STATE OF SEBASTIAN INLET REPORT 2012

An Assessment of Inlet Morphologic Processes, Shoreline Changes, Sediment Budget and Beach Fill Performance

By

Gary A. Zarillo, Florian Brehin, Leaf Erickson and Clarice Cote

Department of Environmental and Marine Systems Florida Institute of Technology

150 University Blvd.

Melbourne, FL 32901

Executive Summary

The annual update of the State of Sebastian Inlet includes six major areas of work: 1) an update of the analysis of volume contained in the inlet sand reservoirs, 2) analysis of morphologic changes within the inlet system, 3) analysis of the sand budget based on the results of the sand volume analysis, 4) an update of the shoreline change analysis, 5) analysis of partitioning of sand grain size fractions through the inlet system, and 6) a numerical modeling analysis of morphological changes and sediment transport in the littoral zone.

The sand volumetric analysis includes the major sand reservoirs within the immediate inlet system and sand volumes within the extended sand budget cells to the north and south of Sebastian Inlet. The volume analysis for each inlet sand reservoir extends from 2004 to 2012. Similar to the volumetric analysis described in previous state of the inlet reports, most inlet sand reservoirs are in a long-term dynamic equilibrium characterized by occasional large seasonal changes in volume superimposed on longer term trends of a lower order of magnitude. An example of this is the volume history of the Sebastian Inlet flood shoal, which has undergone little net volume change between 2004 and 2011, but can experience seasonal variations that exceed 50,000 cubic yards. The most noticeable shift in the flood shoal volume is a decrease of about 43,000 cubic yards between the winter and summer surveys of 2012. This change is considered to be temporary and due to excavation of the sand trap in winter-spring of 2012, which effectively cuts off the sediment supply to the flood shoal.

Likewise, the Sebastian Inlet ebb shoal has experienced gradual net gain in volume since 2004 along with larger seasonal variations in volume that include occasional sand volume gains and losses in a range of 50,000 to 100,000 cubic yards. In the most recent period of 2010 to 2012 the ebb shoal has decreased in volume by about 30, 000 cubic yards, whereas the lower ebb shoal has increased in volume by about 30,000 cubic yards.

Annual gains in sediment volume in the Sebastian Inlet sand trap are about 30,000 cubic yards based on analysis after the 1993, 1999, and 2007 sand bypass projects. According to model tests described in the 2011 State of the Inlet Report, the total volume and rate of annual gains in the sand volume may increase after the planned sand trap extension is completed in 2013.

The dynamic equilibrium of sand reservoirs associated with Sebastian Inlet is also reflected in sediment budget calculations. Whereas net changes in sediment budget cells, including the cell that contains Sebastian inlet sand reservoirs, are relatively small over a 20-year period, seasonal changes in any of the cells can occasional exceed 100,000 cubic yards. In this report the sand budget for the Sebastian Inlet region is reported at several different time scales, including longer time scales of 6 to 10 years and shorter time scales of 3 to 5 years. Over the most recent time period of 2010 the sand budget cell that includes all sand reservoirs associated with the inlet has retained very little sand and over certain seasons has given up more than 85,000 cubic yards of material to be bypassed across the inlet

Similar to the sand volume analysis, the results of shoreline mapping from survey data vary considerably by time scale. Over the 10-year time scale from 2002 to 2012, shoreline changes south of the inlet reflected the position of beach fill placement in 2003, 2007, and2011 and 2012. These projects provided sections of advancing or stable shoreline. The section of beach 15,000 feet north of Sebastian Inlet during the summer 2002 to summer 2012 period was

subject to shoreline recession. On the shortest time scales, shoreline change and change rates were spatially variable and largely reflect seasonal beach conditions, as well as fill placement in the 2011-2012 period. Over the shortest time period analyzed, 2007 to 2013 net shoreline gains were prevalent over most areas when comparing summer to summer shoreline positions. These areas include a section from R190 to R219 north of the inlet and from about R17 to R30 south of the inlet. Shoreline advancements in the R17 to R30 are thought to result from retention of fill material drifting south from the 2003 and 2007 fill projects plus the results of more recent fill projects from upland sand sources. The areas from R1 to R15 were outside the immediate zone of recent fill projects completed in 2011, but include much of the beach nourished in 2003 and renourished in 2007, as well as sand from the Sebastian Inlet Sand Trap. Thus, dispersal of fill material in this area including the 2007 and 2012 sand bypass project from the inlet sand trap have limited shoreline recession from R2 to R15 in the 2007 to 2012 period.

For the two modeling time periods in 2011, predicted sedimentation patterns were in good agreement with measured data. The model was particularly successful in reproducing the sand deposition on the north fillet reservoirs, in the sand trap and on the shoreface in the south part of the domain, which are characterized by hard-bottom through nearshore reef. On a larger scale, model results showed deposition at R16 and beyond which suggested that large sand bodies moving alongshore were trapped by complex reef morphology. For both time periods, the model overestimated the changes on the ebb shoal. These issues are mitigated by using multiple sediment grain sizes as input to the sand transport calculations, as well as by increasing the coverage of hard bottom. Model predicted volume changes are verified by measured volumetric changes of the individual inlet reservoirs.

Table of Contents

List of Figures

List of Tables

Introduction and Previous Work

The report extends the analysis of the Sate of Sebastian Inlet from the publication of the 2011 report through the summer months of 2012. In the original 2007 report, sand volume changes, sand budget, and morphological changes between 1989 and 2007 were examined (Zarillo et al. 2007). In addition, shoreline changes were documented between 1958 and 2007using aerial images and between 1990 and 2007 using field survey data. In the 2009 report, these analyses were updated along with the addition of a numerical modeling analysis to simulate existing conditions and to examine the potential performance of two engineering projects. These included a hypothetical extension to the south jetty to improve navigation and limited excavation of the lower ebb shoal for beach-compatible sand. All of these analyses are updated in the 2012report, including a more comprehensive analysis using the numerical model. Specific focus was given to comparing longer term shoreline and morphologic changes since 2000 with shorter term changes later in the decade. Likewise, comparisons were made between the longer term sand budget from 2000 to 2011 with the sand budget over shorter time intervals between 2002 and 2011. Recommendations are made for applying the results of State of the Inlet Analysis to the ongoing Sebastian Inlet Management Plan.

2.0 Sand Volume Analysis Methods

Hydrographic surveys of the inlet system and surrounding beaches were conducted annually by Sebastian Inlet Tax District (SITD) since the summer of 1989. Starting in winter 1991, surveys have been performed on a semiannual basis. Offshore elevation data are gathered by conventional boat/fathometer surveying methods from -4 ft to -40 ft in accordance with the Engineering Manual for Hydrographic Surveys (USACE, 1994). As shown Figure 1, the study area includes not only the entire inlet system (ebb shoal, throat, sand trap and flood shoal), but also the adjacent beaches approximately 30,000 ft north (Brevard county) and 30,000 ft south (Indian River County) of the inlet with beach profiles taken about every 500 ft. Such a comprehensive dataset provides excellent support for volumetric calculations of inlet shoal and morphologic features, as well as for the analysis of changes in shoreline position through a “zero contour” extraction technique. This data source is also very valuable for calibrating models and other decision making tools. Additional datasets used for this report update include surveys

performed in winter 2012 and summer 2012. The spatial resolution is much greater due to the use of multibeam sonar in the south region.

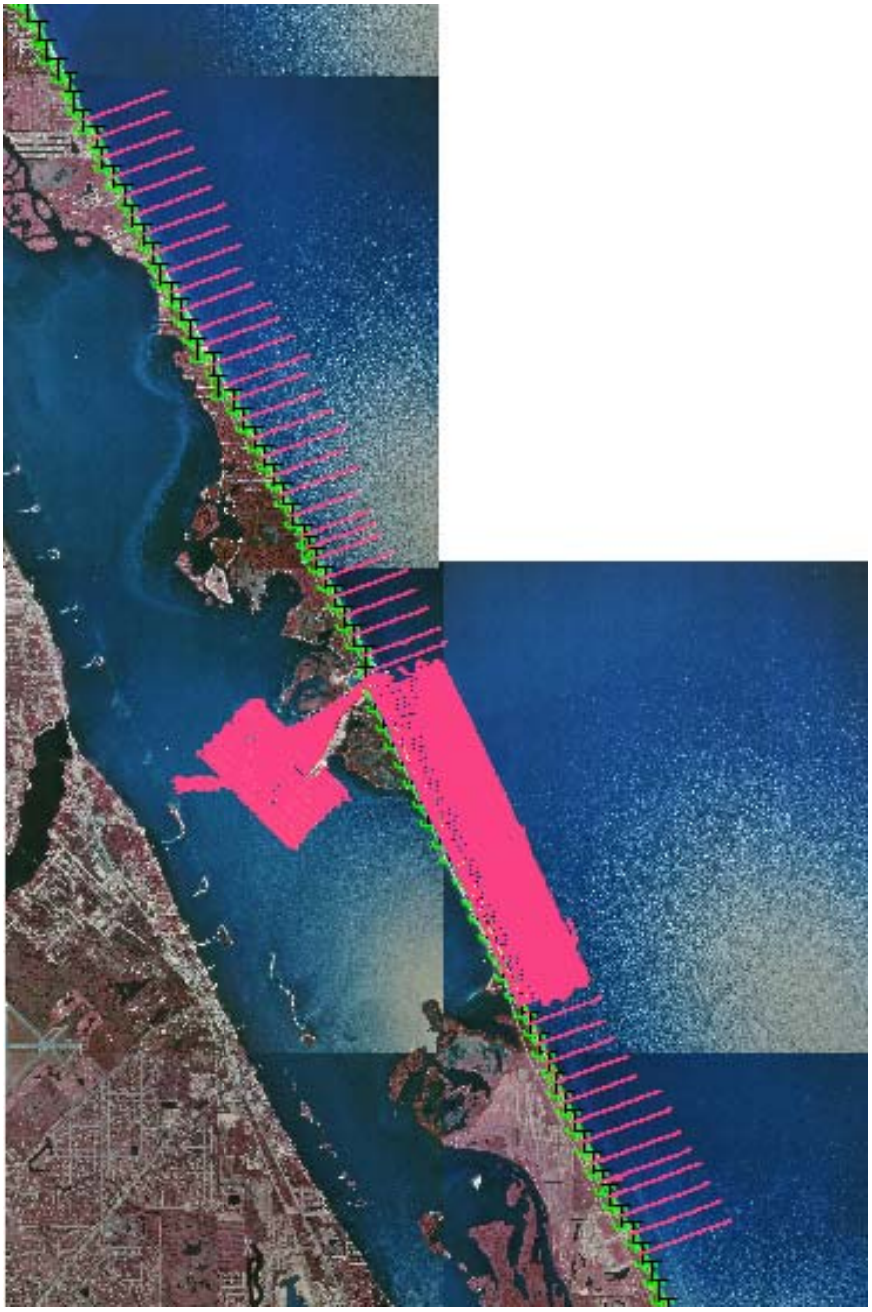

Figure 1.Extent of hydrographic survey (2012 winter)

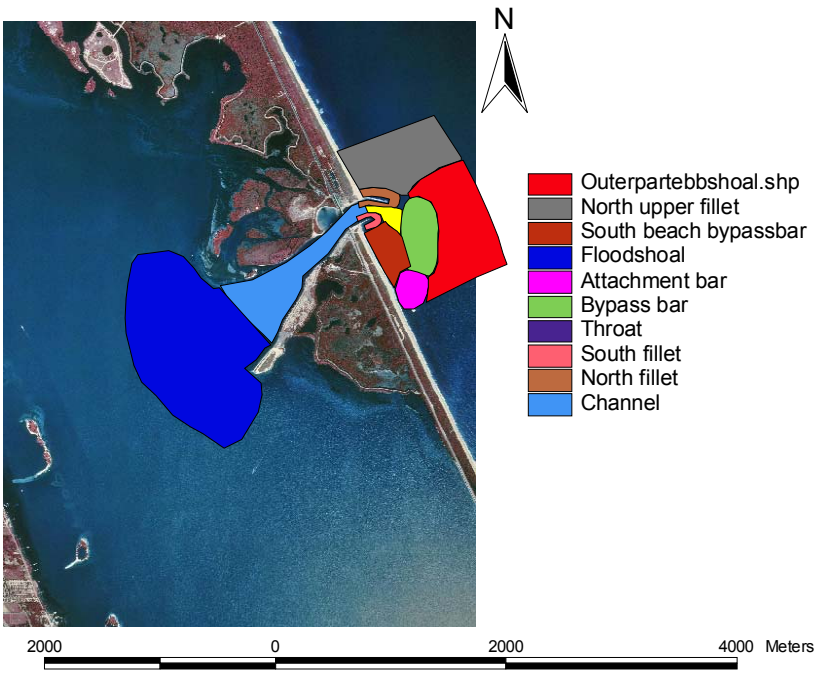

Figure 2. Morphologic features forming the inlet system reservoir

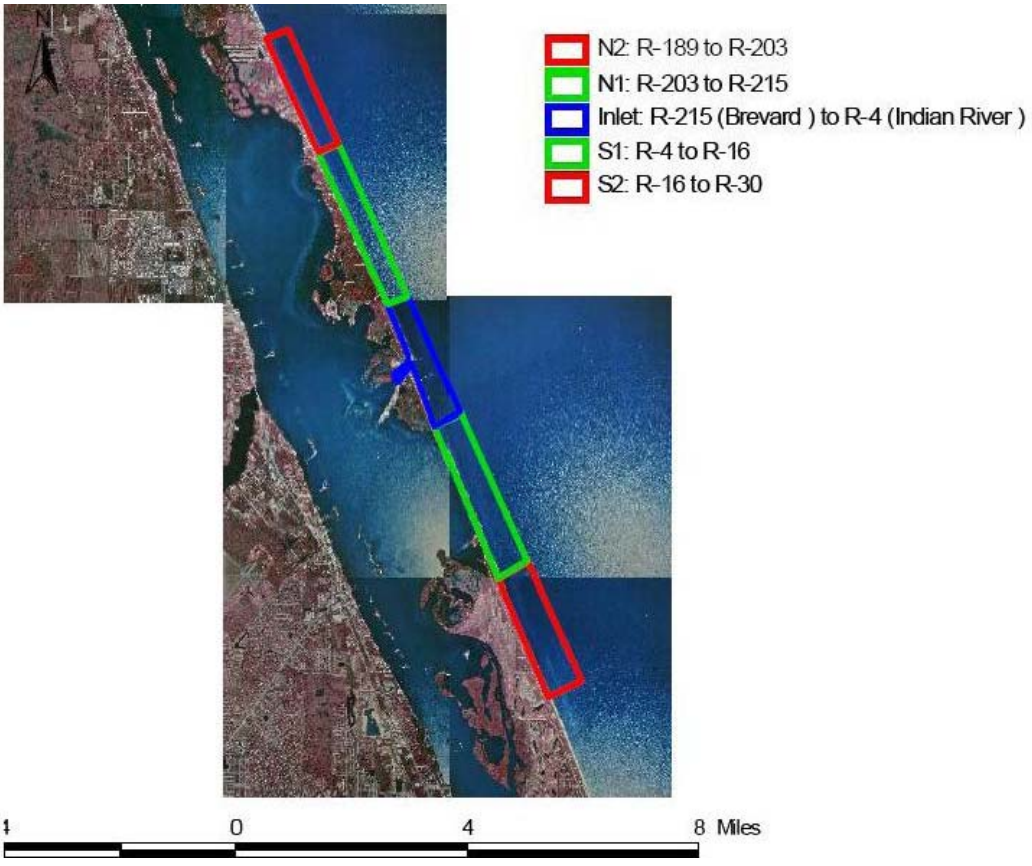

Figure 3. Sand budget cells. Note the inlet cell does include the flood shoal

Table 1. Summary of Hydrographic Surveys (Source: Sebastian Inlet Tax District)

Survey Date	Ebb shoal	Channel	Sand trap	Flood shoal	North beach (ft)	South beach (ft)
Jul-90	x	x	x	x	3000	12 000
Jan-91 *[1]	x	x	x	x	3000	15 000
Jul-91	x	x	x	x	3000	15 000
Jan-92 *[2]	x	x	x	x	10 000	15 000
Jul-92	x	x	x	x	3000	20 000
Jan-93	x	x	x	x	30 000	30 000
Jul-93	x	x	x	x	25 000	30 000
Jan-94	x	x	x	x	10 000	20 000
Jul-94	x	x	x	x	10 000	20 000
Jan-95	x	x	x	x	10 000	20 000
Jul-95	x	x	x	x	10 000	20 000
Jan-96	x			x	15 000	20 000
Jul-96	x	x	x	x	15 000	20 000
Jan-97	x	x	x	x	20 000	20 000
Jul-97	x	x	x	x	20 000	20 000
Jan-98	x	x			20 000	20 000
Jul-98	x	x	x	x	20 000	20 000
Jan-99	x	x	x		30 000	30 000
Jul-99	x	x	x	x	30 000	30 000
Jan-00	x	x	x		30 000	30 000
Jul-00 *[3]	x	x	x	x	30 000	30 000
Jan-01	x	x	x	x	30 000	30 000
Jul-01	x	x	x	x	30 000	30 000
Jan-02	x	x	x	x	30 000	30 000
Jul-02	x	x	x	x	30 000	30 000
Jan-03	x	x	x	x	30 000	30 000
Jul-03 *[4]	x	x	x	x	30 000	30 000
Jan-04						
Jul-04	x	x	x	x	30 000	30 000
Jan-05	x	x	x		30 000	30 000
Jul-05	x	x	x		30 000	30 000
Jan-06	x	x	x	x	30 000	30 000
Jul-06	x	x	x	x	30 000	30 000
Jan-07	x	x	x	x	30 000	30 000
Jul-07	x	x	x	x	30 000	30 000
Jan-08	x		x		30 000	30 000
Jul-08	x	x	x	x	30 000	30 000
Jan-09	x	x	x	x	30 000	30 000
Jul-09 *[5]	x	x	x	x	30 000	30 000
Jan-10 *[5]	x	x	x	x	30 000	30 000
Jul-10 *[5]	x	x	x	x	30 000	30 000
Jan-11 *[5]	x	x	x	x	30 000	30 000
Jul-11 *[5]	x	x	x	x	30 000	30 000
Jan-12 *[5]	x	x	x	x	30 000	30 000
Jul-12 *[5]	x	x	x	x	30 000	30 000

Remarks:

1. Poor coverage, no jetty fillet of north beach
2. Poor coverage of north beach, transects every 3000 ft
3. missing section of lower shoreface between R-1 and R-4
4. Poor coverage of flood shoal
5. Multibeam data

3.0 Sand Volume Analysis Results

Results presented in the volumetric analysis are divided into 2 subsections and include two additional surveys: winter 2012, and summer 2012 (Figure 4 and Figure 5). Section 1 presents the volumetric evolution of the sand reservoirs or features in the inlet system (Figure 2) with plots of net seasonal and cumulative volume change over time. All plots cover the period from summer 2004 to summer 2012. Section 2 presents the volumetric evolution of the inlet littoral cells (masks) used for the sand budget computation (Figure 3). The calculated net seasonal volume changes (ΔV) serve as inputs to the sand fluxes (ΔQ) for the budget calculations.

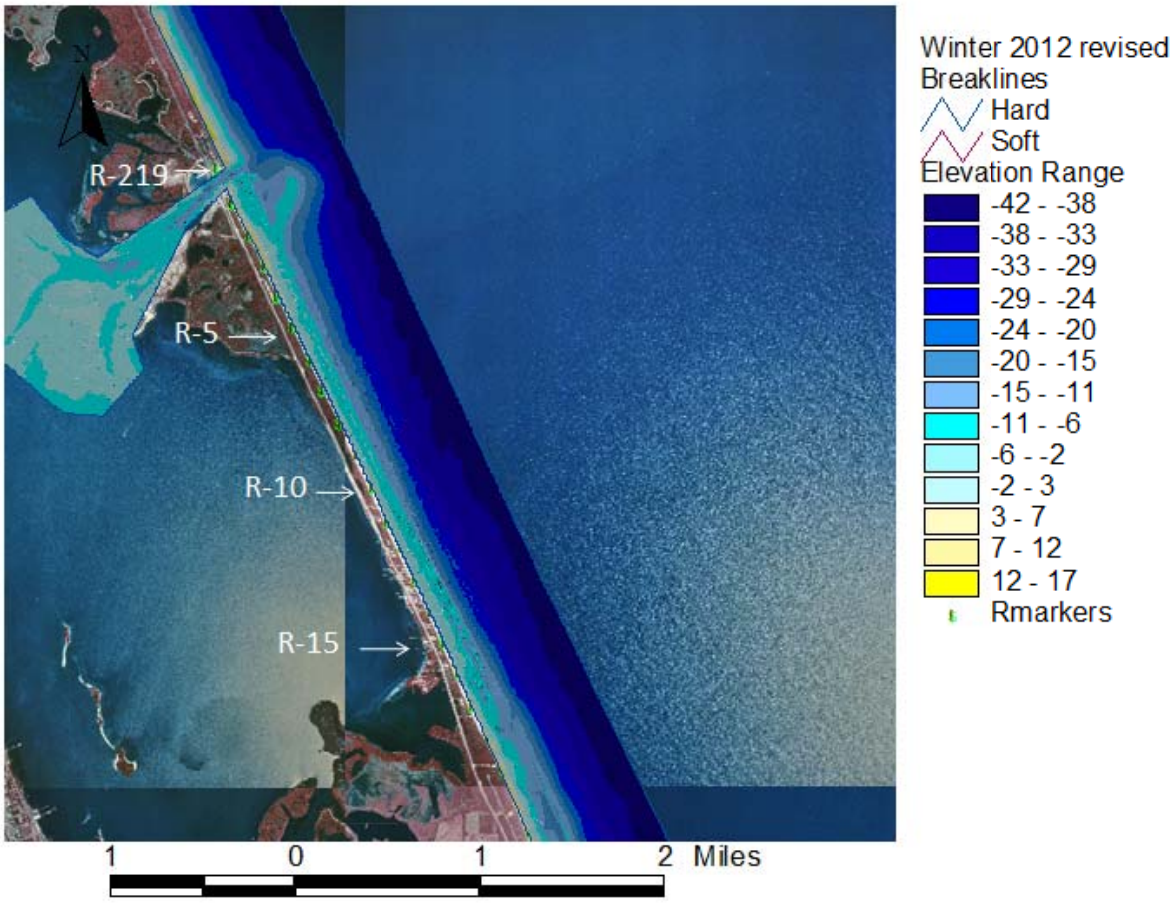

Figure 4. Bathymetric surface (TIN) generated using winter 2012 survey data.

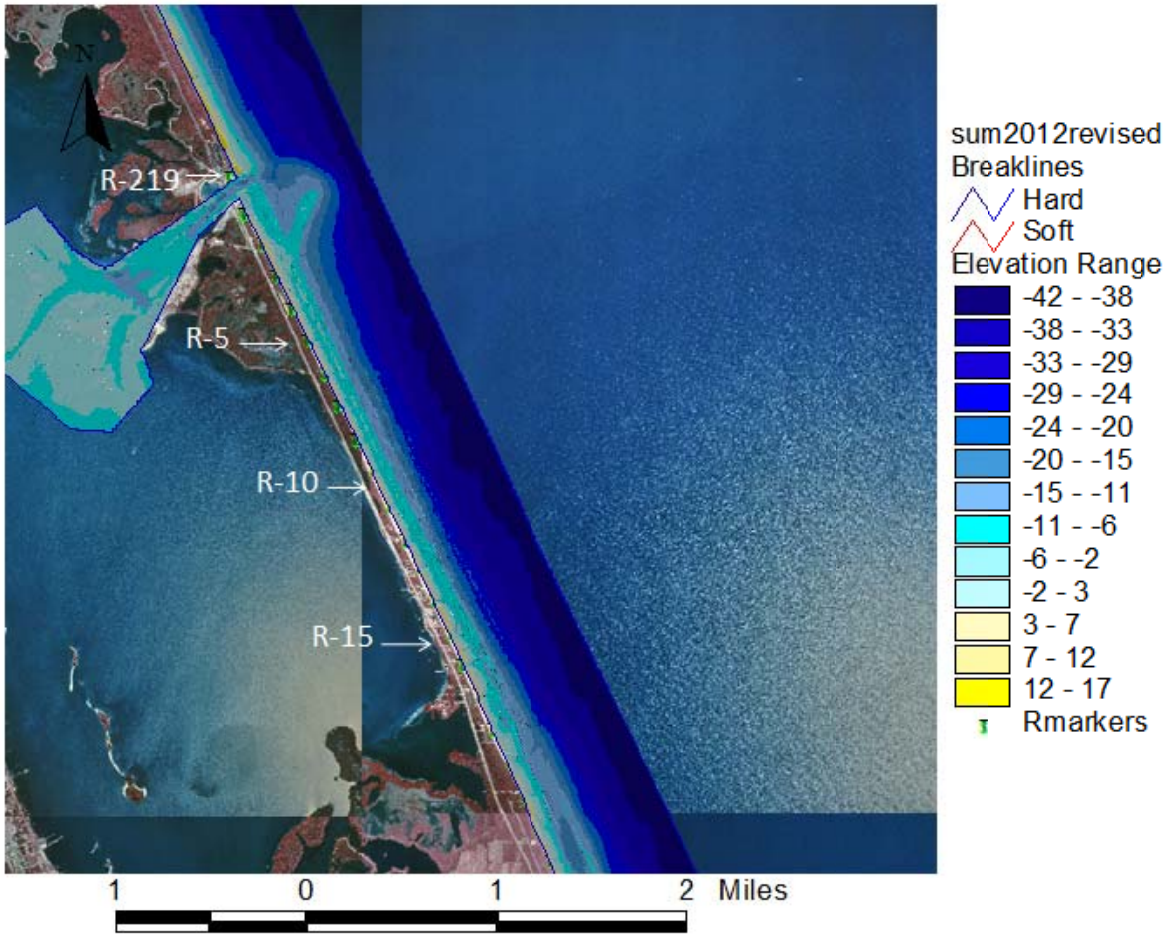

Figure 5. Bathymetric surface (TIN) generated using summer 2012 survey data.

3.1 Volume Analysis: Individual Inlet Reservoirs

The volumetric evolution of the ebb shoal (Figure 6) shows small volume gain from summer 2011 to winter 2012 (+413 cu. yd.), followed by a loss (-12,770 cu. yd.) from winter 2012 to summer 2012. Cumulative changes reached approximately +31,000 cu. yd. since 2004. The volumetric evolution of the outer ebb shoal (Figure 7) shows relatively small volume changes for the two time periods considered with a loss(-113 cu. yd.) from summer 2011 to winter 2012 and a gain (+31,928 cu. yd.) from winter 2012 to summer 2012. Cumulative volume changes reached 185,000 cu. yd. since 2004.

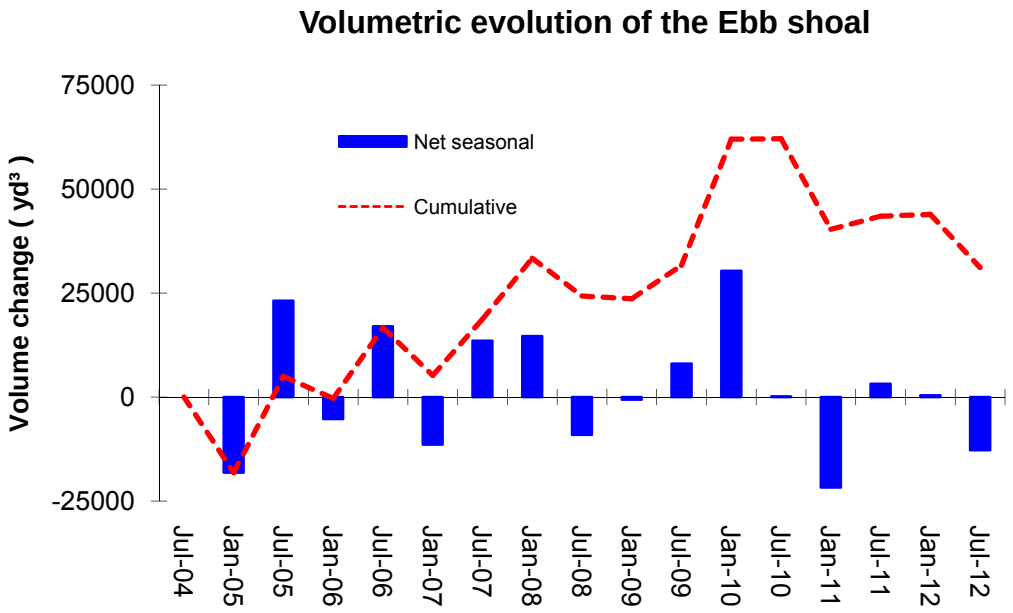

Figure 6. Volumetric evolution of the ebb shoal from summer 2004 to summer 2012

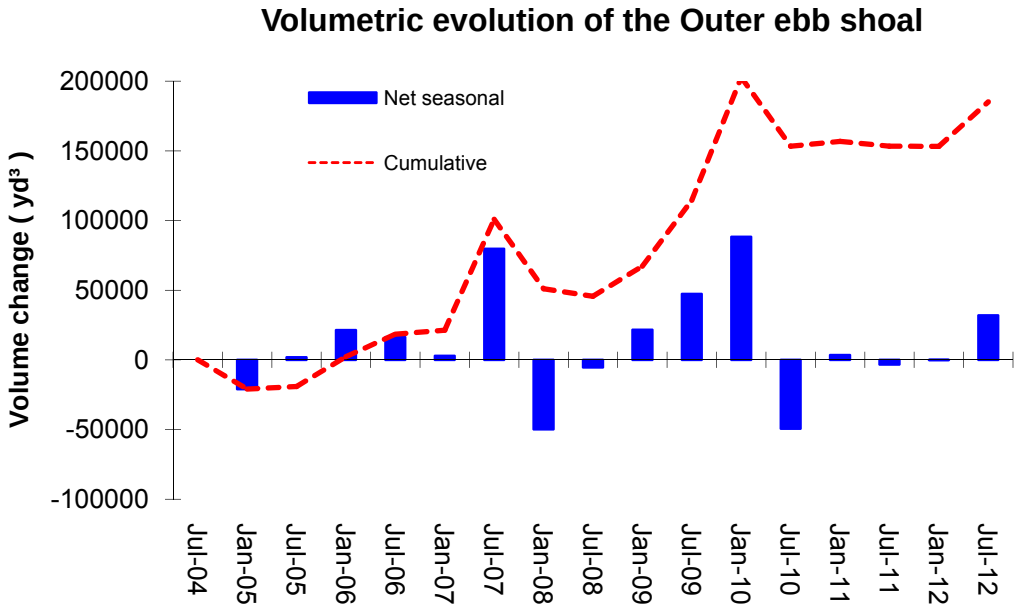

Figure 7. Volumetric evolution of the outer ebb shoal from summer 2004 to summer 2012

The volumetric evolution of the attachment bar (Figure 8) shows volume gain from summer 2011 to winter 2012 and a loss from winter 2012 to summer 2012 (respectively +14,388

cu. yd. and -6,397cu yd.). This resulted in a negative cumulative volume change value of -187 cu. yd. since 2004. Net seasonal volume changes for the south jetty fillet reservoir (Figure 9) shows volume losses from summer 2011 to winter 2012 (-5,924 cu. yd.), followed by gains(+2,568 cu. yd.) from winter 2012 to summer 2012. As illustrated by the dotted line, the seasonal changes cumulated to about +366 cu. yd. since 2004.

The beach section located immediately north of the attachment bar, including the area from the south jetty to R2, According to (Figure 10, the reservoir experienced minimal volume changes over the past two surveys: the reservoir gained +2,760 cu. yd. from summer 2011 to winter 2012 and gained +85 cu. yd. from winter to summer 2012. Cumulative change reached +15,699 cu. yd. since the winter 2004 survey. The reservoir has exhibited a seasonal pattern since winter 2008 consisting of gains between fall and winter and losses during spring and summer. The absence of a volume gain peak between winter and summer 2012 indicates that beach fill material from the spring 2012 mechanical bypassing project has not been back passed from the project area and therefore most of the sand remained on the beach face.

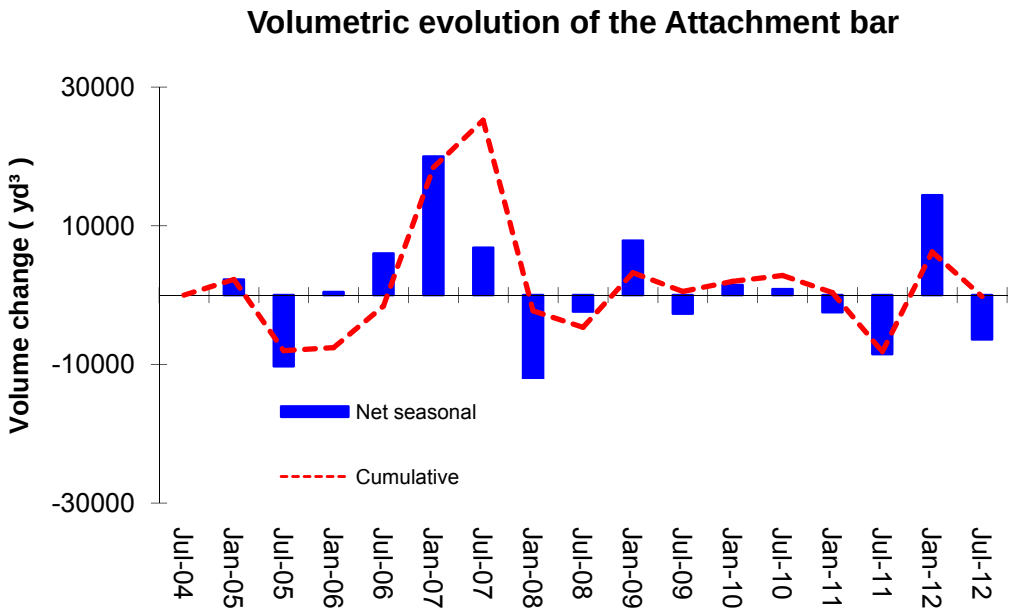

Figure 8. Volumetric evolution of the attachment bar from summer 2004 to summer 2012

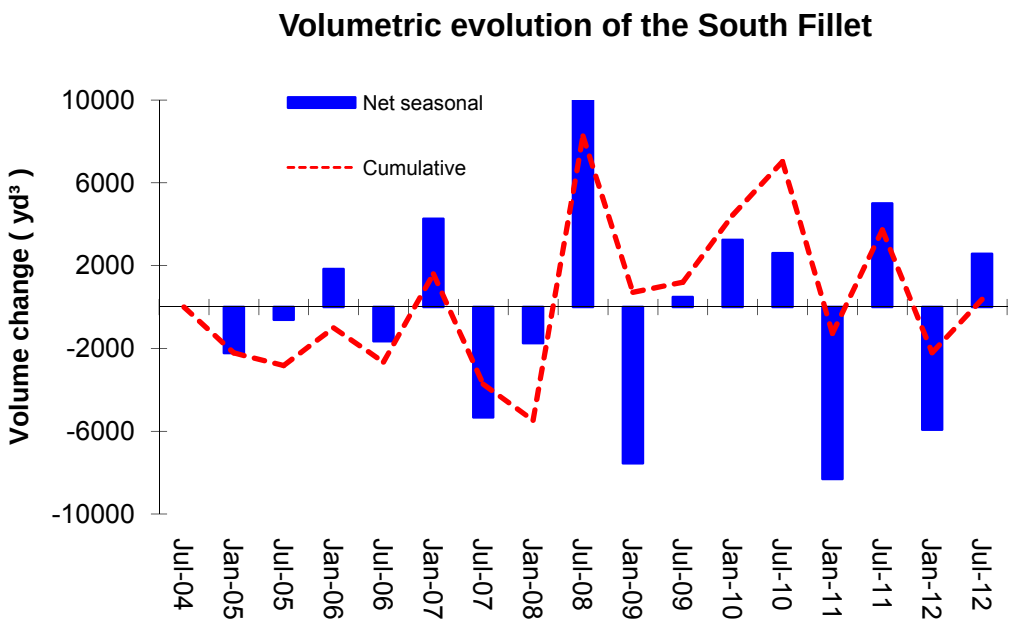

Figure 9. Volumetric evolution of the south fillet from summer 2004 to summer 2012

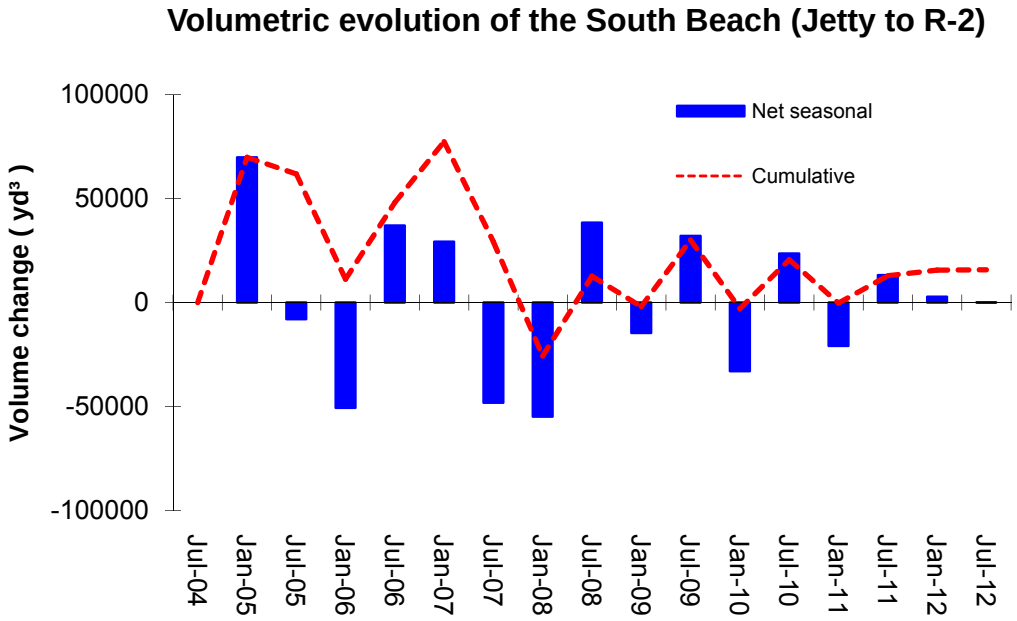

Figure 10. Volumetric evolution of the south beach from summer 2004 to summer 2012

The volumetric evolution of the reservoirs located in the vicinity of the north jetty (north fillet and upper north jetty fillet) is presented in Figure 11and Figure 12, respectively. The

volumetric evolution of the north jetty fillet (Figure 1) shows a volume loss of -7,886 cu. yd. from summer 2011 to winter 2012 followed by a gain of +2,173 cu. yd. from winter 2012 to summer 2012. As suggested by the dotted line, the cumulative volume change approximated -8,350 cu. yd. over the past 8 years.

As shown in Figure 12, the upper north fillet experienced small gains from summer 2011 to winter 2012 (+11,934 cu. yd.), followed by significant losses (approximately +5,199 cu. yd.) which cumulated to +38,631 cu. yd. over the past 8 years.

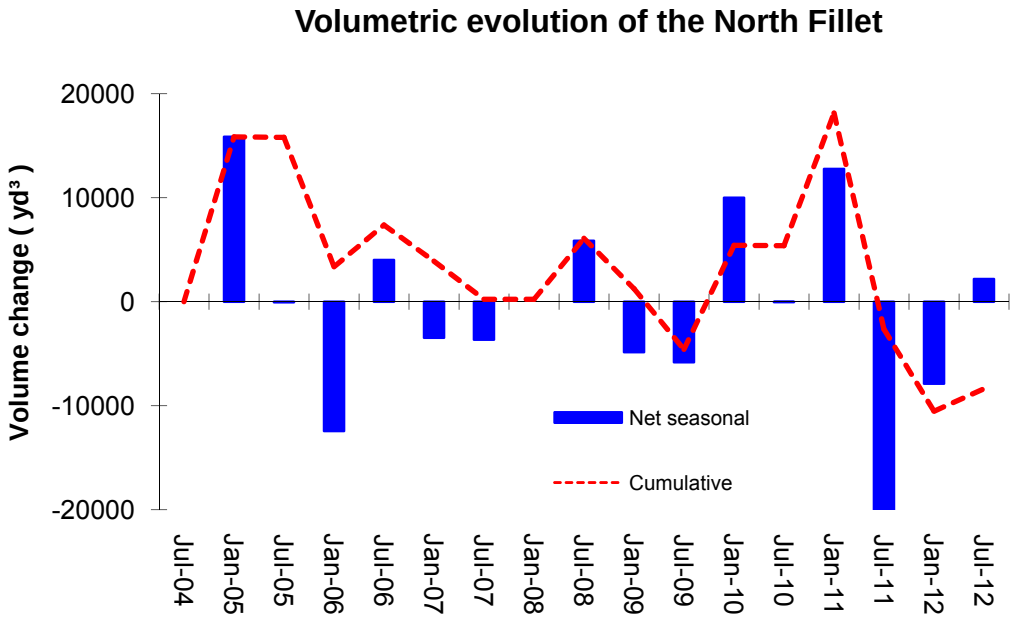

Figure 11. Volumetric evolution of the north fillet from summer 2004 to summer 2012

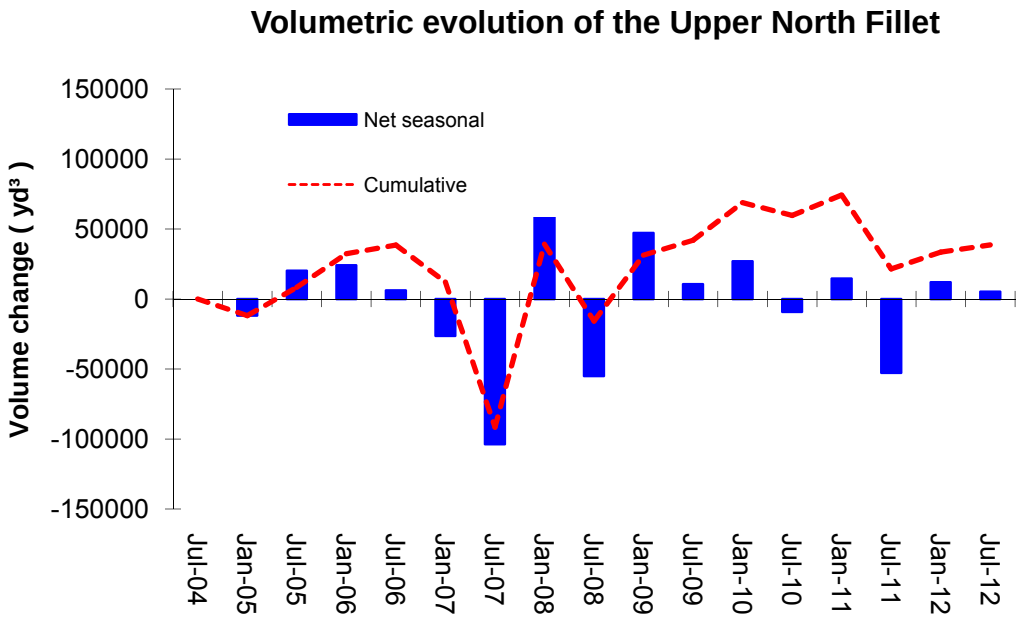

Figure 12. Volumetric evolution of the upper north fillet from summer 2004 to summer 2012

The volumetric evolution of the sand trap is presented in Figure 13. From summer 2011 to winter 2012, the accumulation of sand in the trap reached approximately +15,537 cu. yd., followed by the loss of-80,610 cu. yd. (from winter 2012 to summer 2012). The figure illustrates the mechanical bypassing of spring 2012 with the removal of approximately 90,000 cubic yards of sand from the sand trap. Volumetric changes for the flood shoal (Figure 14) showed losses from summer 2011 to winter 2012 (-25,747 cu. yd.), and from winter 2012 to summer 2012 (-42,738 cu. yd.). The large losses observed from winter 2012 to summer 2012 were in part due to the channel dredging project (30,000 cubic yards) completed in spring 2012, along with the sand trap dredging/mechanical bypassing project. Other factor that might have influenced volume change is sand trap dredging; in fact the two back-bay reservoirs are inter-related and large volume losses within the flood shoal were already documented in the past, in the surveys following a dredging project (1999, 2007).

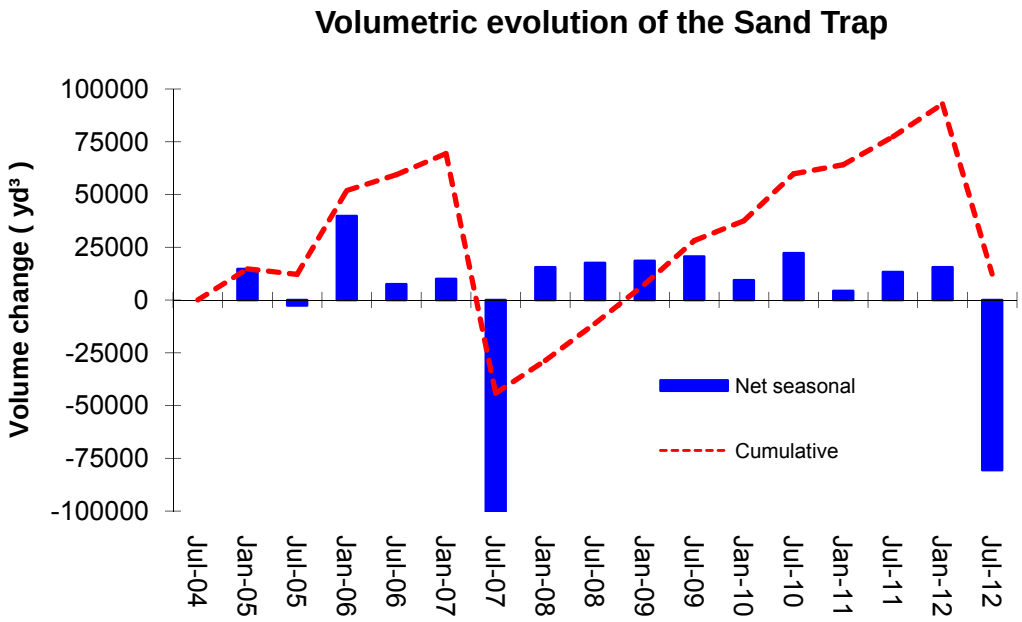

Figure 13. Volumetric evolution of the sand trap from summer 2004 to summer 2012

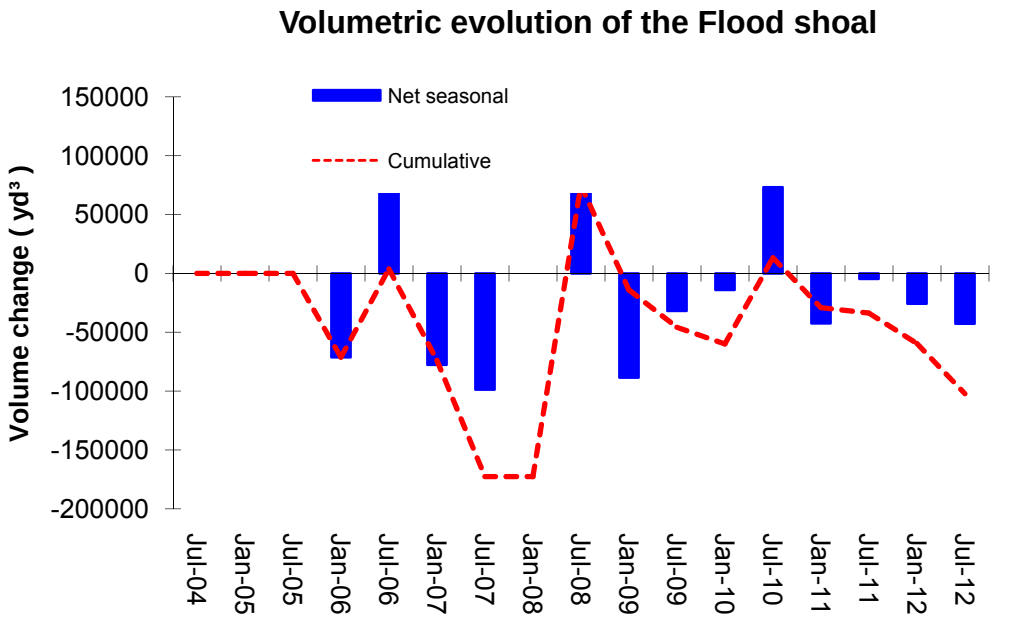

Figure 14. Volumetric evolution of the sand trap from summer 2004 to summer 2012

Overall, volume changes of all reservoirs were well within the range of previous estimates (Zarillo et al. 2007, 2009, 2010, 2011). It must be noted that the sand reservoirs in the inlet vicinity (north and south jetty filets, south beach, and attachment bar) experienced cumulative changes over the past 8 years close to 0, suggesting that even though they experienced large seasonal changes, they remained in dynamic equilibrium. The volumetric changes of the reservoirs located in the inlet back-bay (sand trap and flood shoal) were most impacted by the spring 2012 mechanical bypassing project and channel extension, with large losses for both sand trap and flood shoal. Sand trap dredging tends to decrease the amount of sand that reaches the flood shoal via tidal current transport therefore increasing volumetric losses. The large seasonal fluctuations in the sedimentation were further highlighted in the bathymetric change analysis section.

3.2 Volume analysis: Sand Budget Cells

The sediment budget calculations discussed in the report depend on the analysis of individual sand budget cells. Consistent with earlier versions of the report (Zarillo et al.2007, 2009, 2010, 2011), five computational masks were created to define the sand budget cells (Figure 3). The inlet cell encompassing the nearshore zone from R215 in Brevard County to R4 in Indian River County included the ebb and flood shoals and all other reservoirs discussed in the previous section. Annualized volume changes (ΔV) for each cell, calculated over different time periods, were added to the sand budget equation to calculate the littoral sand transport in and out of each reservoir/cell. Annualized placement and removal volume data were also included to account for dredging/mechanical bypassing and beach fill activities in the cells concerned. This is presented in Table 2 in the sand budget section (Section 6.1). Time series of volumetric change for the five littoral cells (masks) since 2004 are presented in Figure 15 through Figure 19, ranging from the northernmost to the southernmost distal cells.

Volume changes for the N2 cell, the section between R189 and R203, are presented in Figure 15. Results indicated volume gain (+116,079 cu. yd.) during the period from summer 2011 to winter 2012, followed by a smaller gain (+66,130cu. yd.) during the next cycle of

survey, from winter to summer 2012. As indicated by the dotted line, cumulative change for the N2 cell approximated +51,298 cu. yd. since 2004.

Volume changes for the N1 cell, the section between R203 and R215, are presented in Figure 16. The cell gained approximately +237,401 cu. yd. of sand between summer 2011 and winter 2012, followed by a smaller gain (+18,218 cu. yd.) between winter 2012 and summer 2012. Cumulative volume change approximated -320,624 cu. yd. over the past 8 years.

Overall the magnitude of the seasonal changes for both N2 and N1 cells was well within the magnitude observed during the past 8 years. Both cells shared similar volume change trends, and volume changes have been in phase since 2007.

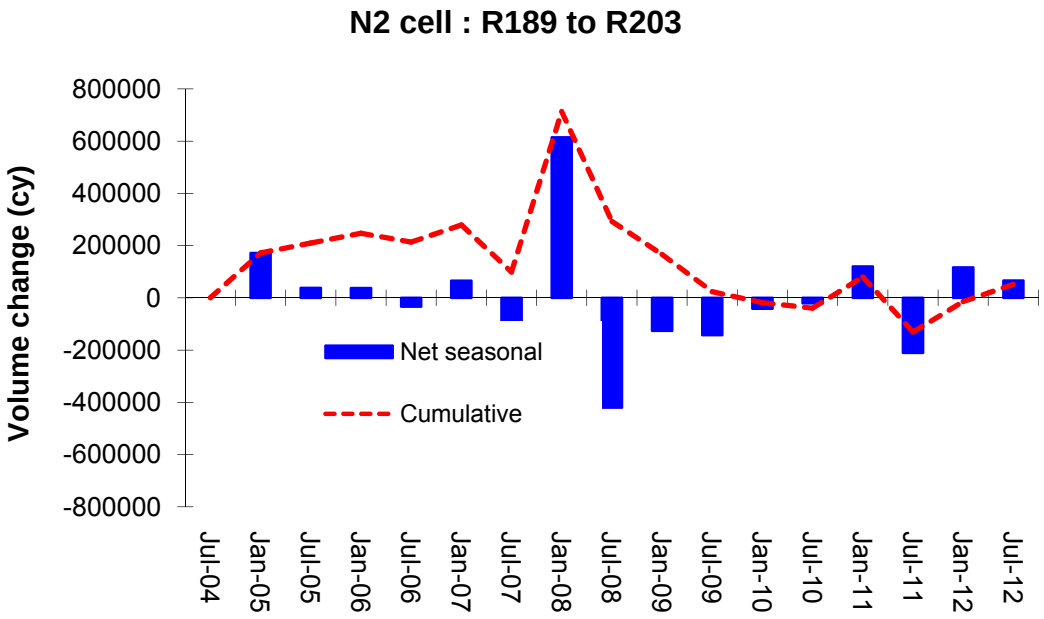

Figure 15. Recent volumetric evolution of the N2 sand budget cell

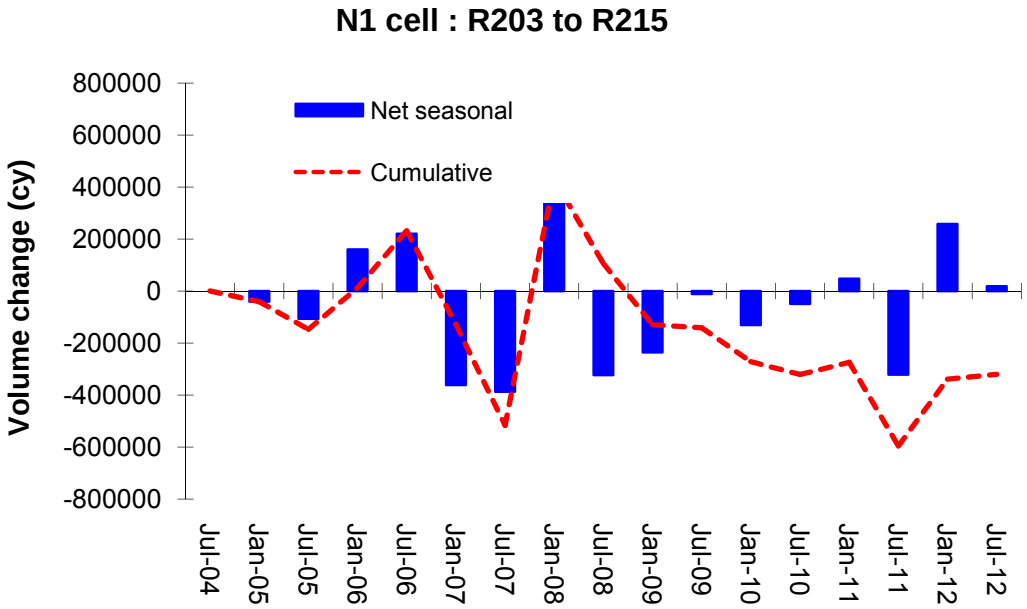

Figure 16. Recent volumetric evolution of the N1 sand budget cell

Volume changes for the inlet cell are presented in Figure 17. The inlet cell experienced consecutive volume sand gains from summer 2011 to winter 2012 and from winter 2012 to summer 2012 (+85,164 cu. yd. and +19,373 cu. yd., respectively). Cumulative volume changes were positive for the 8-yr time period, and reached +148,009cu. yd. Net volume change remained positive over this short time periods remained positive even though 90,000 cubic yards. of sand were removed from the sand trap.

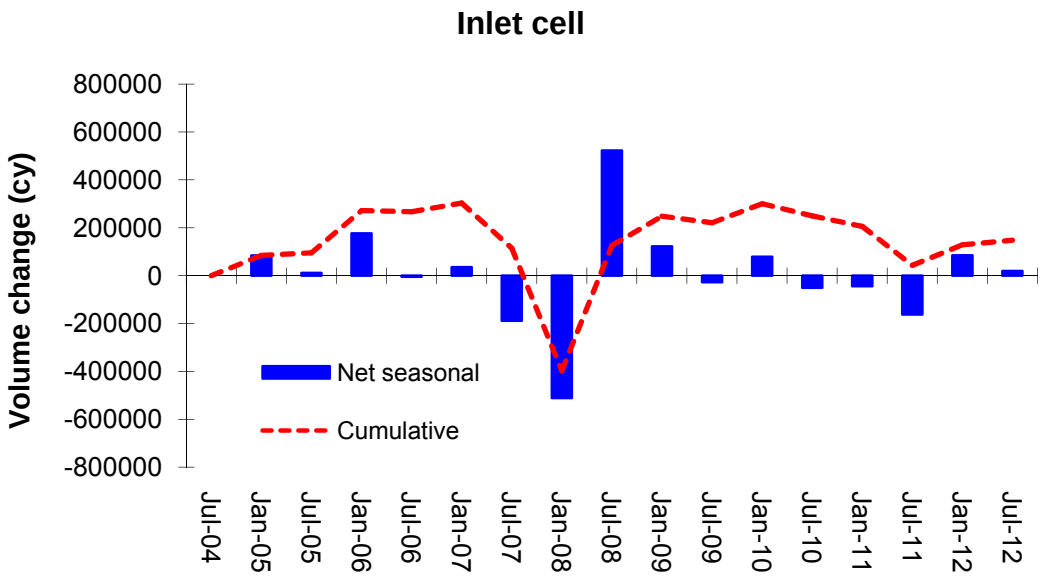

Figure 17. Recent volumetric evolution of the Inlet sand budget cell

The volumetric evolution of the S1 cell, situated directly south of the inlet cell between R4 and R16, is presented in Figure 18. The cell gained approximately +230,854 cu. yd. of sand between summer 2011 and winter 2012, followed by another gain of +63,847 cu. yd. between winter 2012 and summer 2012. Cumulative volume change values remained negative over the long-term (-191,038 cu. yd. for the 8-yr period). There was no signature of the spring 2012 mechanical bypassing project in the summer 2012 survey data, suggesting that beach fill material has remained on the beach face. This is later verified in the survey-based shoreline change section which highlights significant shoreline advancement in the project zone (up to +120 ft).

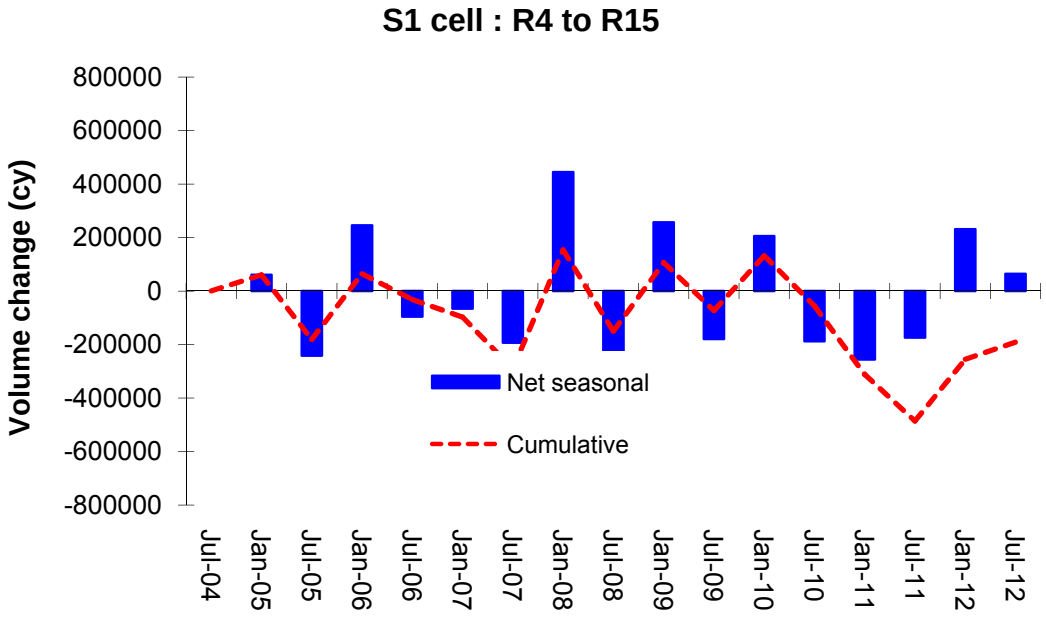

Figure 18. Recent volumetric evolution of the S1 sand budget cell

The volumetric evolution of the S2 cell, located between R16 and R30, is presented in Figure 19. The cell experienced significant net volume gain from summer 2011 to winter 2012 (+233,059 cu. yd.) followed by a significant loss (-126,958 cu. yd.) from winter 2012 to summer 2012. As represented by the dotted line, cumulative change showed a gain of +31,843 cu. yd. over the 8-year period from 2004 to 2012. The large gains experienced from summer 2011 to winter 2012 could be a signature of the +45,000 cu. yd. beach fill that took place in winter 2011 from R26.5 to R30.

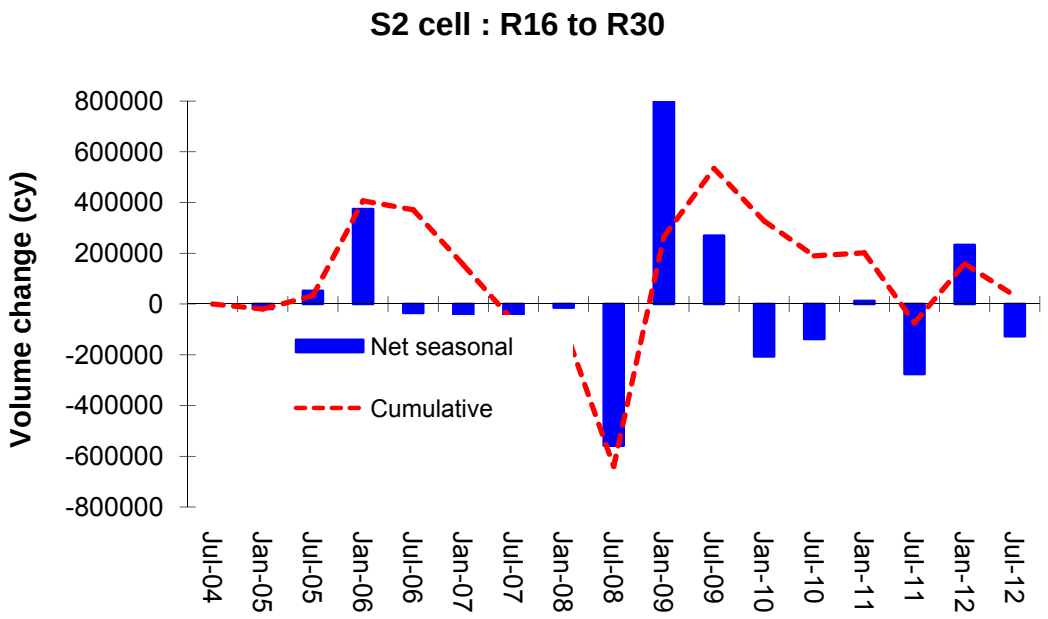

Figure 19. Recent volumetric evolution of the S2 sand budget cell

4.0 Bathymetric/Morphologic Changes Methods

The analysis uses the same dataset and overall methodology as the sand volume analysis described in the section above. The bathymetric changes section is subdivided according to the time period of analysis. Section 5.1 presents the seasonal changes from summer 2010 to summer 2011 (Figure 20 and Figure 21. The net bathymetric changes over a 15-year and 20-year period are presented in Appendix A. In the color code for figures depicting topographic change, blue represents erosion, whereas red indicates deposition. Topographic changes were combined with results from shoreline changes and sand budget calculations for a better understanding of the sedimentation processes.

5.0 Bathymetric/Morphologic Change Results

5.1 Seasonal changes: 2011-2012

Net topographic changes between summer 2011 and winter 2012 (Figure 20) indicated that the greatest deposition occurred on the north jetty fillet and upper north fillet/lower shoreface off R219 (+4 ft) as well as in the northern domain (R204 –R213). Significant deposition (+2 to +3 ft) was also observed on the upper shoreface between R2 and R6, and south of R16 (+2 to +3 ft). Other areas that experienced deposition included the inner part of the ebb shoal (+1 to +2 ft), the edge of the flood shoal (ramp) and the sand trap (+1 to +2 ft). Significant scour (-2 to -3 ft) was observed on the upper shoreface between R1 and R2,and on the seaward part of the ebb shoal. Scour up to -3 ft was also observed between R15 and R30 in a pattern following the reef occurrence.

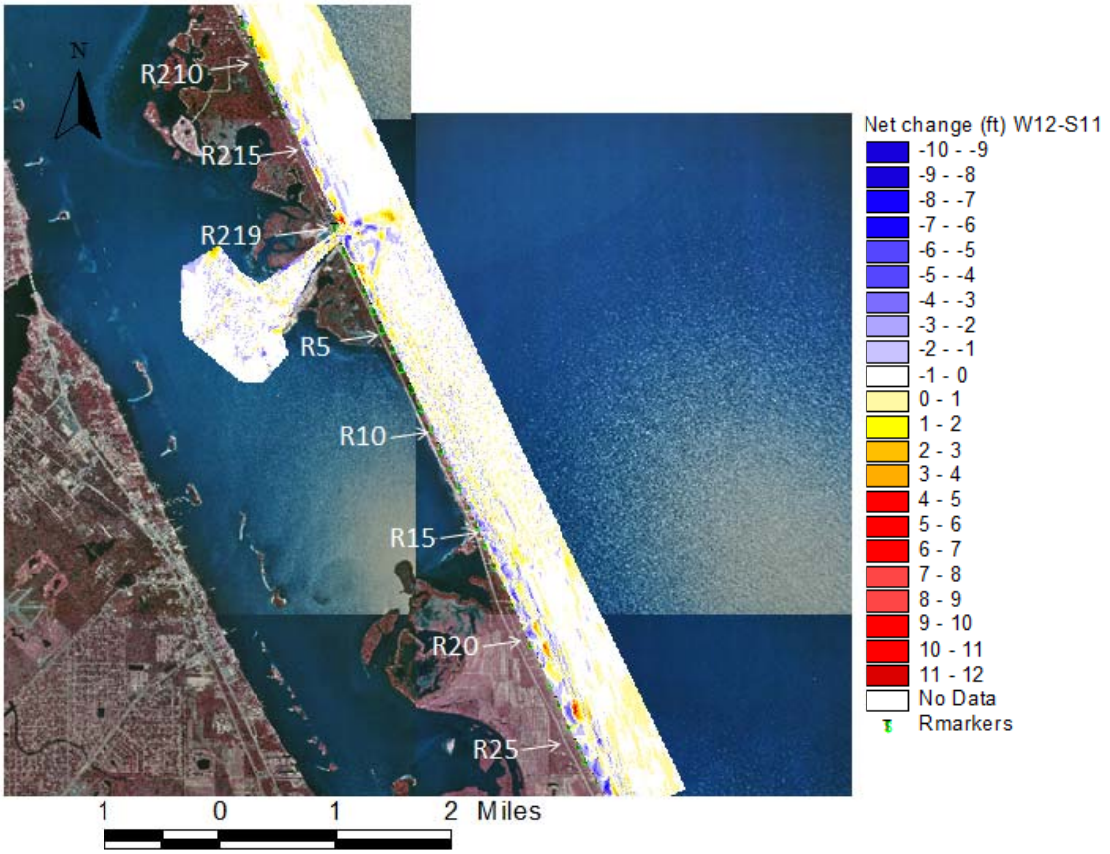

Figure 20. Net topographic changes from summer 2011 to winter 2012

Net topographic changes between winter 2012 and summer 2012 are presented in Figure 21. Significant deposition up to +5ft is observed on the overall beach face and upper shoreface

section from R4 to R20. Significant scour (-6 to -8 ft) was observed in the sand trap and in the channel to the ICW on the western side of the flood shoal. The Figure clearly illustrates the spring 2012 mechanical bypassing project and the volumetric changes discussed in the above sections. For the north domain, similar trends of deposition/erosion were observed on the upper shoreface to the exception of the zone between R204 and R213 (minimal scour as opposed to significant deposition between summer 2011 and winter 2012). The abnormal deposition observed could be related to natural sand backpassing from the inlet (improbable) or strong south littoral drift transporting beach fill material away from project areas up north.

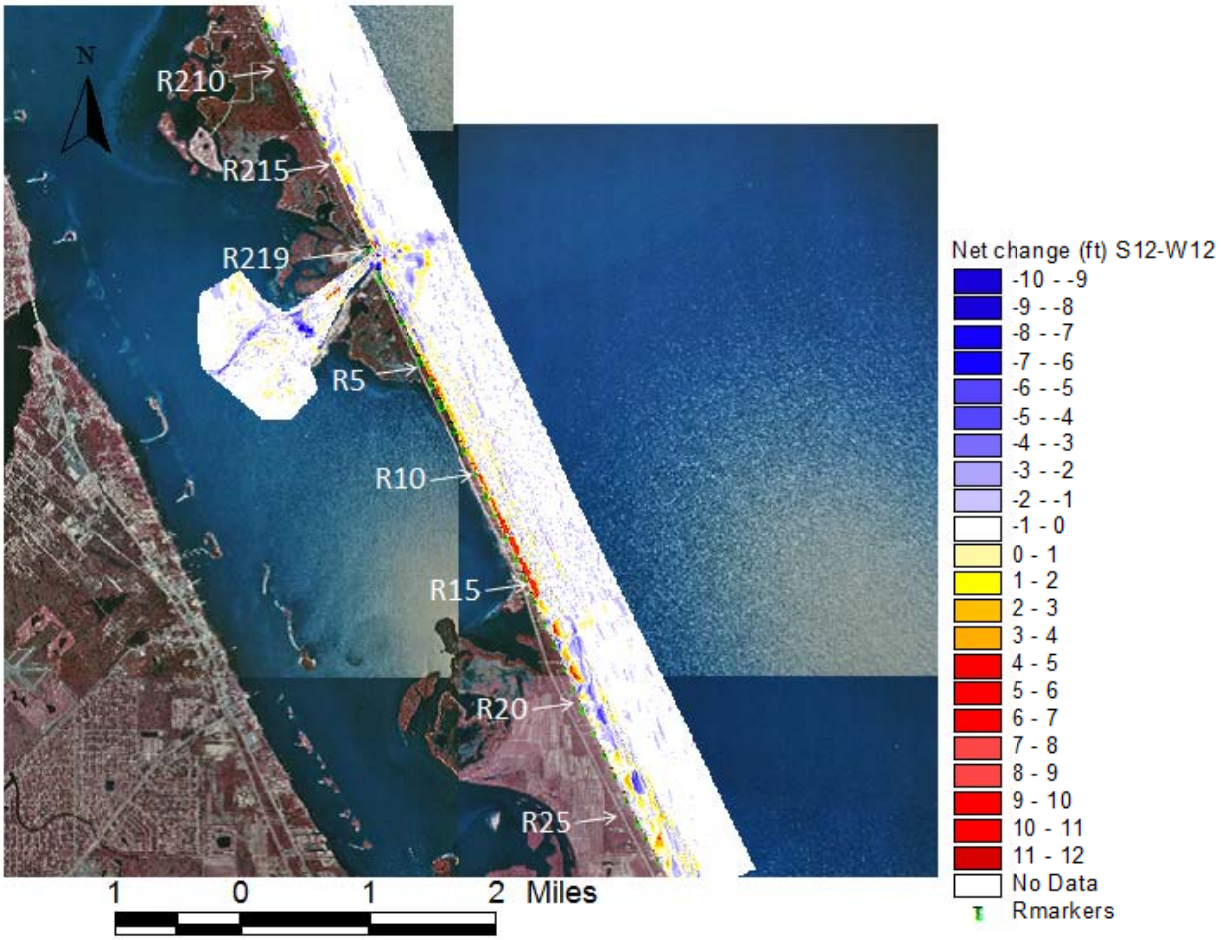

Figure 21. Net topographic changes from winter 2012 to summer 2012

6.0 Sand Budget Update 2012: Methods

A sediment budget uses the conservation of mass to quantify sediment sources, sinks, and pathways in a littoral cell environment. It is used to quantify the effects of a changing sediment supply on the coastal system and to understand the large-scale morphological responses of the coastal system. The sediment budget equation is expressed as:

$$\sum Q_{source} - \sum Q_{\sin k} - \Delta V + P - R = residual \qquad \text{Equation 1}$$

The sources (Q_{source}) and sinks (Q_{sink}) in the sediment budget together with net volume change within the cell (ΔV) and the amounts of material placed in (P) and removed from (R) the cell are calculated to determine the residual volume. For a completely balanced cell the residual would equal zero (Rosati and Kraus, 1999). Figures 22 schematically shows how calculations are made within each cell of the sediment budget model.

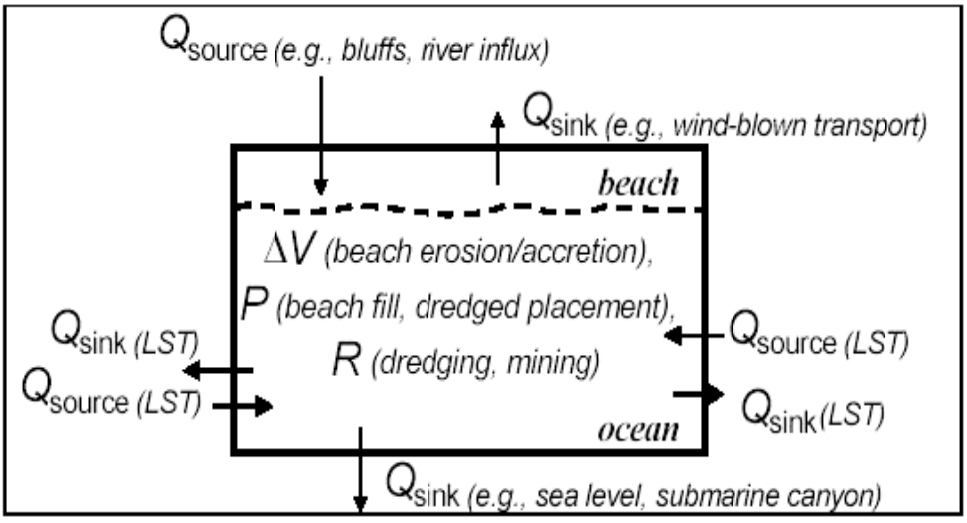

Figure 22. Schematics of a littoral sediment budget analysis (from Rosati and Kraus, 1999).

Determination of net volume change for the local sediment budgets for Sebastian Inlet, FL was based on volumetric analysis masks discussed earlier. The budget encompasses the area between monuments R189 in Brevard County to monument R30 in Indian River County. Since variability of the seasonal signal overshoots the average range of values in the sediment budget,

the temporal scale of the calculations is based on several time periods ranging from two to ten years from summer 2002 to summer 2012. The computation cells (masks) that were used to establish the local sediment budget are schematically shown in the volumetric section (see Figure 3). Volume changes for each mask were determined according to the methods described above in the net topographic changes section and input into the Sediment Budget Analysis System (S.B.A.S) program, provided by the Coastal Inlet Research Program. Details of these procedures can be found in the technical report by Rosati et al. (2001).Based on the longshore transport estimates from the Coastal Tech study (1988) and other estimates, an input value (Q_{source}) of 100,000 yd^3/yr was chosen. The placement values (*P*) into the S1 (R4 to R16) and S2 cells (R16 to R30) correspond to the beach fill projects and were included in the calculations. Removal of sand (R) through mechanical bypassing was included (*R*) to account for the Spring 2007 and 2012 dredging projects of the sand trap. However, removal of sand (R) through offshore losses was assumed to be zero for all cells, as the boundaries of the masks extend beyond the depth of closure. Placement and removal values are annualized and presented in Table 2

6.1 Sand Budget Results

This section is divided into two subsections corresponding to a time period. The first section contains discussion of the sand budget over the long term (5 to 10 years), while the next section discusses sand budget calculations for shorter time periods (2 to 4 years). The budget uses calculated annualized volume change per cell as inputs. The yearly beach fills material and the sand trap dredged material is accounted for in the S1 and S2 cells (R4-R16 and R16-R30, respectively).

Table 2.Annualized placement (beach fill) and removal (dredging) volumes for the time periods used in the inlet, S1, and S2 cells for sand budget calculations

	Time period	Season	Placement S1 (cy/yr)	Placement S2 (cy/yr)	Removal Inlet (cy/yr)
Long term	2002 to 2012	winter	89,000	4,550	9,500
		summer	101,000	13,150	21,500
	2005 to 2012	winter	43,000	6,500	13,600
		summer	60,000	13,200	30,715
	2007 to 2012	winter	60,000	9,100	19,000
		summer	84,000	26,300	43,000
Short term	2008 to 2012	winter	0	11,375	0
		summer	30,000	32,875	30,000
	2009 to 2012	winter	0	15,170	0
		summer	40,000	43,800	40,000
	2010 to 2012	winter	0	22,750	0
		summer	60,000	65,750	60,000

Interpretation of the fluxes, especially those leaving the southernmost cell (S2, R16-R30) must consider that the sand budget assumes a fixed input of +100,000cy/yr at the first north cell (N2). Sand transport was assumed to flow north to south. Positive numbers indicate an increased flux toward the south, which was likely representative of the Sebastian Inlet area on a larger scale, whereas negative results indicate a reversal of sediment transport to the next cell north. Thus a negative volume change for a cell meant that volume was gained in a south cell or was available for that cell.

Long-term sand budget

The net annualized volume changes and associated fluxes for long-term periods are presented in Table 3(summer budget) and Table 4 (winter budgets), and are illustrated in Figure 23 through Figure 25. The annualized volume changes for the N2 cell calculated for the summer budgets (Table 3) were -51,772 cy/yr (10-yr), -22,614 cy/yr (7-yr), and -9,462 cy/yr (5-yr). Fluxes out of the N2 cell ranged from +109,462 cy/yr (5-yr) to +122,614 cy/yr (7-yr) and +151,572 cy/yr (10-yr). The annualized volume changes for the N1 cell were -73,680 cy/yr (10-yr) and -24,722 cy/yr (7-yr). However the annualized net change for the 5 years and budget reached +39,243 cy/yr therefore decreasing the flux out of N1 down to +70,219 cy/yr for that

time period. Fluxes out of the N1 cell ranged from +147,337 cy/yr to +225,251 cy/yr for the 7-yr and 10-yr budgets respectively. The annualized volume changes for both the N1 and N2 cells were much larger in the 10-yr winter budget calculations, with values of -76,499 cy/yr and -85,108 cy/yr, respectively for those two cells. Volume change values for both the N2 and N1 cells were comparable to the summer budget values for the 7-yr and 10-yr budgets. For the 5-yr budget, the trend was reversed for N1, with a negative ΔV of -41,930 cy/yr.

As shown in the summer budget calculations (Table 3), the inlet and southern cells experienced more variability in the annualized volume changes as compared to the north cells. For the 10-yr budget, the inlet, S1 and S2 cells experienced negative ΔV's (-14,038 cy/yr, -77,258 cy/yr, and -47,945 cy/yr, respectively). For the 7-yr budget, the annualized volume change for the inlet cell was positive (+7,484 cy/yr) whereas relatively small negative changes were observed for the S1 and S2 cells (-1,423 cy/yr and -94 cy/yr, respectively). For the 5-yr budget (winter 2007 to winter 2012), all southern cells experienced positive annualized volume changes, ranging from +6,709 cy/yr (inlet) to +19,997 cy/yr (S2). The annualized change for the S1 cell was close to the S1 cell, (+19,945 cy/yr).

All sand budget calculations indicated a positive flux out of the S2 cell, ranging from +90,868 cy/yr (summer 2007 to summer 2012) to +457,142 cy/yr (summer 2002 to summer 2012).The flux out of the S2 cell for the 7-yr budget from summer 2005 to summer 2012 was +183,855 cy/yr. Fluxes out of the inlet cell were reduced by volume gains in the cell and were combined with the annualized removal of 21,500 cy/yr (10-yr budget), 30,715 cy/yr (7-yr budget), and 43,000 cy/yr (5-yr budget). The signature of the recent mechanical bypassing project is evident in the long-term summer calculations, with fluxes out of the inlet cell that were much smaller than those in the winter calculations. Some of the variability can be explained by the large removal values over the shorter time scales. The fluxes out of the S2 cell for the winter budgets were larger in the 5-yr and 7-yr calculations and ranged from +218,295 cy/yr (7-yr) to +316,162 cy/yr (5-yr). The flux out of S2 was reduced to +296,458 cy/yr in the 10-year winter budget. Sand placement values (P) have helped increasing the fluxes in both the summer and winter budgets. For the S1 cell, placement values totalized +101,000 cy/yr (10-yr budget), +60,000 cy/yr (7-yr budget), and +84,000 cy/yr (5-yr budget) in the summer calculations. For the winter budget, values were +89,000 cy/yr (10-yr), +43,000 cy/yr (7-yr), and +60,000 cy/yr (5-

yr). Placement values for the S2 cell were much smaller, varying from +4,550 cy/yr (10-yr), +6,500 cy/yr (7-yr), and +9,100 cy/yr (5-yr) for the winter budgets. Placement values for the summer budgets were +13,500 cy/yr (10-yr), +13,200 cy/yr (7-yr), and +26,300 cy/yr (5-yr). All the above fluxes were well within the range calculated for other long-term periods (Zarillo et al., 2007, 2009, and 2010).

Table 3.Annualized volume changes per cell and flux for several long-term periods (summer budget

Time period	Summer 2002 to Summer 2012		Summer 2005 to Summer 2012		Summer 2007 to Summer 2012	
Sediment budget cell	Δ V (cy/yr)	Q (cy/yr)	Δ V (cy/yr)	Q (cy/yr)	Δ V (cy/yr)	Q (cy/yr)
North2	-51,572	151,572	-22,614	122,614	-9,462	109,462
North1	-73,680	225,251	-24,722	147,337	39,243	70,219
Inlet	-14,038	217,789	7,484	109,138	6,709	20,510
South1	-77,258	396,047	-1,423	170,561	19,997	84,513
South2	-47,945	457,142	-94	183,855	19,945	90,868

Table 4.Annualized volume changes per cell and flux for several long-term periods (winter budget)

Time period	Winter 2002 to Winter 2012		Winter 2005 to Winter 2012		Winter 2007 to Winter 2012	
Sediment budget cell	Δ V (cy/yr)	Q (cy/yr)	Δ V (cy/yr)	Q (cy/yr)	Δ V (cy/yr)	Q (cy/yr)
North2	-38,623	138,623	-26,617	126,617	-58,676	158,676
North1	-44,556	183,179	-42,536	169,153	-41,930	200,605
Inlet	1,374	172,305	6,324	149,229	-34,882	216,487
South1	-14,617	275,922	-45,029	237,259	-31,412	307,899
South2	-15,987	296,458	25,464	218,295	837	316,162

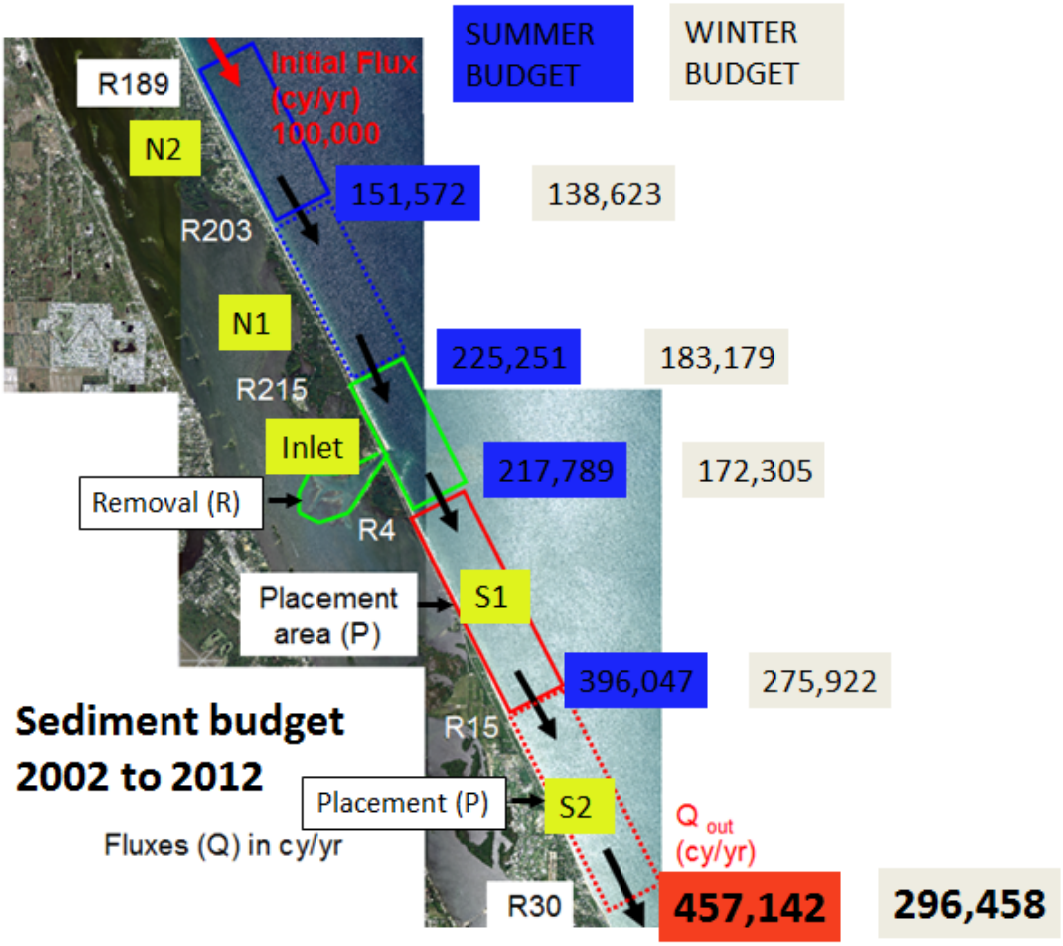

Figure 23. Sand budget calculations from 2001 to 2011 (10-year budget)

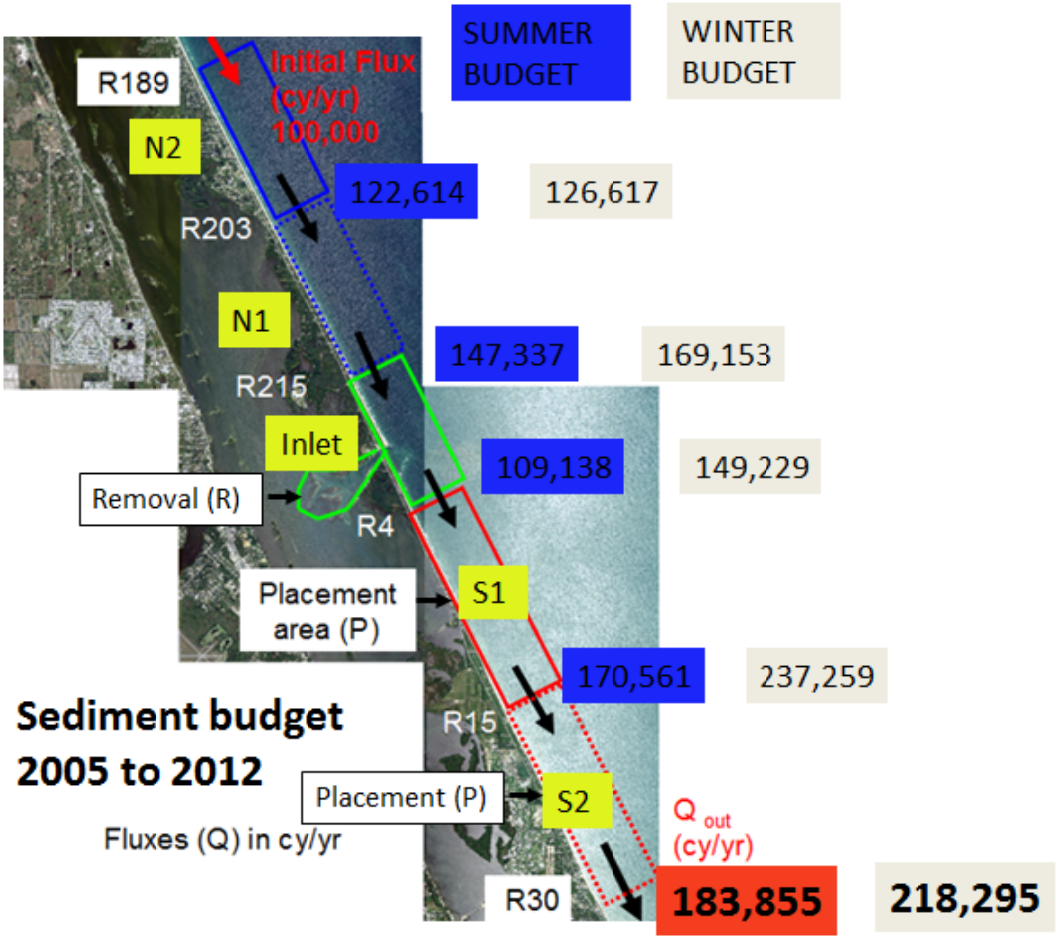

Figure 24 Sand budget calculations from 2005 to 2012 (7-year budget)

.

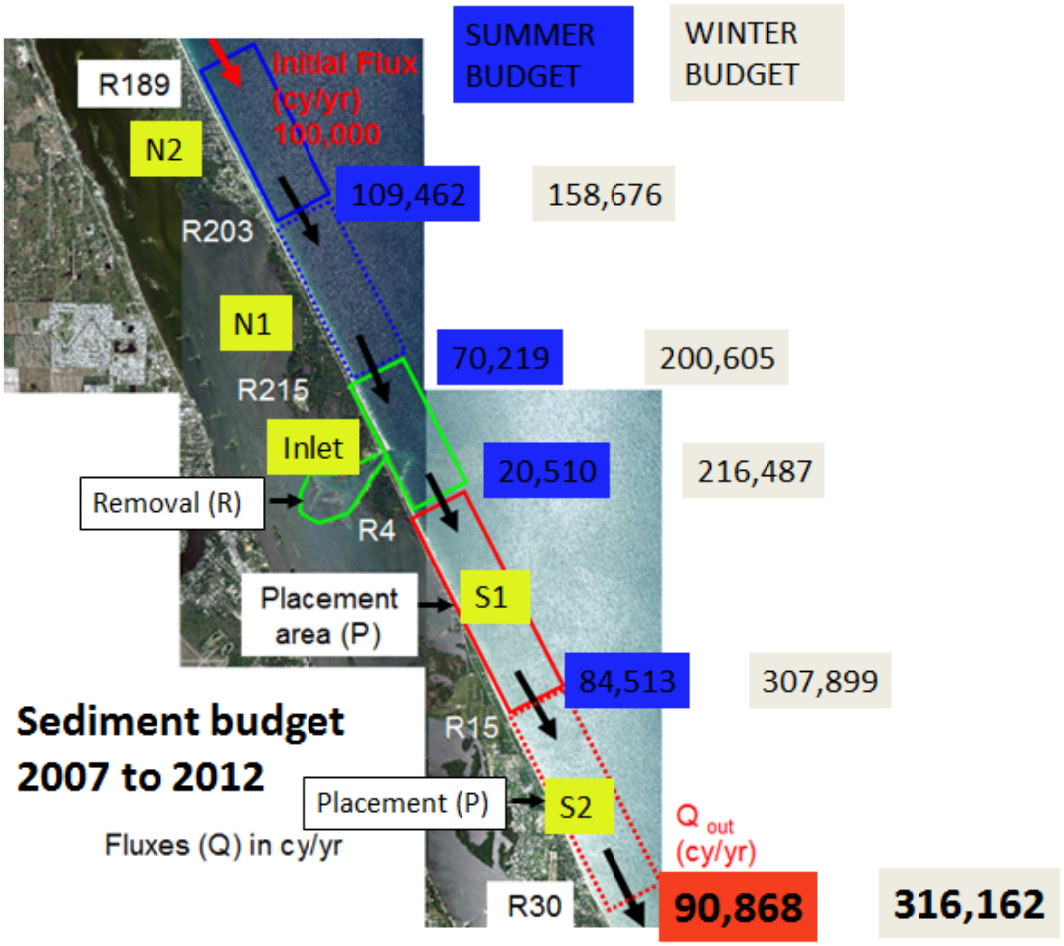

Figure 25. Sand budget calculations from 2007 to 2012 (5-year budget)

Short-term sand budget

The annualized changes and associated fluxes for short-term periods are presented in Table 5 (summer budgets) and Table 6 (winter budgets). The fluxes out of the southernmost cell S2 in the summer calculations ranged from +136,327 cy/yr (4-yr budget) to +425,250 cy/yr (3-yr budget). The flux out of S2 totalized +317,211 cy/yr in the 2-yr budget from summer 2010 to summer 2012. The winter sand budget calculations presented in Table 6 showed less variability as compared to summer calculations. For the 4-year budget from winter 2008 to winter 2012, the flux was +395,725 cy/yr, whereas fluxes reached +440,618 cy/yr and +517,839 cy/yr for the 3-yr and 2-yr sand budgets, respectively.

Table 5.Annualized volume changes per cell and flux for several short-term periods (summer budget

Time period	Summer 2008 to Summer 2012		Summer 2009 to Summer 2012		Summer 2010 to Summer 2012	
Sediment budget cell	Δ V (cy/yr)	Q (cy/yr)	Δ V (cy/yr)	Q (cy/yr)	Δ V (cy/yr)	Q (cy/yr)
North2	-60,292	160,292	9,358	90,642	45,545	54,455
North1	-106,574	266,865	-59,708	150,350	448	54,007
Inlet	5,491	231,375	-24,389	134,740	-51,001	45,007
South1	-10,108	271,483	-39,346	214,086	-67,702	172,710
South2	168,031	136,327	-167,364	425,250	-78,752	317,211

Table 6.Annualized volume changes per cell and flux for several short-term periods (winter budget)

Time period	Winter 2008 to Winter 2012		Winter 2009 to Winter 2012		Winter 2010 to Winter 2012	
Sediment budget cell	Δ V (cy/yr)	Q (cy/yr)	Δ V (cy/yr)	Q (cy/yr)	Δ V (cy/yr)	Q (cy/yr)
North2	-181,960	281,960	-60,270	160,270	1,972	98,028
North1	-191,978	473,938	-69,569	229,839	-33,374	131,403
Inlet	131,405	342,533	-39,912	269,752	-85,894	217,297
South1	-102,002	444,535	-120,372	390,124	-193,528	410,825
South2	60,185	395,725	-35,324	440,618	-84,264	517,839

The N2 cell experienced large variability among the different time periods. Values ranged from -60,292 cy/yd (4-yr budget) to +45,545 cy/yr (2-yr budget). The annualized volume change for the 3-yr budget was +9,358 cy/yr. For the winter calculations (Table 6), annualized volume changes were -181,960 cy/yr (4-yr), -60,270 cy/yr (3-yr), and +1,972 cy/yr (2-yr). For the summer budget calculations Fluxes leaving the N2 cell totalized +160,292 cy/yr (2008-2012),+90,642 cy/yr (2009-2012), and 54,455 cy/yr (2010-2012). For the winter calculations, fluxes were +281,960 cy/yr, 160,270 cy/yr, and +98,028 cy/yr for the same time periods as discussed above. Annualized volume changes for the N1 cell were negative for the 4-yr and 3-yr summer budgets, with values of -106,574 cy/yr and -59,708 cy/yr for the two budget periods. The annualized volume change for the 2-yr period from summer 2010 to summer 2012 was +448 cy/yr. This ΔV value for that time period is opposed to the largely negative value calculated for

the winter budget (-33,374 cy/yr), whereas values for the 3- and 4-yr winter budgets were comparable in magnitude with the summer values (-69,569 cy/yr and -191,978 cy/yr, respectively). Fluxes leaving the N1 cell for the summer budget were much larger in the 4-yr budget (+266,865 cy/yr) than in the 3-yr and 2-yr budgets (+150,350 cy/yr and +54,007 cy/yr, respectively). The winter fluxes out of N1 were also the largest in the 4-yr budget (+473,938 cy/yr). Fluxes decreased to +229,839 cy/yr (3-yr), and +131,403 cy/yr (2-yr). Overall sand transport direction occurred from north to south in the three short term budgets above.

For the inlet cell, annualized volume changes for the summer budget (Table 5) reached +5,491 cy/yr (4-yr), but were negative for both 3-yr and 2-yr periods (-24,389 cy/yr and -51,001 cy/yr, respectively). As shown in Table 5, the annualized volume change for 4-yr budget was increased in the winter calculations (+131,405 cy/yr). Negative changes were observed for the 3-yr and 2-yr periods and totalized -39,912 cy/yr and -85,894 cy/yr for the two periods. Winter fluxes leaving the inlet cell were increased by the sand losses and cumulated to +269,752 (3-yr) and +217,297 cy/yr (2-yr), while fluxes out of the inlet cell for the 4-yr budget was decreased to +342,533 cy/yr. The summer fluxes were reduced for all budget periods and reached +231,375 cy/yr (4-yr), +134,740 cy/yr (3-yr) and +45,007 cy/yr (2-yr).

One of the factors affecting the value of the fluxes in the summer sand budget and particularly the flux reduction of the 2-yr budget was due to the integration of the removal (R) value. As listed in Table 3, the value was the largest for that period (-60,000 cy/yr) whereas it was reduced for the 3-yr and 4-yr budgets (-40,000 cy/yr and -30,000 cy/yr, respectively). Removal values for the winter sand budgets was 0for all three time periods, because the mechanical bypassing project occurred in Spring 2012 and therefore was included only in the summer calculations.

Summer sand budget calculations for the S1 cell (Table 5) indicated overall negative annualized volume changes (ΔV): values were -0,108 cy/yr (2008-2012), -39,346 cy/yr (2009-2012) and -67,702 cy/yr (2010-2012). Fluxes leaving the cell were increased by those volume losses and totalized +271,483 cy/yr, +214,086 cy/yr and +172,710 cy/yr for the 4-yr, 3-yr, and 2-yr budgets. The annualized volume changes for the winter budget (Table 6) were much larger with values of -102,002 cy/yr, -120,372 cy/yr, and -193,528 cy/yr for the same sand budget periods. The large negative values observed in the winter sand budgets significantly increased

the fluxes out of S1 (444,535 cy/yr, 390,124 cy/yr, and 410,825 cy/yr for the 4-yr, 3-yr and 2-yr budgets). One other factor influencing those fluxes was the placement value. Placement values for the summer budgets were fairly large and totalized +30,000 cy/yr between 2008 and 2012, +40,000 cy/yr between 2009 and 2012 and 60,000 cy/yr between 2010 and 2012. Values for the winter budgets were equal to zero since no beach fill occurred in that time period.

Annualized volume changes for S2 showed variability in the summer sand budgets calculations (Table 5). Volume changes were negative for the 2-yr and 3-yr budgets (-78,752 cy/yr and -167,634 cy/yr, respectively), which contrasted with the +168,031 cy/yr for the 4-yr budget. Winter sand budget calculations (Table 6) indicated the same annualized volume change trends, for all budget periods, with values of +60,185 cy/yr (4-yr), -35,324 cy/yr (3-yr), and -84,264 cy/yr (2-yr).

For the summer sand budget, fluxes leaving the S2 cell reached +136,327 cy/yr (4-yr), +425,250 cy/yr (3-yr) and +317,211 cy/yr (2-yr). For the winter budget, fluxes values were comparable (+395,725 cy/yr, +440,618 cy/yr, and +517,839 cy/yr for the 4-yr, 3-yr, and 2-yr periods, respectively). Sand placement values (P) have helped increase the fluxes in the summer budget. Placement values were larger for the summer budget and totalized +32,875 cy/yr (4-yr), +43,800 cy/yr (3-yr), and +65,750 cy/yr (2-yr). Annualized placement volumes were reduced during the winter budget calculations (+11,375 cy/yr, +15,170 cy/yr, and 22,750 cy/yr for the 4-yr, 3-yr, and 2-yr budgets). Sand budget calculations over smaller time scales were more likely to be influenced by seasonal peaks. More variability was observed in the inlet, S1, and S2 cells due to beach fill placement, and complex sand trapping/sedimentation along the reef lines.

7.0 Survey-Based Shoreline Analysis Methods

Analysis of the shoreline position derived from hydrographic surveys was based on digitizing the zero-contour to represent the shoreline. The zero-contour represents the same elevation as the mean water line (MHW) for the NGVD 1929 vertical datum used during the ground surveys. The advantage for using surveys to determine the shoreline position was the improved temporal resolution since hydrographic surveys are typically performed on a seasonal basis at Sebastian Inlet. However, there is a trade-off for spatial resolution because transects were typically spaced 500 ft to 1,000 ft apart. As described in the methods section on analyzing the evolution of inlet reservoirs, generating a survey-based shoreline began with generating contour plots using the ImageAnalyst© extension in Arcview3.2©. Once the XYZ data files from hydrographic surveys were contoured, the extension was also used to highlight the zero-contour so that this one interval could be digitized to represent the position of the shoreline. Once highlighted, the zero-contour was extracted by hand-tracing the contour using shoreline-generating tool in BeachTools© (Hoeke et al. 2001). To determine the change in shoreline position, a common baseline with a NAD27 projection running along the SRA1A was created manually using BeachTools©. This extension was also used to generate perpendicular transects from this baseline to the digitized shoreline every 500 ft, which roughly corresponded to the interval used in the ground surveys. A total of 120 transects were generated including 60 transects north and 60 transects south of the inlet. For detailed methodology on the shoreline change calculations, the reader is referred to previous reports (Zarillo et al., 2007, 2009, 2010).

8.0 Survey-Based Shoreline Analysis Results

The survey-based shoreline section is divided into two subsections of time periods, and includes the most recent surveys (winter and summer 2012). The first section presents the changes over the short-term (seasonal) and the second section focuses on the long-term.

8.1 Survey-based shoreline analysis

The survey-based shoreline section is divided into two subsections of time periods, and includes the most recent surveys (winter and summer 2012). The first section presents the changes over the short-term (seasonal) and the second section focuses on the long-term.

Short term/seasonal changes

Shoreline changes between summer 2011 and winter 2012 are presented in Figure 26. The north section retreated from R190 to R215 (-10 to -75ft) to the exception of several scattered advancement peaks (up to +40 ft) near R192, R201, and R208. The section from R215 to the north jetty at R219 experienced significant advancement ranging from +20 to +110 ft. The south section experienced retreat up to -75ft near the south jetty (R1) and advancement up to +50 ft from R2 to R3 (attachment bar). From R4 to R16, the calculated shoreline changes were minimal and characterized by advancement from R4 to R10 (+10 ft), retreat from R10 to R15 (-20 ft) and advancement near R15-R16 (+20 ft). The magnitude of shoreline changes in the remaining southern part of the domain was much greater: significant retreat (up to -100ft)was observed from R17 to R28, while the shoreline near R29-R30 advanced up to +120 ft.

Shoreline changes between winter 2012 and summer 2012 are presented in Figure 27. The north section advanced from R190 to R204 (+50 to +100 ft). Shoreline retreat occurred from R206 to R208 and from R211 to R214 (-60 ft and -40 ft, respectively). The section near the north jetty at R219 also experienced retreat of -40 ft. Zones of advancement (up to +120 ft) were found near R205 - R206, R208 – R211, and R214 – R216. The south beach section was characterized by a neat signal of the spring 2012 mechanical bypassing project. From R1 to R25, significant shoreline advancement was observed, ranging from +30 to +175 ft and peaking between R12 and R15. The section from R25 to R30 retreated up to -100 ft. As shown in Table 7, the mean overall change rate for the entire south section (R1 to R30) between summer 2010 and summer 2012 was +11.86 ft/yr. according to the EPR method. The mean overall change rate values decreased drastically when calculated over longer time periods (2.07 ft/yr. and 3.17 ft/yr. for the periods from 2002-2012 and 2007-2012, respectively). However, those values remained fairly large compared to the north section which experienced small positive rates for both the 2- and 5-year periods (2.8 ft/yr. and 3.4 ft/yr., respectively). Between 2002 and 2012 (10-yr period), the calculated mean overall change rate became negative (-1.24 ft/yr.).

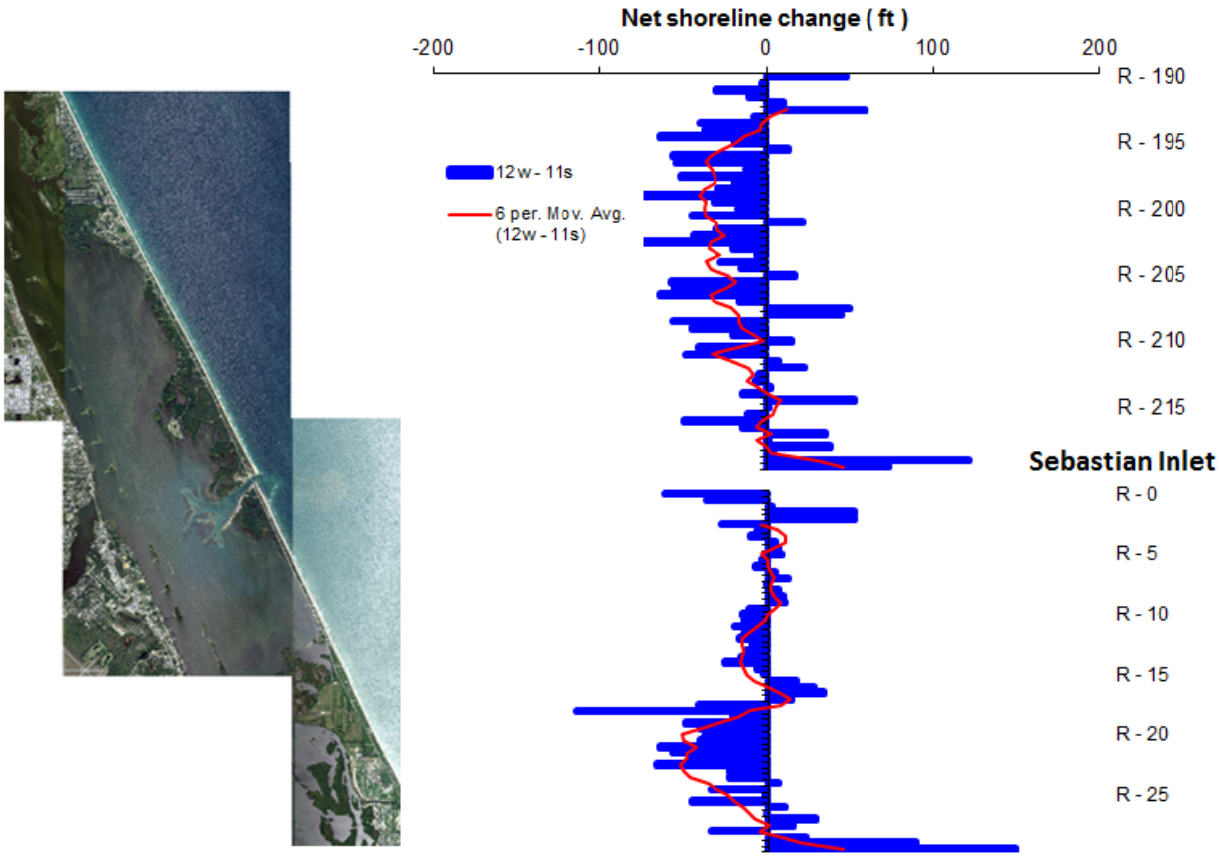

Figure 26. Survey-based shoreline change (ft) from winter 2011 to winter 2012.

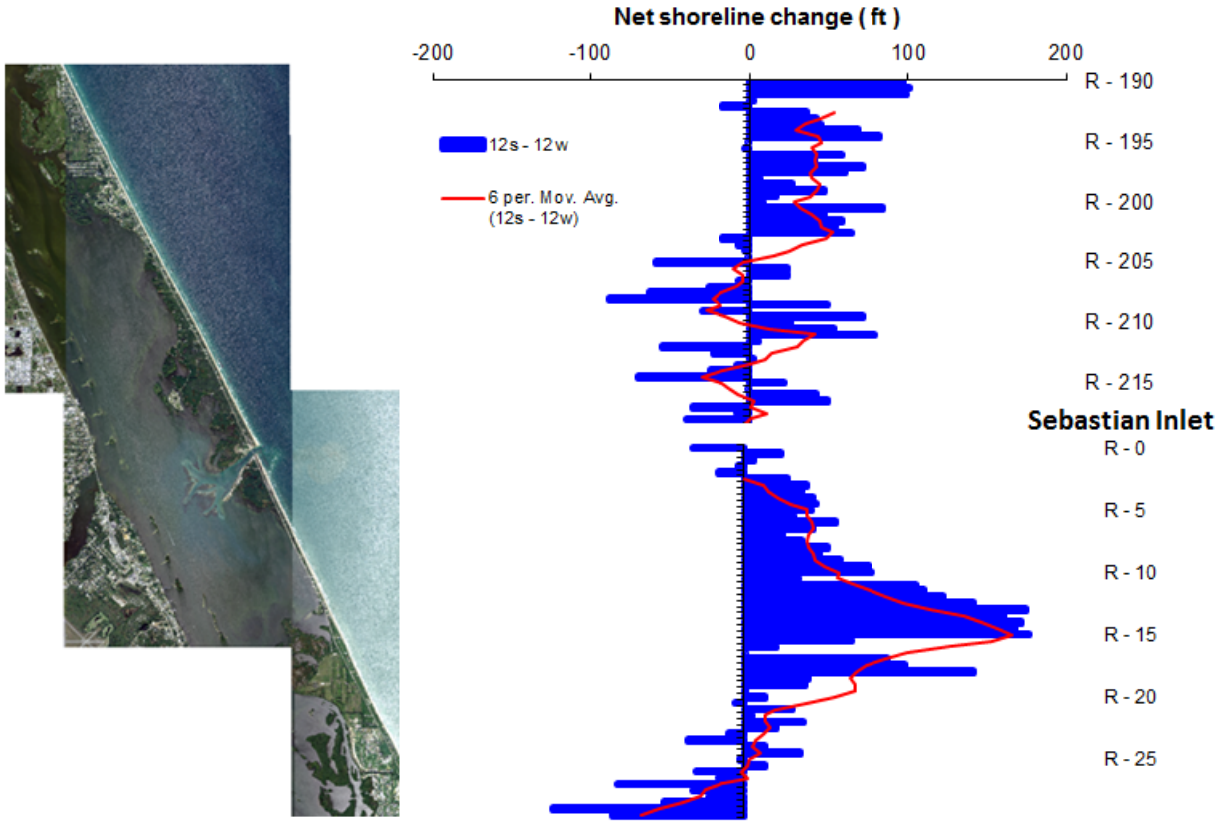

Figure 27. Survey-based shoreline change (ft) from winter 2012 to summer 2012

Table 7.Summary of results (including mean shoreline position) from the EPR and LR methods for survey data sources, North and South domains only extents

			LR		EPR			
Spatial Extent	**Temporal Range**	**Mean Shoreline (ft)**	**Change Rate of Mean Shoreline (ft/yr)**	**Change Rate (ft/yr)**	**Mean Change (ft)**	**Mean Annualized Change (ft/yr)**	**Mean Overall Change (ft)**	**Mean Overall Change Rate (ft/yr)**
North	2002to 2012	357.1287	0.4270	0.4270	-1.3793	-1.6940	-12.4133	-1.2413
	2007 to 2012	359.0588	2.9484	2.9484	4.2469	3.5388	16.9875	3.3975
	2010to 2012	360.1778	2.8323	NAN	5.6647	2.8323	5.6647	2.8323
South	2002to 2012	382.6634	1.2429	1.2429	2.3033	0.9857	20.7295	2.0729
	2007 to 2012	383.8549	4.8248	4.8248	3.9693	1.0046	15.8772	3.1754
	2010to 2012	393.7569	11.8586	NAN	23.7172	11.8586	23.7172	11.8586

Shoreline changes between summer 2011 and summer 2012 (Figure 28) showed similar trends than those observed between winter 2012 and summer 2012. The north section experienced advancement from R190 to R204, along with a succession of advancement/retreat zones (approximately 3,000ftwavelengths) from R205 to R219. The south section is characterized by significant advancement from R2 to R20, which peaked between R14 and R16 (+120 ft). From R20 and beyond, shoreline retreated up to -50 ft. Abnormal retreat occurred near the south jetty at R1 (-100 ft).

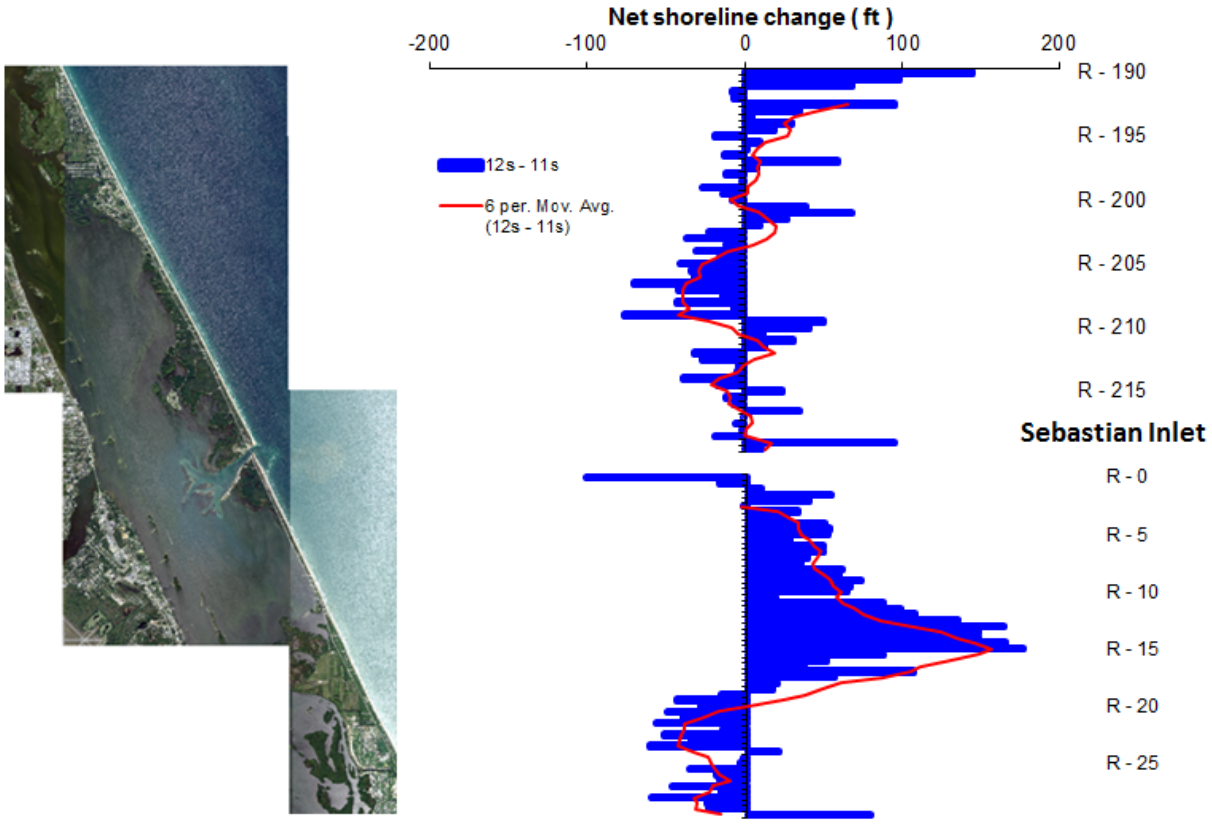

Figure 28. Survey-based shoreline change (ft) from summer 2011 to summer 2012

Long-term shoreline changes

Long-term shoreline change was assessed through a 5-year and 10-year time periods between 2002 and 2012. The time periods were designed to match with aerial images dates so comparisons could be made with image-based shoreline changes. Decadal shoreline change between summer 2002 and summer 2012 is presented in Figure 29. The north section experienced advancement ranging from +20 to +120 ft between R markers R190 and R202. From R203 to R219 the shoreline retreated with values ranging from -25 to -120ft, with the exception of minimal advancement/peaks near R204 and R210-R212 (+20 ft). The most significant retreat (-120 ft) occurred near R208 and R212. The south section experienced advancement (+50 ft) between R1 and R5 (south of the attachment bar) and minimal retreat between R5 and R8 (-5 to -15ft). The following section from R9 to R20 experienced advancement ranging from +20 to +100 ft, followed by retreat (up to -75 ft) between R25 and R30.The long term shoreline change plots illustrated well the effect of the mechanical bypassing projects in maintaining a stable/advancing shoreline in the southern section. Both 5-year and 10-

year plots indicated overall advancement (up to +75 ft) from R1 to R20. Trends indicated a healthy/advancing shoreline, even though the section from R20 to R30 experienced minimal retreat for both time periods. This was verified by the statistics presented in Table 7,which showed mean overall changes reaching 20.7 ft and 15.9 ft for the 5 and 10-yr periods, respectively.

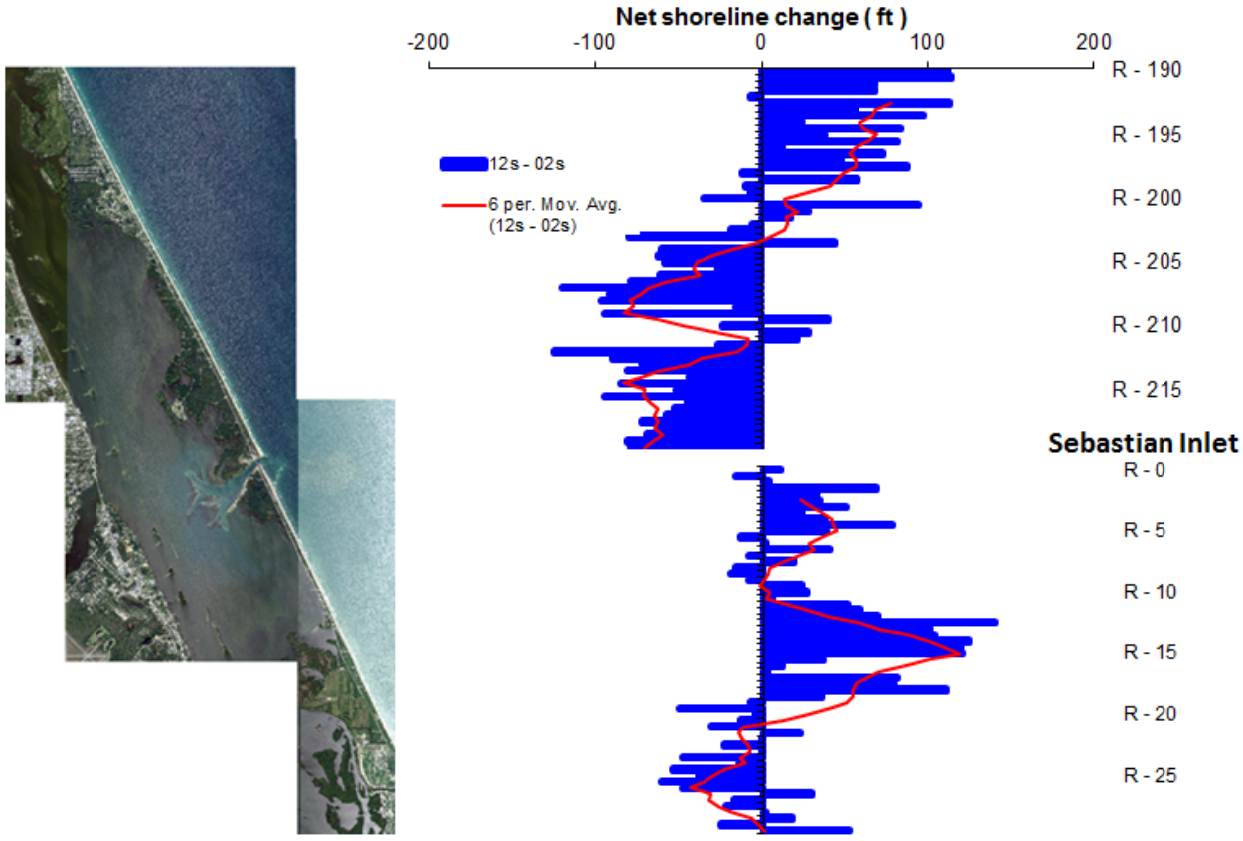

Figure 29. Survey-based shoreline change (ft) from summer 2002 to summer 2012

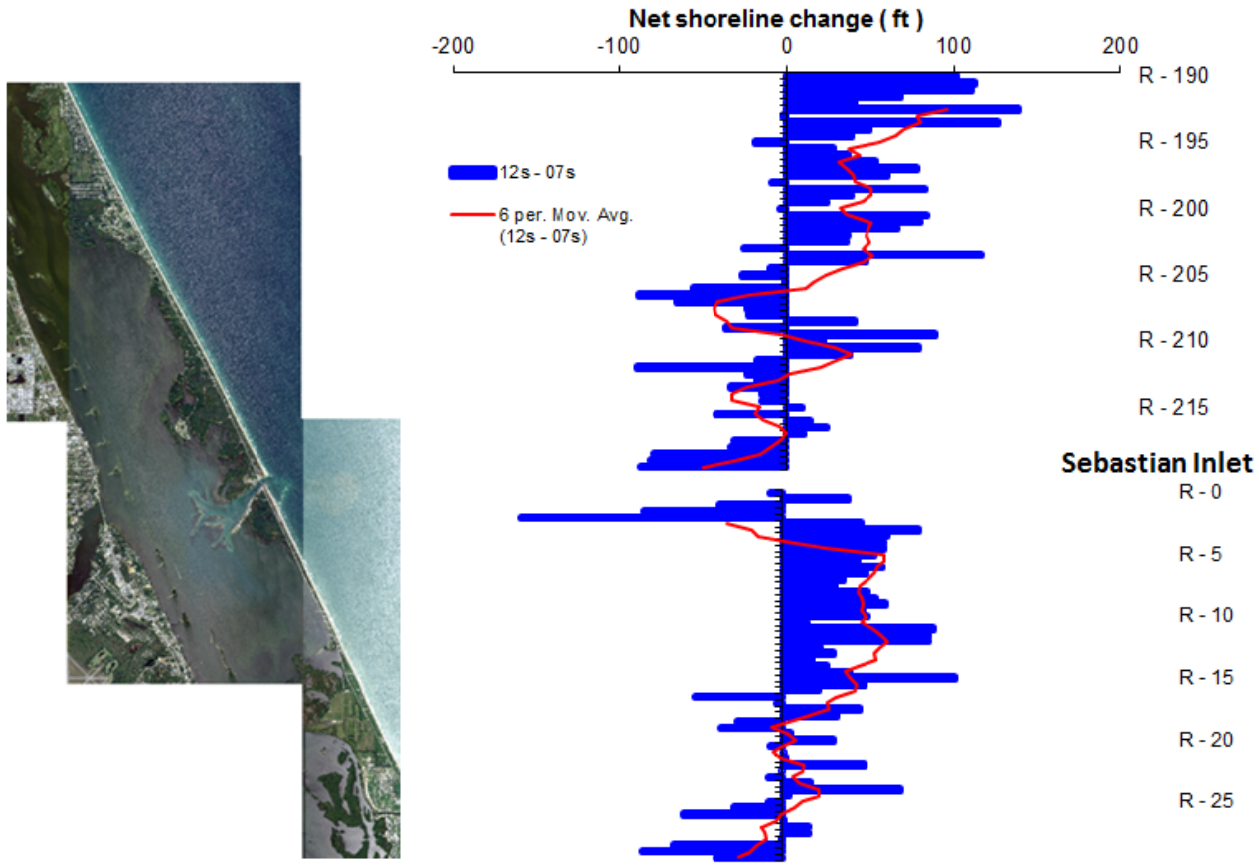

Figure 30. Survey-based shoreline change (ft) from summer 2007 to summer 2012

The comparison between survey-based (summer 2012) and aerial-based (July 2012) shoreline position is presented in Figure 31 and Figure 32 for the north and south sections, respectively. Results indicated similar trends, with the overall image shoreline positioned between +50 ft to +100 ft seaward of the survey (zero contour shoreline). This was consistent with results from previous Sebastian Inlet work (Zarillo et al., 2011). However, spatial variability existed in the trends and reversals occurred both in the north (R190 to R196, and R202) and in the south domains (between R11 and R16, and at R18) with the survey shoreline located seaward of the image shoreline. This suggested the beach-fill signature was more evident in the survey-based shoreline.

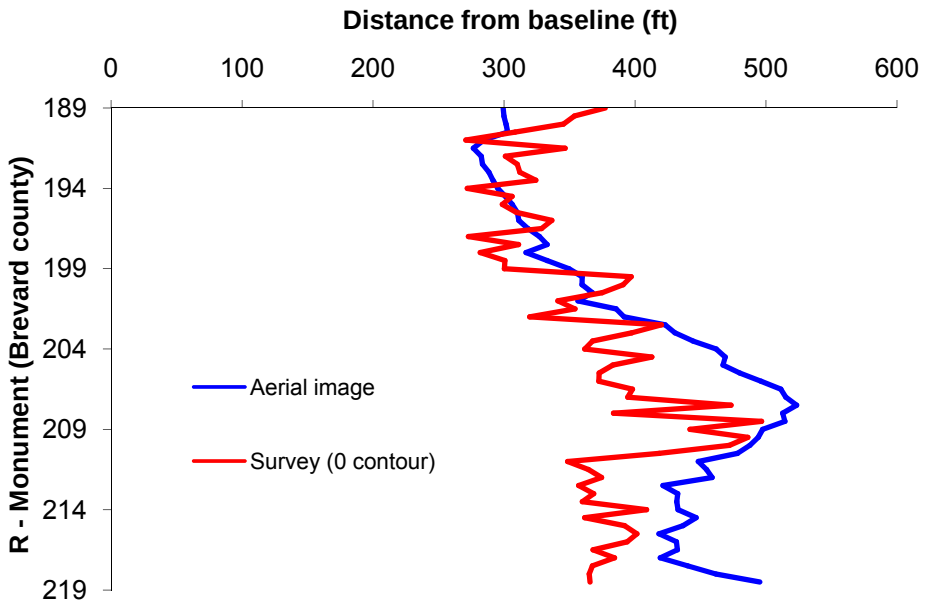

Figure 31. Comparison of aerial vs. survey based shoreline position for summer 2012 (North domain)

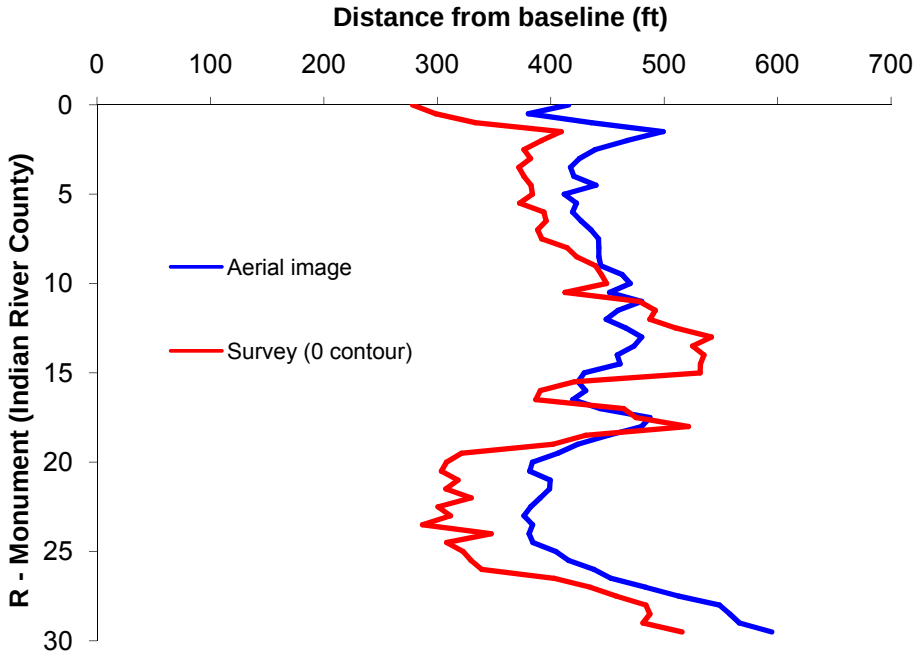

Figure 32. Comparison of aerial vs. survey based shoreline position for summer 2012 (South domain)

It must be stated that single values/peaks of either advancement or retreat (at one transect location) much larger than the nearby data, like those encountered around the north and south jetties, can be attributed to the low spatial resolution of survey data and the extrapolation. Such data have to be interpreted with caution. Net topographic changes can be used to detect any abnormal sedimentation pattern, which may have contributed to such drastic shoreline change.

Additional care must be taken in accounting for the seasonal variability, which is possible through the use of those biannual survey data. The average position of the shorelines for all winter vs. summer surveys (since 2000) is presented for the north and south domains in Figure 33 and Figure 34, respectively. For the north domain, the average summer shoreline position was seaward of the winter shoreline position (up to +20 ft near R196 and R205), which induced a wider beach in summer. However, this pattern was reversed between R210 and R213 and near the north jetty (R217 to R219). This observation can be explained by increased southward littoral transport in winter which fills more sand in the jetty fillet and upper shoreface therefore shifting the zero contour shoreline seaward (nearly +100 ft). Volumetric gains for the jetty reservoirs were documented in the winter surveys (Section3.1).

The same trend (summer shoreline seaward of the winter shoreline) was also observed within the south domain, with a maximum difference reaching approximately +40 ft (between R10 and R15). Such spatial variability could be related to beach-fill projects occurring during the summer surveys of 2003, 2007, 2011 and 2012. Some variability/reversals were also found directly south of the attachment bar system (R3 to R5). These were geomorphic zones dominated by local sand transport, and gains in sediment were documented during the winter months, possibly from increased sand bypassing driven by nor'easters. Related volumetric evolution of the inlet system was discussed in Section 3.1 of this report.

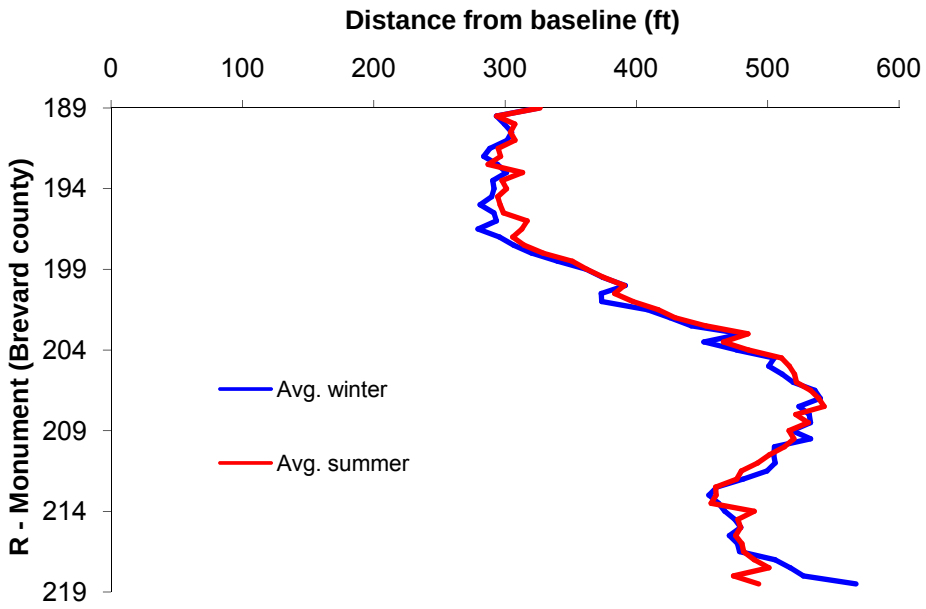

Figure 33. Average survey-based shoreline position (winter vs. summer) for the north domain

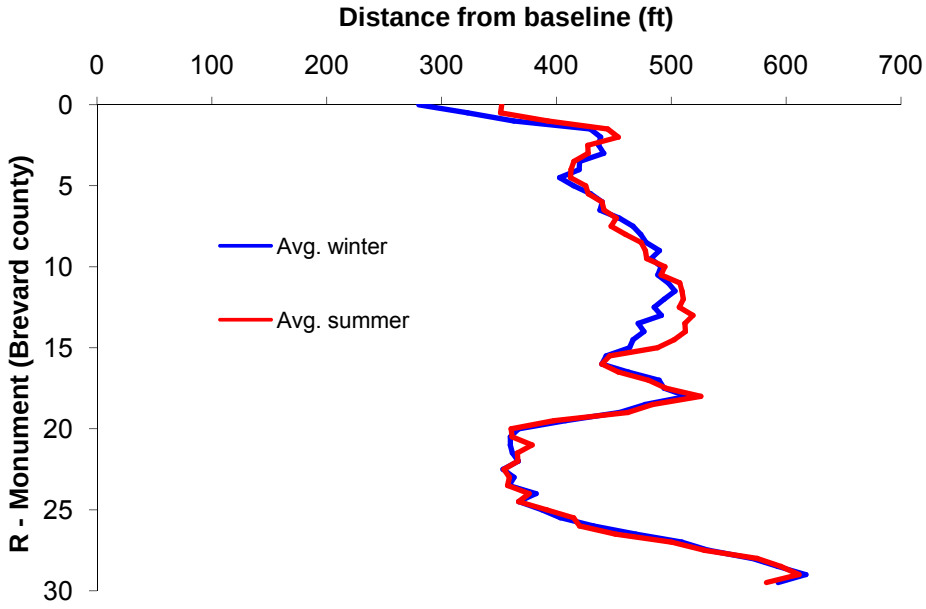

Figure 34. Average survey-based shoreline position (winter vs. summer) for the south domain

Shoreline advancement following the recent mechanical bypassing/beach-fill project was well illustrated by the shoreline changes between winter 2012 and summer 2012 (Figure 27). Survey-based shoreline changes reached +100 ft (near R15) and the plot further suggested that beach-fill sand had remained within the project zone. The comparison of aerial-based vs. survey-based shoreline changes (Figure 32) showed that shoreline advancement was more evident in the survey/zero contour shoreline change calculations and that there was no clear beach-fill signal in the image-based shoreline changes. This was consistent with results from both EPR and LR methods (Table 7) that showed large mean overall changes (ft) and mean overall changes rates (ft/yr.) for the south section over the short and longer terms. The above results (mean overall changes and mean overall change rates) were much smaller for the aerial-based shoreline changes, especially those calculated over the long term (5-yr and 10-yr). According to EPR method, the aerial-based shoreline change rates for the entire south section (R1 to R30) ranged from -2.8 ft (0.26 ft/yr.) to -11.45 ft (-1.85 ft/yr.) for the 10-yr (02-12) and 5-year (07-12) periods, respectively. The trends were verified by the LR method. The summary results Tables were discussed further in the aerial-based shoreline changes section of this report (Section 9).

The shoreline positions of the south beach segment were plotted between summer 2010 and 2012 for both the image-based and survey-based calculations (Figure 35 and Figure 36, respectively). The 2012 survey shoreline (Figure 36) was located seaward than the 2010 shoreline (values ranging from +20 ft between R4 and R16 to +100 ft between R11 and R16) whereas image-based shoreline (Figure 35) overlaid at those locations (no signature of beach-fill). It must be noted that the 2012 image-based shoreline was located +50 ft seaward than the 2010 shoreline between monuments R20 and R30, while the 2010 and 2012 survey-based shorelines overlaid in that zone. Some of the variability could be explained by the differences in spatial resolution between image-based and survey-based shoreline change calculations. Other relevant information to the aerial imagery flight must be considered as well to fully understand the differences observed.

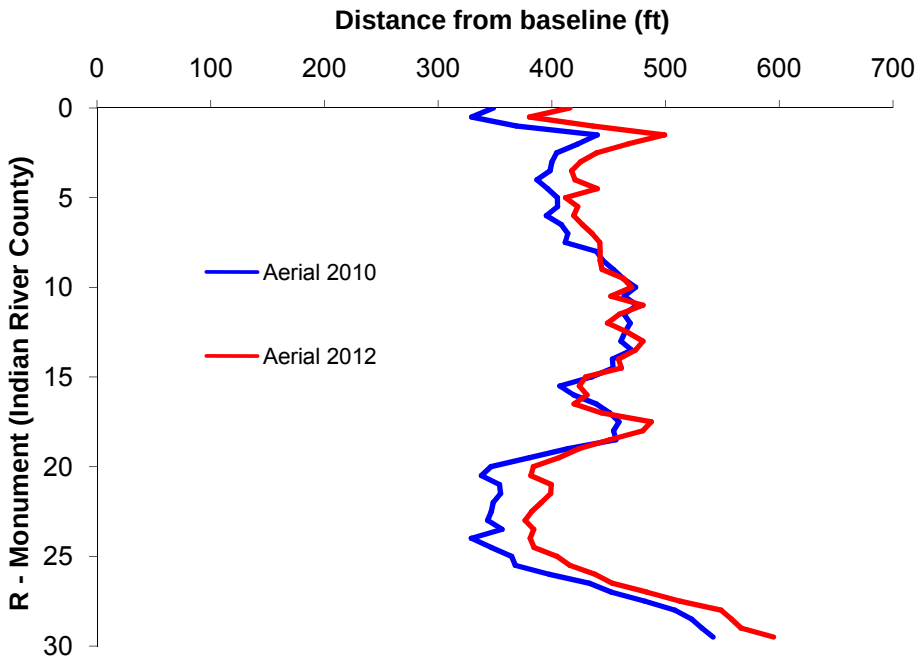

Figure 35. Comparison of image-based shoreline position between 2010 and 2012

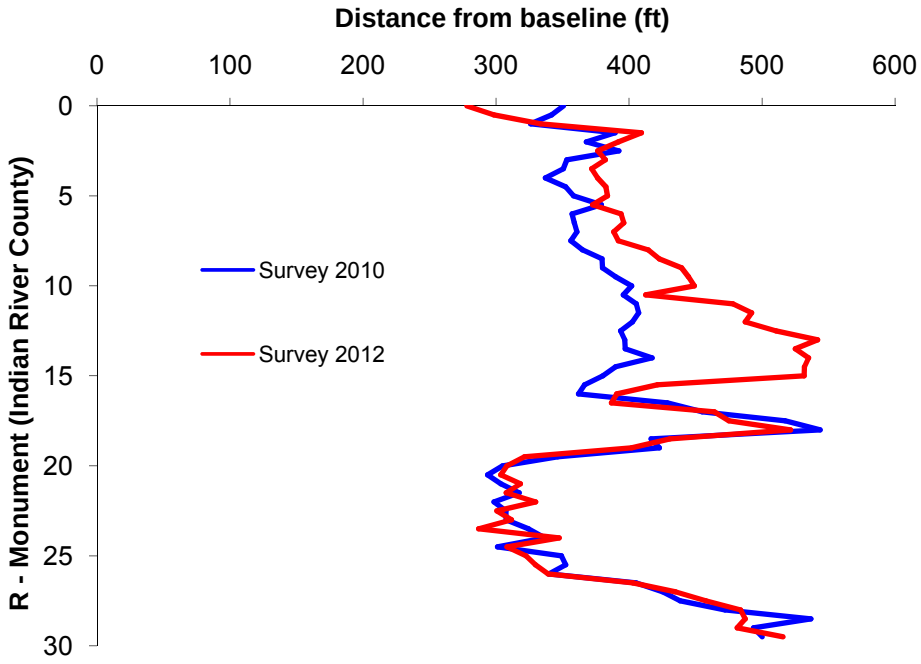

Figure 36. Comparison of survey-based shoreline position between 2010 and 2012

9.0 Analysis of Shoreline Changes from Aerial Imagery

Shoreline positions were digitized from the geo-referenced aerial imagery for a domain covering approximately 7 miles north to 7 miles south of Sebastian Inlet, FL (~75,000 ft, Table 8). Changes to the shoreline position were determined by comparing 30 time series of transects generated every 25 ft along the coast. Tables 8 and 9 indicate the extent of coverage for each of the time series used in the analysis according to the total number of transects and the alongshore distances. Transects were generated using the BeachTools© extension for ArcView3.2© from a standardized baseline (~SR A1A) to the wet/dry line (low-tide terrace). The change in shoreline position was determined by subtracting the distances along each transect between time-series of interest. Shoreline change rates were calculated using both the End Point Rate (EPR) and Linear Regression (LR) methods (Crowell et al., 1993; Morton et al., 2002). For details on the methodology the reader is referred to the previous report. In this version of the report, long-term changes and rates of change have been updated for the time spans of 1958-2012 (historical) and the short-term analysis covered the years 2002-2012 (recent). An additional short-term analysis section has been included to account for the changes occurring since the previous report, spanning from 2007-2012 (recent), as well as those changes occurring during the 2011-2012 (update) time span.

Table 8. Domain of shoreline analysis from aerial imagery

Domains	Transect ID	R Marker	Miles
North	0-1480	180.5-219	7.0
South	1508-2974	0-37.5	6.9
N3	0-880	160.5-203	4.2
N2	880-1364	203-216	2.3
N1	1364-1480	216-219	0.6
Inlet	**1365-1645**	**BC216-IRC4**	**1.3**
S1	1508-1627	0-3.5	0.6
S2	1627-212-	3.5-16	2.3
S3	2120-2974	16-37.5	4.0

Table 9.Summary of transect coverage.

Year	Extent of Coverage					North					South				
	#	Distance		Transects		#	Distance		Transects		#	Distance		Transects	
	Transects	feet	miles	start	end	Transects	feet	miles	start	end	Transects	feet	miles	start	end
1943	2442	61050	11.6	531	2972	950	23750	4.5	531	1480	1465	36625	6.9	1508	2972
1958	2300	57500	10.9	0	2299	1481	37025	7.0	0	1480	792	19800	3.8	1508	2299
1968	1853	46325	8.8	1118	2970	363	9075	1.7	1118	1480	1463	36575	6.9	1508	2970
1970	405	10125	1.9	1369	1773	112	2800	0.5	1369	1480	266	6650	1.3	1508	1773
1972	1349	33725	6.4	501	1895	934	*23350	4.4	501	*1480	388	9700	1.8	1508	1895
1974	2144	53600	10.2	831	2974	650	16250	3.1	831	1480	1467	36675	6.9	1508	2974
1978	2038	50950	9.6	935	2972	546	13650	2.6	935	1480	1465	36625	6.9	1508	2972
1980	1943	48575	9.2	1	1943	1480	37000	7.0	1	1480	436	10900	2.1	1508	1943
1981	2011	50275	9.5	964	2974	517	12925	2.4	964	1480	1467	36675	6.9	1508	2974
1983	1621	40525	7.7	25	1645	1456	36400	6.9	25	1480	138	3450	0.7	1508	1645
1984	1818	45450	8.6	1153	2970	328	8200	1.6	1153	1480	1463	36575	6.9	1508	2970
1986	1251	31275	5.9	536	1786	945	23625	4.5	536	1480	279	6975	1.3	1508	1786
1988	1777	44425	8.4	1124	2971	357	8925	1.7	1124	1480	1393	*34825	6.6	1508	*2971
1989	1757	43925	8.3	199	1955	1282	32050	6.1	199	1480	448	11200	2.1	1508	1955
1992	1989	49725	9.4	958	2946	523	13075	2.5	958	1480	1439	35975	6.8	1508	2946
1993	1891	47275	9.0	91	1981	1390	34750	6.6	91	1480	474	11850	2.2	1508	1981
1995	2975	74375	14.1	0	2974	1481	37025	7.0	0	1480	1467	36675	6.9	1508	2974
1996	1070	26750	5.1	1305	2374	176	4400	0.8	1305	1480	867	21675	4.1	1508	2374
1997	987	24675	4.7	1315	2301	166	4150	0.8	1315	1480	794	19850	3.8	1508	2301
1998	943	23575	4.5	1405	2347	76	1900	0.4	1405	1480	840	21000	4.0	1508	2347
1999	963	24075	4.6	1382	2344	99	2475	0.5	1382	1480	837	20925	4.0	1508	2344
2002	2973	74325	14.1	2	2974	1479	36975	7.0	2	1480	1467	36675	6.9	1508	2974
2004	2965	74125	14.0	10	2974	1471	36775	7.0	10	1480	1467	36675	6.9	1508	2974
2006	2972	74300	14.1	3	2974	1478	36950	7.0	3	1480	1467	36675	6.9	1508	2974
2007	2678	66950	12.7	176	2853	1305	32625	6.2	176	1480	1346	33650	6.4	1508	2853
2008	2693	67325	12.8	159	2851	1323	33075	6.3	159	1480	1345	33625	6.3	1508	2851
2009	2678	66950	12.7	153	2846	1329	32225	6.3	153	1480	1339	33475	6.4	1508	2846
2010	2678	66950	12.7	153	2846	1329	32225	6.3	153	1480	1339	33475	6.4	1508	2846
2011	2678	66950	12.7	153	2846	1329	32225	6.3	153	1480	1339	33475	6.4	1508	2846
2012	2678	66950	12.7	153	2846	1329	32225	6.3	153	1480	1339	33475	6.4	1508	2846

* 1972: gap in North: 1150 ft, id 808-853

* 1988: gap in South: 1800 ft, id 2034-2104

9.1 Results

The results presented and discussed in this section on image-based shoreline change will focus on the linear regression method. However results obtained through the use of the end-point-rate (EPR) method are also included (Table 10) despite its use being subject to several disadvantages. For example, if either shoreline is uncharacteristic, the resulting rate of change will be misleading; also data between the endpoints that is ignored may produce rates that do not capture important trends or changes in trends, especially as temporal variation increases (Dolan et al. 1991). The reader is referred to the earlier version of the report for more information on both (the linear regression and end-point-rate) of method used.

Table 10.Average rate of change for EPR and LR methods (ft/yr).

Extent		Method	('58-'12)	('02-'12)	('07-'12)	('11-'12)
N-S		EPR	-0.0007	-1.8912	-2.8689	-27.2979
		LR	0.3873	-1.5284	-1.9504	-24.7109
Brevard Co.	N	EPR	0.2369	-4.0746	-3.9170	-34.4579
		LR	0.7222	-2.8468	-2.1257	-30.8516
Indian River Co.	S	EPR	-0.3985	0.2710	-1.8475	-20.2074
		LR	0.0481	-0.1932	-1.7680	-18.4442
Brevard Co.	R180.5 – 203 (N3)	EPR	-0.0036	-3.4679	-2.0464	-32.2756
		LR	0.5229	-2.5106	-0.7663	-26.5972
	R203 – 216 (N2)	EPR	0.5819	-4.1870	-4.5081	-35.3301
		LR	0.9450	-2.8149	-2.8430	-35.3301
	R216 – 219 (N1)	EPR	0.2969	-7.3828	-12.7374	-44.4601
		LR	1.2973	-5.5028	-9.4028	-44.4601
Indian River Co.	R1 – 3.5 (S1)	EPR	1.6803	5.1090	3.9419	3.3079
		LR	2.9650	5.2442	0.7178	3.3079
	R3.5 – R16 (S2)	EPR	-0.7603	-0.5871	-5.3092	-22.0538
		LR	0.7994	-1.0740	-5.5464	-22.0538
	R16 – 37.5 (S3)	EPR	-0.7868	0.0617	-0.4633	-22.8584
		LR	-0.7913	-0.4411	0.0561	-19.4363
Inlet		EPR	0.9699	-0.5494	-4.1180	-19.8336
		LR	2.1914	0.3099	-4.0646	-20.1510

In general, both methods yielded similar results with most of the values in the same order of magnitude and with either a positive or negative trend in concordance with each other. The remainder of this section will provide more details on the results obtained for each of the periods updated.

Historical Period (1958-2012)

As compared to 1958, the distance from the baseline to the wet/dry line has advanced by as much as +74 ft along transects immediately north of the inlet and close to +90 ft just south of the south jetty (Figure 37) according to the results obtained with the EPR method. This method also indicates that the average change in shoreline position from 1958 to 2012 is -0.04 ft of retreat at an average rate of -0.0007 ft/yr (Table 10). Despite the indication by the end-point-rate (EPR) method of shoreline retreat along most of the study extent from 1958 to 2012, the linear regression (LR) method indicates that the long-term trend is toward accretion (Figure 38). Close to seventy percent of the 14 miles of the study area is accreting at an average rate of +0.39 ft/yr, while only twenty-eight percent (28%) of the region shows erosion patterns (Figure 38, Table 11).

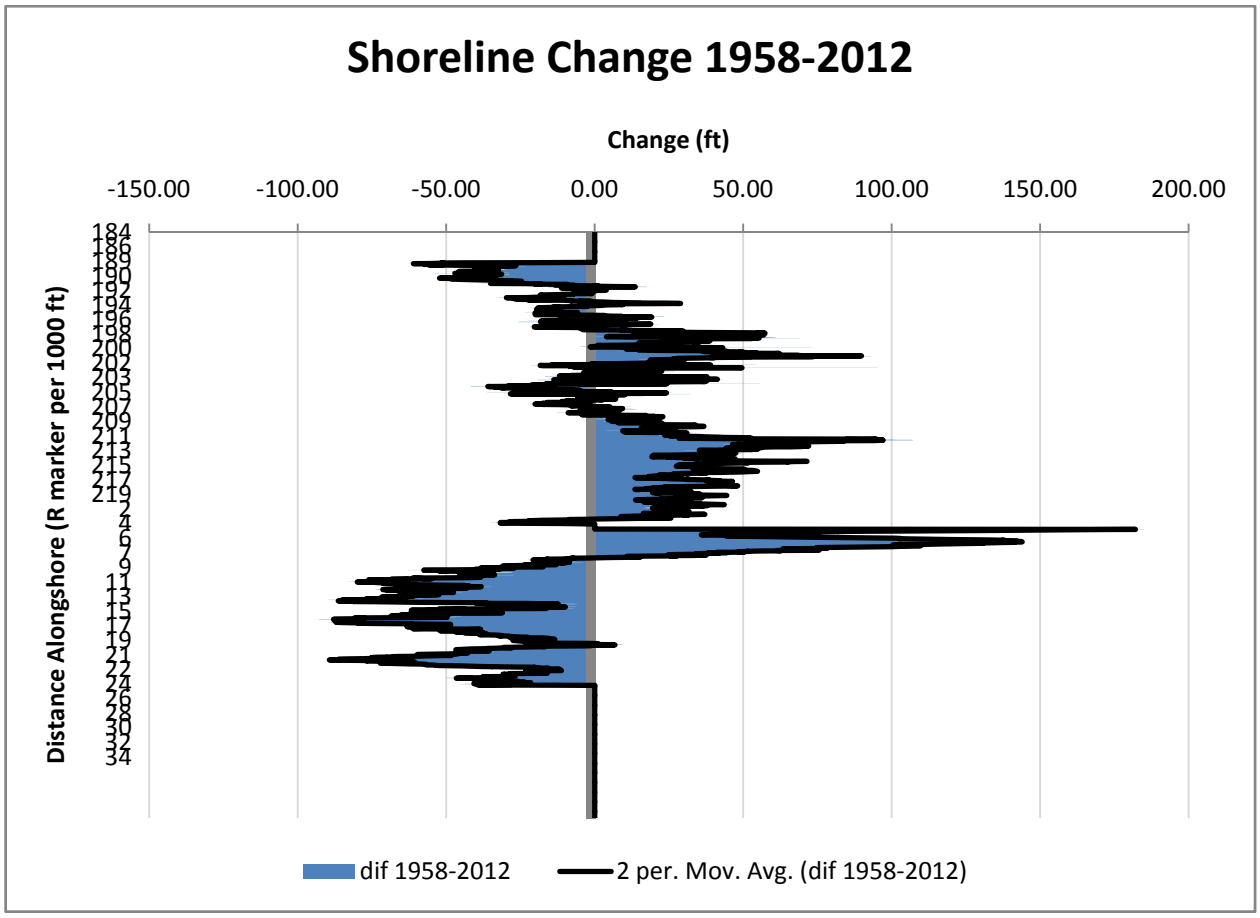

Figure 37.Change (ft) shoreline positions, 1958-2012.

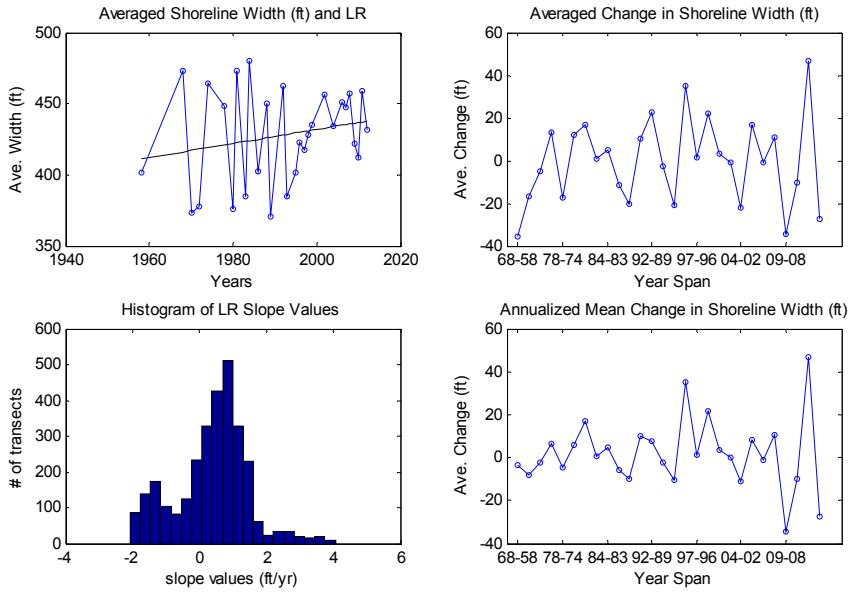

Figure 38. Average shoreline position with LR (top) and histogram indicating number of transects and slope value (bottom for the entire domain and for inlet domain (right), 1958-2012.

Table 11.Summary of short-term changes for the recent period (1958-2012)

Extent	Range (ft/yr)	Average LR (ft/yr)	Erosion %	Accretion %
North to South	-2.07 to +4.06	+0.3871	28.40	70.69
North	-0.86 to +2.16	+0.7222	15.67	84.33
South	--2.07 to +4.06	+0.0481	41.79	58.21
N3	-0.86 to +2.16	+0.5229	26.33	73.67
N2	+0.13 to +1.84	+0.9450	0	100
N1	+0.86 to +1.58	+1.2973	0	100
Inlet	0 to +4.06	+2.1914	0	90.39
S1	+2.21 to +4.06	+2.9650	0	100
S2	+0.03 to +2.56	+0.7994	0	100
S3	-2.07 to +0.95	-0.7913	71.70	28.30

The greatest area of accretion occurs just south of the inlet between the jetty and the attachment bar (S1) from R2 to R4 with a maximum of +4.06 ft/yr at an average of +2.97 ft/yr. In contrast, the region from R16 to R 37 (S3) is predominantly erosional with an average rate of change of -0.79 ft/yr including the maximum erosion rate of -2.07 ft/yr for the entire domain of the study area (near R-26). The northern sub-domain is also predominantly accreting with only smaller regions in N3 showing erosional trends near R-185 and R-200 in Brevard County.
The left side of Figure 3 highlights the percentage of erosion vs. accretion for the entire domain during this fifty-four year period, whereas the right side of Figure 39 is a plot of all the shoreline positions used in the study.

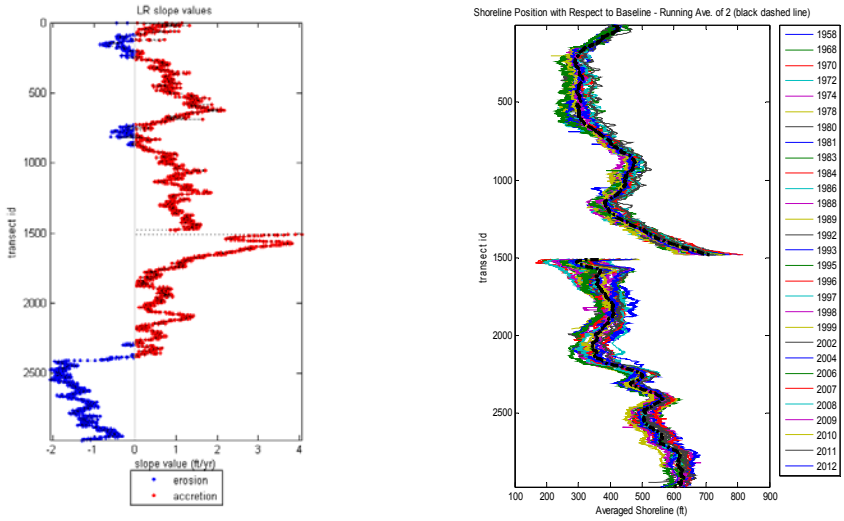

Figure 39. Percent erosion and accretion (left) and shoreline position (right), 1958-2012

Recent Period (2002-2012)

The trend obtained by analyzing nine time series of data representing the last eleven years of shoreline change indicates the beaches along the 14 mile domain are predominantly eroding (Figures 40, 41, and 42). In this case both methods (EPR and LR) are in agreement that the majority of the study area is experiencing erosion. Approximately seventy-three percent (73%, Table 12) of the entire area from north to south is erosional with an average rate of change of -1.53 ft/yr. The area immediate to the south jetty down to R-4 seems to have advanced the shoreline position to about +51.09 ft, while the entire north extent has receded to an average of -40.75 ft at -4.07 ft/yr (Figure 40). A closer inspection to each sub-domains indicate all sub-cells are erosional but two (S1 and Inlet, Figure 5). The region immediately south of the inlet from R2-R5 (sub-cell S1) is the only area in which accretion is occurring 100% with a rate of change of +5.24 ft/yr.

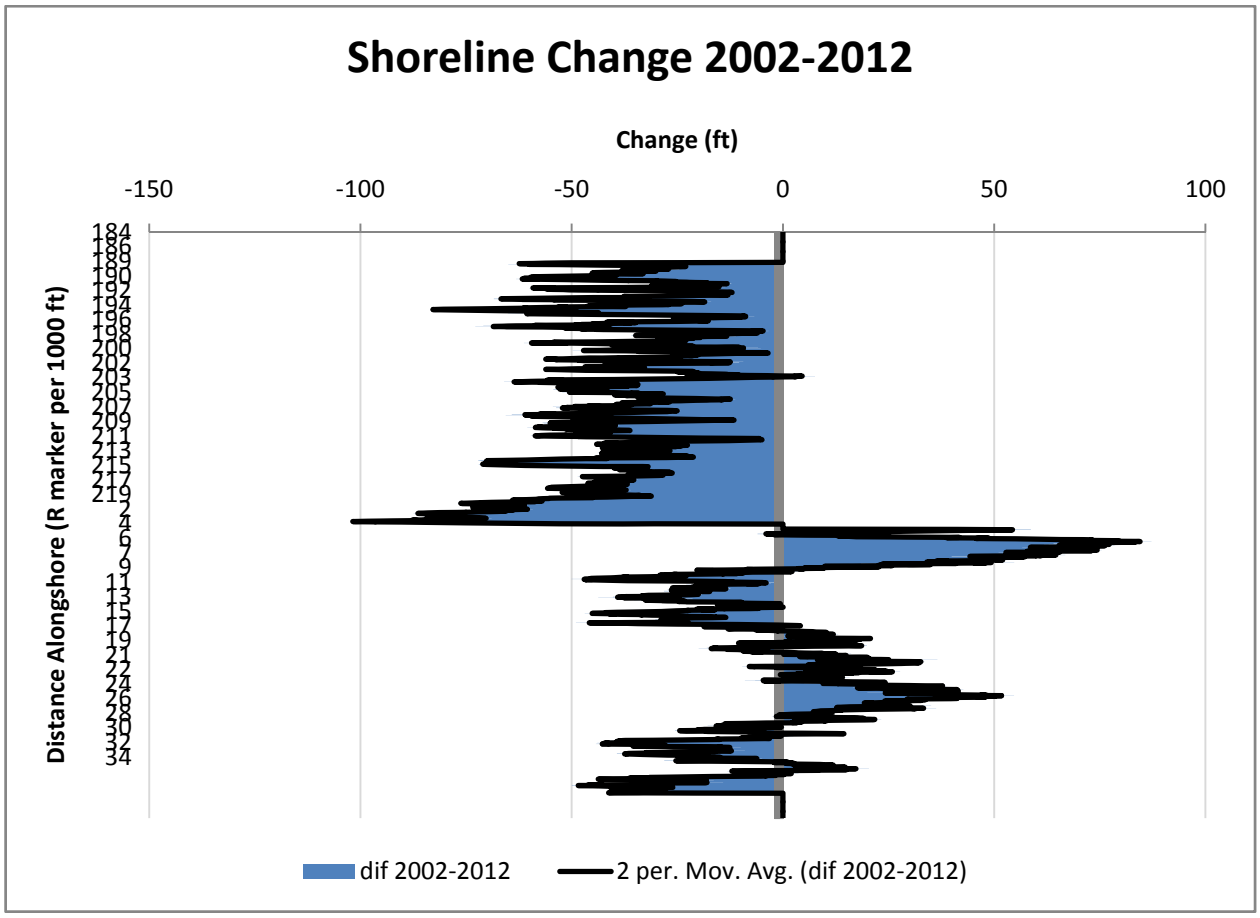

Figure 40. Change in shoreline position from2002-2012

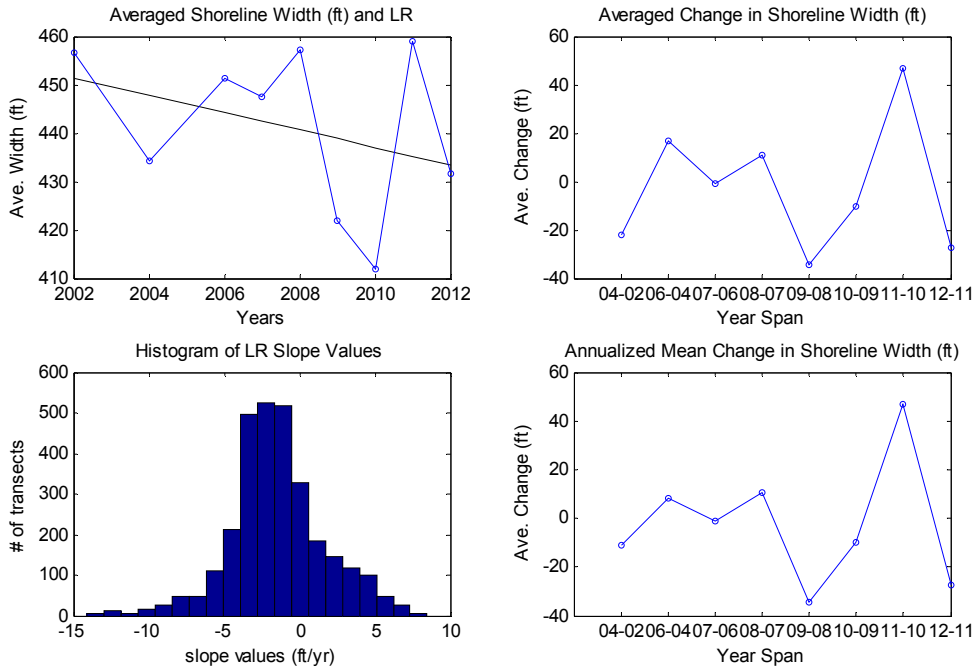

Figure 41. average shoreline position with LR (top) and histogram indication number of transects and slope value(bottom)for entire (left) domain and for the inlet domain (right), 2002-2012

Table 12.Summary of short-term changes for the recent period (2002-2012)

Extent	Range (ft/yr)	Average LR (ft/yr)	Erosion %	Accretion %
North to South	-14.09 to +8.49	-1.5284	73.21	25.82
North	-14.09 to +8.49	-2.8468	95.68	4.19
South	-12.64 to +7.76	-0.1932	51.87	48.13
N3	-14.09 to +8.49	-2.5106	94.21	5.56
N2	-5.83 to +0.84	-2.8149	97.32	2.68
N1	-8.78 to -3.92	-5.5028	100	0
Inlet	-8.78 to +7.76	+0.3099	41.28	49.11
S1	+2.81 to +7.76	+5.2442	0	100
S2	-4.48 to +5.41	-1.0740	75.71	24.29
S3	-12.64 to +6.22	-0.4411	45.38	54.62

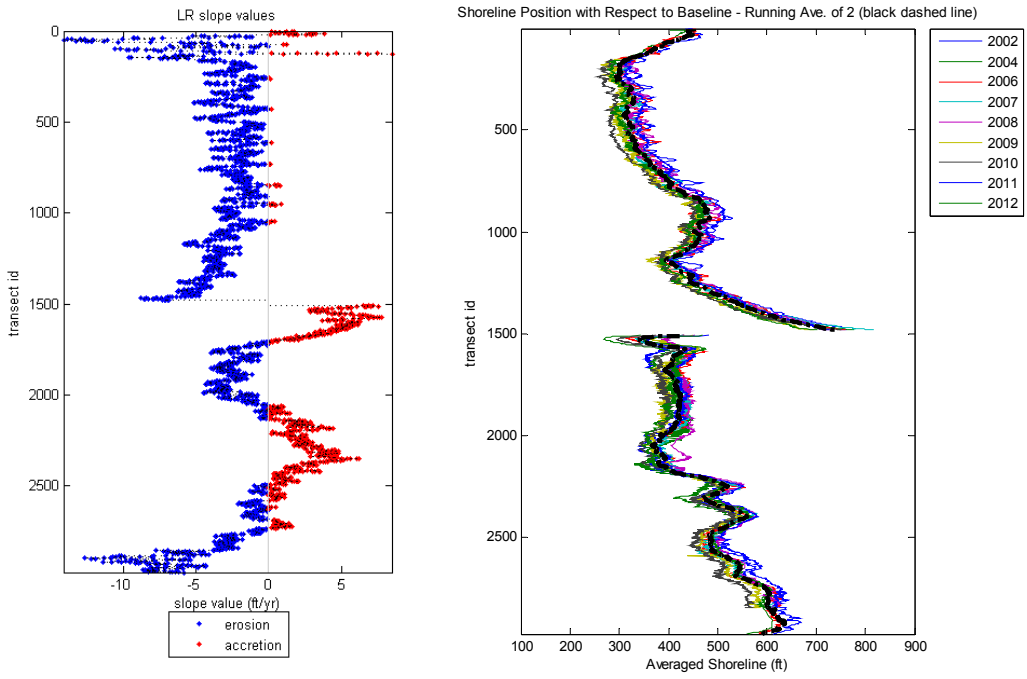

Figure 42. Percent erosion and accretion (left) and shoreline position (right) for 2002-2012.

Latest Update (2007-2012)

Analysis of the more recent shoreline changes from 2007 to 2012 indicate the overall region under study has an average shoreline retreat of -14.34ft (Figures 43, 44 and 45) at a rate of -11.32 ft/yr according to the EPR method (Table 13), and at a rate of -1.95 ft/yr with the LR method. The erosion trend is encountered throughout the majority of the 14 mile extent except for slight accretion in sub-cells S1 and S3.

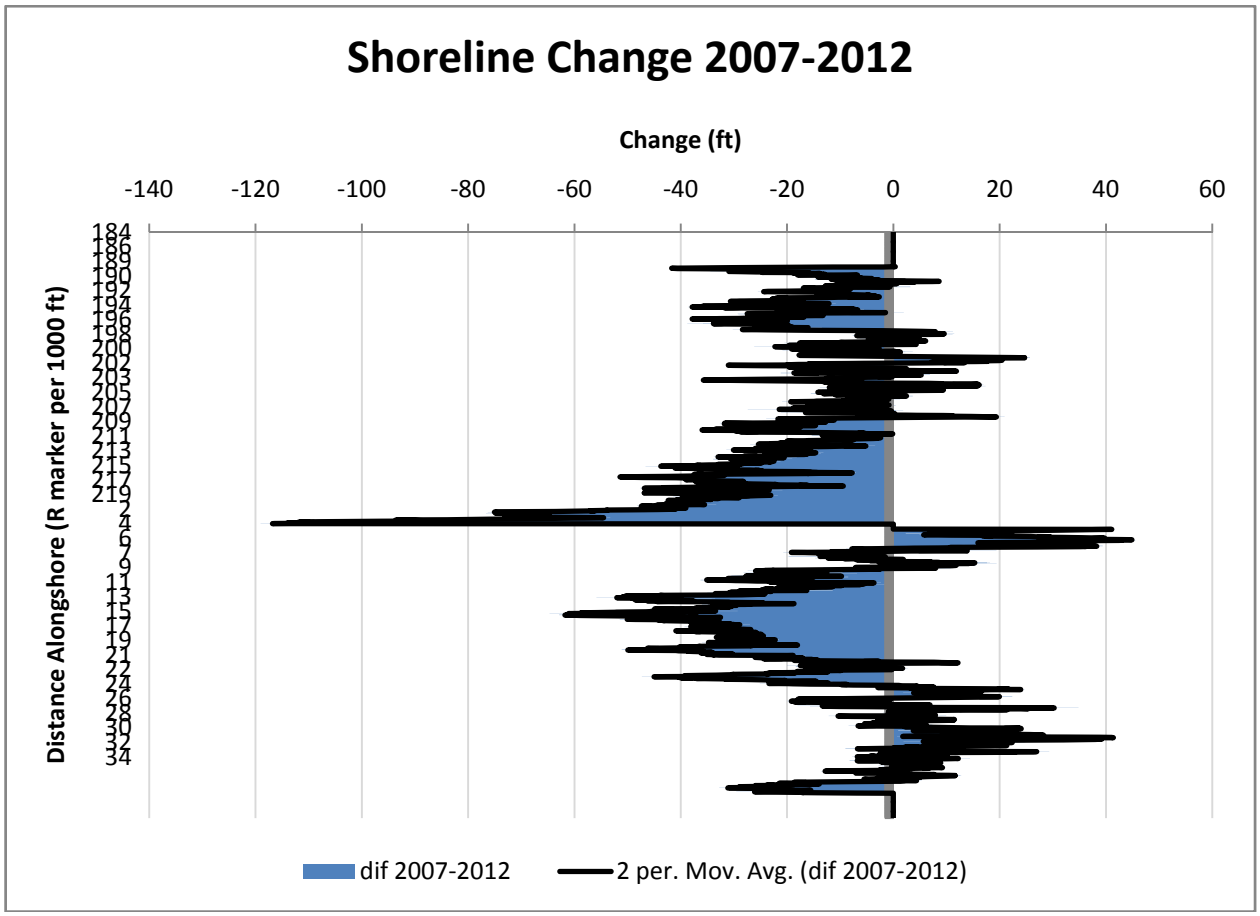

Figure 43. Change (ft) in shoreline position, 2007-2012

The percentages of the areas showing an erosion trend range from 56% at N3 up to 100% erosion in sub-cell N1. The percentages of areas showing accretion trends range from 47.7% up to 58.3% accretion in sub-cells S1 and S3.

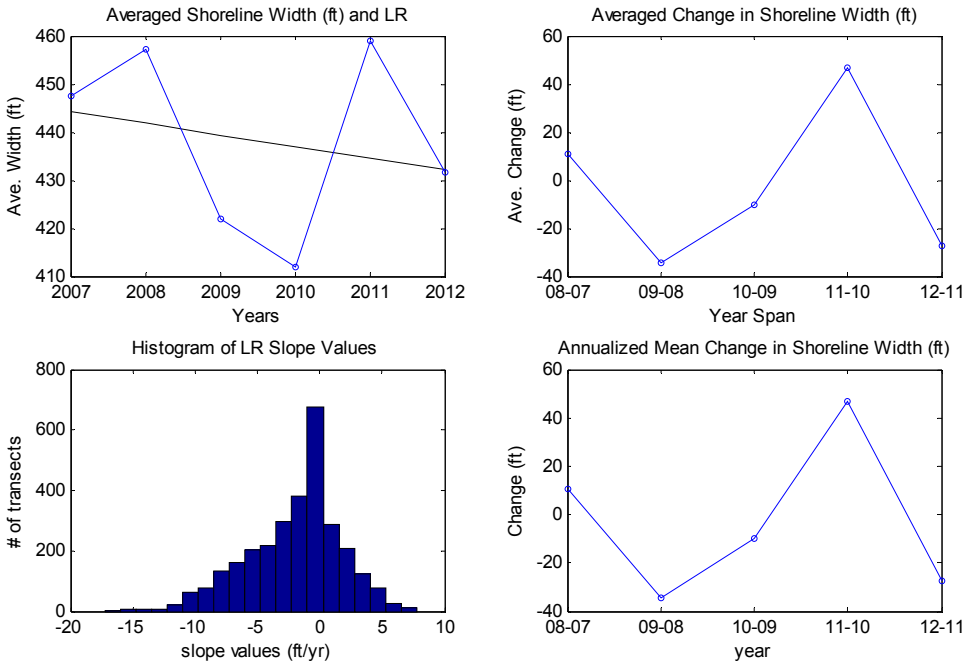

Figure 44. Average shoreline position with LR trend (top) and histogram indicating number of transects and slope value (bottom) for entire domain (left) and for the inlet domain (right), 2007-2012.

Table 13.Summary of short-term changes for the recent period (2007-2012)

Extent	Range (ft/yr)	Average LR (ft/yr)	Erosion %	Accretion %
North to South	-17.27 to +7.79	-1.9504	62.42	27.46
North	-17.27 to +7.79	-2.1257	69.21	20.46
South	-11.30 to +7.59	-1.7680	56.71	35.04
N3	-17.27 to +7.79	-0.7663	55.96	26.67
N2	-8.40 to +4.60	-2.8430	85.77	14.23
N1	-15.79 to -5.29	-9.4028	100	0
Inlet	-15.79 to +6.23	-4.0646	64.41	25.98
S1	-5.07 to +6.23	+0.7178	41.67	58.33
S2	-11.30 to +3.80	-5.5464	92.71	7.29
S3	-11.24 to +7.59	+0.0561	38.13	47.72

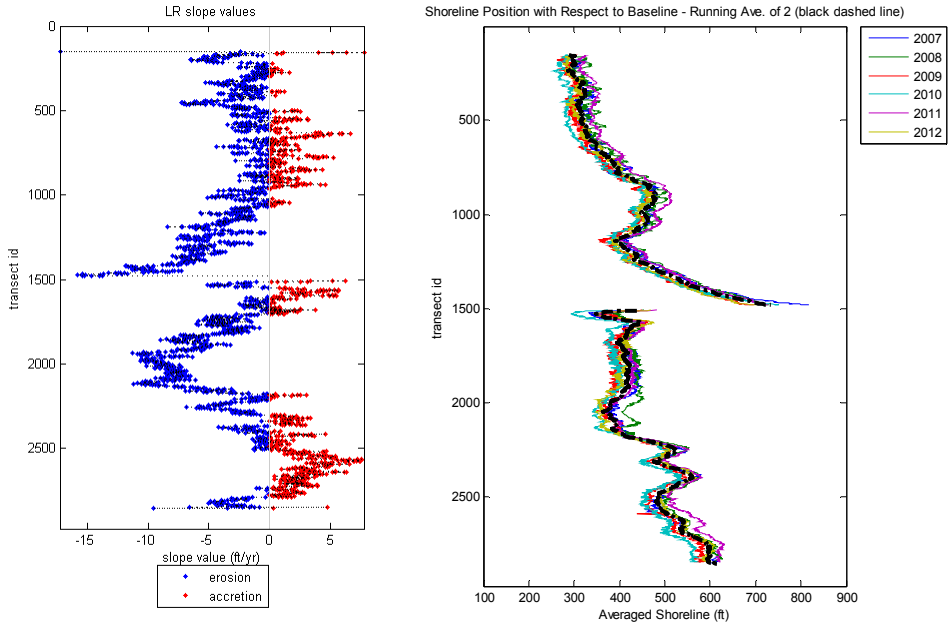

Figure 45. Percent erosion and accretion (left) and shoreline position (right) for 2007-2012.

Latest Update (2011-2012)

Analysis of the most recent shoreline changes from 2011 to 2012 indicate the overall region under study has an average shoreline retreat of -27.3 ft (Figures 46 ,47 and 48) at a rate of -27.3 ft/yr according to the EPR method (Table 14), and at a rate of -24.71 ft/yr with the LR method. The erosion trend is encountered throughout the vast majority of the 14 mile extent, except in the S1 sub-cell domain.

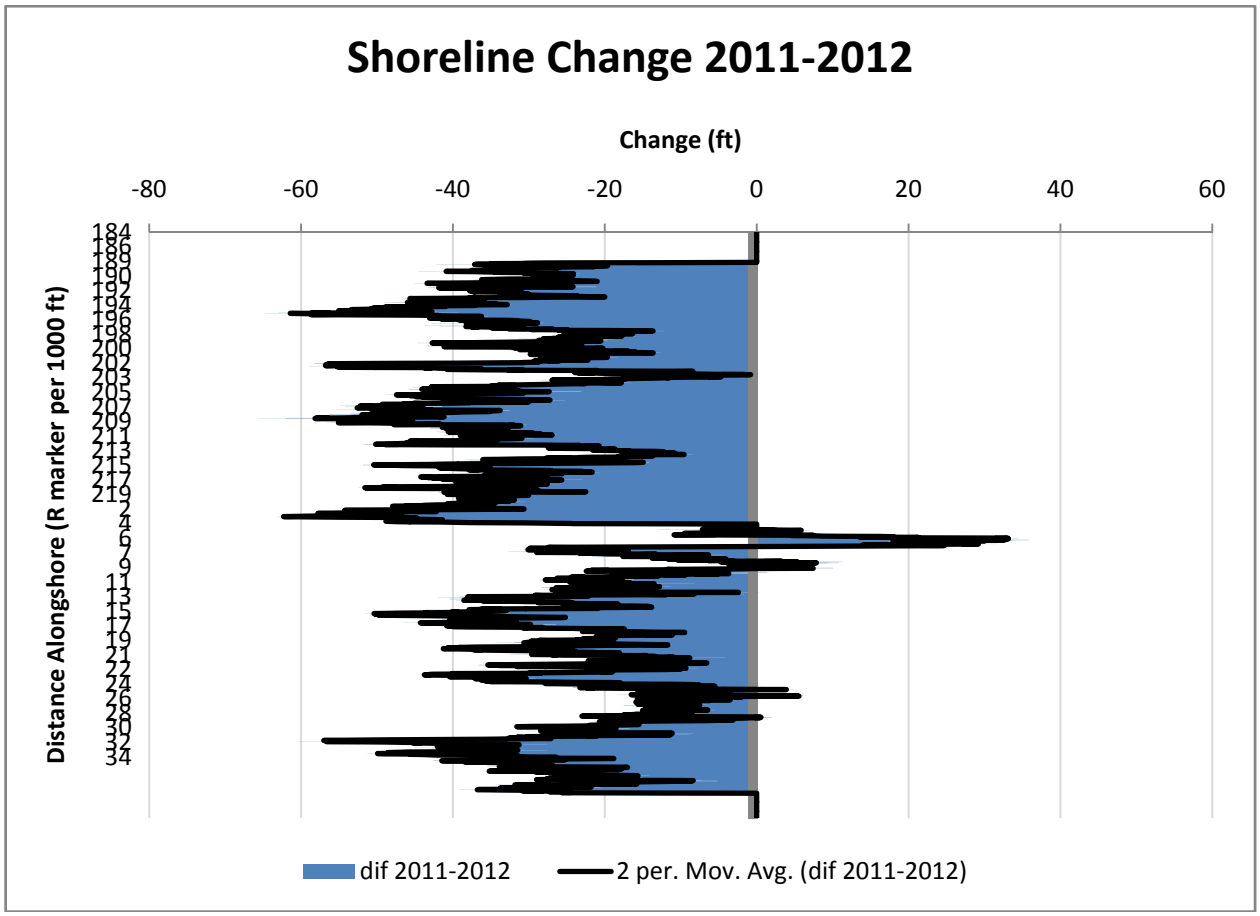

Figure 46. Change (ft) in shoreline position from 2011-2012.

The percentages of the areas showing erosion trend range from 65.8% at Inlet up to 100% erosion in sub-cells N1 and N2. The only sub-cell domain showing accretion was S1 showing accretion at 57.5%.

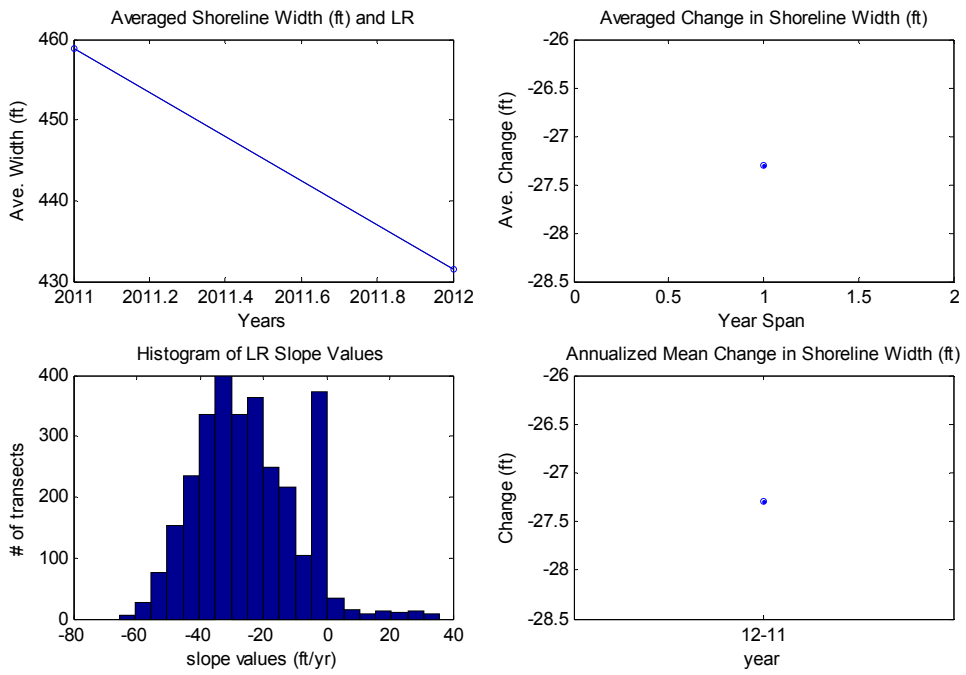

Figure 47. Average shoreline position with LR trend (top) and histogram indication number of transects and slope value (bottom) for the entire domain (left) and for the inlet domain (right), 2011-2012

Table 14. Summary of short-term changes for the recent period (2011-2012)

Extent	Range (ft/yr)	Average LR (ft/yr)	Erosion %	Accretion %
North to South	-65.58 to +35.89	-24.7109	86.12	3.46
North	-65.58 to 0	-30.8516	89.53	0
South	-60.30 to +35.89	-18.4442	84.25	7.02
N3	-64.72 to 0	-26.5972	82.41	0
N2	-65.58 to -8.45	-35.3301	100	0
N1	-63.01 to -22.89	-44.4601	100	0
Inlet	-63.01 to +35.89	-20.1510	65.84	24.56
S1	-32.73 to +35.89	+3.3079	42.50	57.50
S2	-51.68 to +11.30	-22.0538	94.94	5.06
S3	-60.30 to +6.07	-19.4363	83.98	1.05

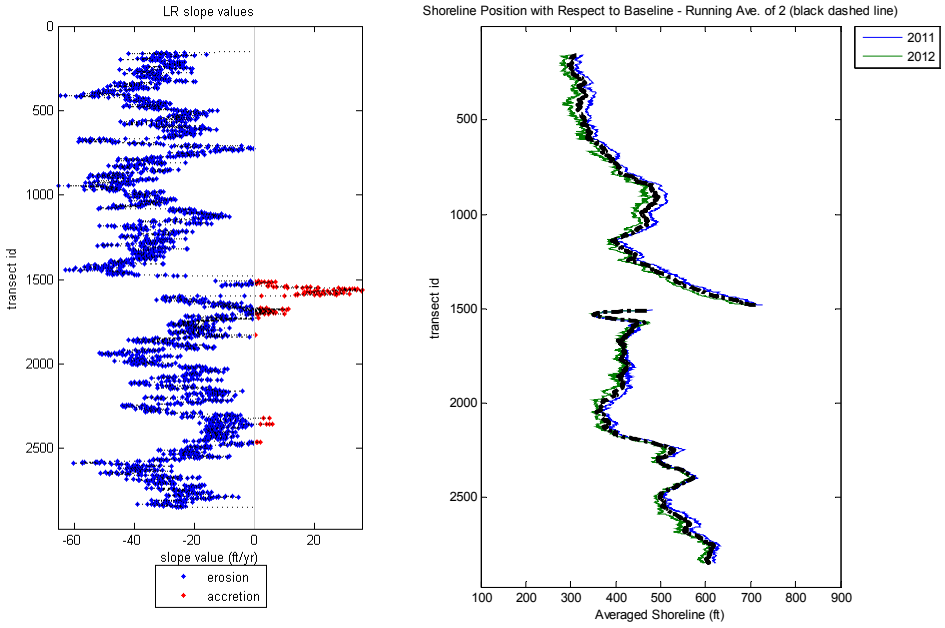

Figure 48. Percent erosion and accretion (left) and shoreline position (right) for 2011-2012.

Tables 15, 16 and 17 provide a summary the aerial image based shoreline changes by time period, major section and by subsections or cells. From these Tables the reader can select longer or shorter time periods to review total changes and rates of change. Annualized changes can be viewed according to both end point (EP) calculation and a linear regression calculation (LR).The overall pattern of shoreline change is similar to that of the sand budget analysis. Over longer time periods the rates of change are smaller. The smaller changes in terms of rates are in the 2002 to 2012 and 2007 to 2012 periods, whereas the largest changes, larger shoreline retreat are observed in the 2011-2012 period. Within the longest period examined, 1959-2012 the rates are moderate and generally positive on the north side of the inlet and negative on the south side of the inlet. Rates and averages can be examined within the shoreline subsections in Tables 16 and 17.

Table 15. Summary of results (including mean shoreline position) from the EPR and LR methods for aerial data sources. North to South, North and South only extents

			LR		EPR			
Spatial Extent	**Temporal Range**	**Mean Shoreline (ft)**	**Change Rate of Mean Shoreline (ft/yr)**	**Change Rate (ft/yr)**	**Mean Change (ft)**	**Mean Annualized Change (ft/yr)**	**Mean Overall Change (ft)**	**Mean Overall Change Rate (ft/yr)**
North to South	1958 to 2012	427.6472	0.3873	0.3871	-0.3101	1.7380	-0.0386	-0.0007
	2002 to 2012	441.2195	-1.5284	-1.5343	-2.5887	-2.2487	-18.9124	-1.8912
	2007 to 2012	438.1471	-1.9504	-2.1415	-2.8806	-2.8806	-14.3447	-11.3154
	2011 to 2012	445.1862	-24.7109	NaN	-27.2979	-27.2979	-27.2979	-27.2979
North	1958 to 2012	459.8163	0.7222	0.7230	1.3072	1.0883	12.7918	0.2369
	2002 to 2012	413.5048	-2.8468	-2.8718	-5.0581	-3.8133	-40.7464	-4.0746
	2007 to 2012	410.2347	-2.1257	-2.3594	-3.9235	-3.9235	-19.5850	-3.9170
	2011 to 2012	417.1612	-30.8516	NaN	-34.4579	-34.4579	-34.4579	-34.4579
INLET	1958 to 2012	467.5451	2.1914	2.1569	2.0027	3.0499	52.3739	0.9699
	2002 to 2012	503.7367	0.3099	0.3050	-0.6868	-1.3548	-5.4941	-0.5494
	2007 to 2012	506.0053	-4.0646	-4.0006	-4.1180	-4.1180	-20.5900	-4.1180
	2011 to 2012	508.1817	-20.1510	NaN	-19.8336	-19.8336	-19.8336	-19.8336
South	1958 to 2012	419.8608	0.0481	0.0481	-0.1605	1.5364	-21.5199	-0.3985
	2002 to 2012	468.7355	-0.1932	-0.1932	-0.1284	-0.6957	2.7096	0.2710
	2007 to 2012	465.6797	-1.7680	-1.9258	-1.8597	-1.8597	-9.2373	-1.8475
	2011 to 2012	472.9392	-18.4442	NaN	-20.2074	-20.2074	-20.2074	-20.2074

Table 16. Summary of results (including mean shoreline position) from the EPR and LR methods for aerial data sources. Sub-cells north extents.

			LR		EPR			
Spatial Extent	**Temporal Range**	**Mean Shoreline (ft)**	**Change Rate of Mean Shoreline (ft/yr)**	**Change Rate (ft/yr)**	**Mean Change (ft)**	**Mean Annualized Change (ft/yr)**	**Mean Overall Change (ft)**	**Mean Overall Change Rate (ft/yr)**
N3	1958 to 2012	346.3603	0.5229	0.5240	-9.6243	-5.7123	-0.1941	-0.0036
	2002 to 2012	351.4301	-2.5106	-2.5490	-4.3542	-3.3023	-34.6793	-3.4679
	2007 to 2012	345.5925	-0.7663	-0.9028	-2.0844	-2.0844	-10.2322	-2.0464
	2011 to 2012	355.8881	-26.5972	NaN	-32.2756	-32.2756	-32.2756	-32.2756
N2	1958 to 2012	449.6023	0.9450	0.9450	0.5953	0.8516	31.4241	0.5819
	2002 to 2012	459.6109	-2.8149	-2.8149	-5.2338	-3.7338	-41.8701	-4.1870
	2007 to 2012	455.2373	-2.8430	-2.8430	-4.5081	-4.5081	-22.5403	-4.5081
	2011 to 2012	461.4271	-35.3301	NaN	-35.3301	-35.3301	-35.3301	-35.3301
N1	1958 to 2012	619.2711	1.2973	1.2973	0.6950	0.7763	16.0310	0.2969
	2002 to 2012	632.2286	-5.5028	-5.5028	-9.2285	-7.5968	-73.8277	-7.3828
	2007 to 2012	624.4564	-9.4028	-9.4028	-12.7374	-12.7374	-63.6869	-12.7374
	2011 to 2012	615.5906	-44.4601	NaN	-44.4601	-44.4601	-44.4601	-44.4601
		(A04)	(A08)	(A11)	(A05)	(A06)	(A09)	(A10)

Table17. Summary of results (including mean shoreline position) from the EPR and LR methods for aerial data sources. Sub-cells south extents.

			LR		EPR			
Spatial Extent	**Temporal Range**	**Mean Shoreline (ft)**	**Change Rate of Mean Shoreline (ft/yr)**	**Change Rate (ft/yr)**	**Mean Change (ft)**	**Mean Annualized Change (ft/yr)**	**Mean Overall Change (ft)**	**Mean Overall Change Rate (ft/yr)**
S1	1958 to 2012	339.7601	2.9650	2.9650	3.2406	4.8955	90.7379	1.6803
	2002 to 2012	393.4435	5.2442	5.2442	6.3863	4.1303	51.0900	5.1090
	2007 to 2012	404.5420	0.7178	0.7178	3.9419	3.9419	19.7093	3.9419
	2011 to 2012	415.9201	3.3079	NaN	3.3079	3.3079	3.3079	3.3079
S2	1958 to 2012	373.0068	0.7994	0.7994	-1.8880	0.0745	-41.0575	-0.7603
	2002 to 2012	404.8166	-1.0740	-1.0740	-0.7339	-2.2176	-5.8711	-0.5871
	2007 to 2012	403.5202	-5.5464	-5.5464	-5.3029	-5.3092	-26.5459	-5.3092
	2011 to 2012	402.2106	-22.0538	NaN	-22.0538	-22.0538	-22.0538	-22.0538
S3	1958 to 2012	511.3955	-0.7913	-0.7913	-2.2197	2.7910	-42.4880	-0.7868
	2002 to 2012	521.1892	-0.4411	-0.4411	-0.5170	-0.3254	0.6169	0.0617
	2007 to 2012	517.7105	0.0561	0.0866	-0.4833	-0.4833	-2.3163	-0.4633
	2011 to 2012	530.2223	-19.4363	NaN	-22.8584	-22.8584	-22.8584	-22.8584
		(A04)	(A08)	(A11)	(A05)	(A06)	(A09)	(A10)

10.0 Quantifying Sediment Texture to Improve Beach Fill Performance

Results of this task provide an improved method for predicting the performance of sand by-pass and beach fill projects contracted by the Sebastian Inlet District. To date topographic surveys combined with model simulations have been used to optimize fill placement in the areas between Indian River County monuments R4 and R20 on the south side of Sebastian Inlet. However, material placed on the beach in this area may be excavated from several local sand sources having a range of textural properties. Sand excavated from the sand trap is in the fine to very fine textural range, whereas material derived from offshore and upland sources may have broader textural distributions that include gravel and coarse sand sizes. The cross-shore equilibrium position of each grain size class depends on how a particular sediment size responds to wave and current forces. Generally, fine sand sizes are stable on the upper beach and berm areas, whereas coarser sands are more stable in the surfzone. Seaward of the surf zone sediment size decreases. Complicating factors include tidal range and storms, which shift the locations and energy level of shoaling and breaking waves. Another complicating factor is the outcropping of rock reefs south of the inlet largely within the surfzone. Present compatibility tests of potential beach fill material use mean, mode, and standard deviations to compare the texture of existing beach and shoreface sand with the texture of the fill material. Simple equilibrium profile models are also used that in part depend on the mean grain size of fill material. None of these methods provide reliable predictions of the stability of fill material of a particular textural range. Rapid movement and partial to complete loss of fill material is a common result of nourishment projects.

To improve the predictability of beach fill performance this task will combine modeling and sediment sampling methods. The CMS model will be used predict the rate of sand transport across the 17 individual gain size classes that are commonly found in beach and nearshore sands in the vicinity of Sebastian Inlet. Field sampling of sand texture across the beach, shoreface, and though Sebastian Inlet in combination with summer and winter topographic surveys will be used to quantify the range of sediment textures. From the combination of model results and sampling, a beach fill coefficient will be calculated that predicts the stability and retention of each of the 17 grain size classes across the beach and shoreface, and over the sandy shoals within Sebastian Inlet. Using the beach fill coefficients, the retention and stability of beach fill sand will be

predicted on a grain size by grain size basis. The methods will predict the percentages of fill sand that will remain in the beach fill envelope as a function of the texture of the fill material.

10.1 Sediment Texture Methods

In June of 2011, 407 surface sediment samples were collected to the north, south, and from the flood and ebb shoals of Sebastian Inlet, Florida. As shown in Figure 49, the shoreline sampling area included a length of 12 miles: 6 miles to the north of the inlet (R191 to R219) and 6 miles to the south of the inlet (R4 to R30).

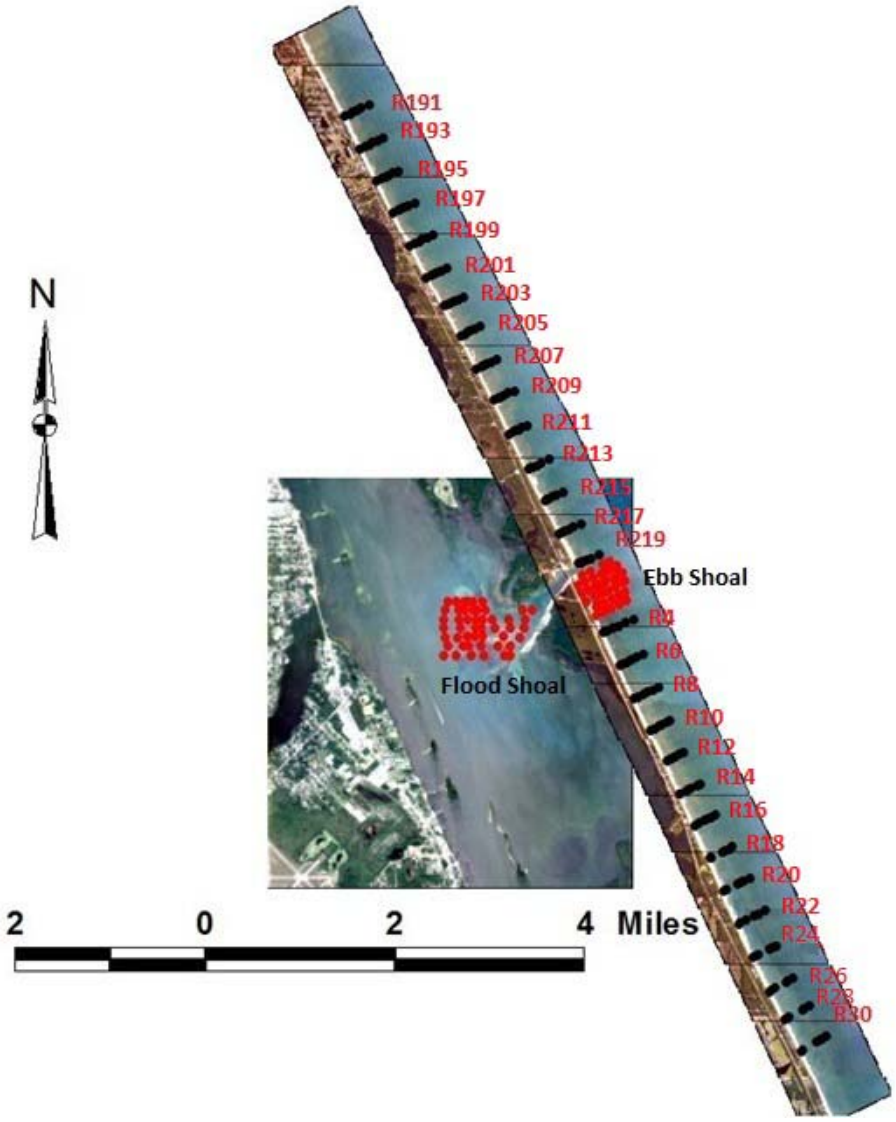

Figure 49. Sampling locations.

The elevation and coordinates of the sample points, expressed in Florida East state plane coordinates, were based on a summer 2011 survey of Sebastian Inlet. On the beach, samples were collected using 4-wheelers equipped with Real Time Kinematic (RTK) GPS. Samples were placed in twirl packs and labeled according to R-marker and lettered "A" through "E" according to position, with "A" being most landward and "E" being most seaward. The offshore samples were collected by free-dive from a boat equipped with RTK GPS. Samples were collected, brought to the surface, and placed in twirl packs on the boat. Samples were again labeled according to range marker and numbered "1" through "6" according to position, with "1" being most landward and "6" being most seaward. On the ebb and flood shoals, samples were collected in the same manner as the offshore samples, and labeled according to the shoal and position they were collected from. If a sample location was on hard bottom, the divers may have deviated slightly from the GPS location in order to collect sediment. In other hard bottom locations, no sediment was available so no sample was taken.

Samples were arranged in order by location. All samples were wet and dry sieved, according to ASTM standards using ASTM standard sieves at half-phi intervals, with the addition of a -4.25 sieve and a 3.75 sieve. In addition to sieving, samples were subject to two levels of high-temperature burns using methods outlined by Dean (1974) and Heiri, et al (1999). Samples were heated to 540° Celsius for a minimum of 6 hours to determine the percentage of organic material in the sediment (inferred to be weight of CO_2). Samples were then heated to 1080° Celsius for a minimum of 6 hours to determine the percentage of calcium carbonates ($CaCO_3$) in the sediment. Sediment statistics were calculated using gINT™ software.

Once sediment statistics were obtained, a comma-delimited file was made for each grain size, which included the sample name, the grain size in millimeters, percent weight retained, and sample coordinates in NAD83. These files were imported into ArcView GIS 3.2 and made into individual contour maps (20 maps total; see Appendix A). Contour maps were also created for mean grain size, modal grain size, standard deviation, and organic and carbonate percentages at each sample location (see Appendix C). From these data the sediment dispersal patterns around the study area can be determined.

10.2 Sediment Patterns at Sebastian Inlet

From the grain size data, the sediment distribution in and around the inlet has been identified. The size terms used are modified Wentworth classifications (see chart in Appendix C). The northern section of the study area (R191 to R219) was predominantly very fine to medium sand, having an average mean grain size of 0.30 mm and an average modal grain size of 0.25 mm. However, the standard deviation in the north section was 0.90. The contour maps(See Appendix A) indicate that the northern section is composed of very fine to medium sands.

The southern section of the study area (R4 to R30) was again very fine to medium sand but slightly coarser having an average mean grain size of 0.47 mm and a modal grain size of 0.40 mm. The standard deviation was again high at 0.93. The contour plots show that this section of the study area is again composed of very fine to medium sands, with coarser sediments at the lower segment of this study area (R20 to R30).

The ebb shoal had an average mean grain size of 0.37 mm and a modal grain size of 0.28 mm, with a standard deviation of 0.65. The contour plots (Appendix A and Appendix B) indicate that the crest of the ebb shoal is dominated by coarse sand whereas the outer perimeter of the shoal, in deeper water, is mainly very fine to fine sand. The flood shoal had the finest mean and modal grain sizes, which were 0.21 mm and 0.14 mm respectively, and a standard deviation of 0.75. The contour plots (Appendix A and Appendix B)show that the flood shoal is mainly composed of very fine to fine sand. Overall, the contour plots show that the 0.09 mm grain size had the greatest percentage of weight retained over the study area.

The sediment patterns found in this analysis clearly show distinctive differences in grain size distribution between the beach and shoreface north of the Sebastian Inlet and the beach and shoreface south of the Inlet. Sediment textures of the ebb and flood shoals are also distinctive and give an indication of sediment partitioning of littoral sands as they enter the inlet system.

The highest carbonate percentages were located mostly offshore in the southern section, as well as the center of the ebb shoal and the throat of the inlet on the southwestern end (Figure 50). The carbonate fraction is largely within the medium to coarse sand range and extends into

the fine gravel range in some areas. High concentrations over the ebb shoal and within the main inlet channel reflect high energy conditions from strong tidal flows that concentrate the coarse shell material. To the south of the inlet down to the vicinity of R30 high carbonate concentrations reflect both the presence of rock reef outcrops that may contribute to shelly, carbonate-rich sediments and the presence of fill material excavated from the carbonate rich sands along the Indian River Shoal, which has been used as a borrow area (Zarillo, 2011).

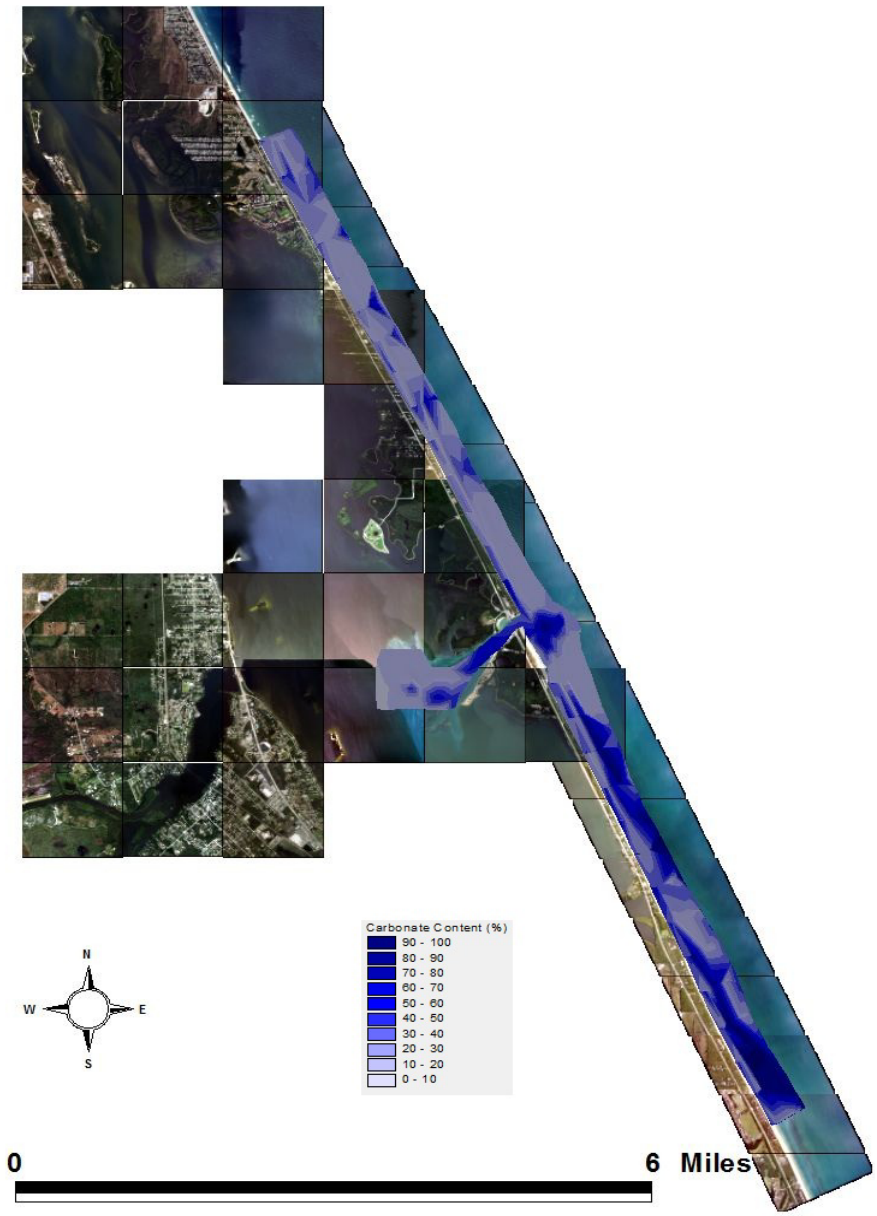

Figure 50. Distribution of carbonate (Shell fragments) percentages within beach, shoreface and inlet sediments showing higher concentrations south of Sebastian Inlet.

The contour plot of modal grain size (Figure 51), similar to carbonate concentrations, shows the influence of beach fill sands to the south of the inlet where modal grain size can be in the range of coarse sand (0.5 -2 mm) on the mid to lower shoreface. On the north side of the inlet coarser model grain sizes are found on the upper shoreface closer to the water line and are more reflective of physical processes rather than concentrations of coarse shell material.

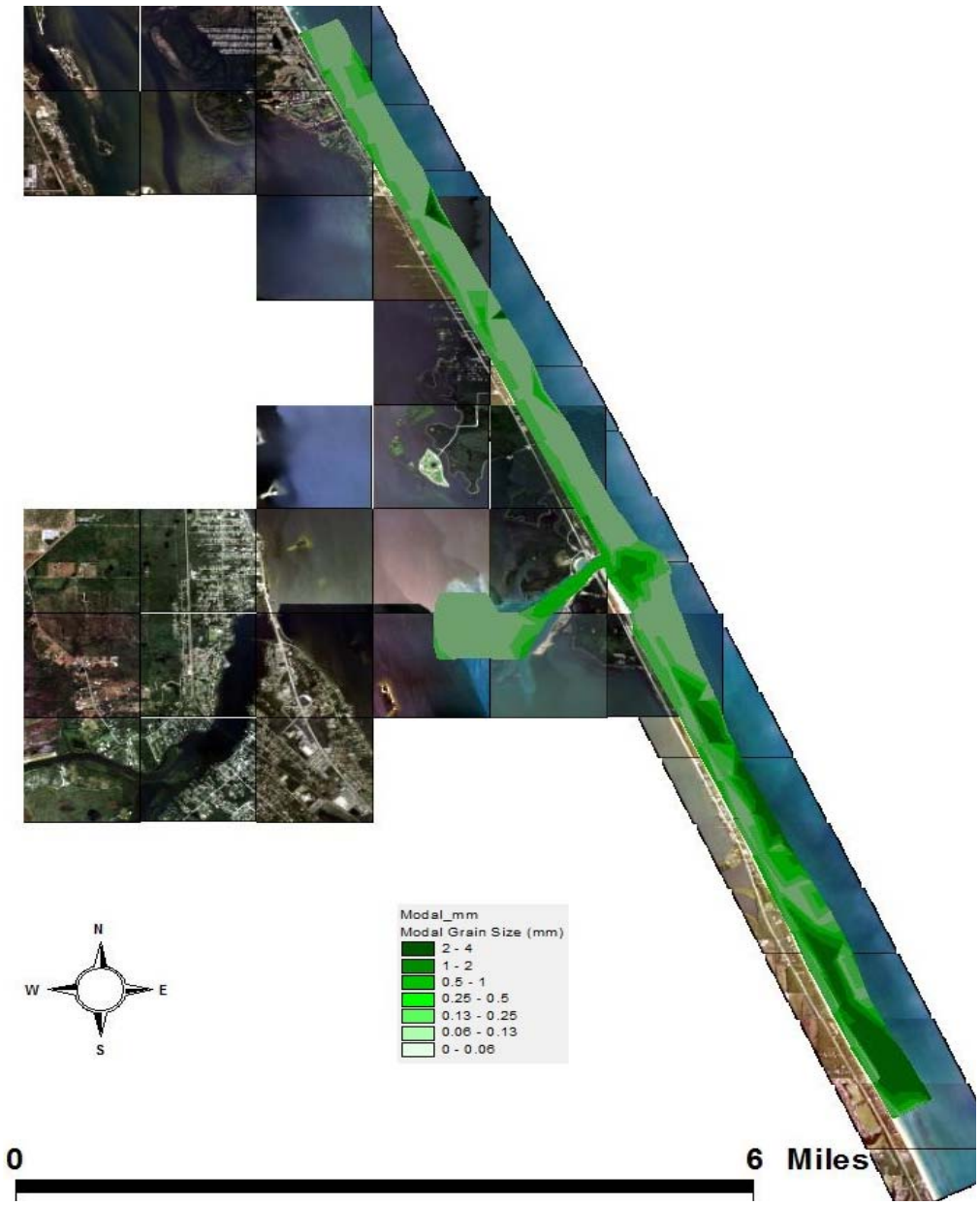

Figure 51. Model (most frequent) grain size within beach, shoreface and inlet sediments.

The occurrence of selected sediment grain size classes to the north and south of Sebastian Inlet, as well as within the ebb and flood shoals of the inlet, give a good indication of sediment transport pathways and the influence of beach fill projects in the area. For example the percentage of 1 mm sand (coarse sand) by weight is highest at the crest of the Sebastian Inlet ebb shoal and areas influenced by rock reef outcrops and recent beach fill projects to the south of the inlet. (Figure 52). Comparison of Figure 52 with Figure 51 (carbonate percentage by weight) shows that coarser sand fractions derived from erosion of rock reef outcrop and offshore shell rich sand sources (Indian River Shoal) are composed largely of carbonate debris.

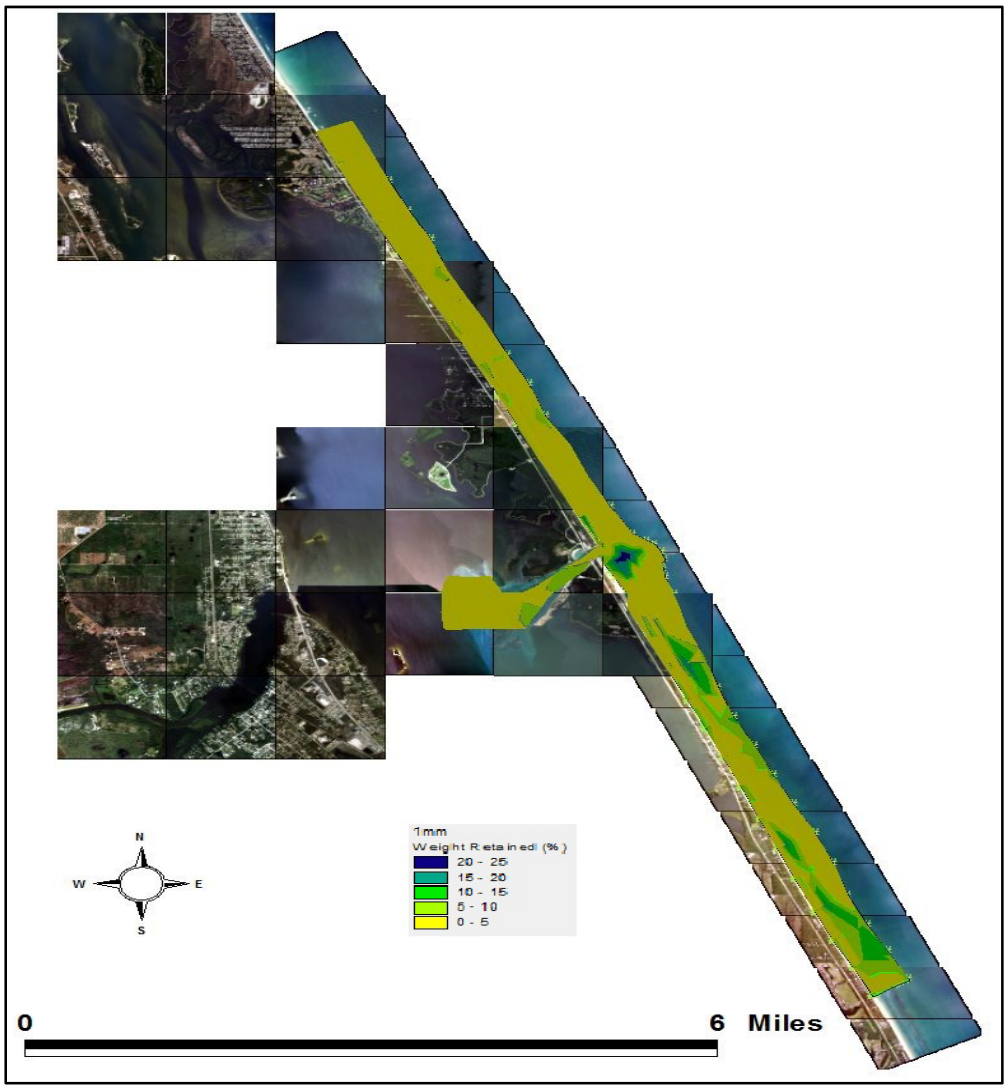

Figure 52. Percent occurrence of 1mm coarse sand by weight.

The occurrence of finer sand fractions to the north of the inlet on the mid to lower shoreface, within the flood shoal, and immediately to the south side of the ebb shoal provides evidence of sediment partitioning in the vicinity of Sebastian Inlet (Figure 53). The abundance of finer grain size classes on the mid to lower shoreface is typical of cross-shore sediment distribution in wave inflected areas having a mixed sized sediment supply (Zarillo, 1985, Liu and Zarillo, 1992). In addition to the influence of beach fill material and rock reef erosion, the higher percentages of coarser material to the south of Sebastian Inlet is due to impoundment of finer sediments from the littoral sand supply within the flood shoal and on the lower south flank of the ebb shoal.

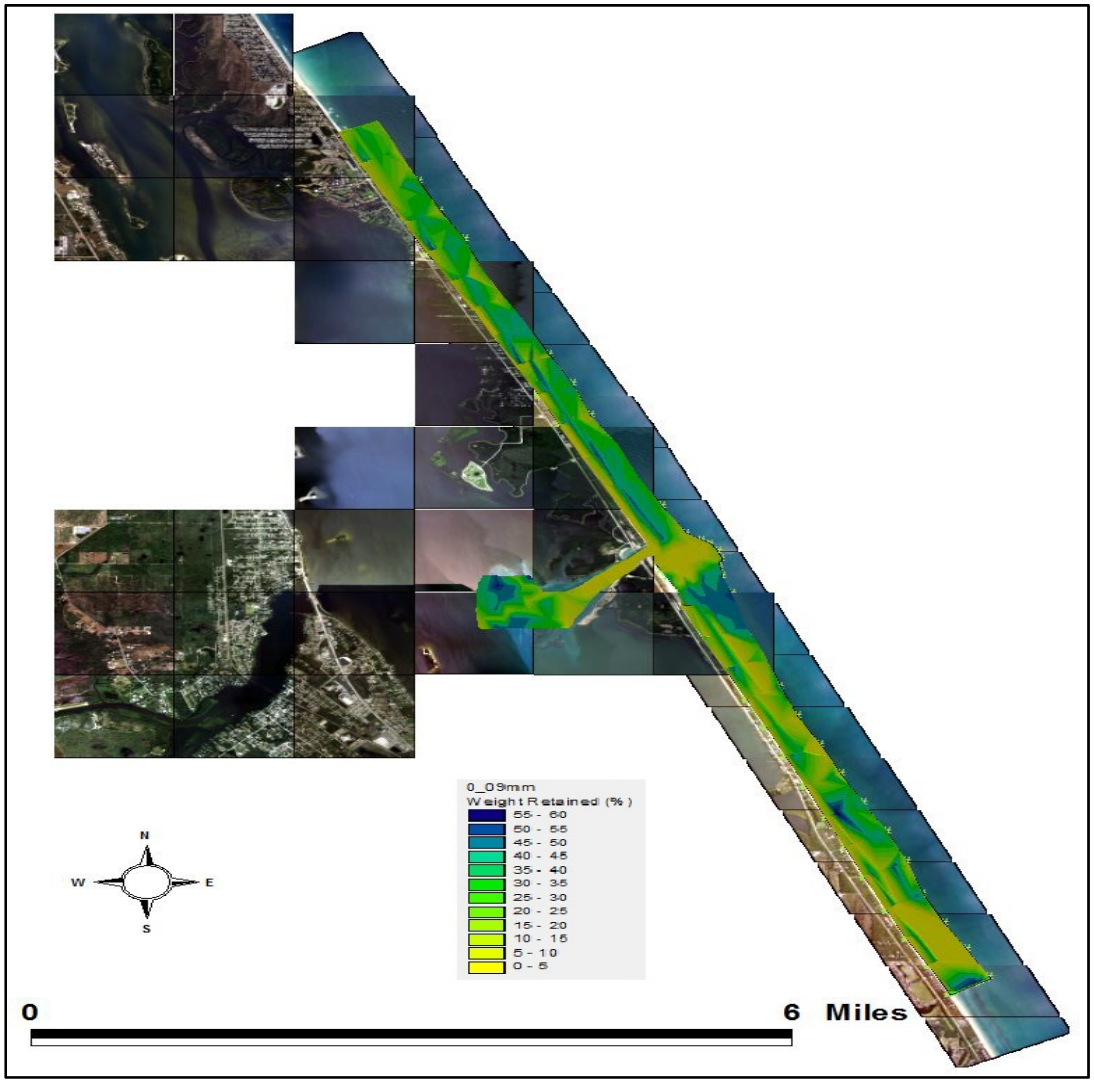

Figure 53. Percent occurrence of 0.09 mm very fine sand by weight.

Figures 54 and 55 further resolve the difference in cross-shore partitioning of sediment size classes to the north and south of Sebastian Inlet. Figure 46 shows the cross-shore distribution of silt to coarse sand and gravel sediment size fractions along with the occurrence of carbonate percentages (shell fragments) by weight percent at a location about 20,000 feet north of Sebastian Inlet. The overall trend is one of fining seaward beginning with medium to fine sand dominating the beach berm area followed by increasing amounts of coarse sand and carbonate percentages down to the shoreline represented by the 0 ft. elevation. On the submerged portion of the shoreface beginning at -3 ft. the percentages of fine very fine sand, and silt increase to a depth of -20 ft. Beyond this depth the very fine sand size class continues to dominate, but is mixed with increased percentages of carbonate materials. At water depths of 0 to -5 ft the size classes occur in sub equal amounts indicating that this is a zone of mixing and mobility subject to variations in mixed sediment sizes due to frequent cross-shore sediment exchange.

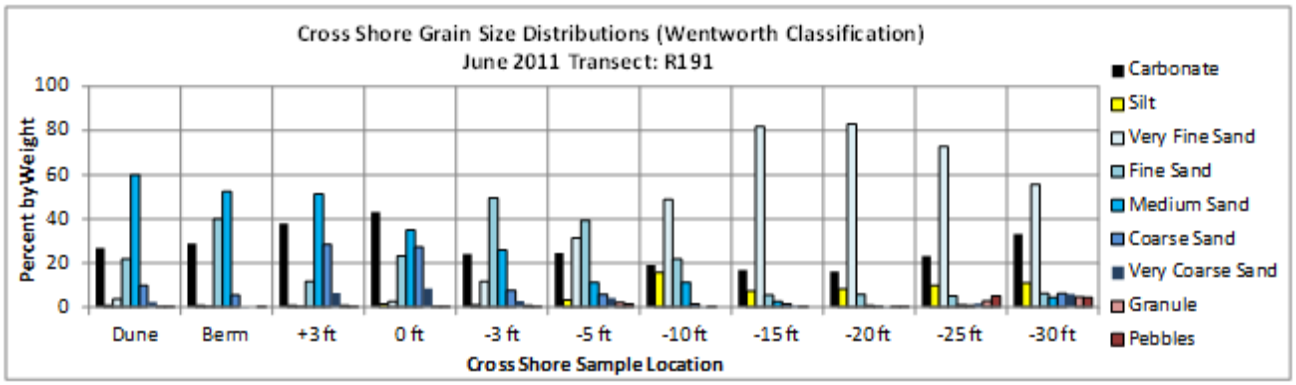

Figure 54. Cross-shore distribution of grain size classes at FDEP R-Marker 191 about 20,000 ft. north of Sebastian Inlet, summer 2011

Figure 55 shows the cross-shore distribution of sediment sizes fraction at about 28,000 feet south of the Sebastian inlet at R-Marker 28. Here medium and coarse sand dominate the beach size fractions along with a substantial amount of carbonate material that enhances the coarse sand fraction. At the 0 ft elevation the carbonate fraction exceeds 60% and is likely to compose a substantial portion of the medium sand to gravel fractions as indicated by the sub equal percentages across this range shown in Figure 55. A more normal fining progression occurs to a depth of -10 ft. where the shoreface sediment is dominated by very fine sand. From

water depths of -15 to -30 ft. the sediments are dominated by the carbonate fraction distributed across the coarse sand to gravel fractions that occur in sub-equal percentages (Figure 55). This patterns shows the influence of nourishment material mostly from the carbonate–rich Indian River Shoal borrow area. This material may have first entered in the system in 2003 during the Ambersand nourishment project when about 600,000 cubic yards of fill was placed between R12 and R17 along with a re-nourishment phase in 2007. More recently (2010) about 175,000 cubic yards of shell rich coarse sediment from an upland source was placed between R26 and R36. Previous analysis of volume exchanges between the upper and lower shoreface indicate that some of the 2003 and 2007 fill materials remain in the system but migrated to the lower shoreface (Zarillo et al, 2007). However the similarity between the sediment distribution between 0ft. and -5ft. and distributions between -15 ft. and -30 ft. indicate that some of the fill material may be still nourishing the lower beach by cross-shore exchanges of coarser grain size fractions.

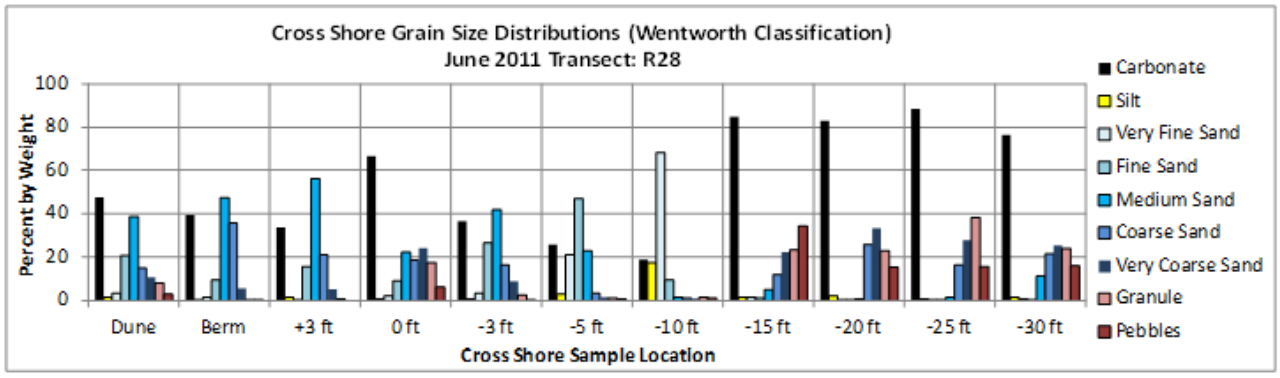

Figure 55.Cross-shore distribution of grain size classes at FDEP R-Marker R28 about 28,000 ft. south of Sebastian Inlet, summer 2011

10.3 Sand Bypassing at Sebastian Inlet

The study of sediment grain size partitioning in the vicinity of Sebastian Inlet is designed as a two part project to be completed over the course of 2 years. In year one a set of summer sediment samples was collected and analyzed as described in Section 9.1 and 9.2 of this report. A second set of winter samples was also collected in January of 2012. This section compares sediment textures and composition between the summer of 2011 and the winter of 2012. Results are interpreted with respect to performance of beach bill material on the south side of Sebastian

inlet and recommendations for selecting beach compatible source materials and optimization of fill placement in future beach replenishment projects.

Figure 56 compares the distribution of the most frequent or modal grain sizes in the vicinity of Sebastian Inlet and south to the location of the R30 FDEP marker. The comparison is between sediment distribution patterns for June 2011 and January 2012. The comparison shows concentrations of coarser sediment on the shoreface south of Sebastian Inlet that are either related to reef rock outcrops in the vicinity of R07 to R16 or to carbonate rich fill material in the R22 to R28 area. In these areas the model and mean grain size can be more than 2mm. The winter-summer modal size patterns are similar, especially in the reef rock area. However the fill related material in the winter sample set is not as widely distributed (Figure 56) compared to the summer 2011 pattern. This indicates that some of the fill material may have dispersed and mixed with finer naturally occurring sands in the area between R22 and R28. A comparison of summer and winter carbonate distribution (Figure 57) Shows a pattern similar to that of modal grain size. The carbonate content of sediment largely is in the form of shell fragments concentrated in fill sands and derived from reef rock outcrops. Concentrations are particularly high in the fill influenced area of R22 to R28, However, like model grain size concentrations of coarse shell is more dispersed by January 2012. Both the modal and carbonate sediment patterns indicate a concentration of coarse sediments over the ebb shoal and bypass bar where breaking waves disperse and re-work finer sediments. Patterns also indicted modernly high concentrations of coarse shell rich sediments though the inlet throat where tidal currents reach high velocities and limit the deposition of finer sands.

Examination of sediment patterns for grain size classes between 1mm and 0.13mm provides evidence of which size classes and being bypassed across the Sebastian Inlet bypass bar (see Figure 2) and which size classes are being retained within the inlet. Figure 58 shows the distribution pattern of the 1mm size class for both the summer of 2011 and winter of 2012. Bother patterns are similar with the exception that concentrations along the beach above the water line are larger in winter 2012. Conversely concentrations of this relatively coarse material are slightly larger over the submerged shoreface in the summer 2011 data set. In both cases high concentration of 1 mm sand are found over the crest of the ebb shoal but largely absent

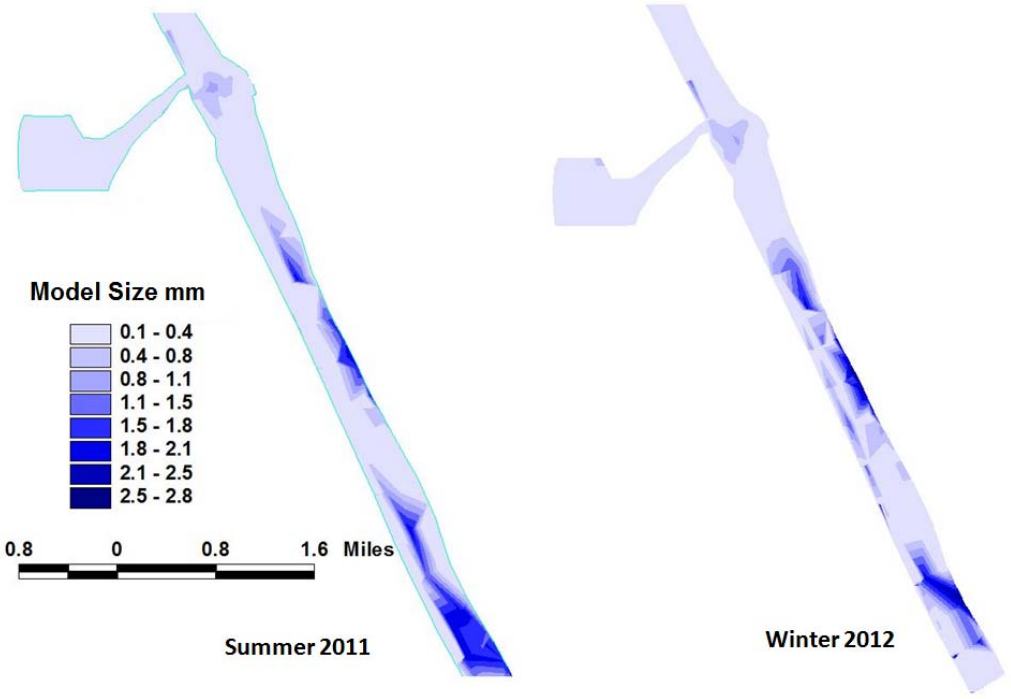

Figure 56. Modal grain size in mm, summer 2011 and winter 2012.

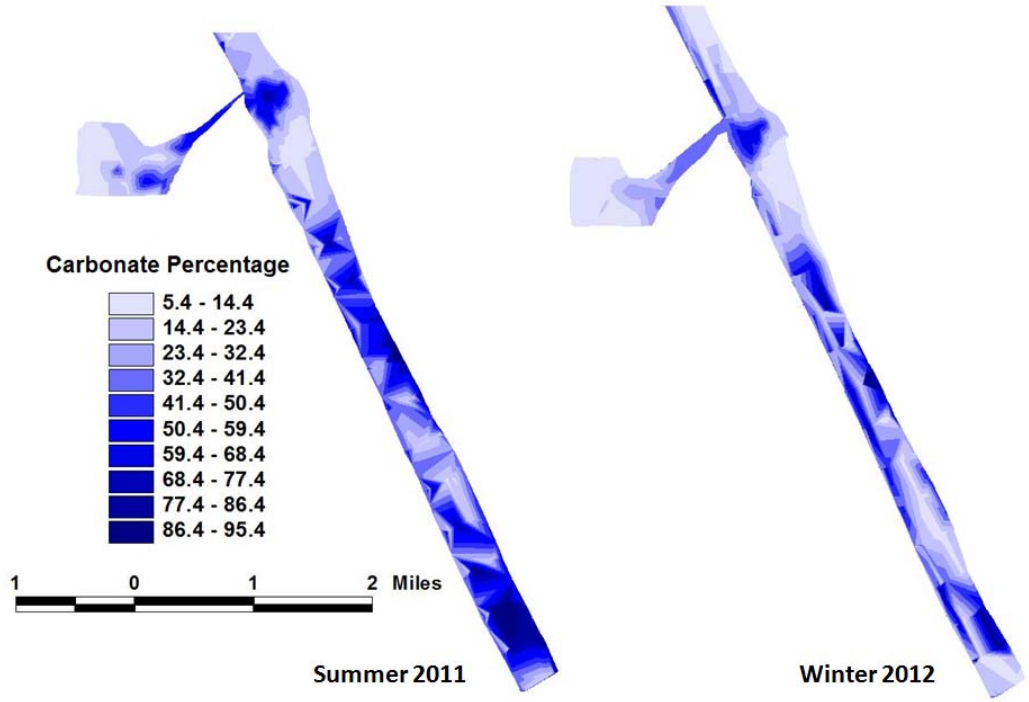

Figure 57. Carbonate percent in surficial sands, summer 2011 and winter 2012.

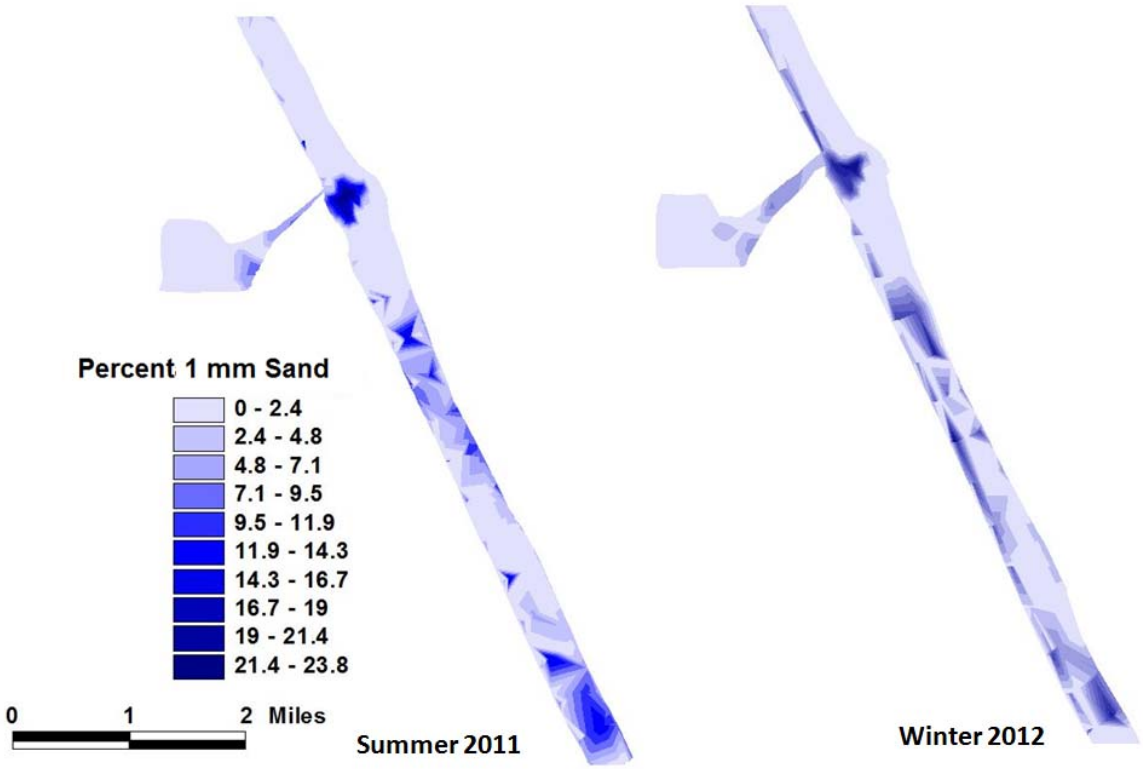

Figure 58. Distribution of 1 mm sand, summer 2011 and winter 2012.

from the bypass bar where it connects to be beach on the south side of Sebastian inlet near R04. This size class is largely composed of shell fragments and other carbonate debris and can be considered most susceptible to transport during higher energy conditions. The patterns indicate cross shore transport onto the beach and concentrations of lag materials as finer sized material is reworked by longshore transport.

Sand size classes finer than 1 mm are distributed in patterns that indicate bypassing around Sebastian Inlet over the seaward flank of the bypass bar (see Figure 2 for location). Figure 59 compares the distribution pattern on the 0.5mm size class for summer of 2011 and winter of 20122. The high concentrations of this class of sediment on the seaward flank of the ebb shoal and across the bypass bar connecting to the beach and shoreface on the south side of the inlet between R2 and R3 is a clear indication of transport past the inlet. The pattern is more organized for the winter 2012 data set showing that most of this size class of sand is concentrated

on the upper shore face and on the beach. This material is also found though the inlet channel in relatively high concentrations. However low concentrations of this class in the flood shoal indicate that it is preferentially bypassed across the inlet.

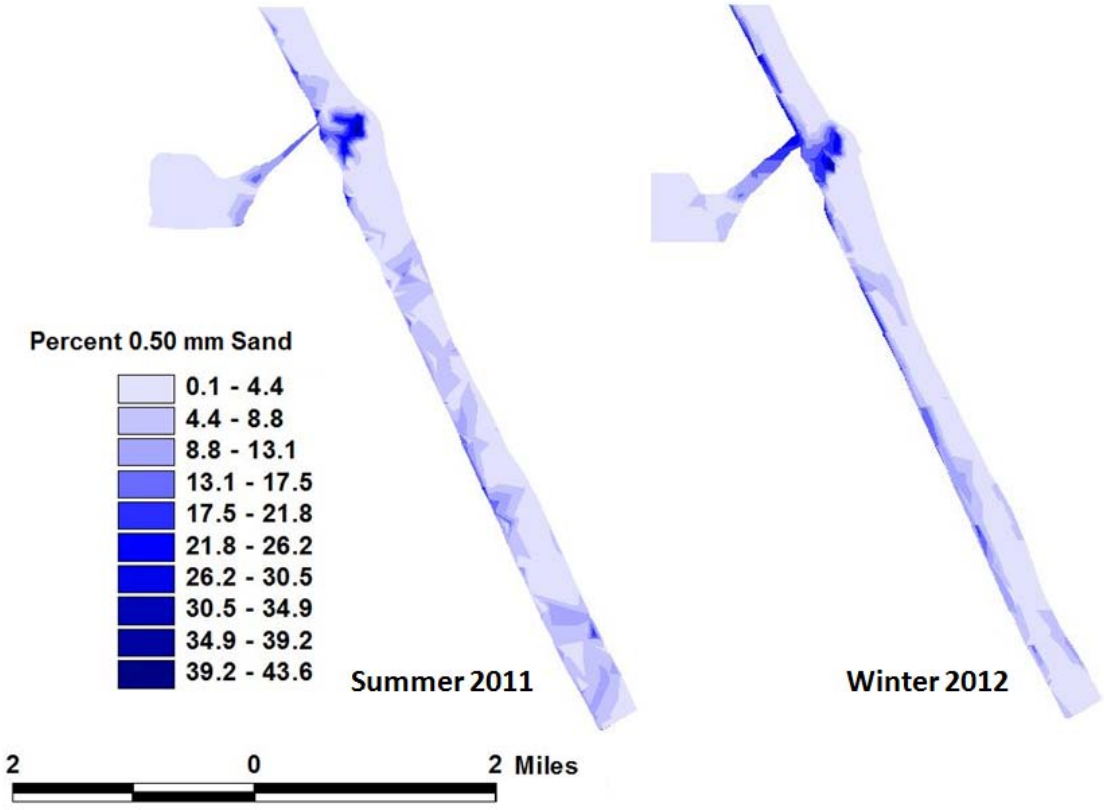

Figure 59, Distribution of 0.50mm sand, summer 2011 and winter 2012.

The distribution of finer sand size classes also indicates bypassing around and incorporation into the shoreface and beach system on the Southside of Sebastian Inlet. Figure 60 shows the distribution of the 0.18 mm class (fine sand). High concentration of this sand are continuous across the inlet and patterns both south and north of the inlet show that this size class is abundant in the shallow sub-tidal sections of the shoreface to depths of about 25 to 30 feet. Where concentrations of the coarser 0.50 mm sand are less. High concentrations of 0.18mm sand in the flood shoal indicate that some of this material is captured by the inlet

Figure 61 shows the distributions of one of the smallest size classes analyzed for distribution though the inlet system. The 0.13mm sand is abundant in the flood shoal and across the shoreface to depths of 30 feet or more. High concentrations north and south of the inlet and on

the seaward flank of the ebb shoal and bypass bar indicate that this material is bypassed across the inlet in the dominant net southward littoral drift. Higher concentrations of this material in the winter destruction patterns along with the more organized pattern of all size classes in the winter data set may indicate more persistent wave energy prior to the sampling period in January of 2012.

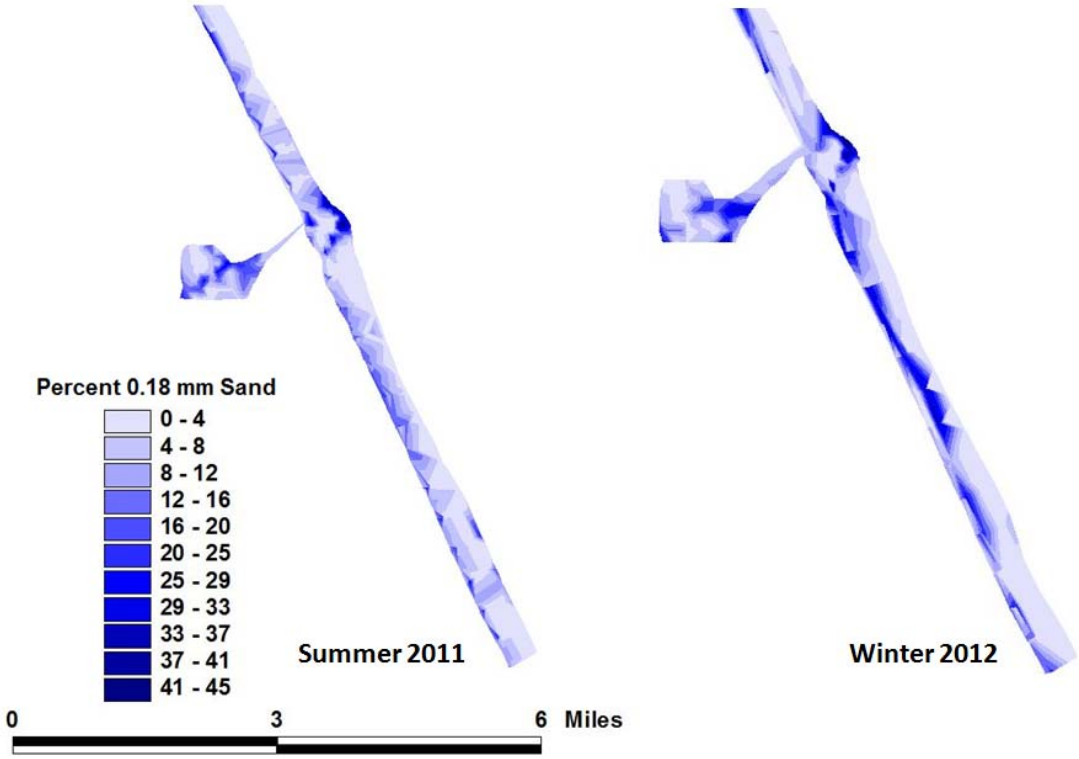

Figure 60. Distribution of 0.18mm sand, summer 2011 and winter 2012

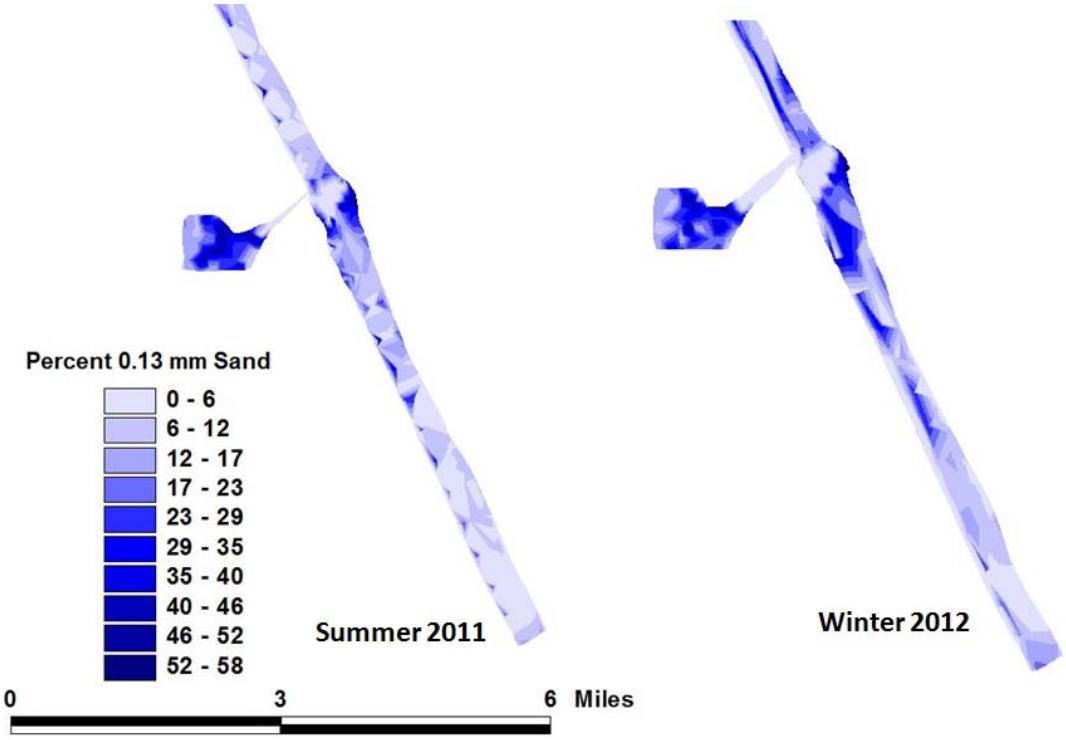

Figure 61. Distribution of 0. 13mm sand, summer 2011 and winter 2012.

The analysis of sediment distribution patterns from 2011 and 2011 shows that Sebastian inlet is bypassing sediment size classes in the medium to fine sand range and is retaining some of the sand in the finer size ranges below 0.18mm. The overall coarse sediments found on the south side of the inlet are the product of coarse shell rich sands placed in this area by recent fill projects and due to the influence of local reef rock outcrops. The indication of sand bypassing in the 2011 to summer 20912 periods is consistent with finding of the sand volume and sand budget analysis described in Section 6. Between 2010 and 2012 the shoals or sand reservoirs of Sebastian inlet have provided a net export of sand to the south side of the inlet. The sand volume analysis described in Section 3. showed sand volume decrease occurred in the ebb shoal and in the fillet on the north side of the inlet, which along with sand bypassed from dredging of the Inlet Sand Trap in Spring of 2012 provided a net sand volume loss for Sebastian Inlet and volume gains on the beach and shoreface areas to the south of the inlet.

11.0 Model Description and Methods

The numerical modeling study was conducted under the coastal modeling system (CMS), which is a physics-based model of waves, flow, sediment transport, and morphology change. The CMS is a product of the Coastal Inlets Research Program (CIRP) at the U.S Army Engineer Research and Development Center (ERDC). The model runs were driven with the hydrodynamic/sediment transport model CMS-Flow (Buttolph et al., 2006) coupled with the wave model (CMS-Wave, Lin et al. 2007), which provided an updated wave field at three-hour intervals. CMS-Flow is a finite-volume, depth-averaged model that calculates water surface elevation and flow velocity. CMS-Flow is coupled with CMS-Wave that calculates spectral wave propagation, including refraction, diffraction, reflection, shoaling, and breaking and also provides wave information for the sediment transport formulas. CMS-Flow can be driven by water surface elevation (WSE) and by wind forcing, as in the present study.

The overall methodology followed the previous inlet reports (Zarillo et al., 2007, 2009, 2010, 2011). However, the upgraded version of SMS allowed for increased grid resolution (smaller cell size) through the use of telescoping grids, multiple sand grain size input, and much faster computational times (implicit code/solver enabling much larger time steps). The hard-bottom coverage used acoustic monitoring surveys performed in the south domain during 2009. The non-equilibrium sand transport formula (NET) was employed, with varying sediment grain size across the shoreface and inlet features mapped within SMS based on the summer 2011 sediment sampling/analysis campaign. The non-equilibrium sediment transport method is based on a total load advection-diffusion approach (Sanchez and Wu 2010). It is based on the Lund-CIRP transport formula (Camenen and Larson 2007) and includes combined waves (breaking and non-breaking) and current. Bed change was then calculated periodically and updated in both the wave and flow models. More information on sediment transport parameters used for the model runs can be found in the following model set-up section. The modeling work is aimed at reproducing the hydrodynamics and sediment transport over the long-term for the entire year 2011 (six-month periods) in order to: 1) calculate morphology/bottom topography change over time and compare it with measured data 2), observe trends in sediment transport over time and calculate a model-based sand budget based on predicted sand transport in the area, and 3)

determine the importance of uniform vs. non uniform/variable sediment grain sizes input into the model domain.

11.1 Model Setup

The model setup section discusses the grid generation process, hard-bottom cells tagging, and the boundary conditions used to drive the simulations. Sediment grain size input is also presented in this section. The results section focuses on the analysis of morphologic and volumetric evolution of the inlet reservoirs over the entire year 2011. Calibration plots of current velocity and wave heights are also provided in the section.

Bottom Topography Grids

The model domain extends north of the Sebastian River to Wabasso, 6 km (3.7 miles) offshore of the barrier island in the Atlantic Ocean (water depth 16 m or 52 ft) and west, reaching past the Indian River Lagoon (IRL) to the mainland. The grid generation process for both CMS-Flow and CMS-Wave requires the preparation of shoreline data, bathymetry, and shape files of hard-bottom (reef or structure). The bottom topography dataset consisted of a combination of high-resolution beach profiles/hydrographic survey data of the inlet system, and surrounding beaches collected bi-annually since 1990 (SID), and offshore data from the Coastal Relief Model using the National Geodetic Data Center's website. In order to take full advantage of the available high-resolution hydrographic survey dataset, both CMS-Flow and CMS-Wave bottom topography grids were upgraded bi-annually, producing model runs that were divided into six-month periods. In this project, the first period ran from January 2011 to June 2011, applying a grid created using the winter 2011 topographic dataset (Figure 62, left). The second period runs until December 31st, 2011, using the summer 2011 topography, as shown in the right panel of Figure 62. The availability of semi-annual survey data was valuable for comparison with predicted data and for assessment of the model performance.

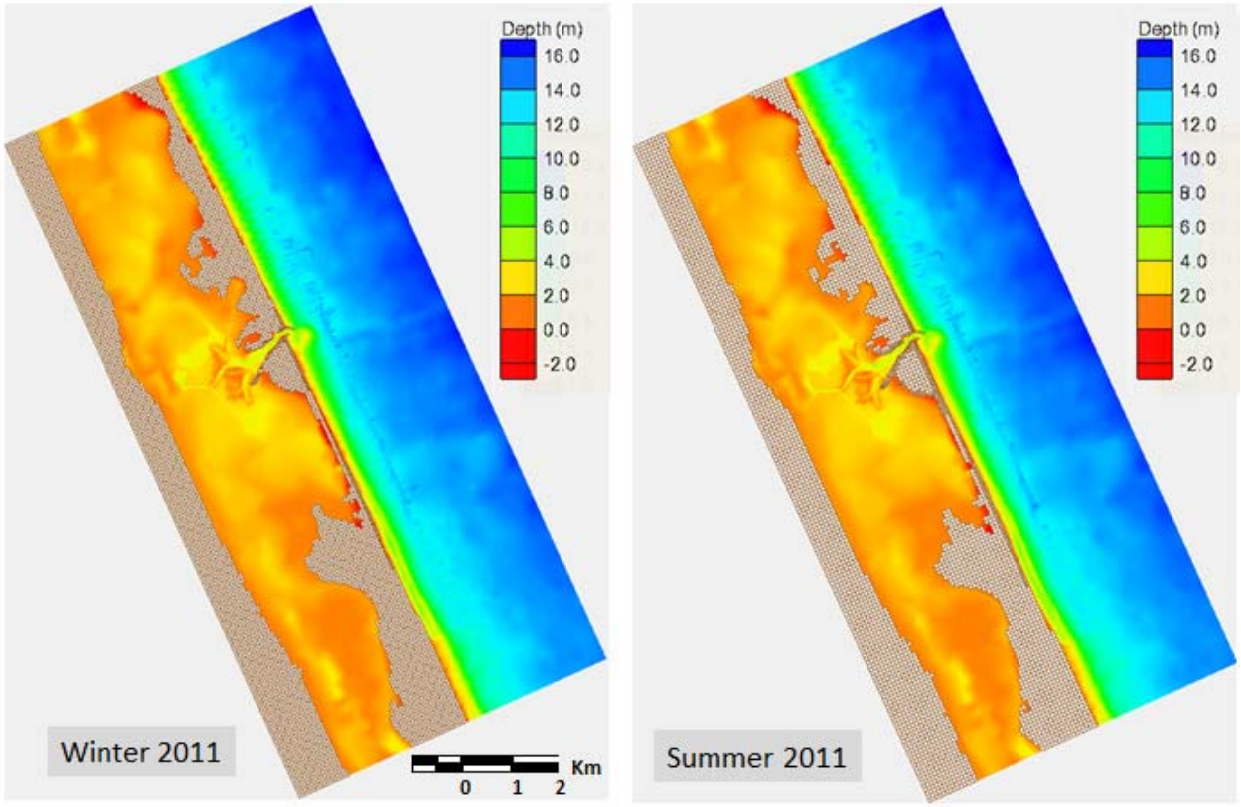

Figure 62. Bathymetry grid generated for summer 2011 model runs

For the circulation/sediment transport model, the grid cell sizes ranged from 20 m to 100 m, whereas the wave model used a uniform grid cell size of 50 m. Specific model grid parameters are listed in Table 18. Observation stations were established to facilitate analysis/extraction of the littoral sediment transport. Stations were selected by tagging 10 consecutive cells every 300m (900 ft), totaling 36 columns (Figure 63, left).These cells extended from the swash zone to depths of approximately -3 m to -4 m (-9 ft to -12 ft), which was considered the area representative of the nearshore processes (swash and longshore) and would capture the littoral sand transported during high-energy events.

Table 18. Model grid domain characteristics (January to June 2010 run)

Number of cells	92,919
Number of rows	191
Number of columns	90
Minimum Z value (m)	-5.59
Maximum Z value (m)	16.23
Angle (°)	24.34
Number of Monitoring stations	X
Number of ocean cells	88,833
Number of land cells	4086
Minimum row height (m)	12.5
Maximum row height (m)	100
Minimum column width (m)	12.5
Maximum column width (m)	100

For each grid, morphological constraints were applied by tagging the non-erodible cells. This study integrated acoustic data collected during the summer of 2009 by the Biological Oceanography Laboratory at Florida Tech on a 25,000-ft segment of beach from the attachment bar (R2) to approximately R30 in water depths ranging from -2 m to -6 m (-6 ft to -20 ft). The methods were the same as for the 2010 report (Zarillo et al., 2010). The acoustic data representing the hard-bottom zones were assembled into GIS files and included in the model runs (Figure 63).

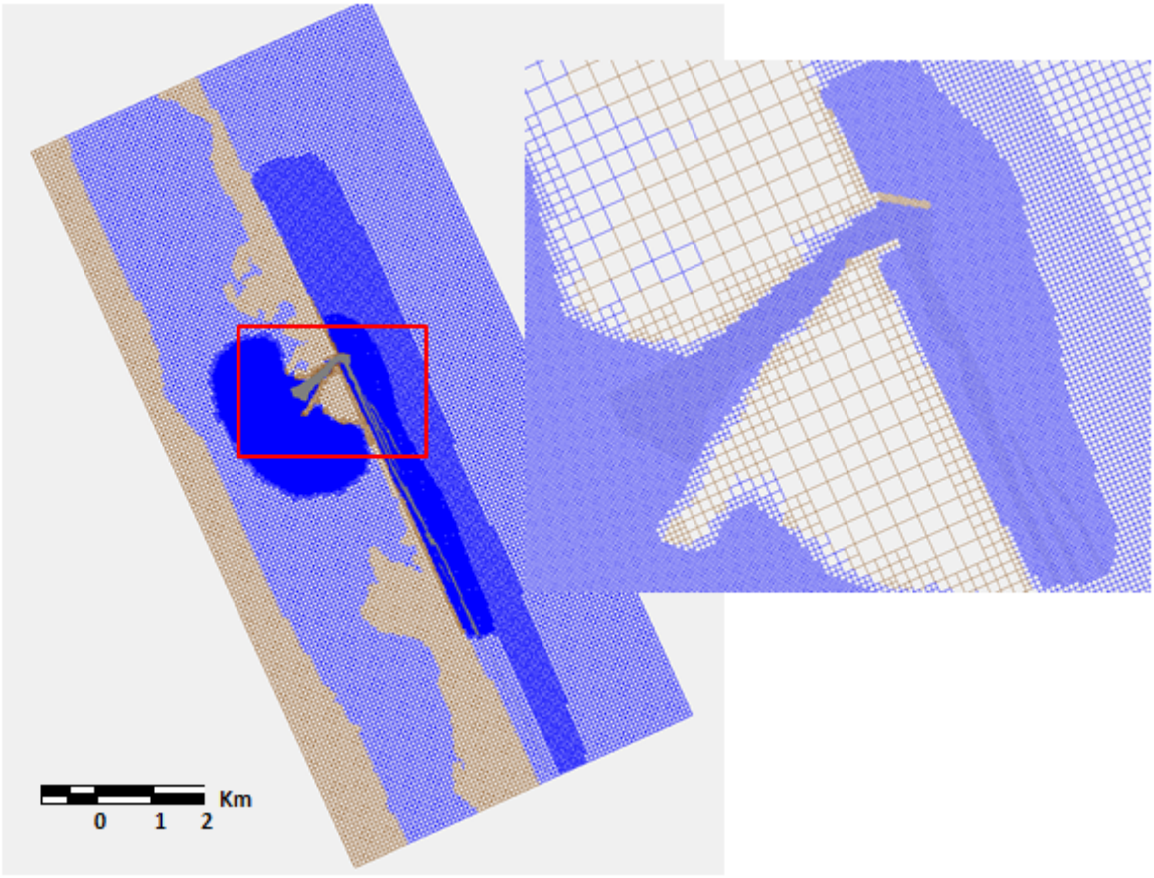

Figure 63. Telescoping grid used for 2011 model simulations

Sand Volume Analysis

In order to complement the net topographic change analysis, sand volumes contained within the Sebastian Inlet area were extracted. The sand reservoirs included the individual inlet cells (Figure 64) and sand budget cells (Figure 65). Volume calculations were performed under SMS, using a combination of the map and GIS tools, by importing the shape files and extracting the volume from the net change predictions.

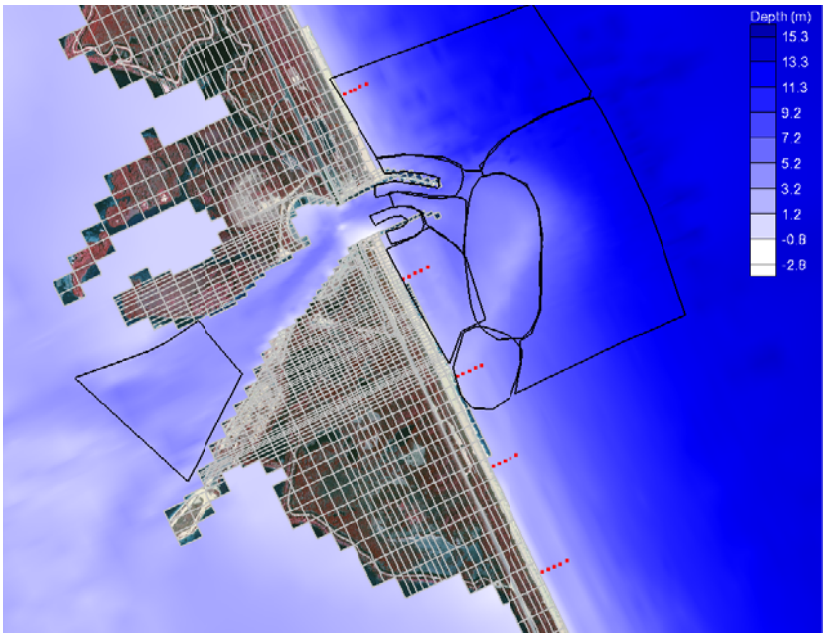

Figure 64. Sebastian Inlet reservoirs shapefiles imported into SMS for sand volume calculations

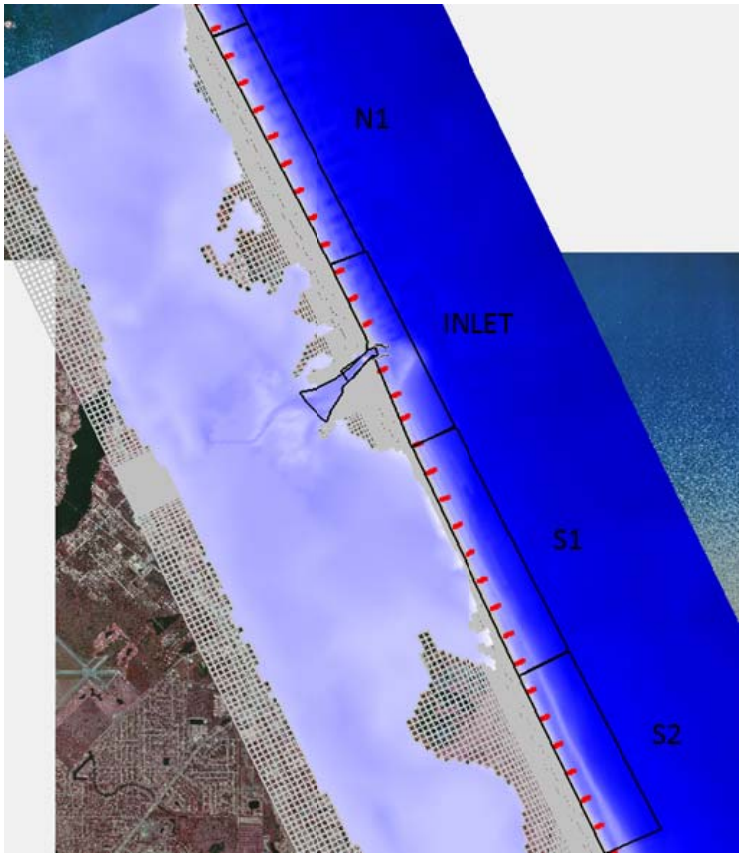

Figure 65. Sand budget cells overlaying the CMS–Flow model grid

Model Boundary Conditions

The model runs consisted of hydrodynamic/sediment transport model (CMS-Flow) hourly output, coupled with the wave model (CMS-Wave), with wave updates every three hours. This process, called steering, allowed interval outputs from each model to be transferred to the other model, thereby updating the inputs prior to continuation of the next interval run. The circulation model was driven by a time series of water surface elevations (WSE). Time series of hourly measurements were inserted at the three boundaries of the model domain consisting of the north lagoon, south lagoon, and the ocean (Figure 66 and Figure 67). The water surface elevation data were based on a prediction from tidal constituents derived from measured data.

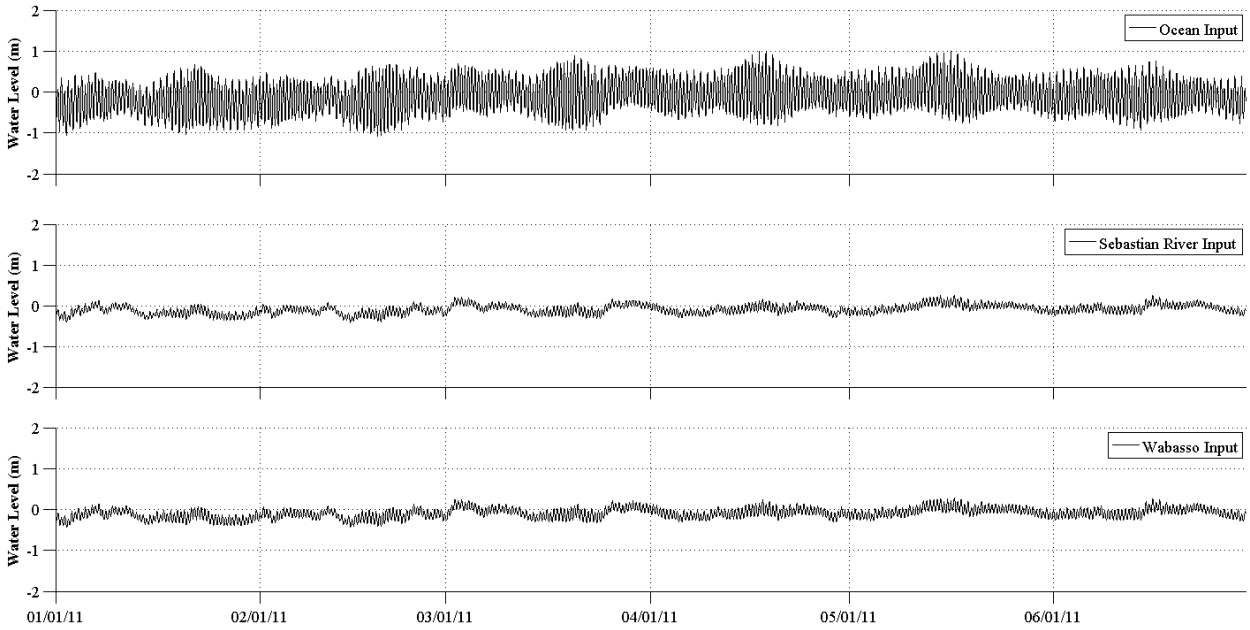

Figure 66. Water surface elevation time series for the three boundaries of the CMS-Flow model domain for the winter 2011 run

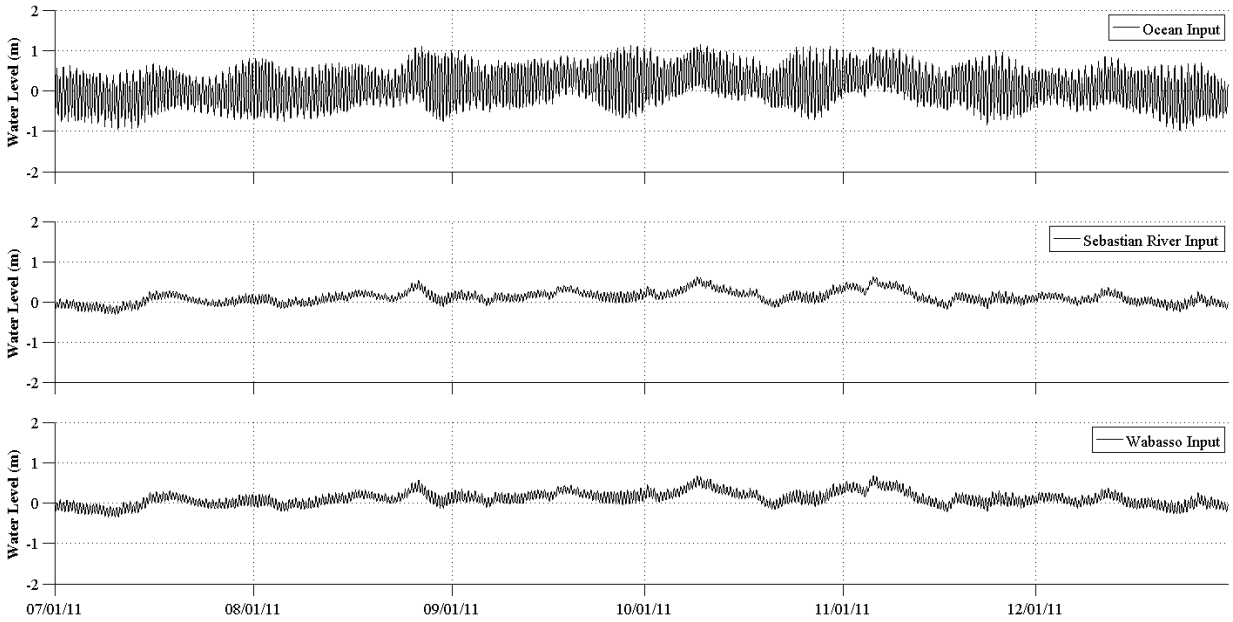

Figure 67. Water surface elevation time series for the three boundaries of the CMS-Flow model domain for the summer 2011 run

Wind data consisted of a time series of hourly wind speed and direction (Figure 68 and Figure 69). Data were collected at the meteorological station located on the north jetty of Sebastian Inlet, which is maintained by the Coastal Engineering Laboratory (CEL) at Florida Tech. The weather monitoring array was located 10 m (33 ft) above the water and included a R.M. Young anemometer, barometric pressure sensor, air temperature sensor, and a Campbell Scientific data logger (CEL website). Wind data were used as input for both circulation and wave models.

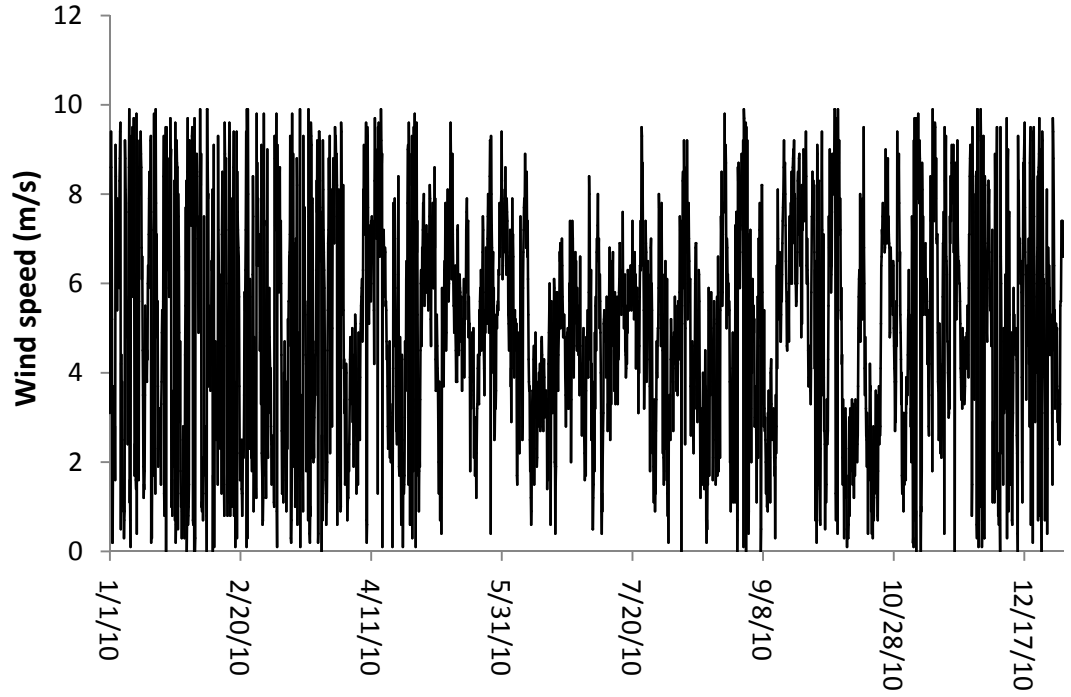

Figure 68. Input wind speeds for CMS-Flow and CMS-Wave simulations

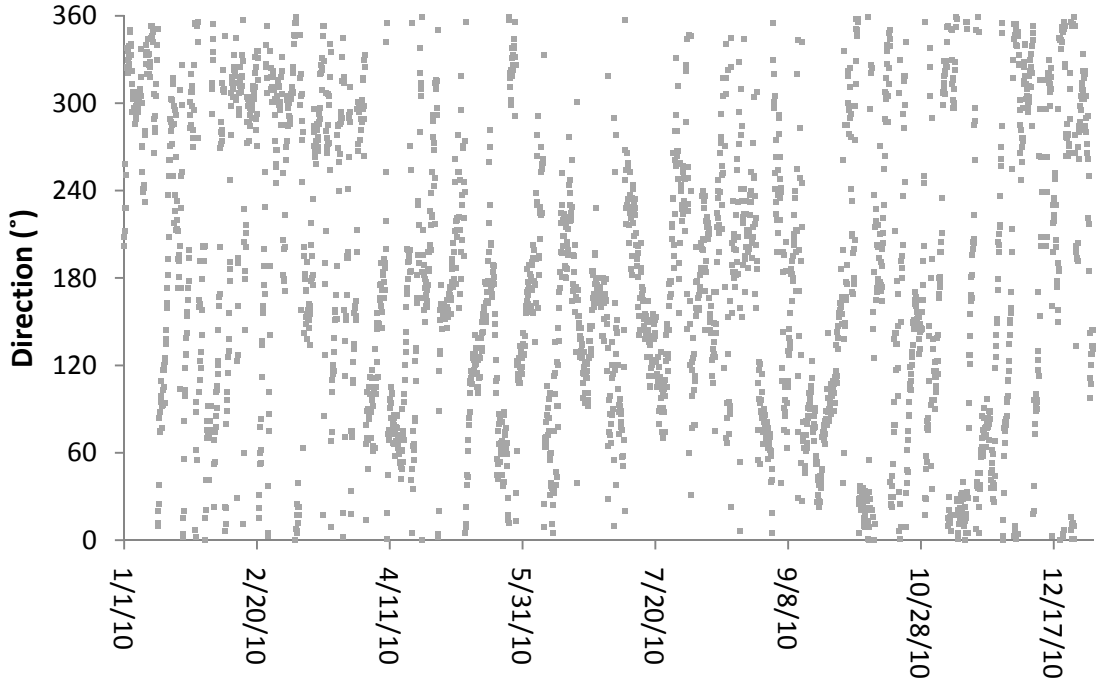

Figure 69. Input wind directions for CMS-Flow and CMS-Wave simulations

The wave model used time series of wave height, period, and direction, as well as spreading parameters, which were derived from hind cast data. The hind cast data were provided by establishing a larger CMS-Wave grid and 2011 archive data from the Wave Watch III third generation wave model developed at NOAA/NCEP for global wave forecasting (Tolman, 2009). The overall methodology, including data extraction and calibration processes were similar to those presented in the previous Inlet reports (Zarillo et al., 2007, 2009, 2010, and 2011). For the calibration of the models, an observation station was tagged at the location of the nearshore wave gage maintained by the CEL. The wave gage setup consisted of four wave gages deployed for one to three months at a time, including a Sontek as the main gage as well as a Nortek AquaDopp and Nortek Aquapro gages. As indicated by Figure 70 and Figure 71, there was a good match between the predicted and the measured wave heights extracted in the nearshore north of the inlet in a water depth of -8 m (24 ft). Important features to notice were 1) the seasonal signal with reduced wave height in summer and 2) the succession of storm events that included wave heights ranging from 1.5 m to 2.5 m (5 ft to 8 ft) approaching from the north-northeast (winter) to the east-southeast (summer).

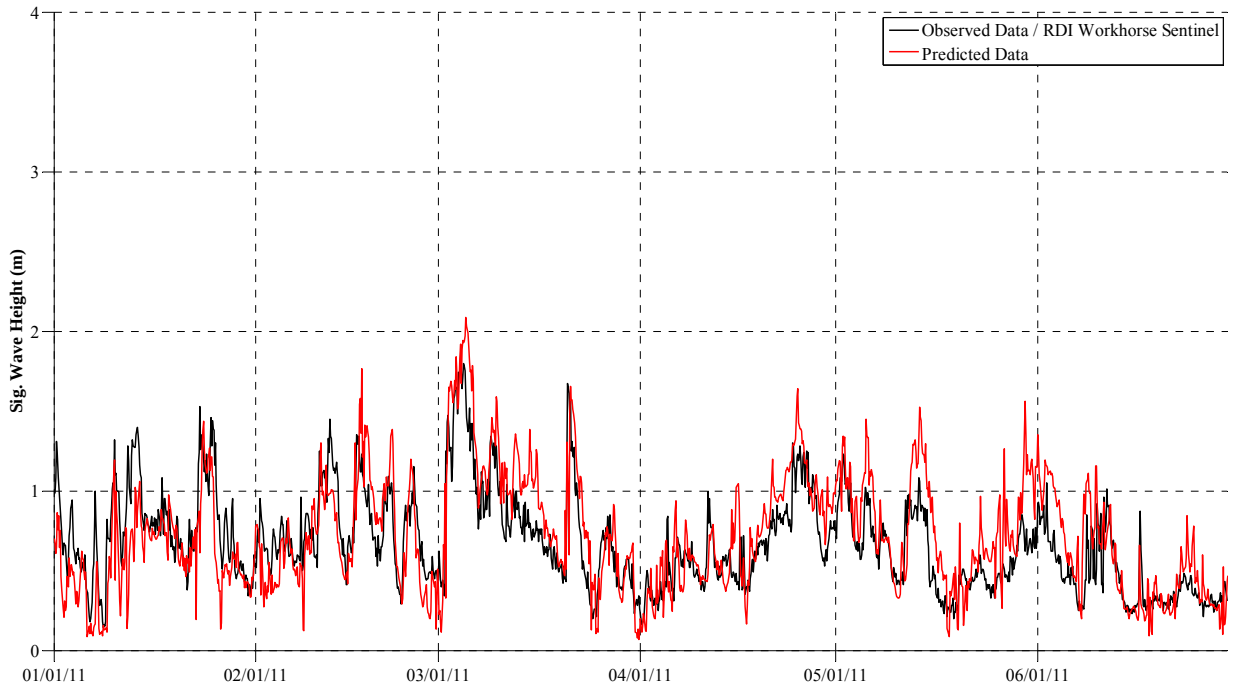

Figure 70. Measured vs. modeled significant wave heights (Hs) from January to June 2011

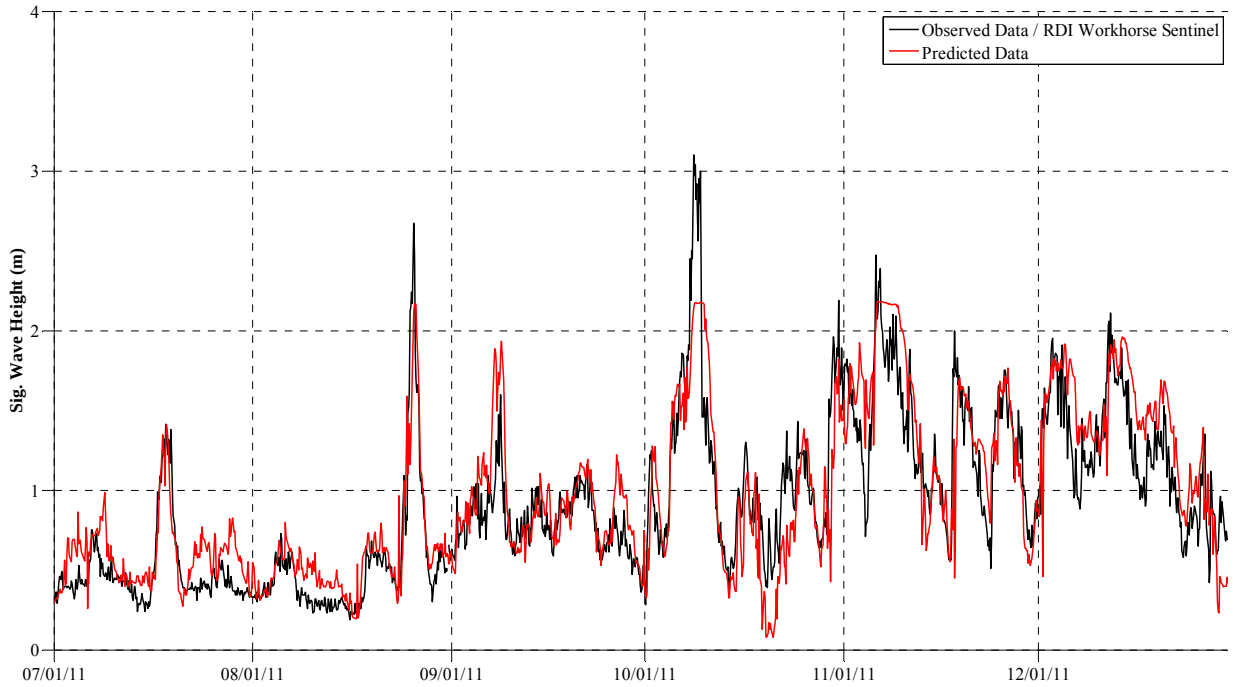

Figure 71. Measured vs. modeled significant wave heights (Hs) from July to December 2011

The 2011 Hurricane season included several strong storms moving along the U.S Atlantic coast, such as Hurricane Irene, and Ophelia. All those storms occurred during the second modeling period and are illustrated in Figure 71.

Sediment transport calculations were performed under the NET Lund formula, using bed load and suspended load scale factors of 1. For model calculations, the sediment transport time step was set to 10 seconds and morphology time step set to 1 hour. Additional information concerning the sediment transport parameters used for the runs is presented in . The mixed size sand fractions in the model sediment bed corresponded to recent sediment sampling (summer 2011). Figure 72 illustrates the mapping of a variable D50 dataset within SMS using GIS masks. The use of the implicit version of the CMS-Flow code enabled an increase of the model hydrodynamic time step from 0.5 to 30sec. which significantly decreased the computational time.

Table 19. Sediment transport parameters used for model simulations

Transport formulation	LUND-CIRP/NET
Bed load scale factor	1
Suspended load scale factor	1
Transport calculation time step (sec)	5
Morphology update *sec)	1
Sediment density (kg/m3)	2650
Water density (kg/m3)	1025
Sediment grain size (mm)	Variable *
Sediment porosity (	0.4
Slope coefficient	1

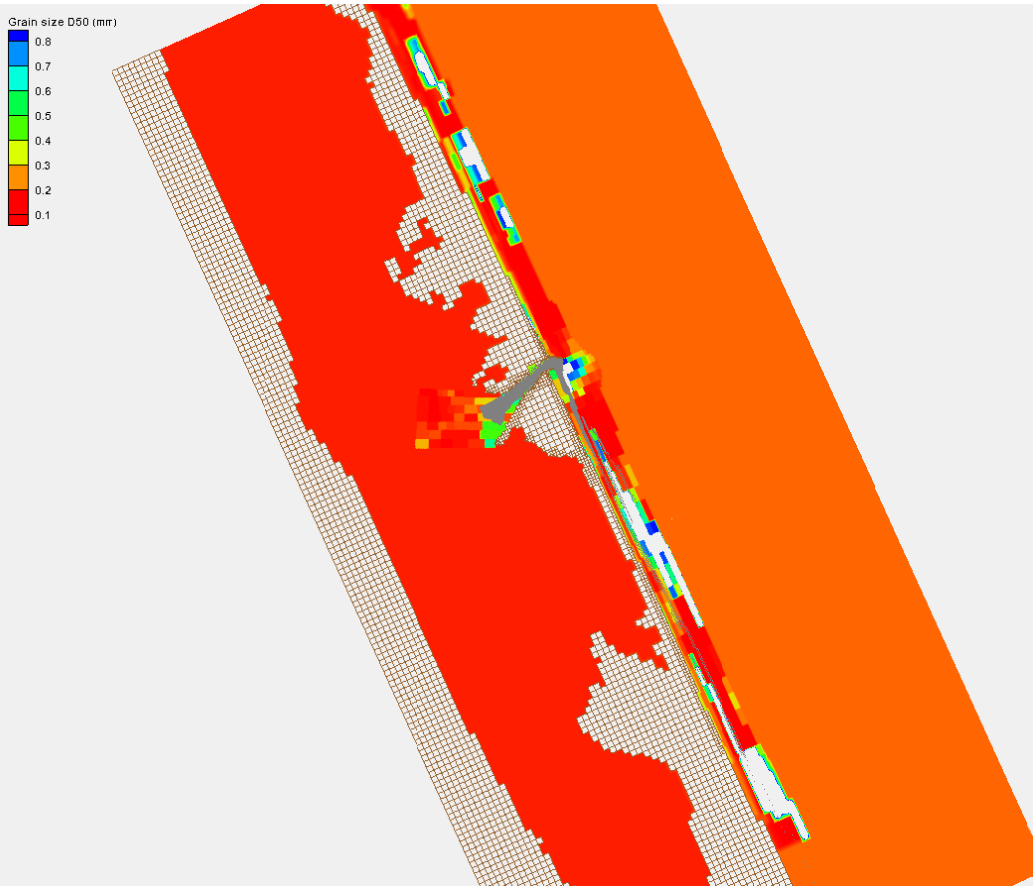

Figure 72. Variable sediment grain size (D50) input into the CMS-Flow model grid

11.3 Model results: Predicted Morphological change

Net topographic analysis

Model results of morphological evolution from the sand transport calculations were used to compute net topographic/morphologic changes for each simulation period. The modeled net changes from January 2011 to June 2011 and from July 2011 to December 2011 were presented in the left panel of Figure 73 and Figure 74, respectively. The corresponding measured morphologic changes were presented in the right panel of the Figures. The color code for the net change is the same as for the measured net topographic changes: blue colors represent erosion, whereas red colors represent deposition.

In the run from January 2011 to June 2011 (Figure 73, left), the model predicted the largest morphologic changes around the ebb shoal, with sand deposition reaching approximately +1.5 m

(+5 ft) on the lower flanks/seaward side and scour (-1.2 m or -4 ft) of the landward side. Model indicated deposition up to +1 m (+3 ft) on the upper shoreface between the south jetty and R2 (attachment bar), in the sand trap, and along the north jetty fillet and lower shoreface of the north beach (R218) near the upper fillet reservoir. For the south domain, the model reproduced deposition onto the upper shoreface of the beaches from R7 to R8, R16 to R18, and R25 to R30. Besides the inner ebb shoal, significant scour (up to -1 m or -3 ft) was predicted at the tip of the north and south jetties, and along the channel banks. Erosion up to -0.5 m (-2 ft) also occurred on the upper shoreface of the north beach (R215-R218), and on the upper shoreface from R4 to R16 and from R22 to R25 (south domain).

In the run from July to December 2011 (Figure 74, left), significant deposition (up to +4 ft or 1.2 m) was observed on the outer ebb shoal, in the flood shoal and onto the lower shoreface between R2 and R5. Deposition of smaller magnitude (up to +3 ft or +1 m) also occurred on the lower shoreface in the south domain and near the north jetty fillet and upper north fillet reservoirs in the north domain (R218-219). Scour up to -4 ft (-1.2 m) was predicted at the edge of the inlet channel and on the inner part of the ebb shoal, and to a lesser extent along the nearshore reef outcrops in the south domain. The above observations were consistent with plots of current velocity, which highlighted the strongest currents in the inlet channel and throat. This verified that the zones experiencing extreme morphologic changes corresponded to high energy zones.

For the two modeling time periods, predicted sedimentation patterns were in good agreement with measured data (right panel of Figure 73 and Figure 74). The model was particularly successful in reproducing the sand deposition on the north fillet reservoirs, in the sand trap and on the shoreface in the south part of the domain, which are characterized by hard-bottom through nearshore reef. On a larger scale, model results showed deposition at R16 and beyond which suggested that large sand bodies moving alongshore were trapped by within complex reef morphology. This was evident in the measured data and the pattern was observed in previous studies (Zarillo et al., 2011).However, the model failed to represent the sedimentation patterns in the flood shoal area as well as the intense scour along the north jetty and adjacent shoreface near R219 during that time period. For both time periods, the model overestimated the changes on the ebb shoal (too much scour at ebb jet) and too much deposition on the lower ebb shoal. These

issues are investigated later in the section by using multiple sediment grain sizes as input to the sand transport calculations, as well as by increasing the coverage of hard bottom. All above changes can be verified by the volumetric changes of the individual inlet reservoirs extracted from the model runs for the two above time periods (Tables 20 through 22).

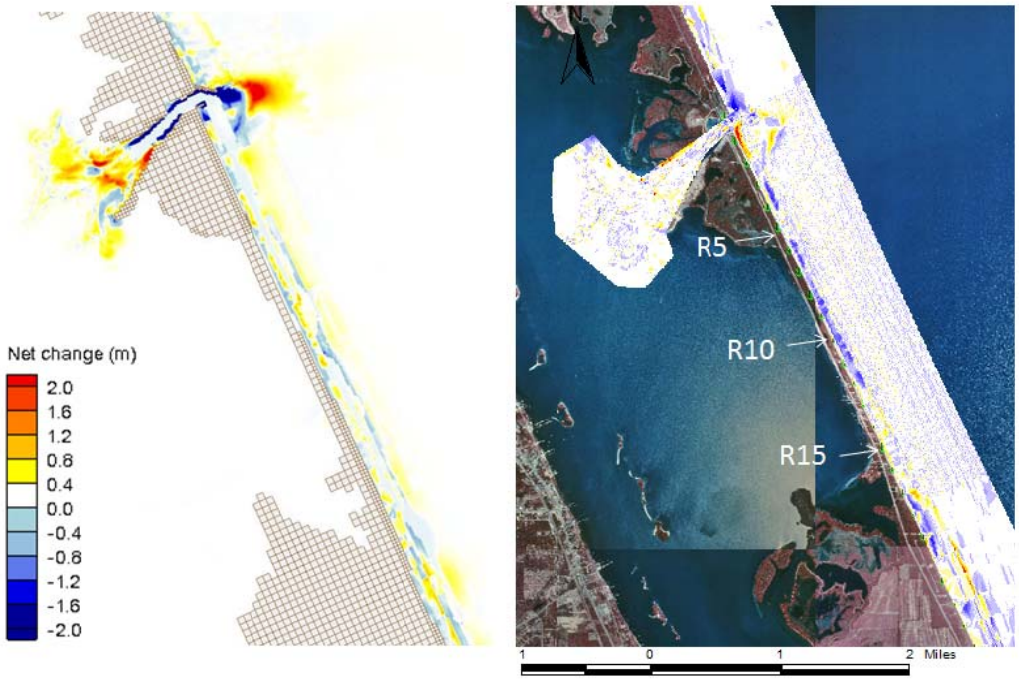

Figure 73. CMS model simulation of net topographic change for January 2011 to June 2011 using variable grain size (left) and measured changes (right)

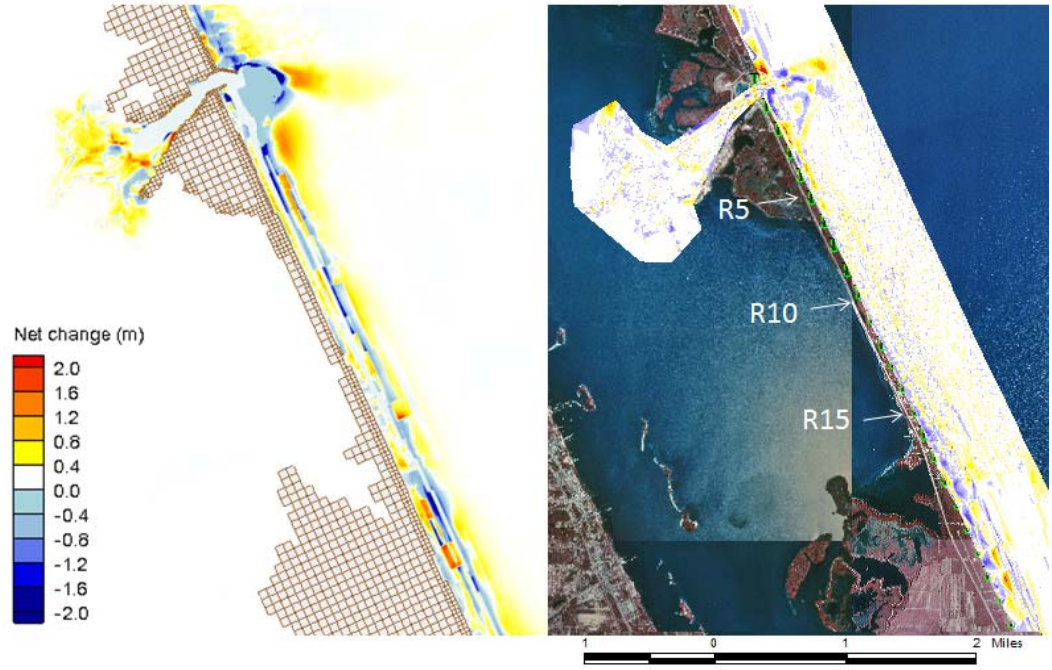

Figure 74. CMS model simulation of net topographic change for June 2011 to December 2011 using variable grain size (left) and measured changes (right)

The influence of variable grain size input into the model calculations for the two time periods considered is presented in Figure 75. The Figure shows that using multiple grain sizes helped refining the morphologic changes around the ebb shoal/bypass bar and the lower shoreface between R2 and R5, which were the zones experiencing the largest predicted morphologic changes. As suggested by Figure 72, these zones were characterized by coarser material (D50). The use of multiple grain sizes did not change the net topographic predictions as much in the other reservoirs of the domain, which are composed of finer sediment. The reduction of scour within the ebb shoal and inlet throat by using a variable grain size (either D50 only or multiple D's) is exemplified in the volumetric analysis below. Additional fine tuning of the model in this dynamic area was performed by selecting additional hard bottom cells to control the erosion and therefore amount of material available for transport and deposition.

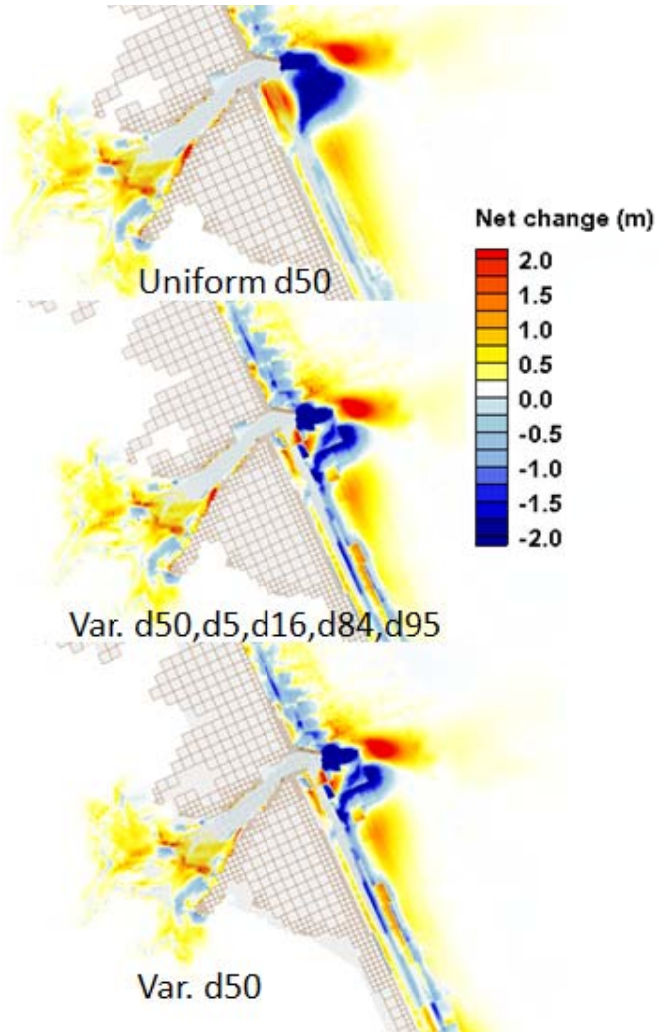

Figure 75. Influence of variable grain size input on morphologic change calculations (summer 2011 run)

The influence of extending the hard bottom within the inlet back bay is illustrated in Figure 76. Increasing the number of hard-bottom cells not only reduced the scour within the inlet channel but also reduced the deposition onto the shoals, therefore providing more realistic results. The model was successful in simulating the hard-bottom zones in the inlet channel by preventing strong currents from scouring the channel.

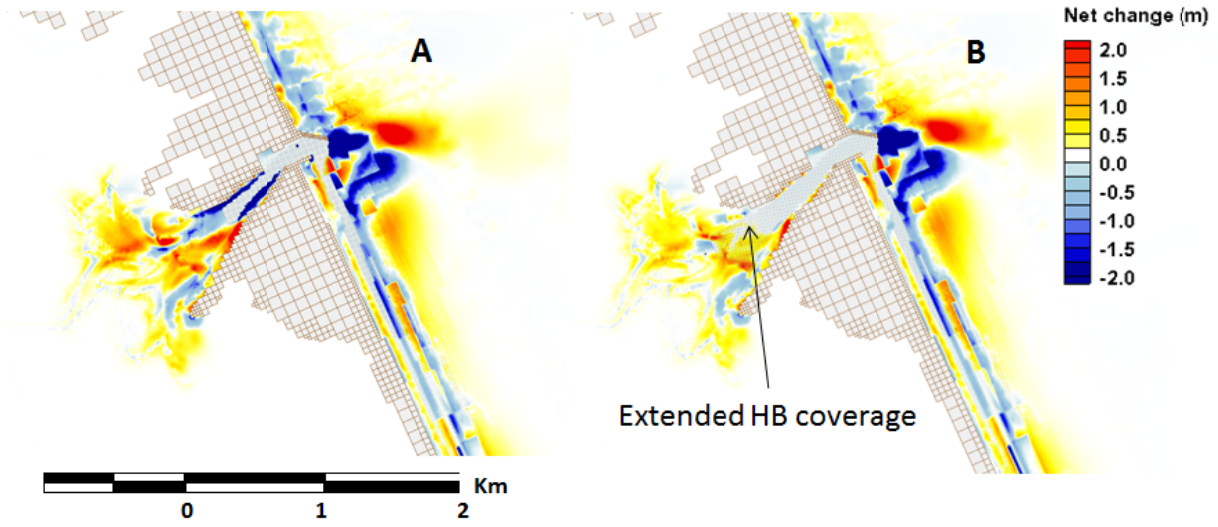

Figure 76. Influence of extending the hard bottom into the inlet back-bay

11.4 Volumetric analysis

Individual inlet reservoirs

Predicted volume changes for the individual inlet domains (see Figure 64) are presented in the following section. The cells were the same as those used in the volumetric analysis section. The results are presented for two time periods corresponding to the model simulations (Table 13 through Table 15)

As shown in Table 20, there was a large variability in the predicted net volume changes for most of the reservoirs in the January to June 2011 runs, particularly as a function of the grain size input. Predicted net volume changes for the south beach varied from +7,579 m^3 to -17,172 m^3 (+9,912 cu. yd. to -22,460 cu. yd.) for the uniform grain size and multiple grain size (5GS), respectively. For the south fillet, predicted net volume change reached -12,642 m^3 or -16,535 cu. yd. (uniform GS) and -9,941 m^3 or -13,002 cu. yd. (5GS). Volume changes remained small for those reservoirs even though the numbers did not match the measured data. Volume changes for the ebb shoal were largely negative and reached -72,455 m^3 or -94,767 cu. yd. under uniform grain size input for sand transport calculations, which decreased to -41,855 m^3 or 54,744 cu. yd. for the multiple grain size (5GS) calculations.

As noted earlier in the predicted morphologic changes section, the use of multiple grain sizes significantly helped reducing the scour in the ebb shoal area which is characterized by coarser grain sizes. However, the model still tremendously overestimated the scour in that zone. In reverse, predicted volume changes for the outer ebb shoal were much larger than the measured changes, and reached +181,609 m^3

(+237,535 cu. yd.) for sand transport calculations with a uniform grain size. Volume changes calculated using multiple grain sizes (5GS) decreased to +99,753 m^3 or +130,471 cu. yd.

For the sand trap, predicted net volume changes reached +88,996 m^3 (+116,402 cu. yd.) as opposed to a measured volume change of +10,130 m^3 (+13,249 cu. yd.). Predicted volume changes for the north fillet varied between -60,557 m^3 (-79,205 cu. yd.) for calculations using multiple grain sizes (5GS) and -102,179 m^3 (-133,645 cu. yd.) for calculations using uniform grain size, as compared to measured change of -15,896 m^3 (-20,791 cu. yd.). As suggested by Table 20 , the amount of erosion was also largely overestimated by the model in the inlet throat (-10,853 m^3 or -14,195 cu. yd. for predicted changes vs. -1,618 m^3 or – 2,116 cu. yd. for measured changes).

For the July to December 2011 model runs, the predicted volume changes are presented in Table 14and Table 15. For the volumetric analysis, changes were made within the model grid to control/limit the overestimation of scour/deposition (sedimentation) in the inlet vicinity. The changes included: 1) the use of "variable D50 only" instead of the multiple grain size using 3GS, and 2) the use of a revised grid with 5GS input that incorporated additional hard bottom cells in the ebb shoal area. This process enabled the determination of which sediment grain size fraction really influenced the sand transport/morphology change calculations the most.

Net volume changes for the south beach reached +1,562 m^3 or +2,043 cu. yd. (predicted using 5GS) and -2,110 m^3 or -2760 cu. yd. (measured). For the south fillet, net volume changes varied between -1,209 m^3 or -1,581 cu. yd. (predicted using variable D50 only) and -1,850 m^3 or -2,419 cu. yd. (predicted using 5GS and revised hard bottom coverage), while measured changes reached -4,529 m^3 or -5,923 cu. yd.

Table 20. Measured vs. predicted volume changes for the inlet reservoirs (January to June 2011 model run)

Reservoir	RUN/CASE	Net volume change (m3)	Area (m2)	Normalized change
South beach	Uniform GS	7579.00	112400	0.07
	Varying 1: 5 GS	-9139.76		-0.08
	Varying 2: 3 GS	-17172.00		-0.15
	Measured	10057.03		0.09
South fillet	Uniform GS	-12642.90	18400	-0.69
	Varying 1: 5 GS	-9941.00		-0.54
	Varying 2: 3 GS	-13417.00		-0.73
	Measured	3824.54		0.21
Ebb shoal	Uniform GS	-72455.00	188000	-0.39
	Varying 1: 5 GS	-41855.90		-0.22
	Varying 2: 3 GS	-104610.00		-0.56
	Measured	2423.64		0.01
Outer ebb	Uniform GS	181609.00	519200	0.35
	Varying 1: 5 GS	99753.00		0.19
	Varying 2: 3 GS	213221.00		0.41
	Measured	-2555.70		0.00
Attachment bar	Uniform GS	6540.00	75312	0.09
	Varying 1: 5 GS	2491.00		0.03
	Varying 2: 3 GS	-1827.00		-0.02
	Measured	-6518.40		-0.09
Sand trap	Uniform GS	88996.00	220000	0.46
	Varying 1: 5 GS	102034.00		0.40
	Varying 2: 3 GS	100810.00		0.46
	Measured	10130.23		0.05
Upper North fillet	Uniform GS	-2942.00	421600	-0.01
	Varying 1: 5 GS	-1523.00		0.00
	Varying 2: 3 GS	2865.00		0.01
	Measured	-40340.32		-0.10
Flood shoal	Uniform GS	129893.00	1382800	0.09
	Varying 1: 5 GS	44527.00		0.03
	Varying 2: 3 GS	122865.00		0.09
	Measured	-3546.94		0.00
North fillet	Uniform GS	-102709.00	44800	-2.29
	Varying 1: 5 GS	-60557.00		-1.35
	Varying 2: 3 GS	-96914.00		-2.16
	Measured	-15896.94		-0.35
Throat	Uniform GS	-10853.00	37500	-0.29
	Varying 1: 5 GS	-13058.00		-0.35
	Varying 2: 3 GS	-20741.00		-0.55
	Measured	-1618.59		-0.04

For the ebb shoal, net volume changes ranged from -83,812 m^3 or -109,621 cu. yd. (predicted using 5GS and revised hard bottom) to -358,714 m^3 or -469,180 cu. yd. (predicted using uniform grain size). Measured volume changes were minimal and reached +316 m^3 or +413 cu. yd. Even if the model still overestimated the volume changes, the use of multiple (5GS) grain size input along with the updated hard-bottom coverage significantly decreased the volume changes. The same trends were observed for the outer ebb reservoir. Net changes ranged from +120,657 m^3 or +157,813 cu. yd. (predicted using uniform grain size) to +146.194 m3 or +191,214 cu. yd. (predicted using variable D50 only). Net changes were reduced to -12,172 m^3 or -15,920 cu. yd. with the use of variable 5GS and the updated hard-bottom coverage, allowing for a better match with measured data (-86 m^3 or -112 cu. yd.).

Net volume change calculations for the sand trap (Table 22) also indicated model overestimation with predicted volumes (using uniform and variable D50 only) in the order of 6 to 7 times larger than measured changes (+11,879 m^3 or +15,537 cu. yd.). This diffeence decreased when the multiple grain size input was used, with predicted net changes reaching +31,544 m^3 or +41,257 cu. yd.

Overall, there was less variability in the net volume changes among reservoirs for the summer 2011 time period. For most of the reservoirs, the volume increase/gain trend was reproduced in the summer 2011 simulations even though the model largely overestimated sand deposition in the reservoir. Overall, volume change differences between predicted and measured decreased with the use of multiple grain sizes in the sand transport formula. It must be noted that the difference between “variable D50 only” and multiple GS was not significant, which suggested that D50 is the controlling grain size/parameter in sedimentation control.

Table 21. Measured vs. predicted volume changes of inlet reservoirs (July 2011 to December 2011 model run)

Reservoir	RUN/CASE	Net volume change (m3)	Area (m2)	Normalized change
South beach	Uniform GS	67673.50	111875	0.60
	Varying 1: 5 GS	1562.70		0.01
	Varying 2: var. D50 only	1561.90		0.01
	Varying 3: 5GS HB rev. ebb	-33019.00		-0.30
	Measured	2110.12		0.02
South fillet	Uniform GS	2071.10	18437.5	0.11
	Varying 1: 5 GS	-1209.40		-0.07
	Varying 2: var. D50 only	-1209.20		-0.07
	Varying 3: 5GS HB rev. ebb	-1850.60		-0.10
	Measured	-4529.77		-0.25
Ebb shoal	Uniform GS	-358714.00	188906	-1.90
	Varying 1: 5 GS	-231973.00		-1.23
	Varying 2: var. D50 only	-231981.00		-1.23
	Varying 3: 5GS HB rev. ebb	-83812.00		-0.44
	Measured	316.40		0.00
Outer ebb	Uniform GS	120657.00	522344	0.23
	Varying 1: 5 GS	146194.00		0.28
	Varying 2: var. D50 only	146214.00		0.28
	Varying 3: 5GS HB rev. ebb	-12172.00		-0.02
	Measured	-86.00		X
Attachment bar	Uniform GS	-4509.30	75312.5	-0.06
	Varying 1: 5 GS	-30473.00		-0.40
	Varying 2: var. D50 only	-30473.00		-0.40
	Varying 3: 5GS HB rev. ebb	-18449.30		-0.24
	Measured	11001.08		0.15

Table 22. Measured vs. predicted volume changes of inlet reservoirs (July 2011 to December 2011 model run)

Reservoir	RUN/CASE	Net volume change (m3)	Area (m2)	Normalized change
Sand trap	Uniform GS	76707.80	220625	0.35
	Varying 1: 5 GS	68587.50		0.31
	Varying 2: var. D50 only	68564.00		0.31
	Varying 3: 5GS HB rev. ebb	31544.50		0.14
	Measured	11879.41		0.05
Upper North fillet	Uniform GS	-7097.00	420377	-0.02
	Varying 1: 5 GS	-3916.00		-0.01
	Varying 2: var. D50 only	-3909.00		-0.01
	Varying 3: 5GS HB rev. ebb	-39005.00		-0.09
	Measured	9124.65		0.02
Flood shoal	Uniform GS	155825.00	1383910	0.11
	Varying 1: 5 GS	152645.00		0.11
	Varying 2: var. D50 only	152647.00		0.11
	Varying 3: 5GS HB rev. ebb	138853.00		0.10
	Measured	-19685.68		-0.01
North fillet	Uniform GS	-67966.00	42968	-1.58
	Varying 1: 5 GS	-76663.00		-1.78
	Varying 2: var. D50 only	-76674.00		-1.78
	Varying 3: 5GS HB rev. ebb	-20648.00		-0.48
	Measured	-6029.59		-0.14
Throat	Uniform GS	-13899.80	37500	-0.37
	Varying 1: 5 GS	-35145.90		-0.94
	Varying 2: var. D50 only	-35148.60		-0.94
	Varying 3: 5GS HB rev. ebb	-7119.00		-0.19
	Measured	2517.98		0.07

11.5 Nearshore Current Analysis

Results of the hydrodynamic model are presented in the Figures below. The Figures highlight the spatial variability in current velocity and direction. Nearshore circulation is presented in Figure 77. The presence of bathymetric features greatly influenced the hydrodynamics and therefore the morphodynamics. This was exemplified by the extraction of cross-sections along the model domain to represent the current magnitude (Figure 78). One cross section was chosen at the Sebastian Inlet gage and the two others on the southern part of the domain. The southern beaches are characterized by nearshore reefs and it is evident that these geomorphic features influence current distribution, mostly by funneling the current in between the reef lines.

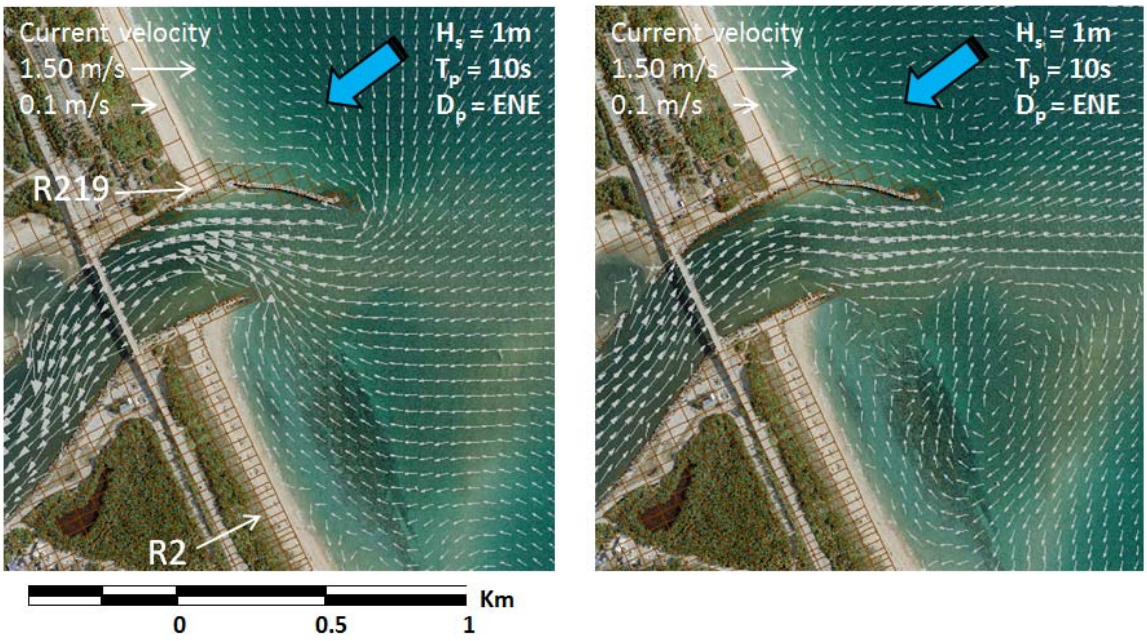

Figure 77.Current velocity vectors near Sebastian Inlet.

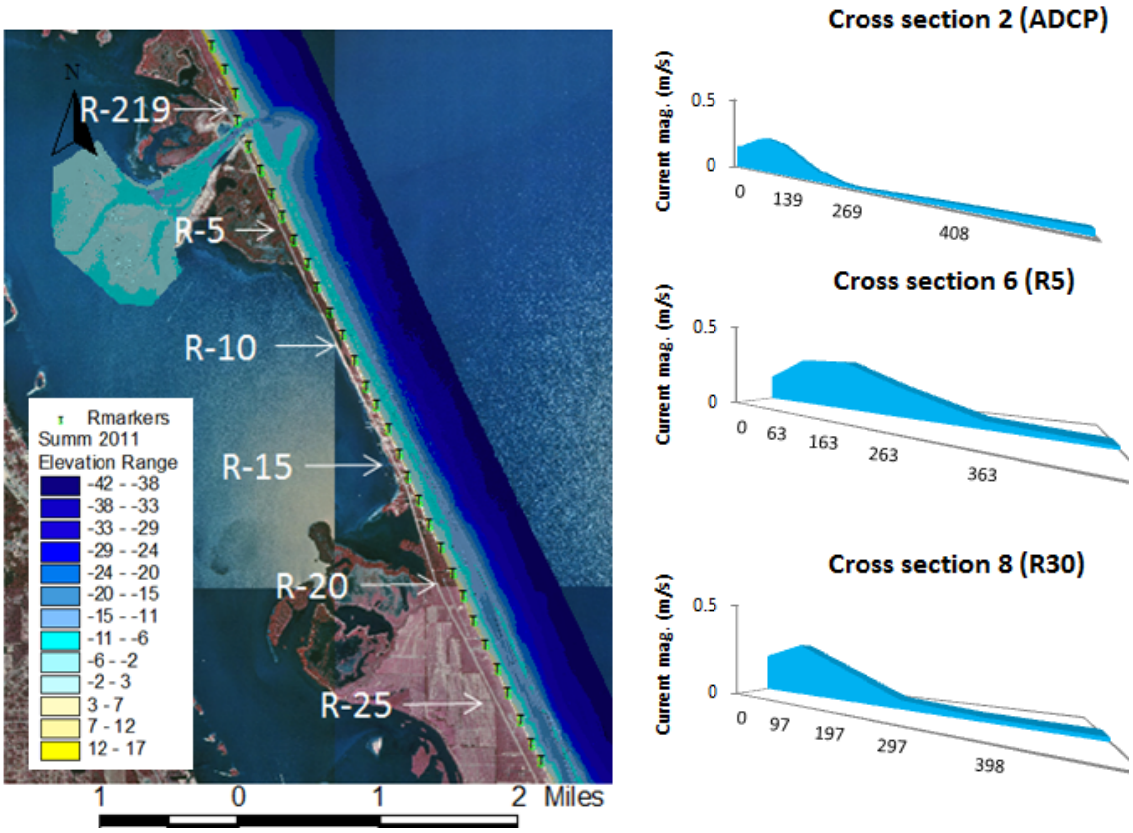

Figure 78. Predicted (CMS) current magnitude cross-section extracted at three stations

Current roses were generated in order to evaluate model performance. As suggested by Figire 79 and Figure 80, the model shows predicted currents focused towards the South East which means the model has been incorporating cross shore current on top of longshore/littoral currents. It can be expected that tagging a cell farther away from nearshore zone would shift the mode to a more southerly direction therefore eliminating some cross shore component.

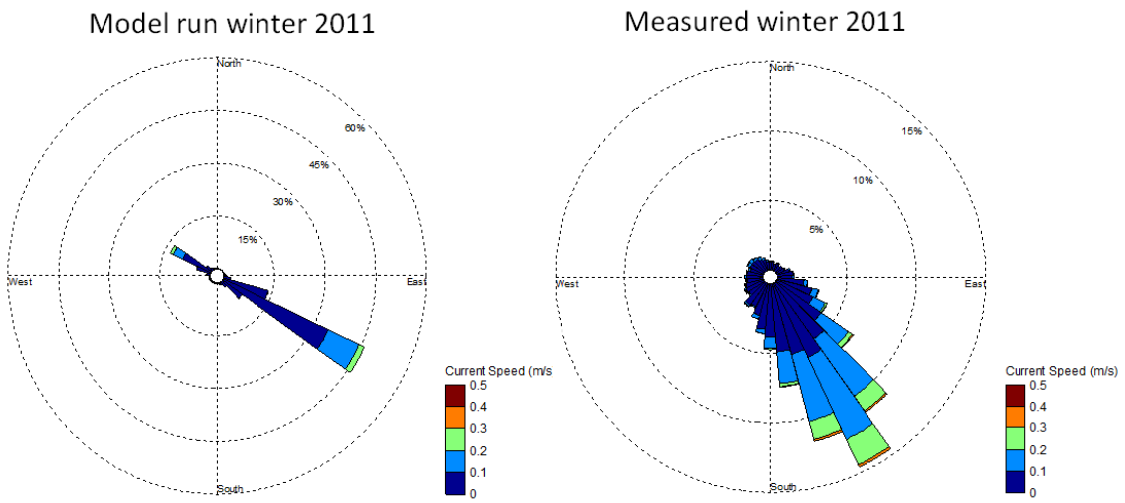

Figure 79. Current rose plots from July to December 2011

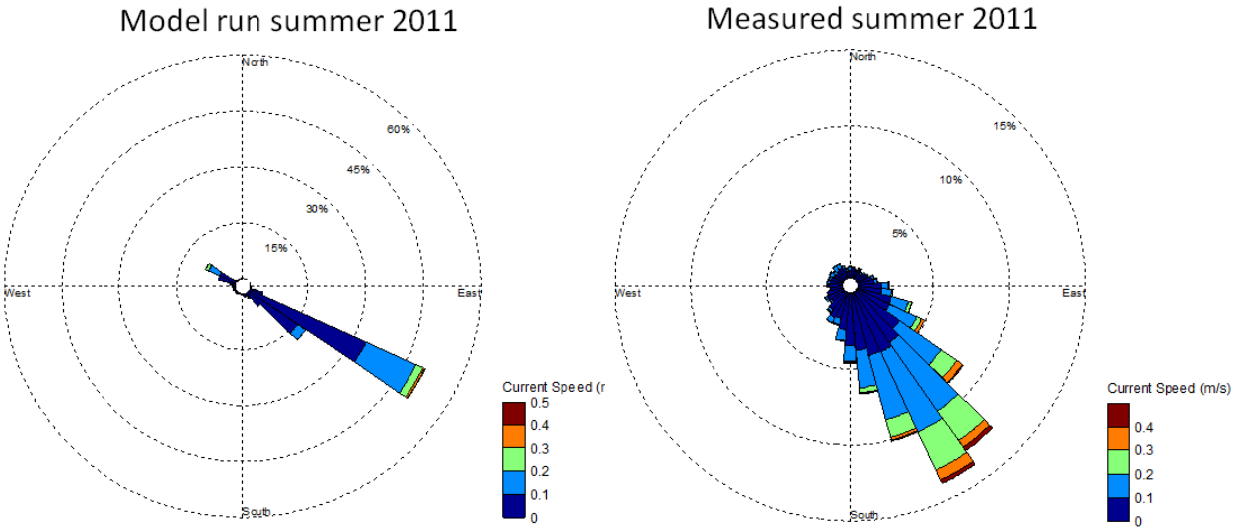

Figure 80. Current rose plots from July to December 2011

12.0 References

Brehin, F.G. and G.A. Zarillo. 2010. Morphodynamic Evolution and Wave Modeling of the Entrance Bar Surfing Break "Monster Hole": Sebastian Inlet, FL. 7th International Surfing Reef Symposium 2010, Sydney, Australia.

Buttolph. A.M., Reed, C.W., Kraus, N.C., Ono, N., Larson, M., Camenen, B., Hanson, H., Wamsley, T., and Zundel, A.K. 2006. Two-dimensional depth-averaged circulation model CMS-M2D: Version 3, Report 2, Sediment transport and morphology change. *ERDC/CHL TR-06-09,* U.S. Army Engineer Research and Development Center, Vicksburg, Mississippi.

Camenen, B., and M., Larson. 2007. A Total Load Formula for the Nearshore. ProceedingsCoastal Sediments '07 Conference, ASCE Press, Reston, VA, 56-67.

Crowell, M., S.P. Leatherman, and M.K., Buckley. 1993. Erosion Rate Analysis: Long Termversus Short Term Data. Shore and Beach, 61 (2):13-20.

Dolan, R., M.S. Fenster, and S.J. Holme. 1991. Temporal analysis of shoreline recession and accretion. Journal of Coastal Research, 7(3):723-744.

USACE. 1994. Engineering Manual for Hydrographic Surveys EM 1110-2-1003 Change 1 (http://www.asace.army.mil) Accessed: October 2010.

Hoeke, R. K. G.A. Zarillo, and M. Synder. 2001. A GIS Based Tool for Extracting ShorelinePositions from Aerial Imagery (BeachTools).*ERDC/CHL CHETN-IV-37*, U.S. Army Engineer Research and Development Center, Vicksburg, MS.

Lin, L., H. Mase, F. Yamada, and Z. Demirbilek. 2006. Wave-Action Balance EquationDiffraction (WABED) model: Tests of wave diffraction and reflection at inlets. ERDC/CHL CHETN-III-73. Vicksburg, MS: U.S. Army Engineer Research and Development Center.

Morton, R. A. 2002. Factors controlling storm impacts on coastal barriers and beaches – Apreliminary basis for real-time forecasting: Journal of Coastal Research (18):486-501.

NOAA National Geodetic Survey (NGS). Coastal Relief Model Offshore Data Sets. (http://www.ngs.noaa.gov) Accessed: October 2010.

Rosati, J.D., Carlson, B. D., Davis, J. E., and T. D., Smith. 2001. "The Corps of Engineers'National Regional Sediment Management Demonstration Program," ERDC/CHL CHETN-XIV-1, U.S. Army Engineer Research and Development Center, Vicksburg, MS.

Rosati, J.D. and N.C., Kraus. 1999. "Formulation of sediment budgets at inlets," CoastalEngineering Technical Note IV-15, U.S. Army Engineer Waterways Experiment Station,Vicksburg, MS.

Rosati, J.D. and N. C. Kraus. 2001. Sediment Budget Analysis System (SBAS). ERDC/CHL. CHETN- XIV-3. U.S. Army Engineering Research and Development Center. Vicksburg, MS.

Ruggiero, P., D, Reid, Kaminsky, G. and J. Allan. 2003. Assessing Shoreline Change TrendsAlong U.S. Pacific Northwest Beaches. July 22 to 26, 2007, Proceedings of Coastal Zone 07, Portland, Oregon.

Tolman, 2010: WAVEWATCH III (R) development best practices Ver. 0.1. NOAA / NWS / NCEP / MMAB Technical Note 286, 19 pp

Wu, W., A. Sanchez, and M. Zhang. 2010. An Implicit 2-D Depth-Averaged Finite-Volume Model of Flow and Sediment Transport in Coastal Waters. June 30 – July 5, 2010, 32nd International Conference on Coastal Engineering (ICCE 2010) Shanghai, China.

Zarillo, G.A. and The Florida Tech Coastal Processes Research Group. 2007. State of Sebastian Inlet Report: An Assessment of Inlet Morphologic Processes, Historical Shoreline Changes, and Regional Sediment Budget, *Technical Report 2007-1*, Sebastian Inlet Tax District, FL.

Zarillo, G.A., Brehin, F.G., and TheFlorida Tech Coastal Processes Research Group. 2009. State of the Inlet Report: An Assessment of Inlet Morphologic Processes, Historical Shoreline Changes, Local Sediment Budget and Beach Fill Performance. Sebastian Inlet Tax District, FL.

Zarillo, G.A., Brehin, F.G, 2010. State of the Inlet Report: An Assessment of Inlet Morphologic Processes, Historical Shoreline Changes, Local Sediment Budget and Beach Fill Performance. Sebastian Inlet Tax District, FL.

Zarillo, G.A. and Bishop, J. 2008. Geophysical Survey of Potential Sand Resources Sebastian Inlet, Florida. Prepared for the Sebastian Inlet Tax District, 29p.

Zarillo, G.A. and Brehin, F.G. 2008. Wave Hind Cast Project Report. Submitted to the Sebastian Inlet Tax District, 18p.

Zarillo, G. A., et. al. "A New Method for Effective Beach Fill Design," *Coastal Zone '85,* 1985.

APPENDIX A: Grain Size Contour Plots: Summer 2011

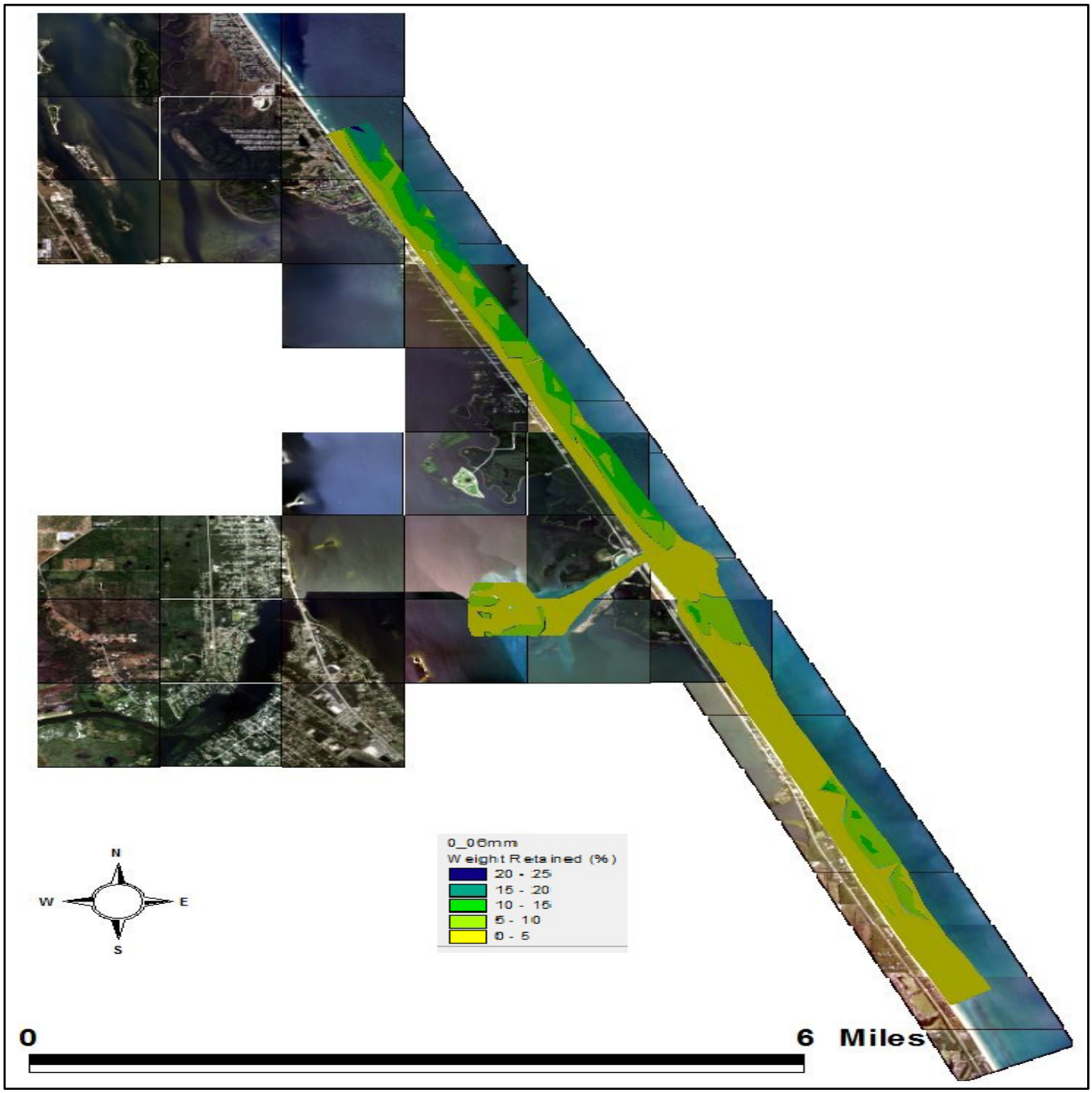

Figure 81. 0.06 mm weight retained (%)

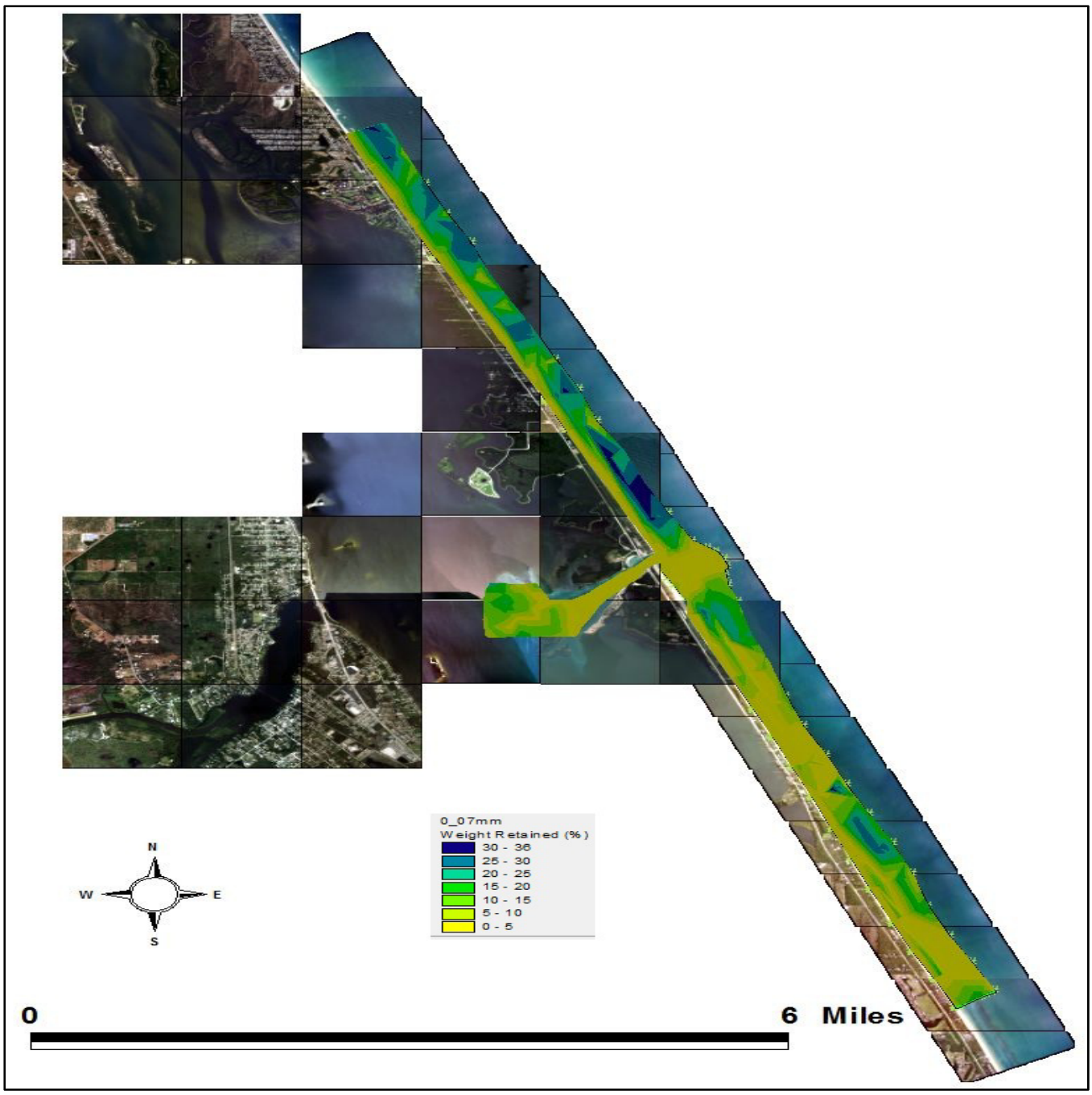

Figure 82. 0.07 mm weight retained (%)

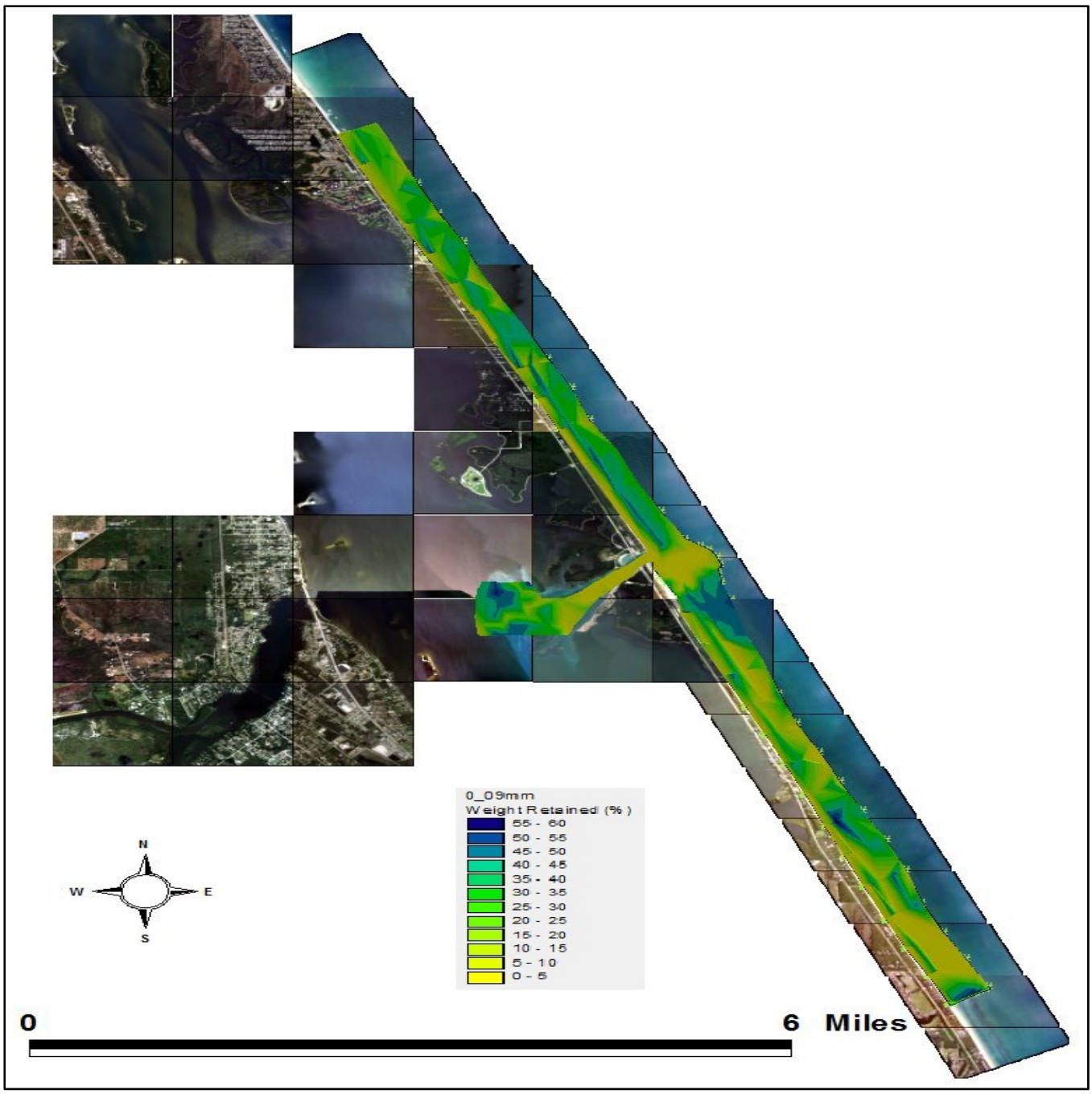

Figure 83.0.09 mm weight retained (%)

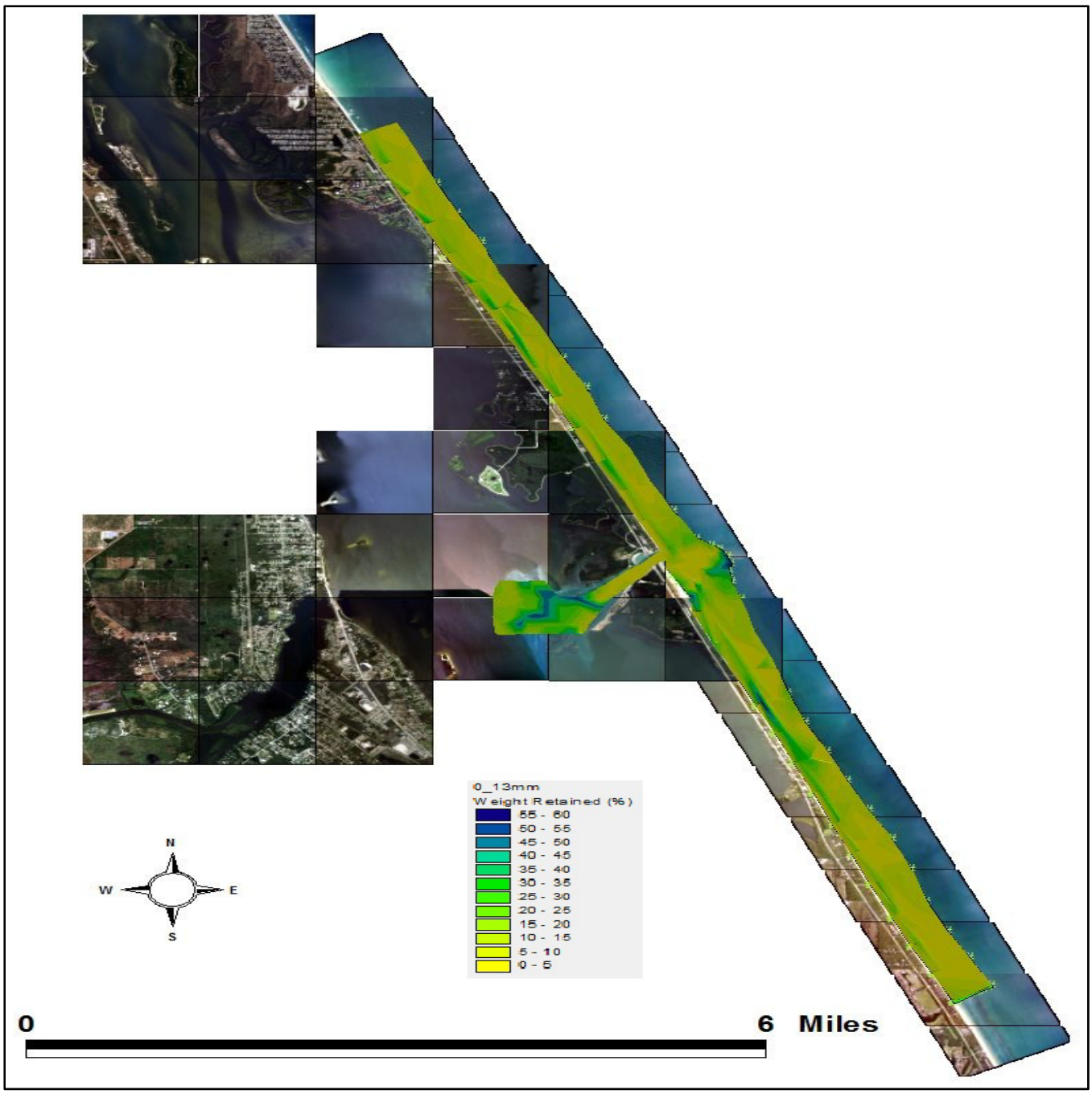

Figure 84.0.13 mm weight retained (%)

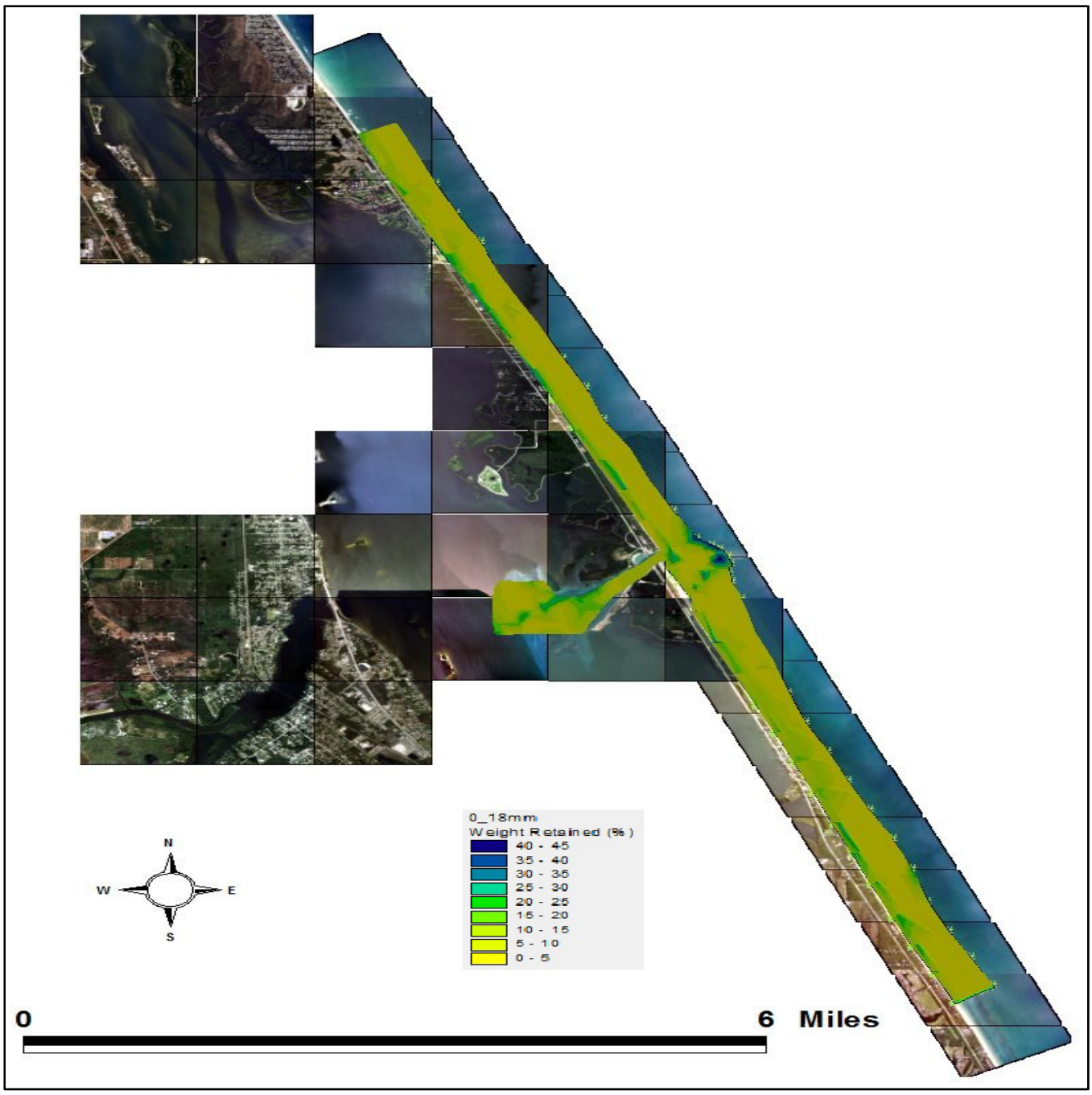

Figure 85. 0.18 mm weight retained (%)

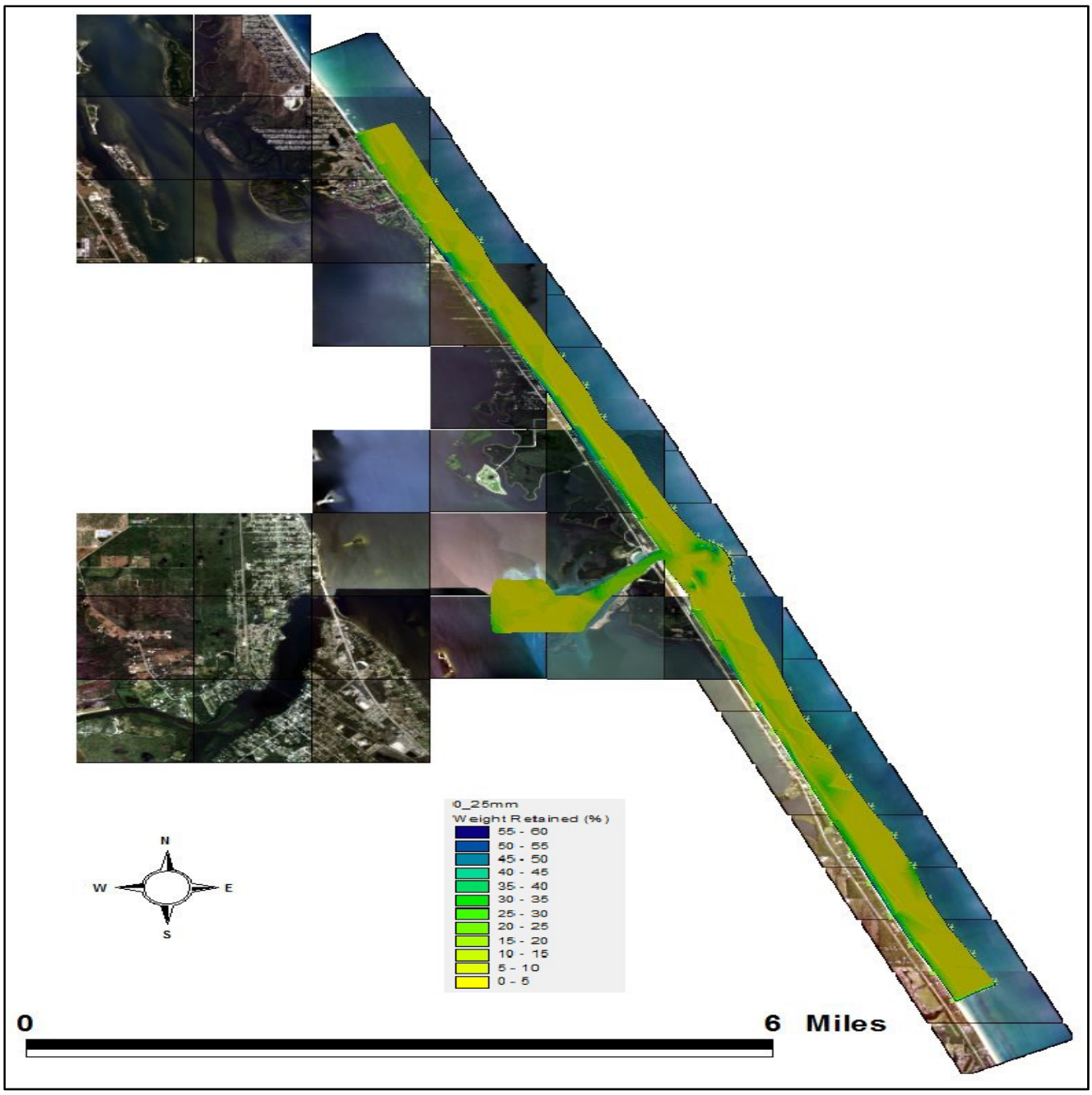

Figure 86. 0.25 mm weight retained (%)

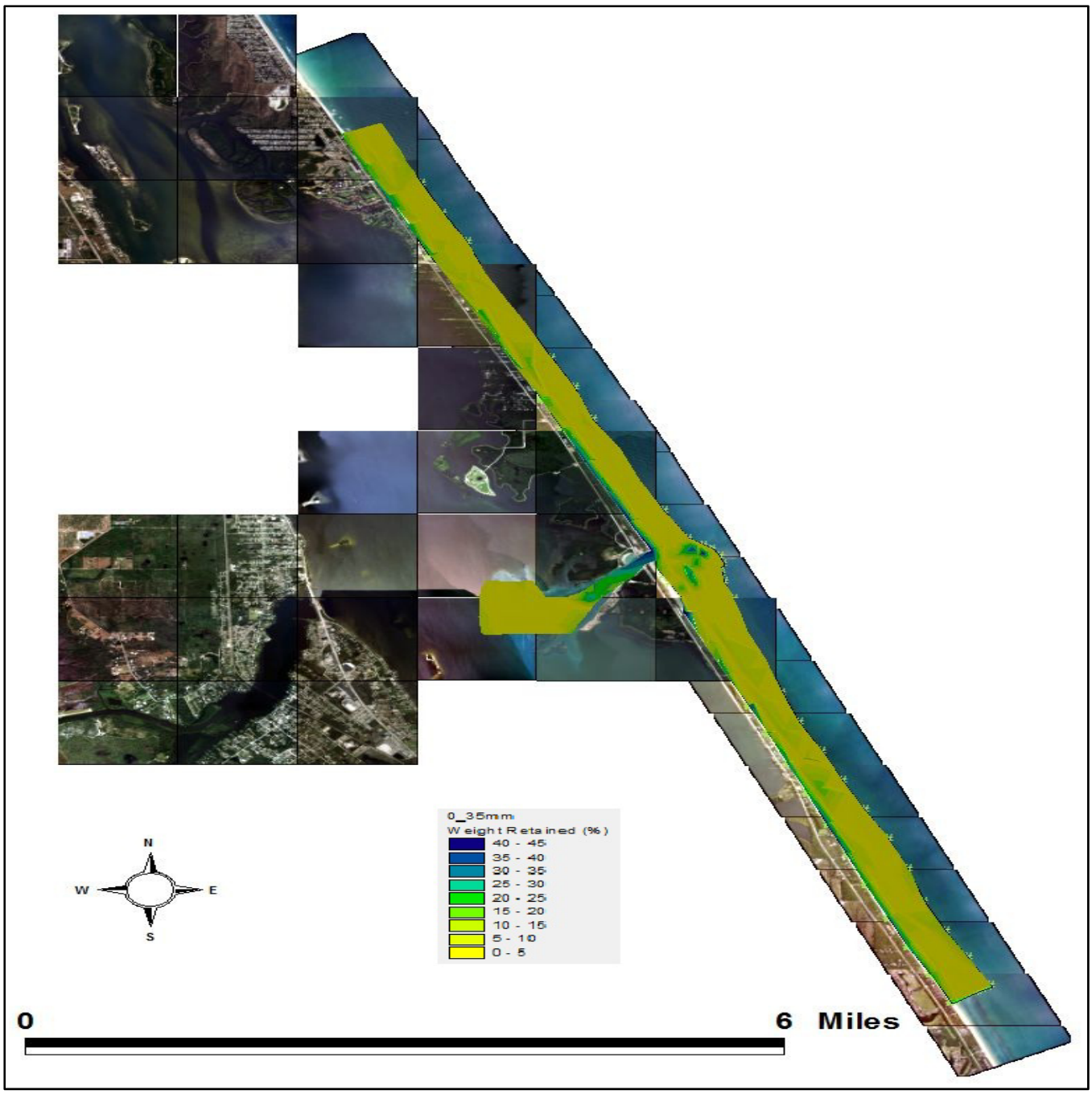

Figure 87. 0.35 mm weight retained (%)

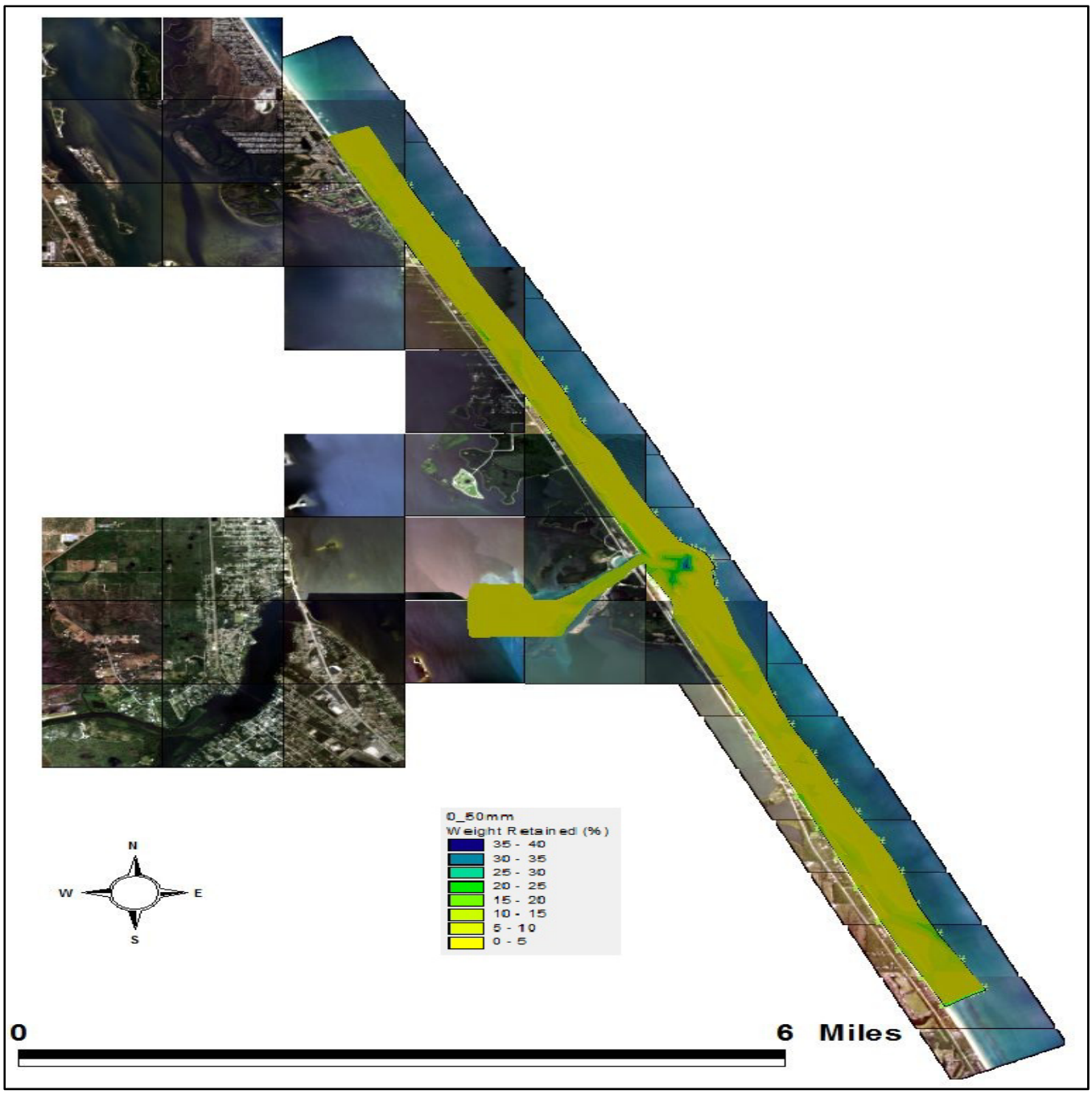

Figure 88. 0.50 mm weight retained (%)

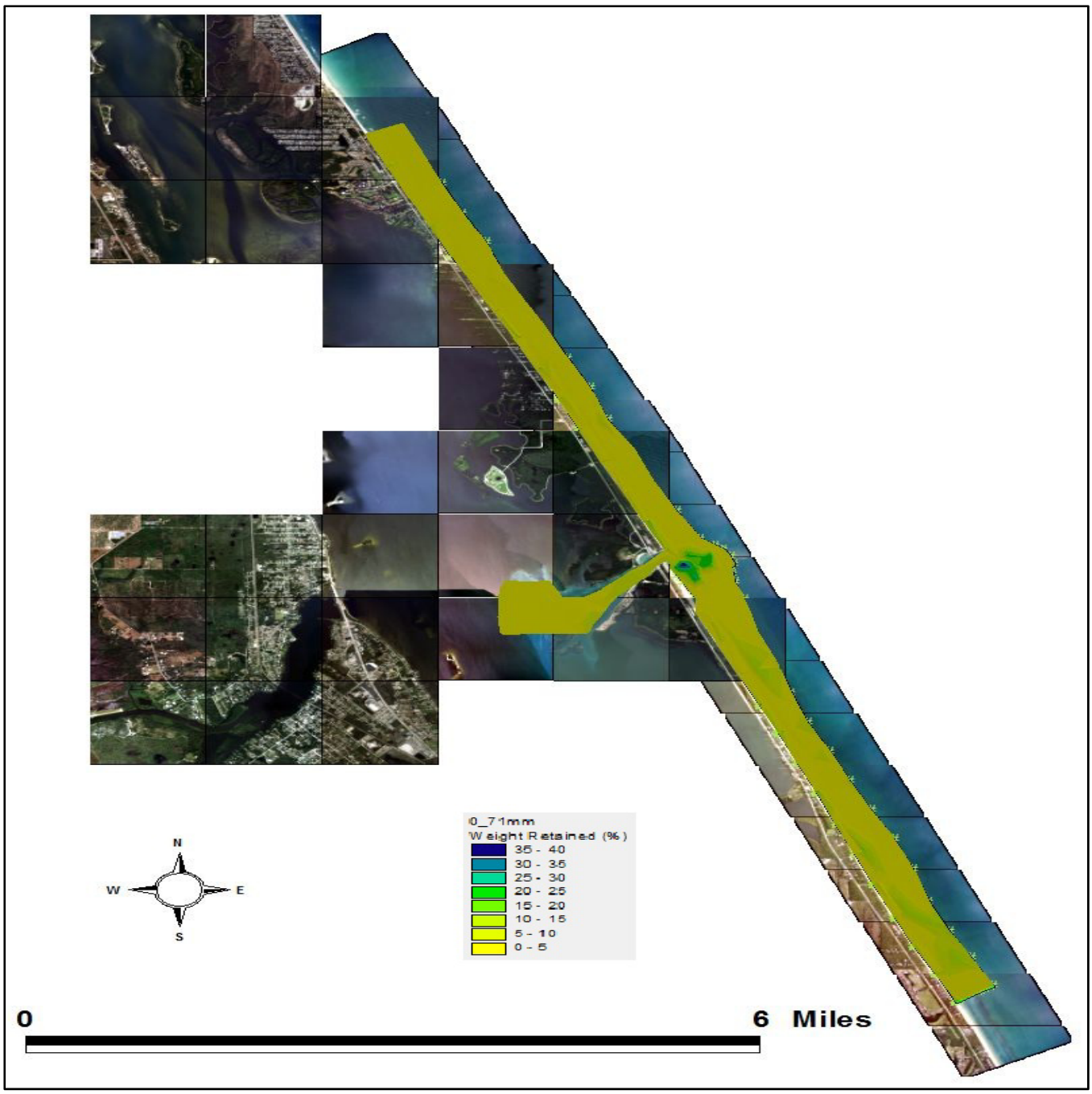

Figure 89. 0.71 mm weight retained (%)

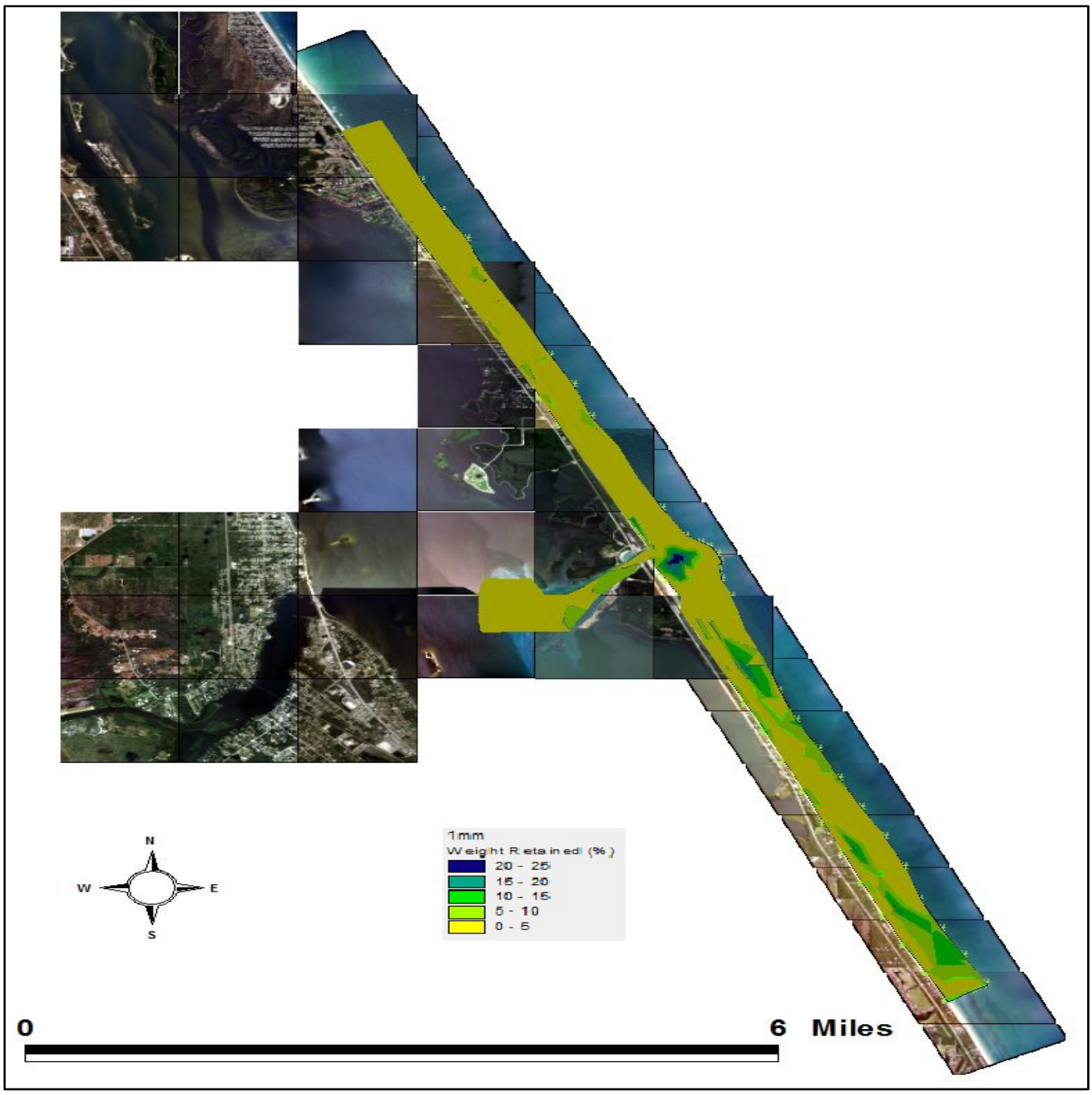

Figure 90. 1 mm weight retained (%)

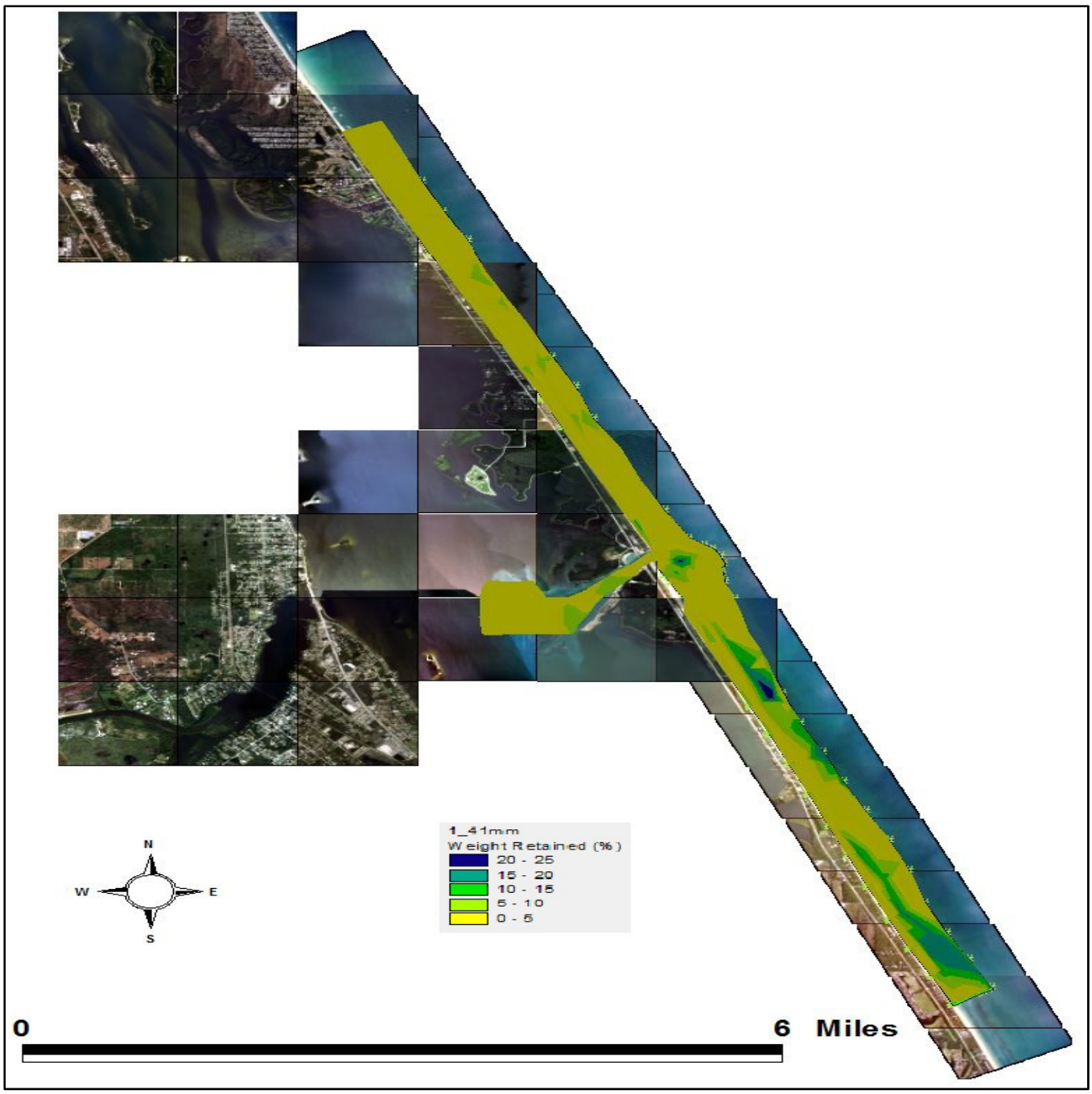

Figure 91. 1.41 mm weight retained (%)

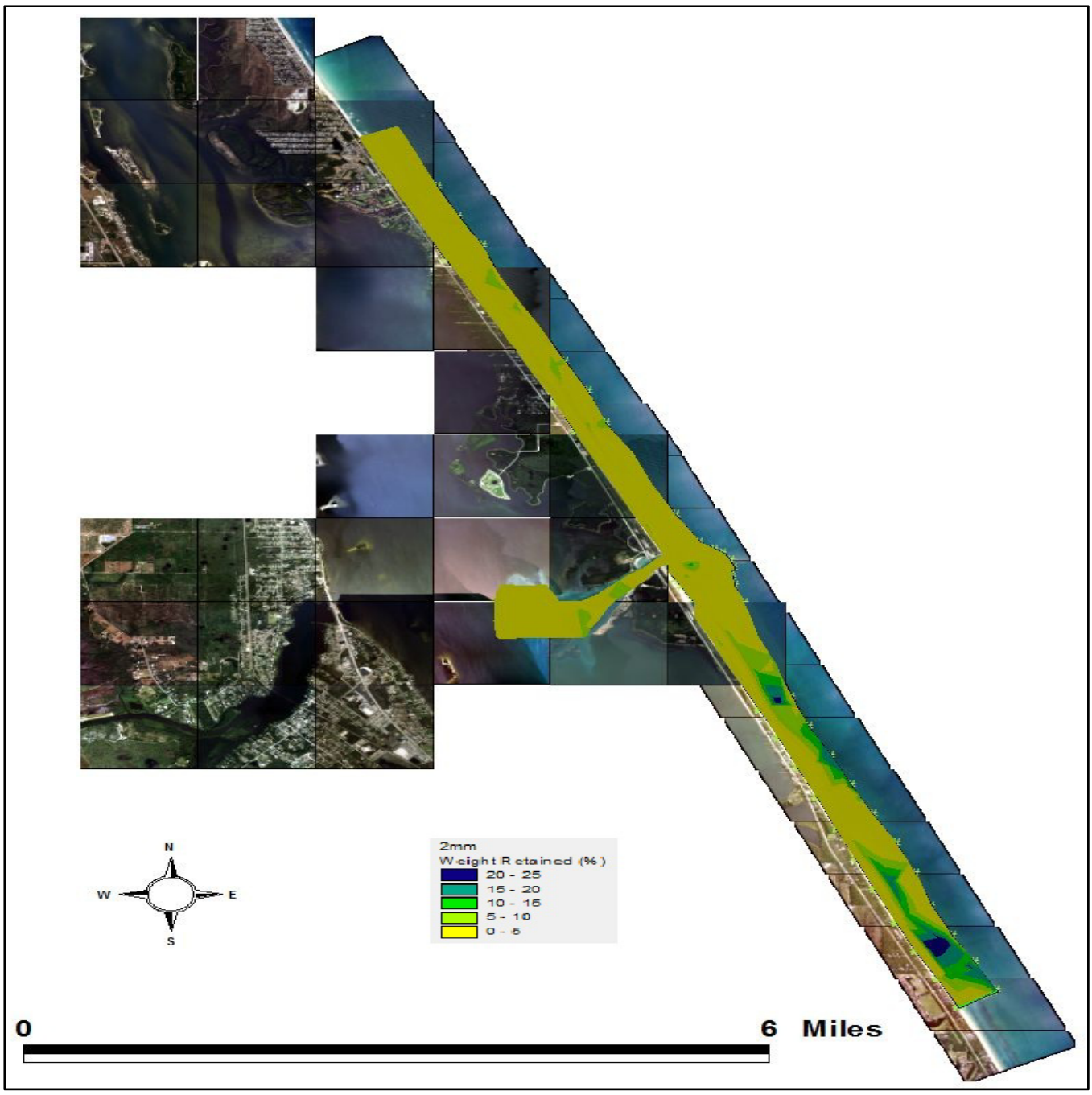

Figure 92. 2 mm weight retained (%)

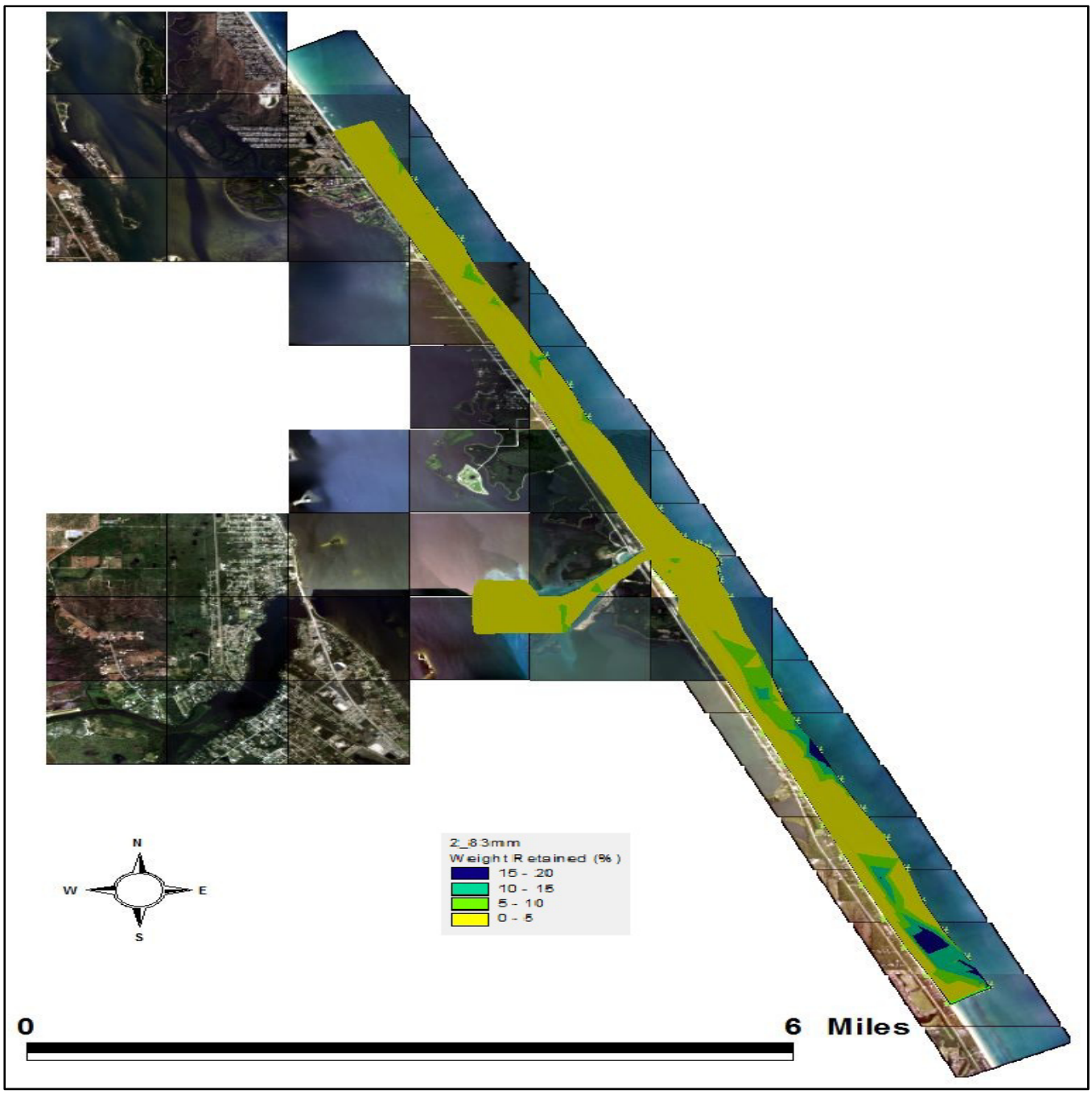

Figure 93. 2.83 mm weight retained (%)

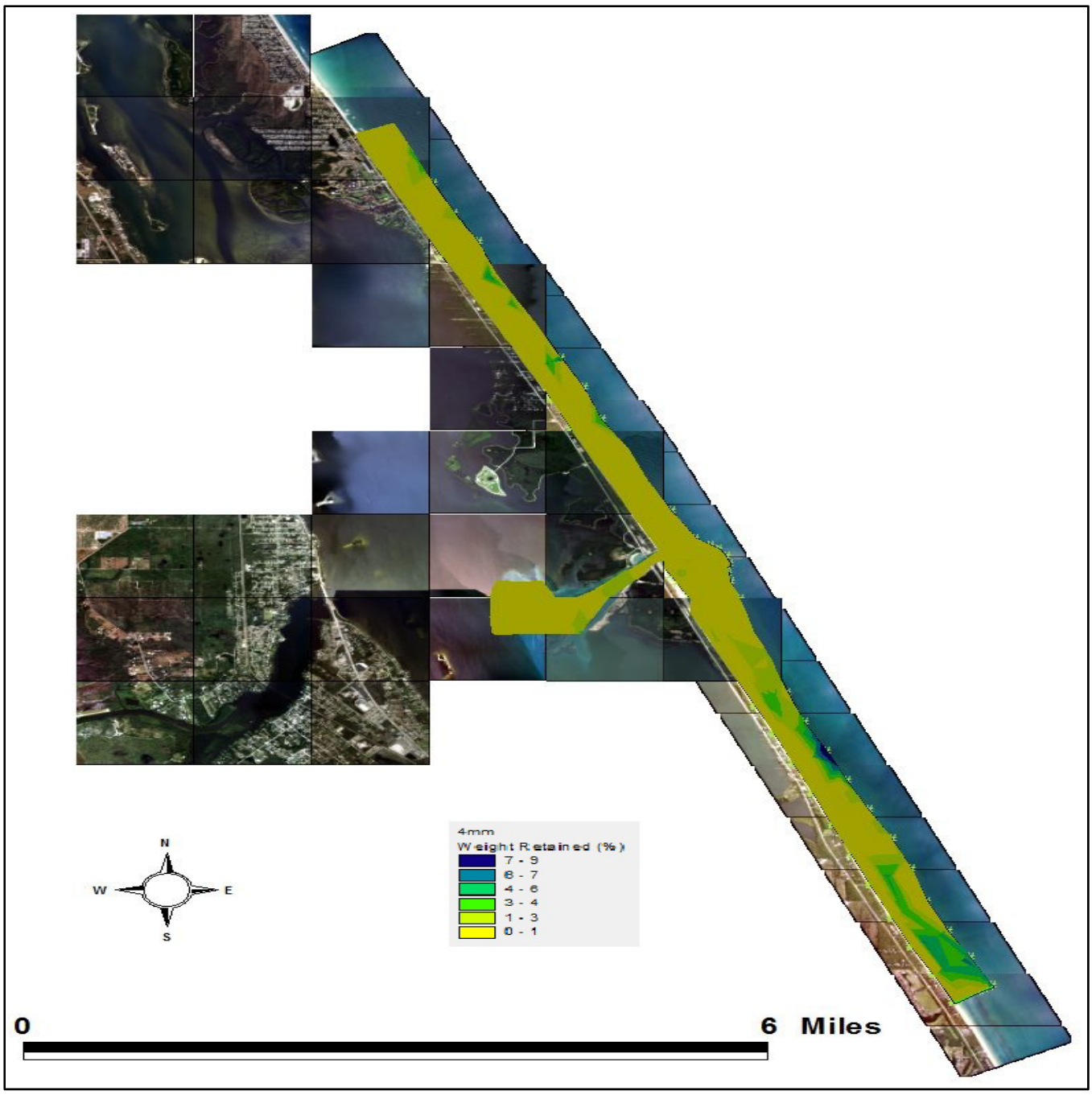

Figure 94. 4 mm weight retained (%)

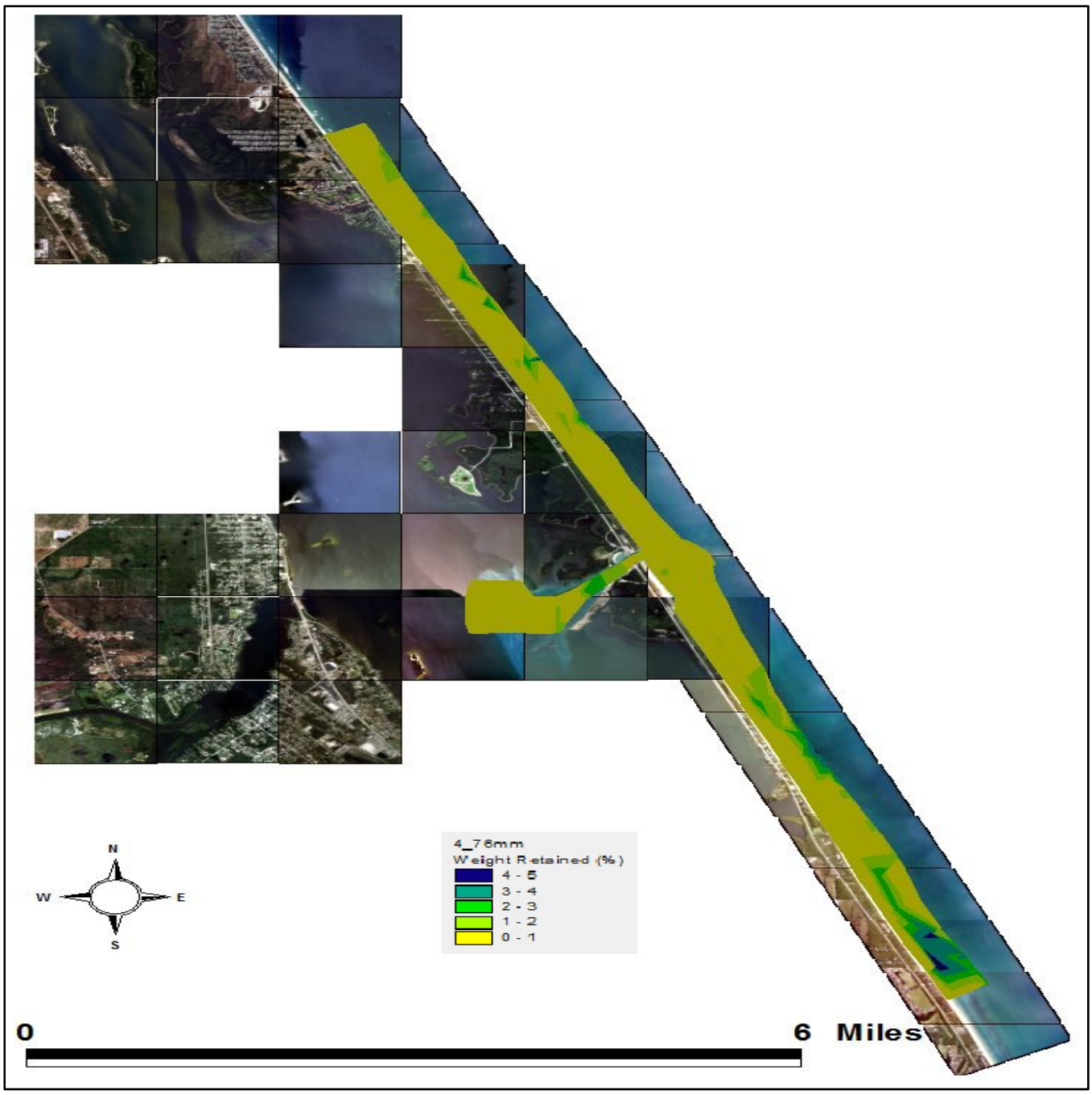

Figure 95. 4.76 mm weight retained (%)

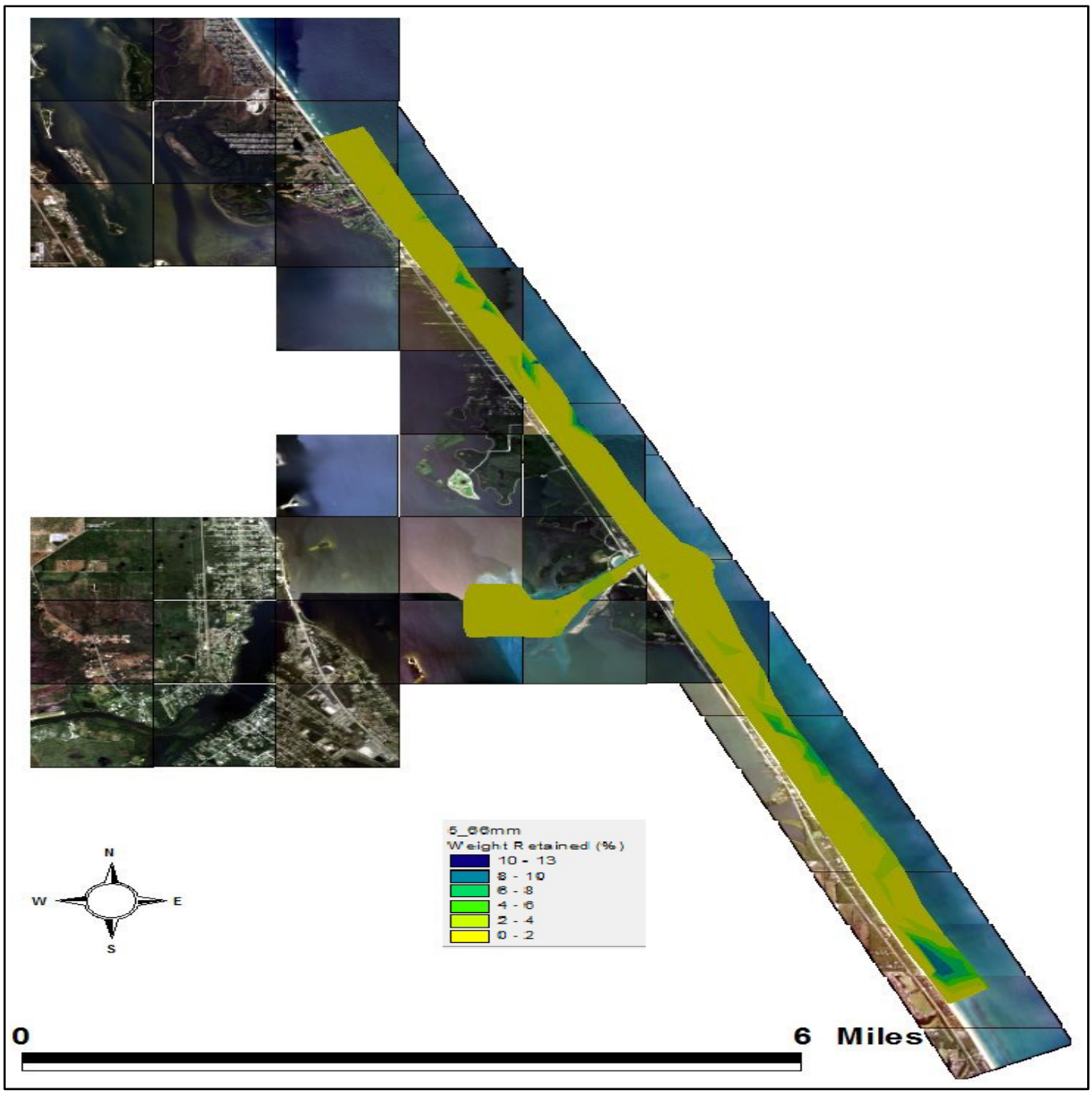

Figure 96. 5.66 mm weight retained (%)

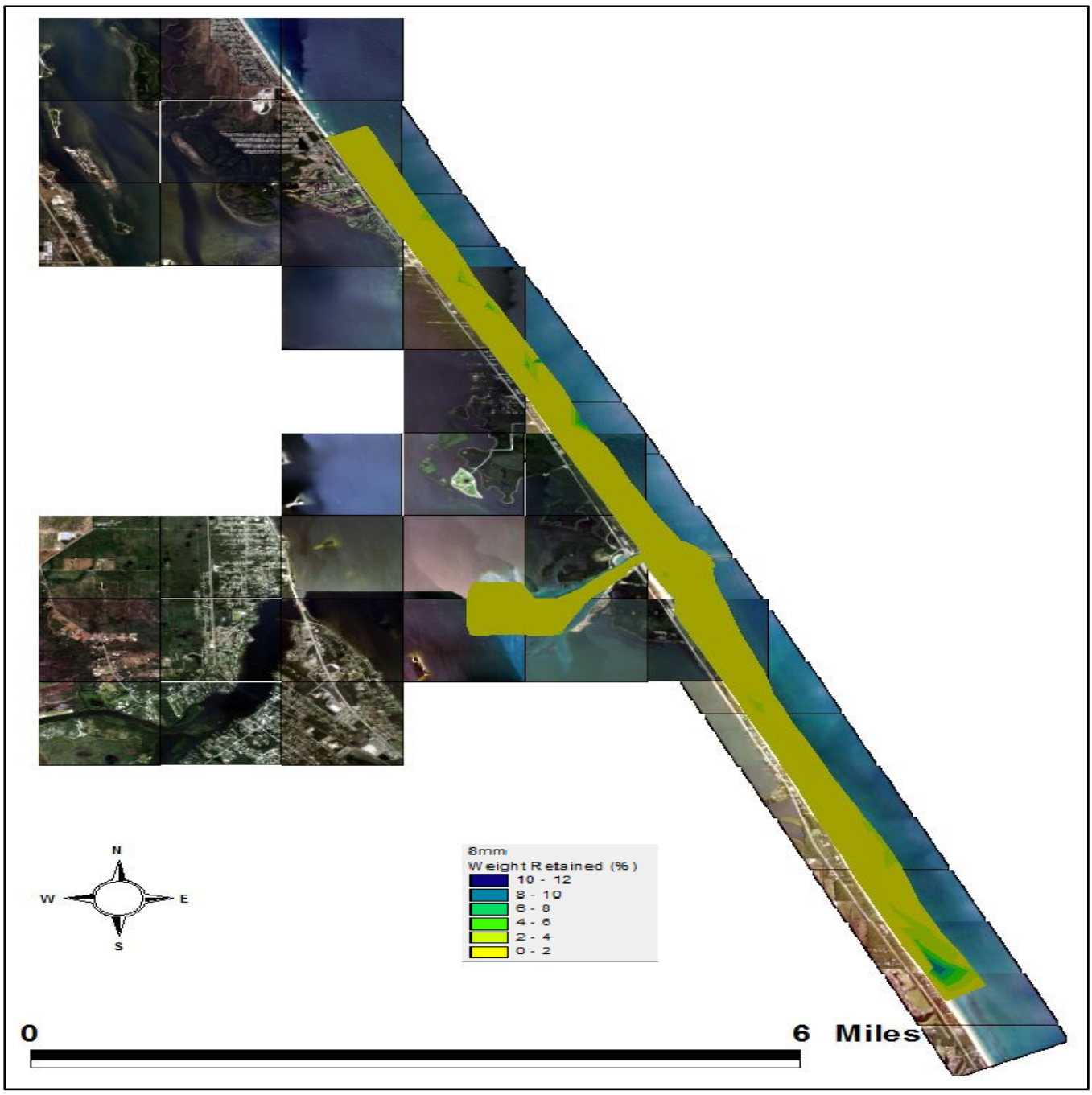

Figure 97. 8 mm weight retained (%)

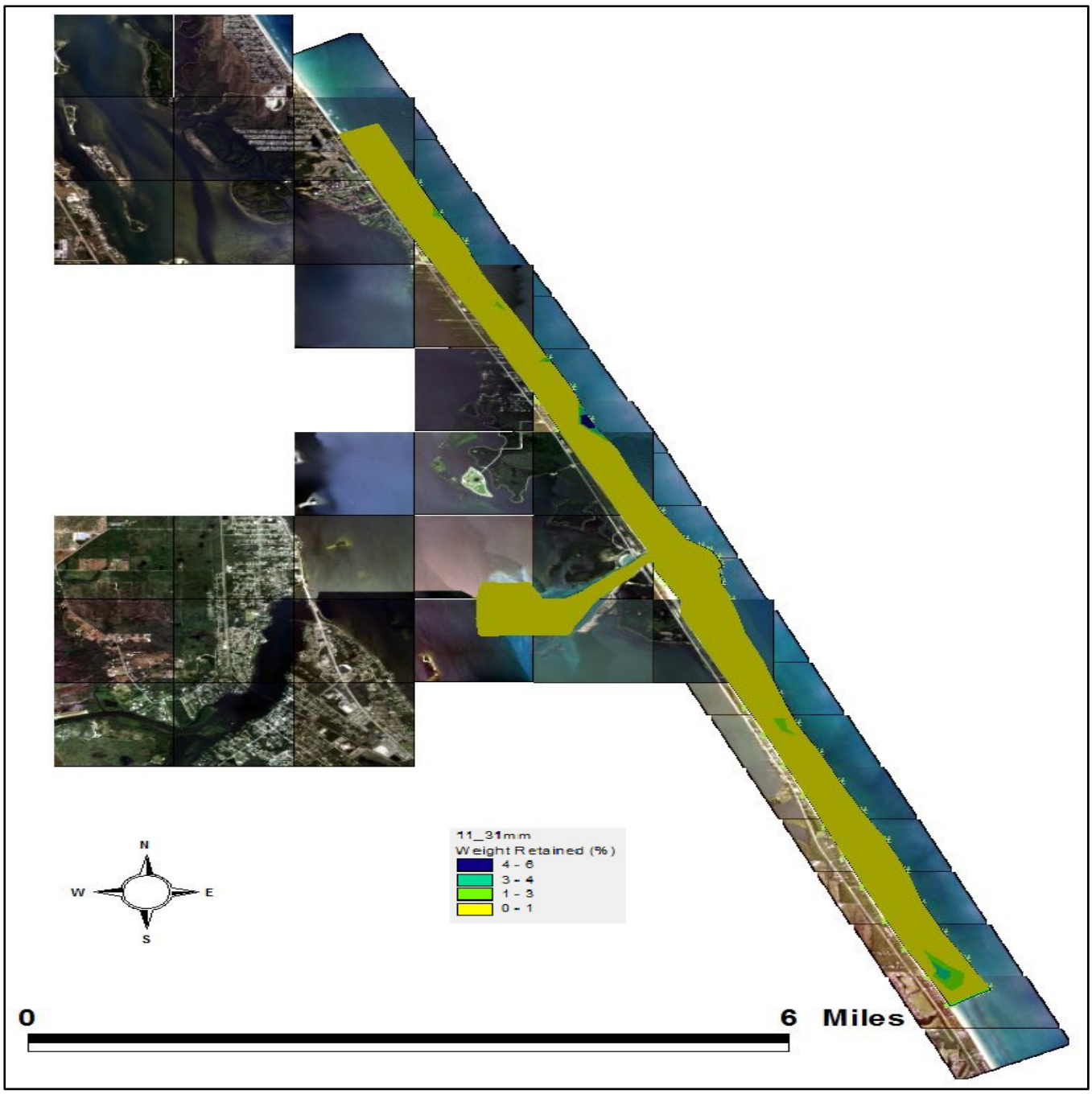

Figure 98. 11.31 mm weight retained (%)

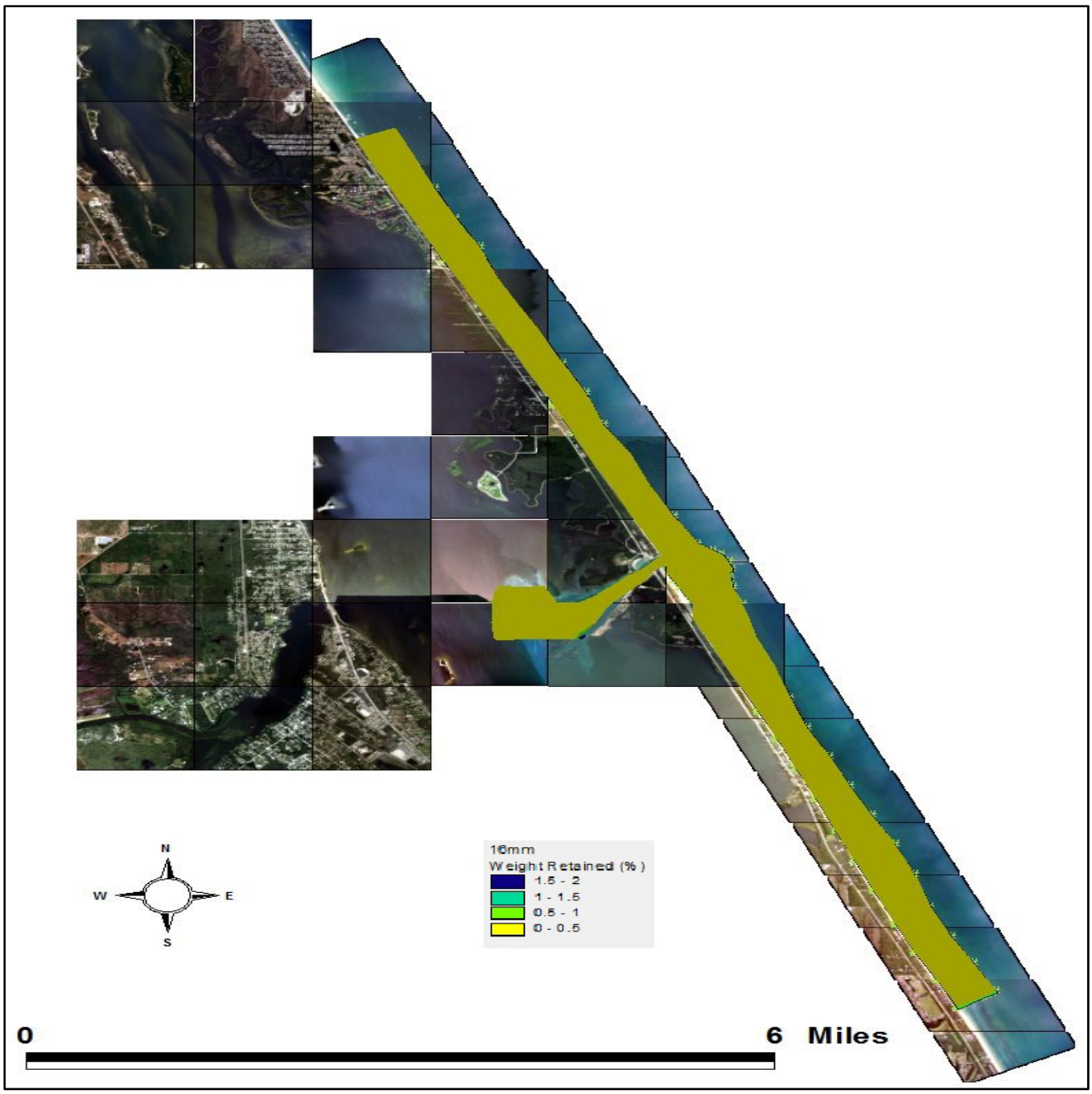

Figure 99. 16 mm weight retained (%)

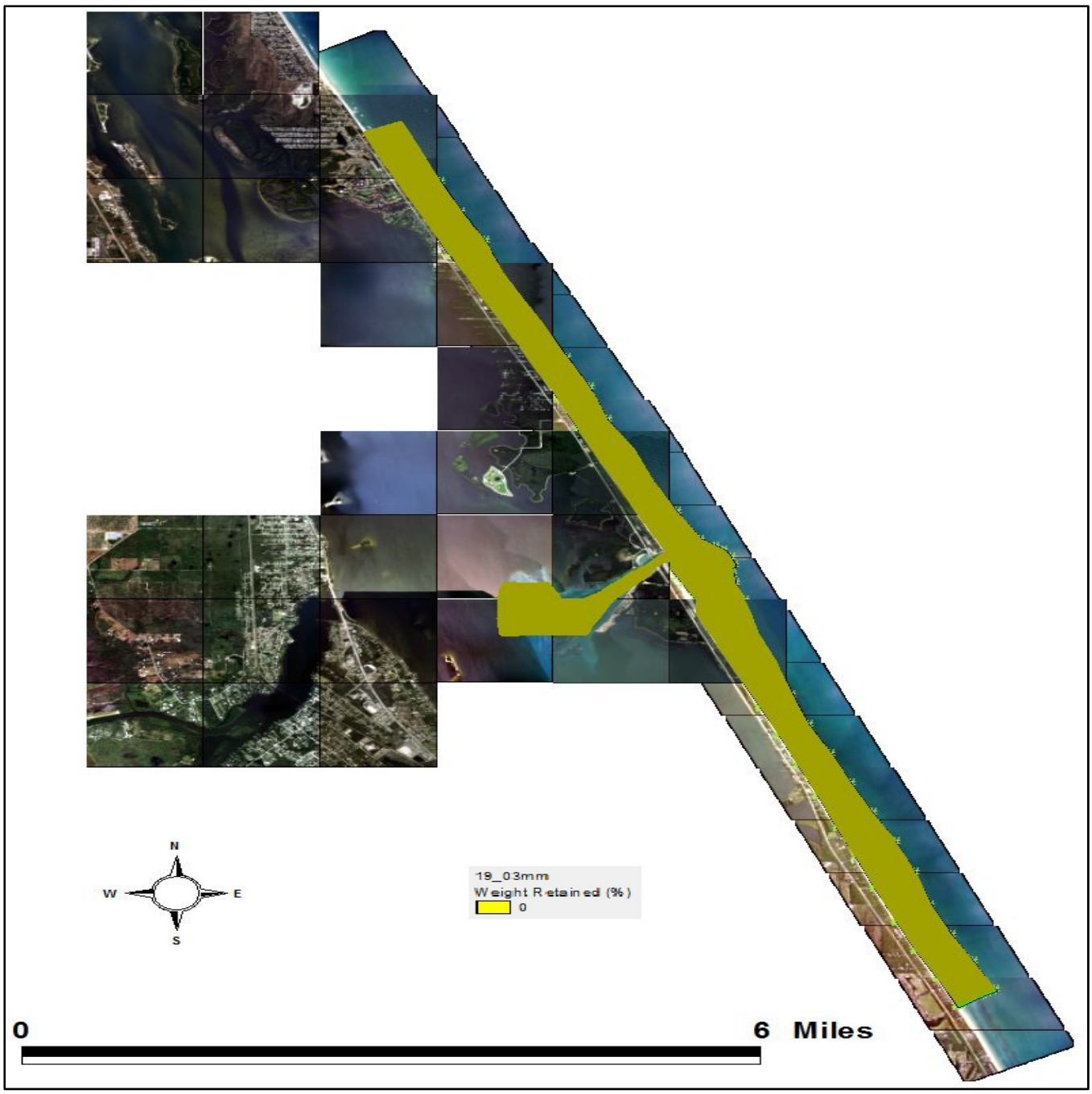

Figure 100.19.03 mm weight retained (%)

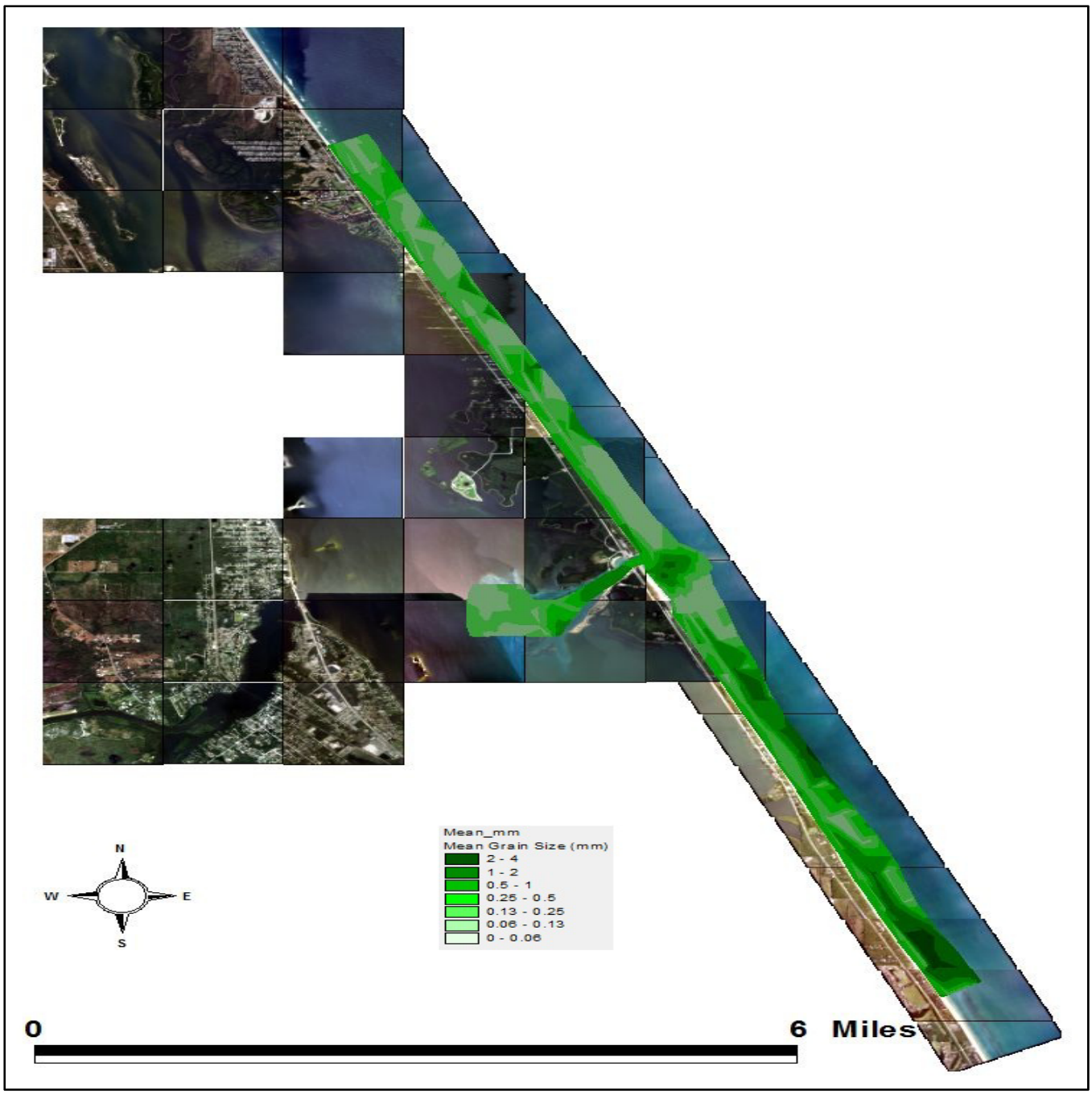

Figure 101. Mean grain size (mm)

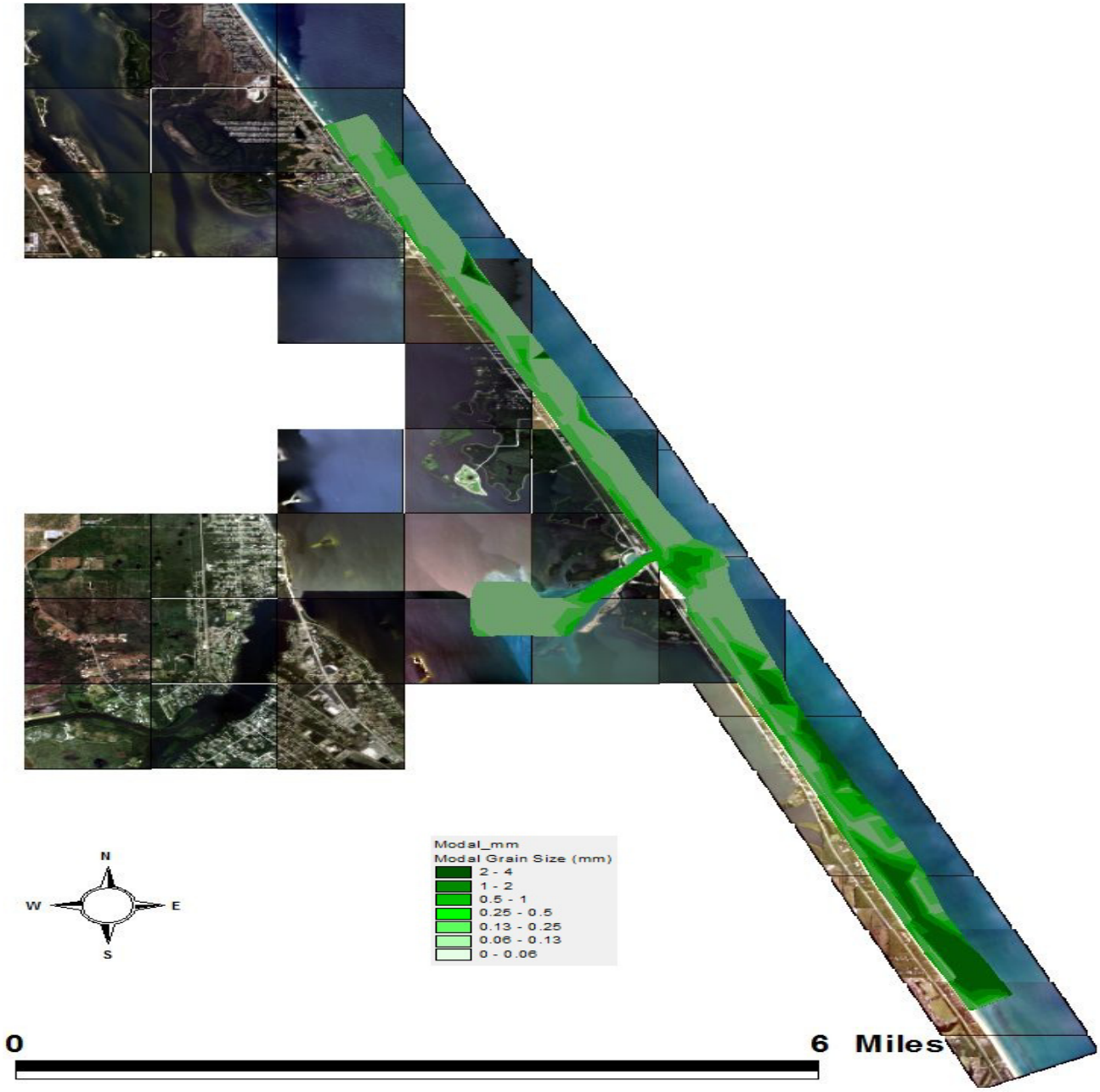

Figure 102. Modal grain size (mm)

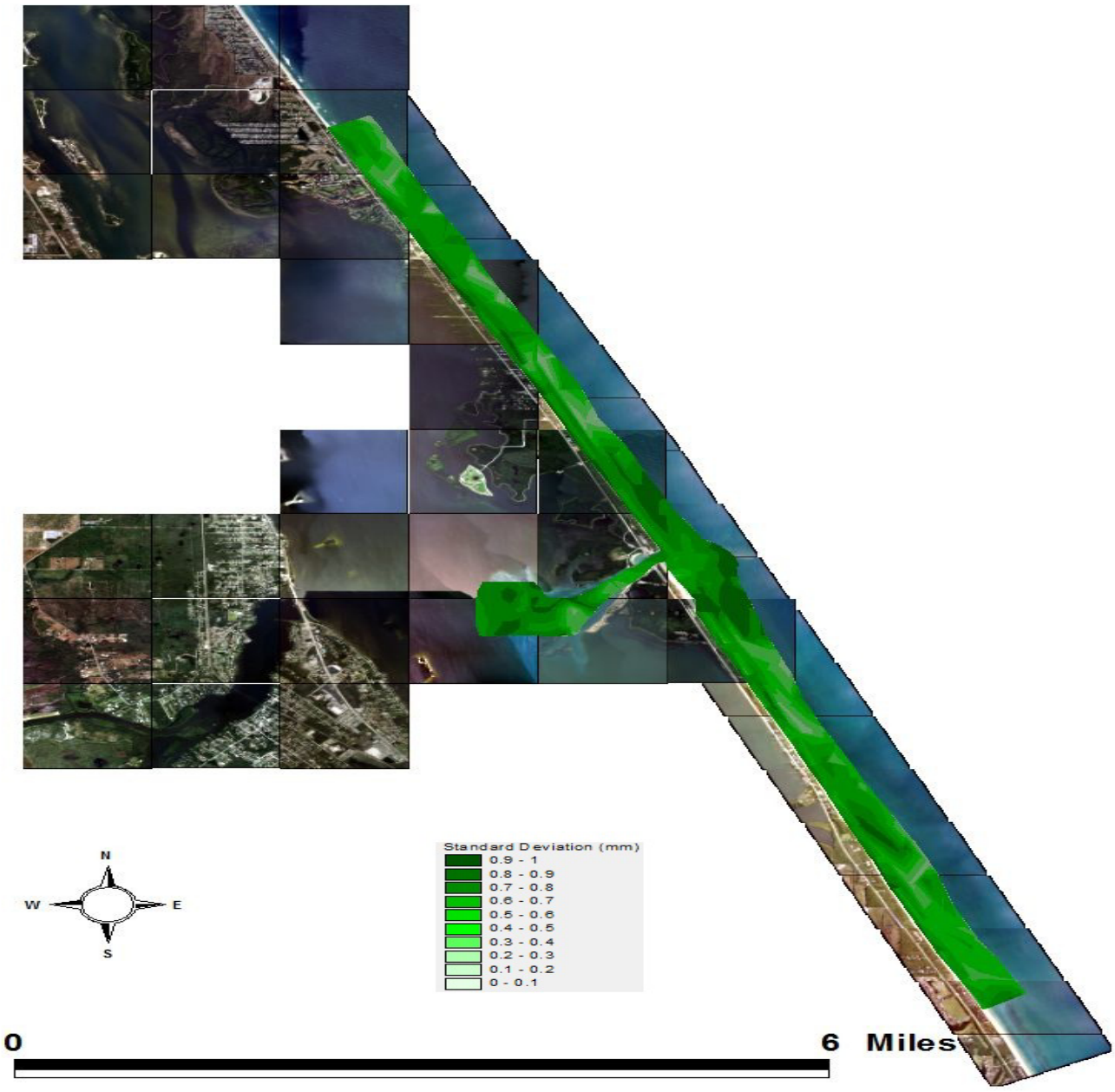

Figure 103. Standard deviation

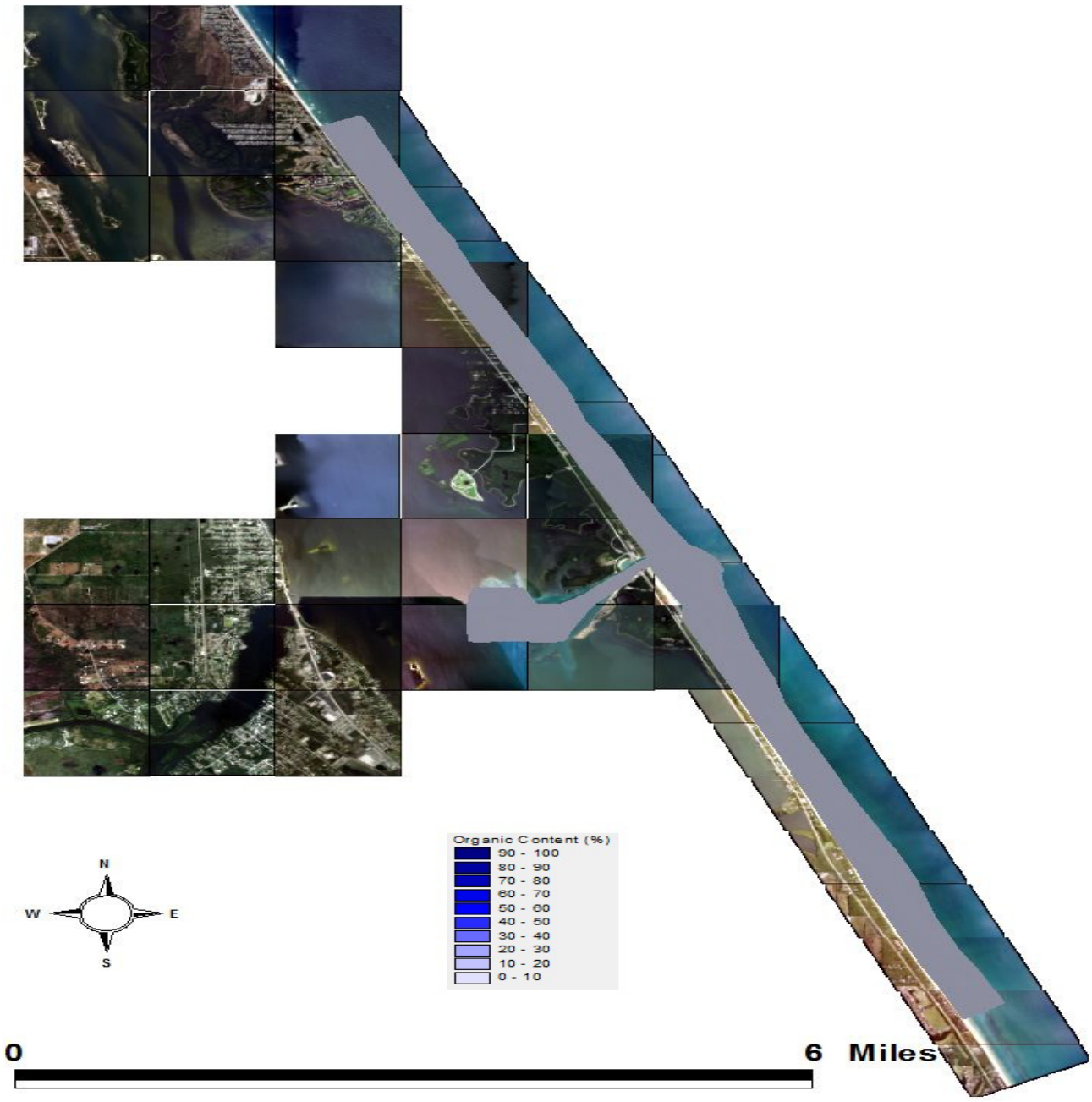

Figure 104. Organic content (%)

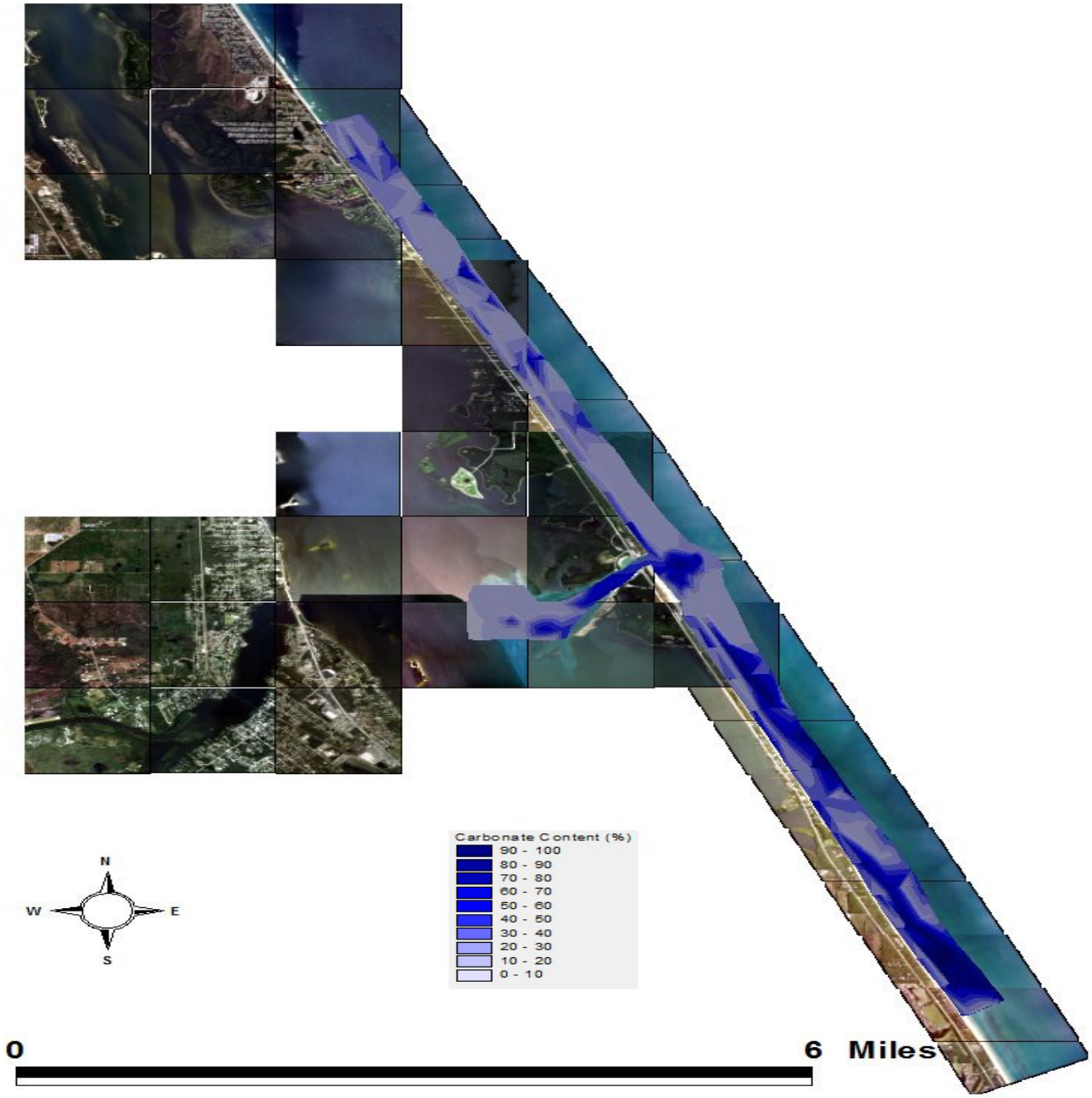

Figure 105. Carbonate content (%)

APPENDIX B: Grain Size Contour Plots: Winter 2012

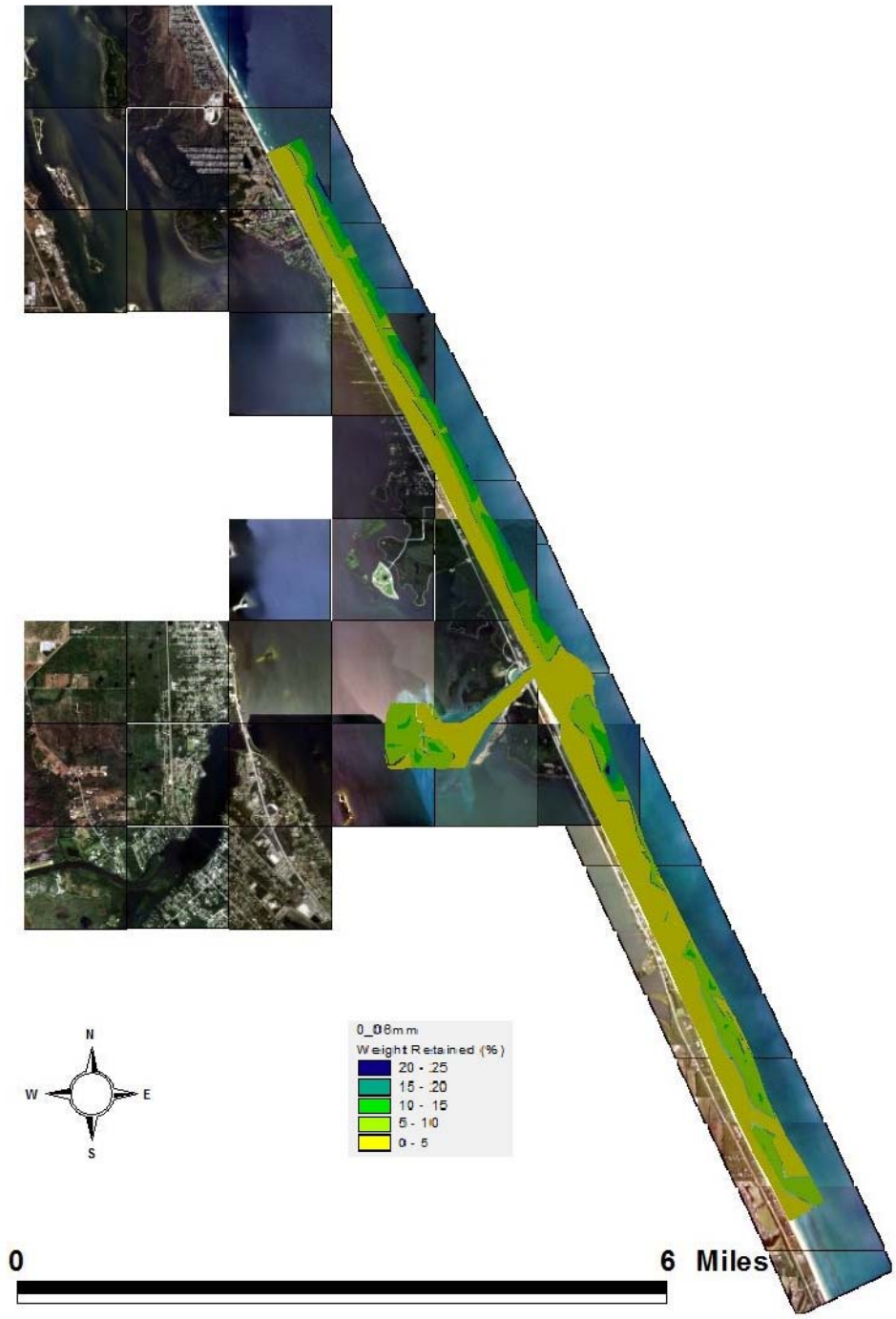

Figure 106. 0.06 mm weight retained (%)

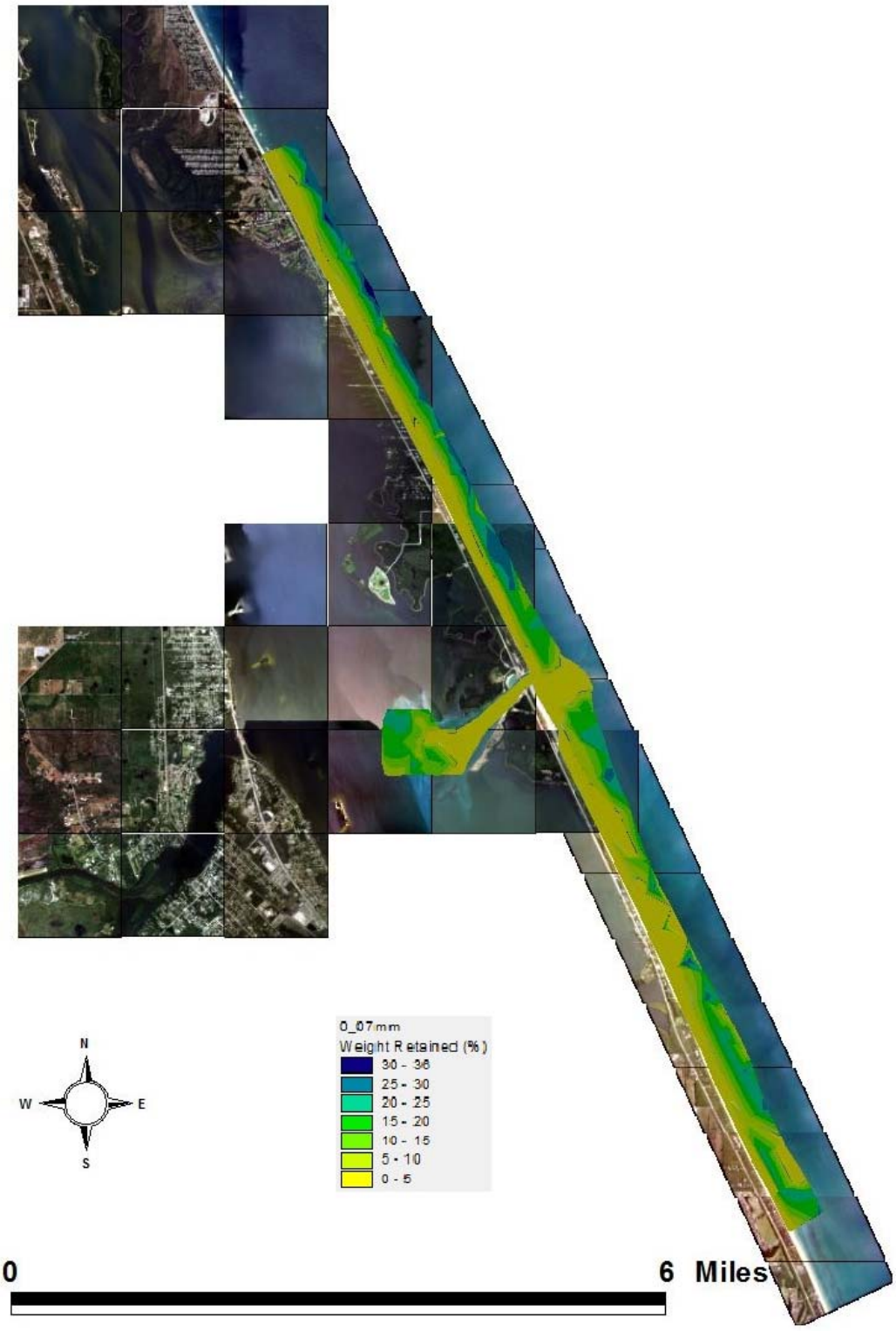

Figure 107. 0.09 mm weight retained (%)

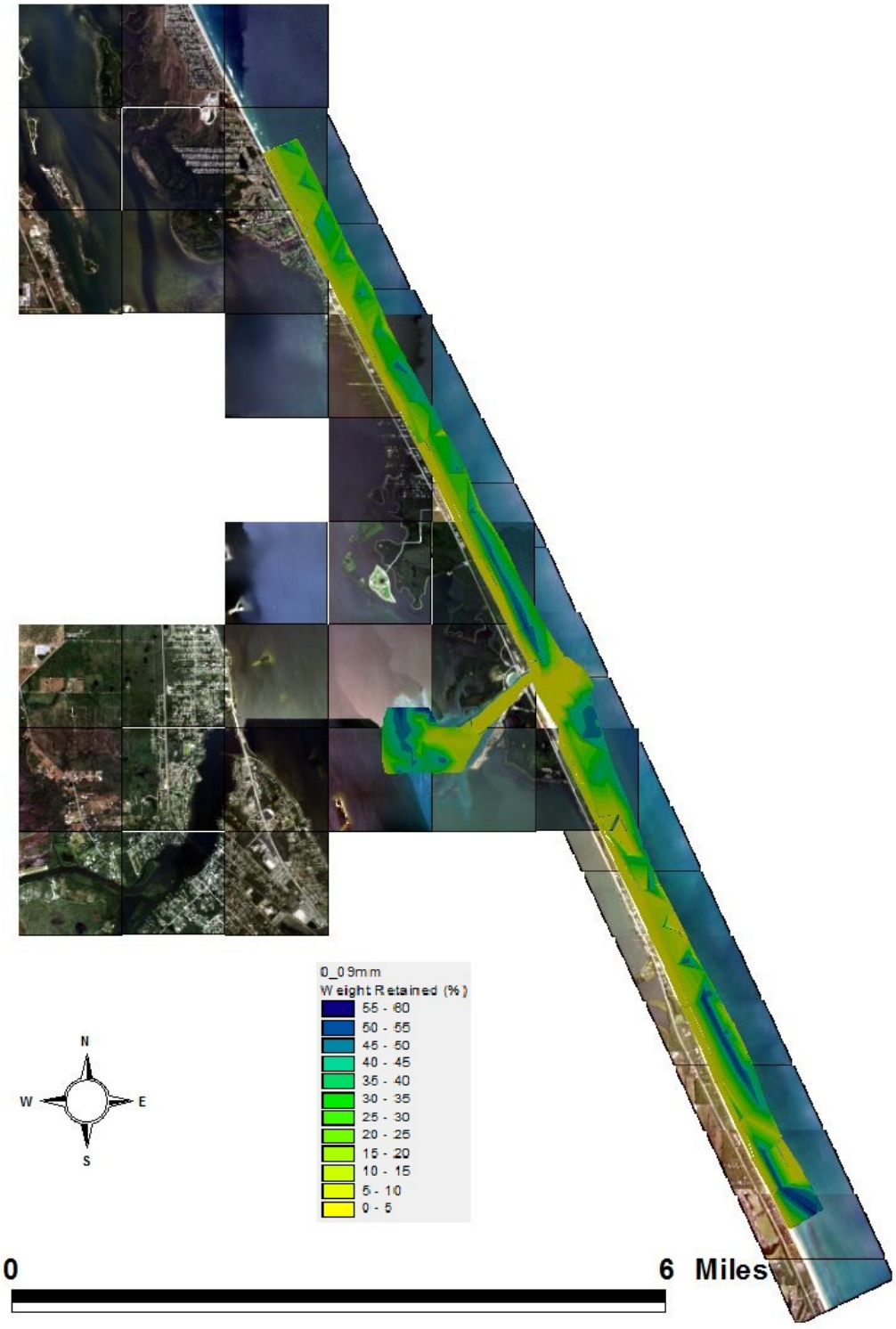

Figure 108. 0.09 mm weight retained (%)

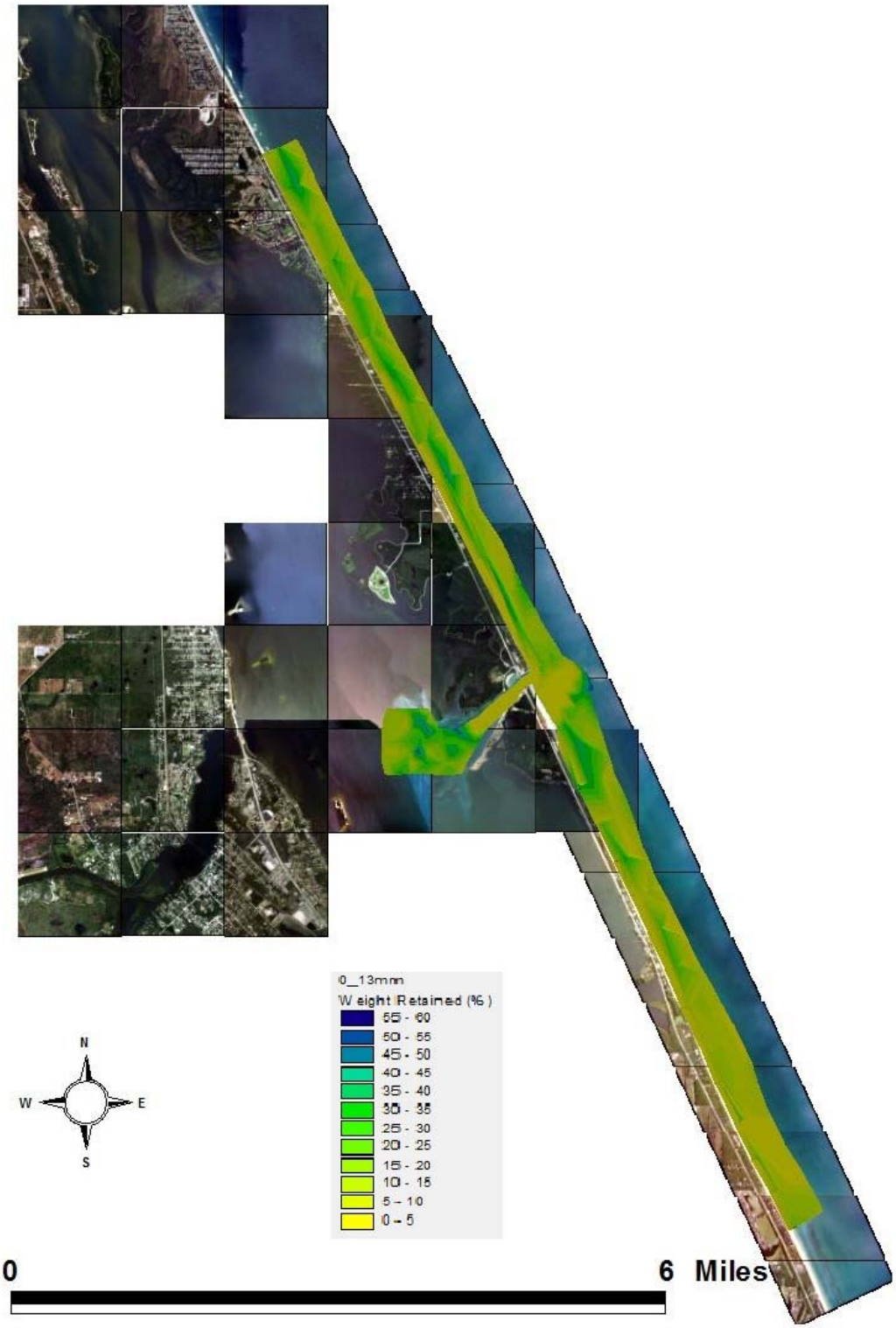

Figure 109. 0.13 mm weight retained (%)

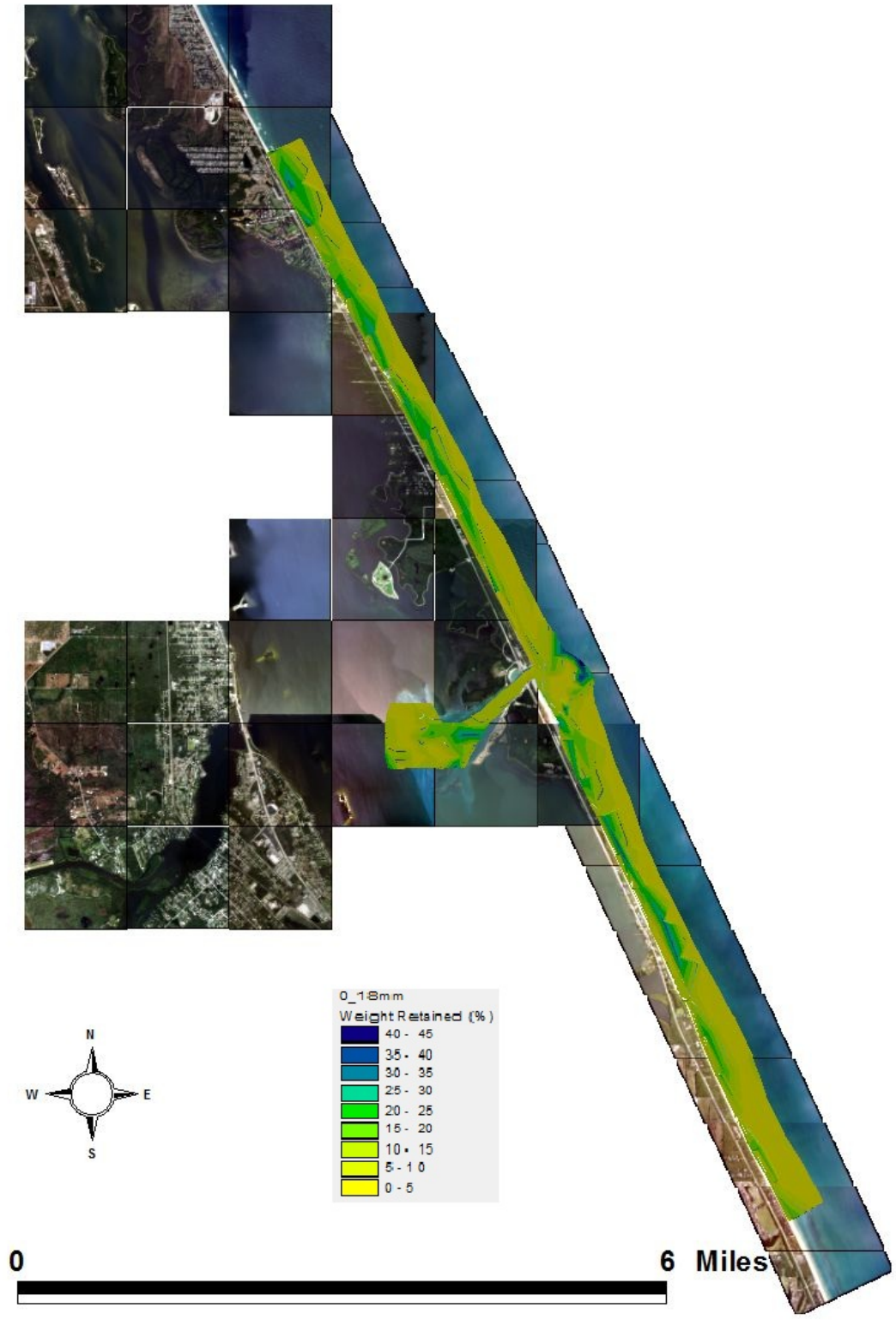

Figure 110.0.18 mm weight retained (%)

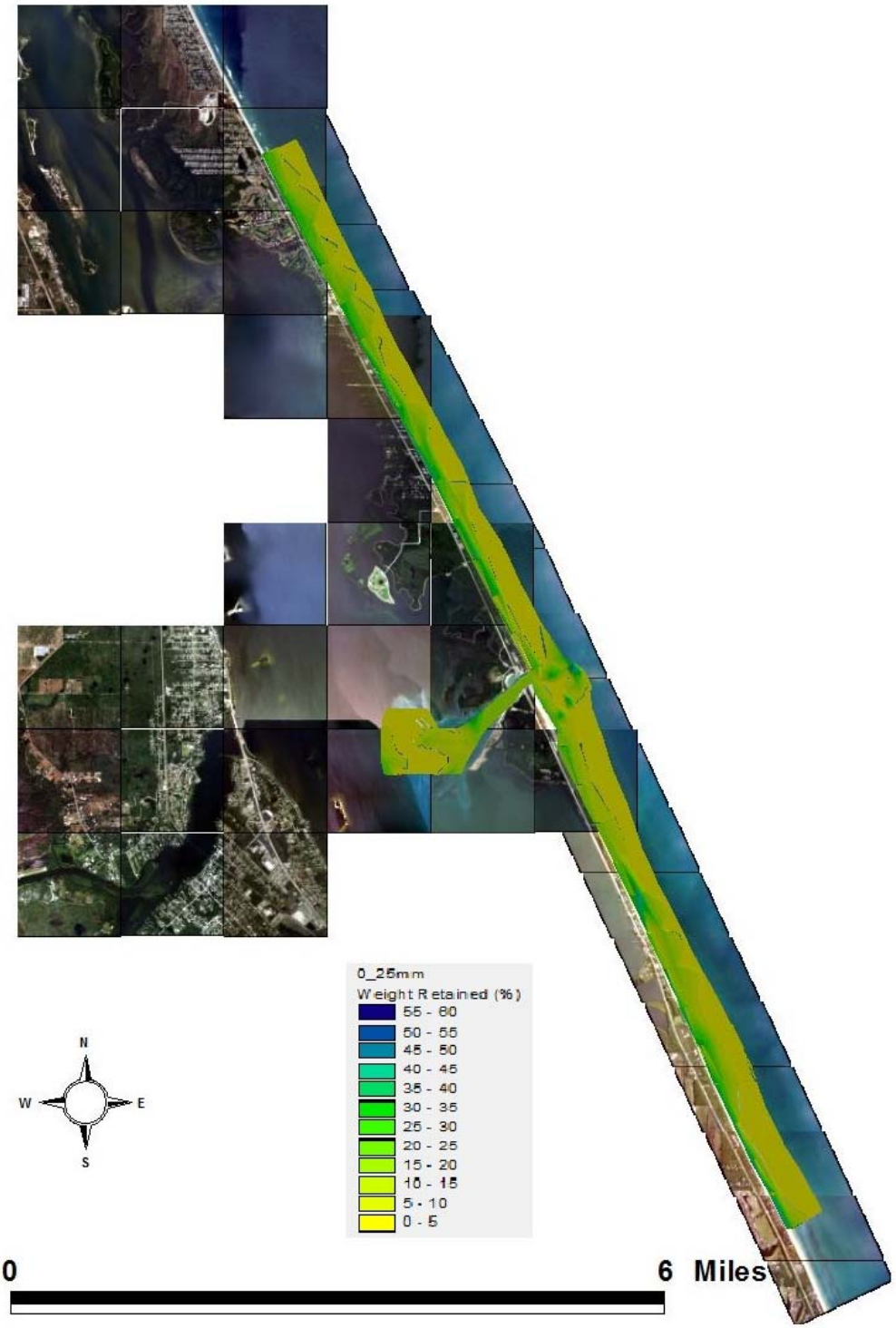

Figure 111.0.25 mm weight retained (%)

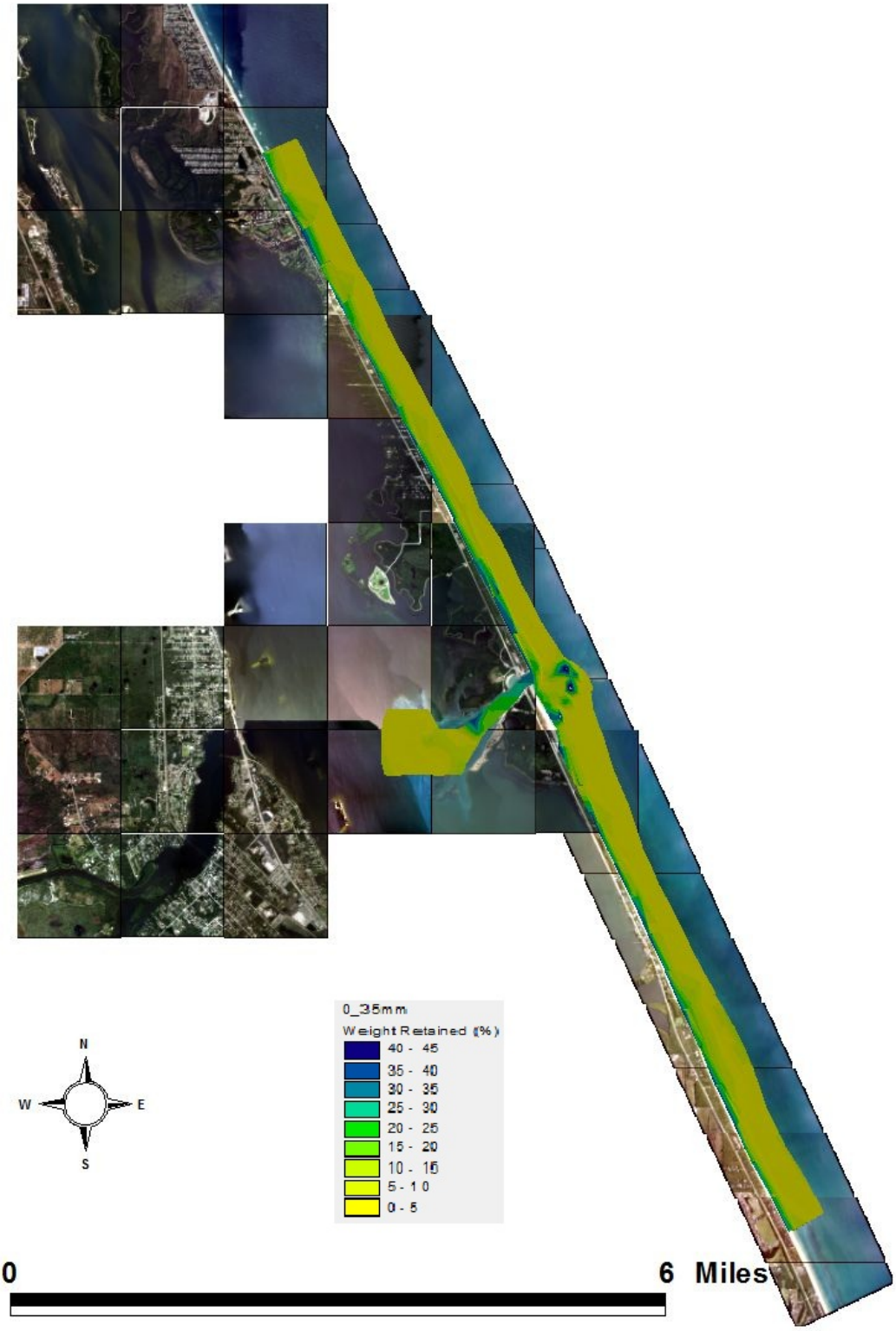

Figure 112.0.35 mm weight retained (%)

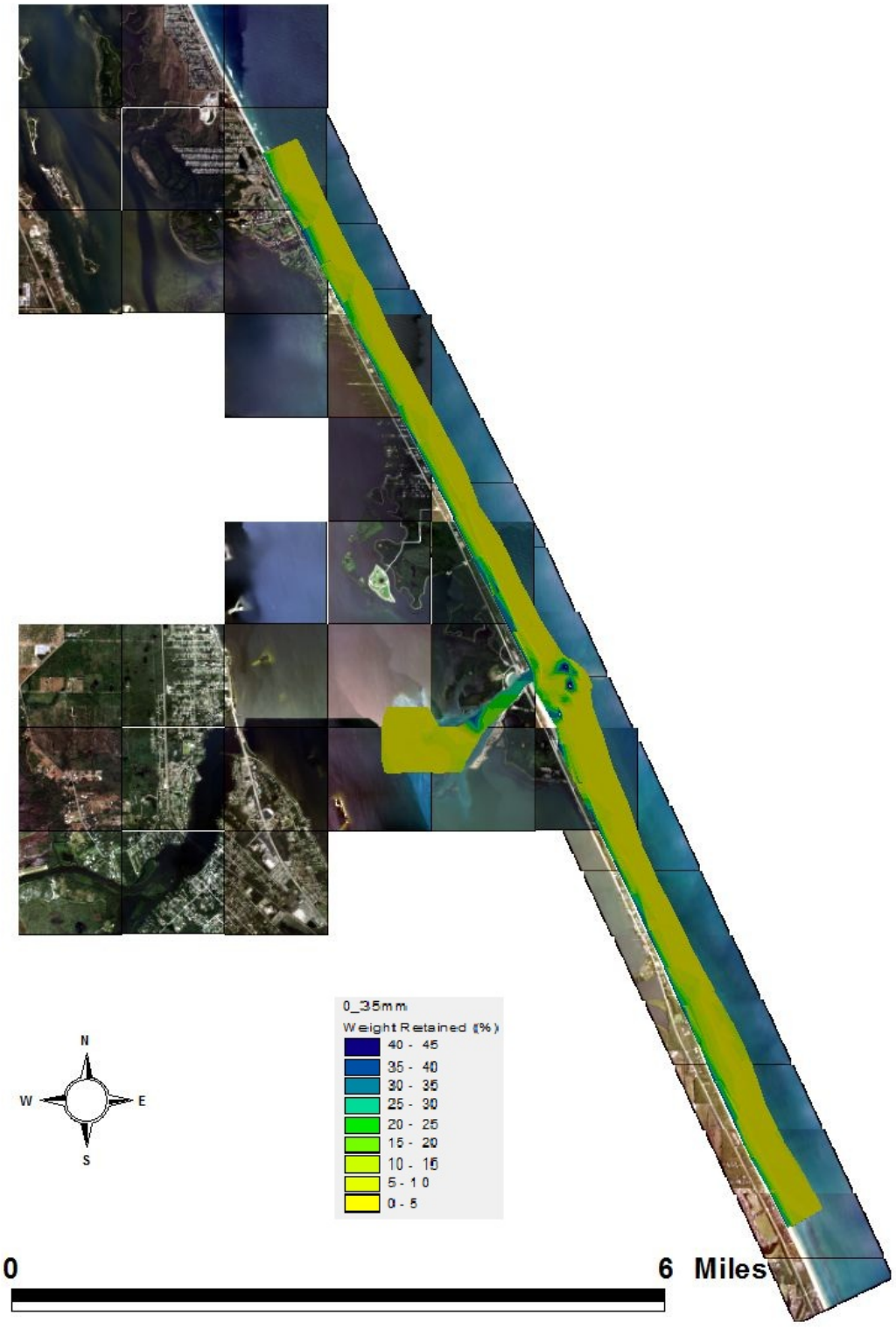

Figure 113.0.50 mm weight retained (%)

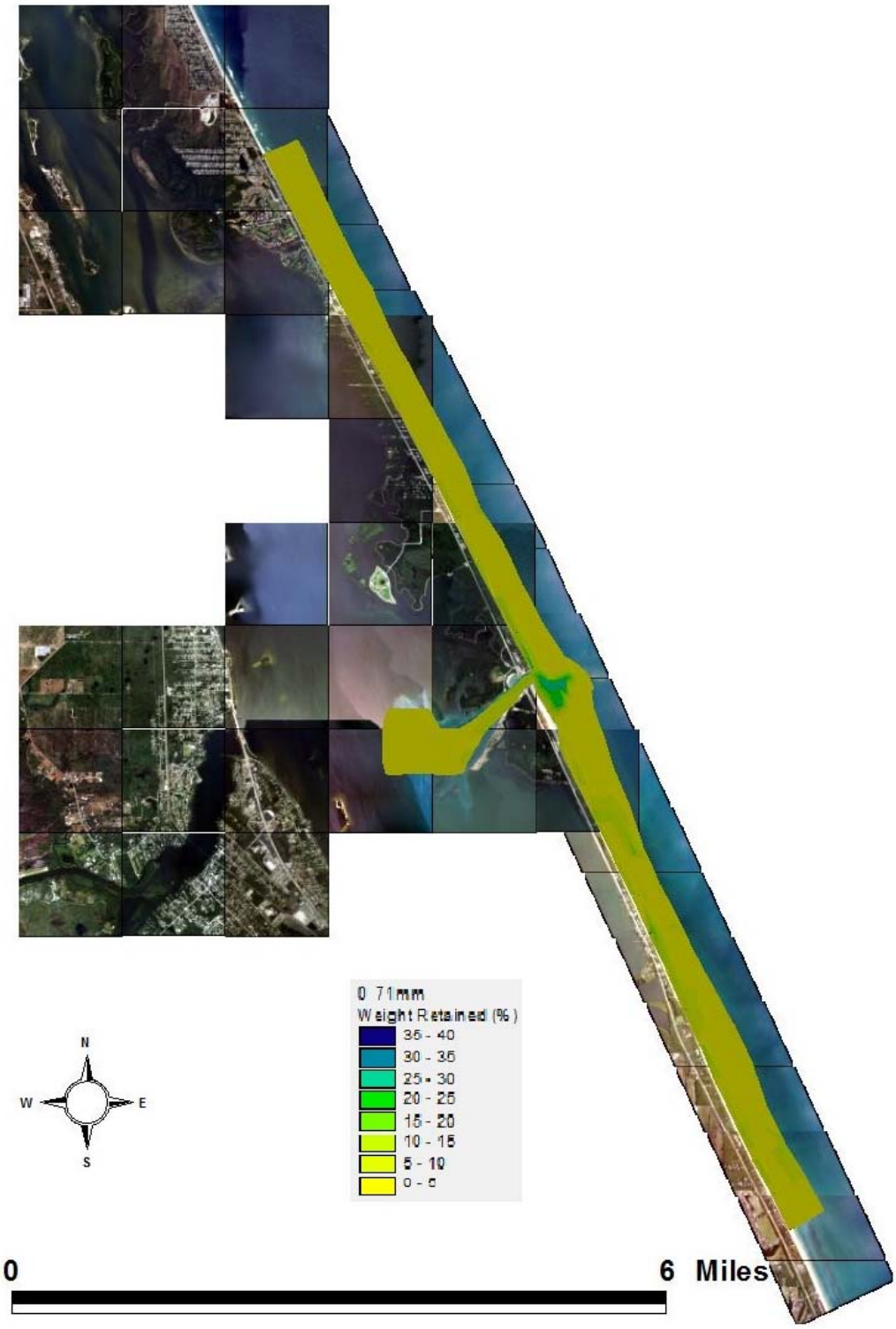

Figure 114.0.71 mm weight retained (%)

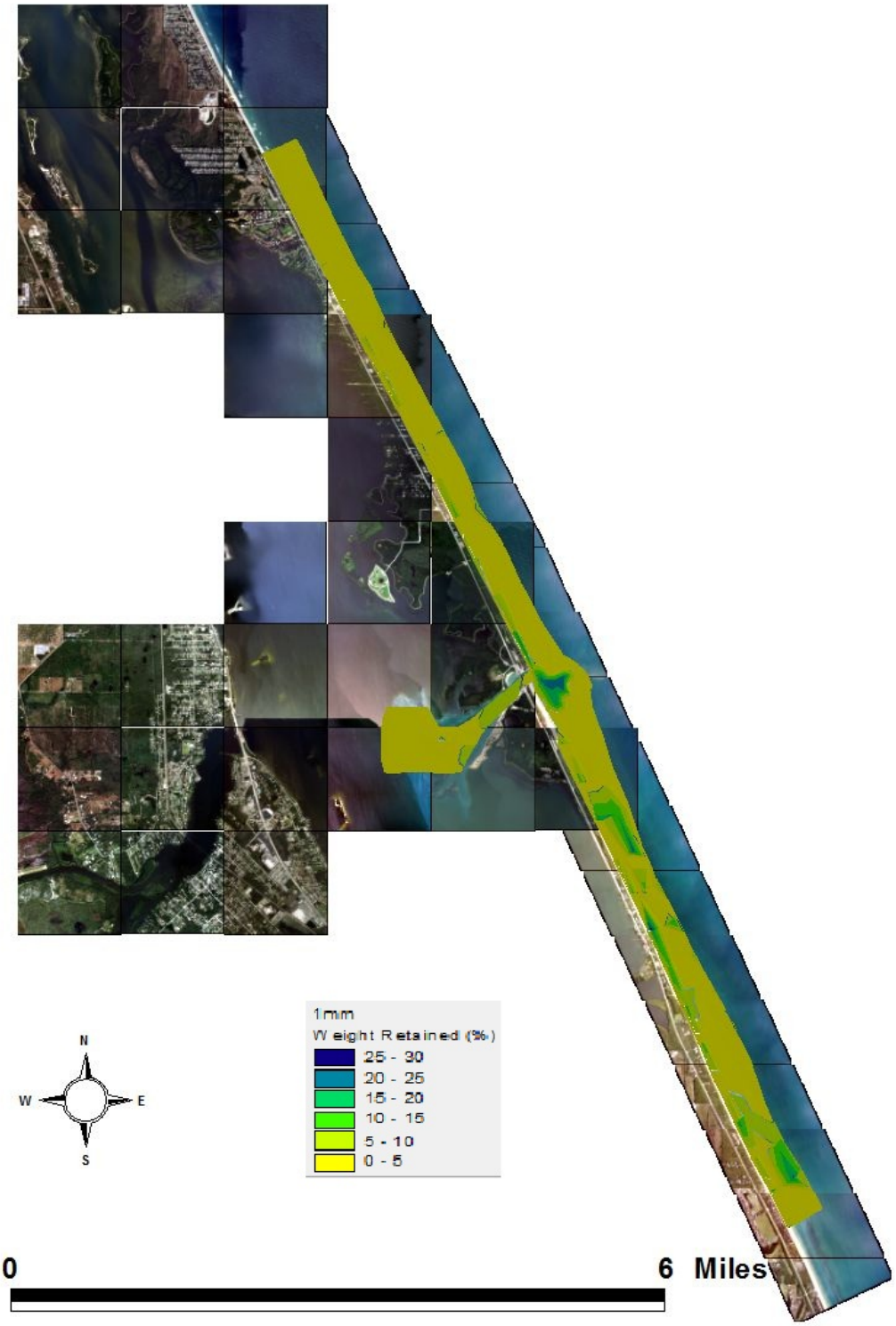

Figure 115.1.0 mm weight retained (%)

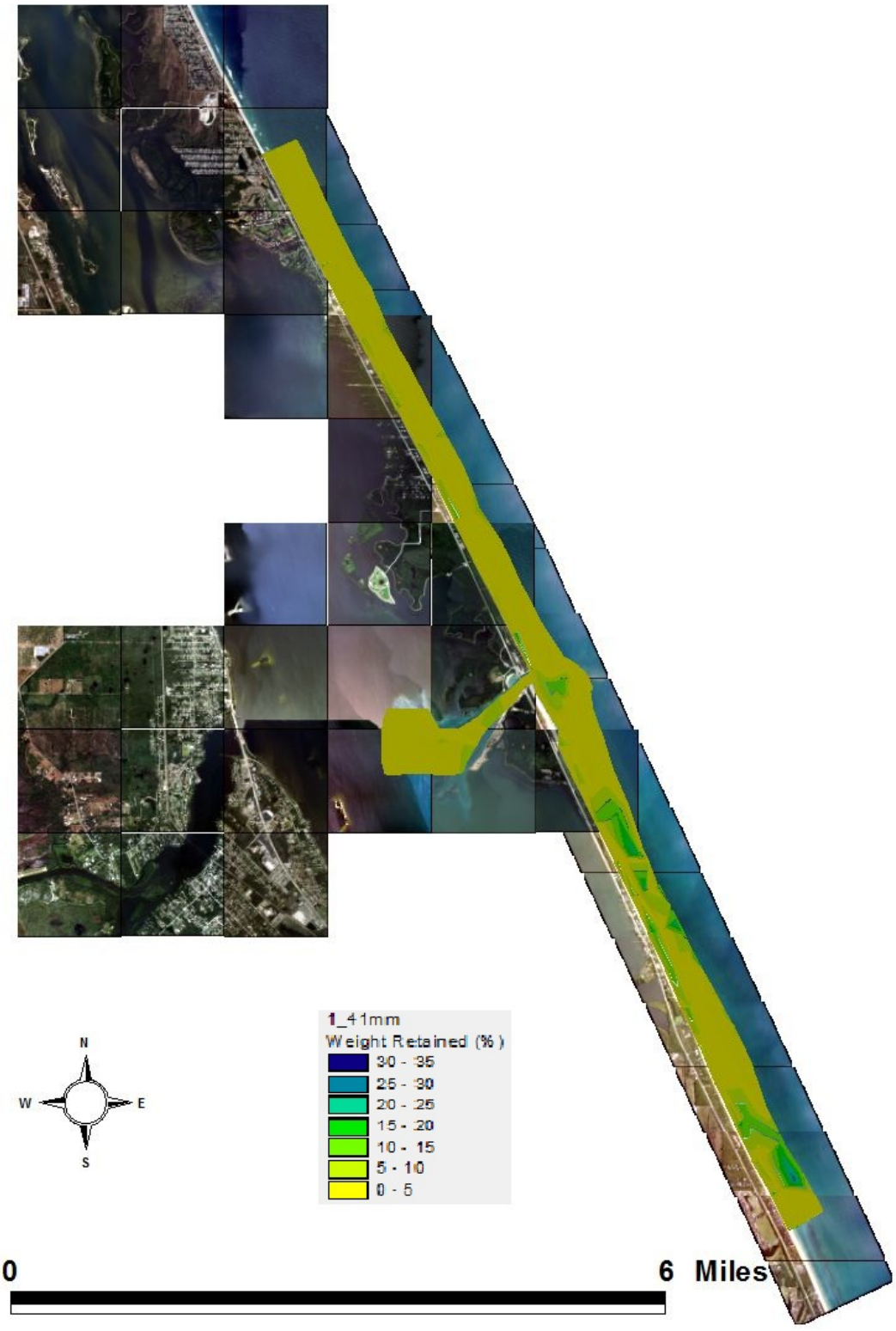

Figure 116.1.41 mm weight retained (%)

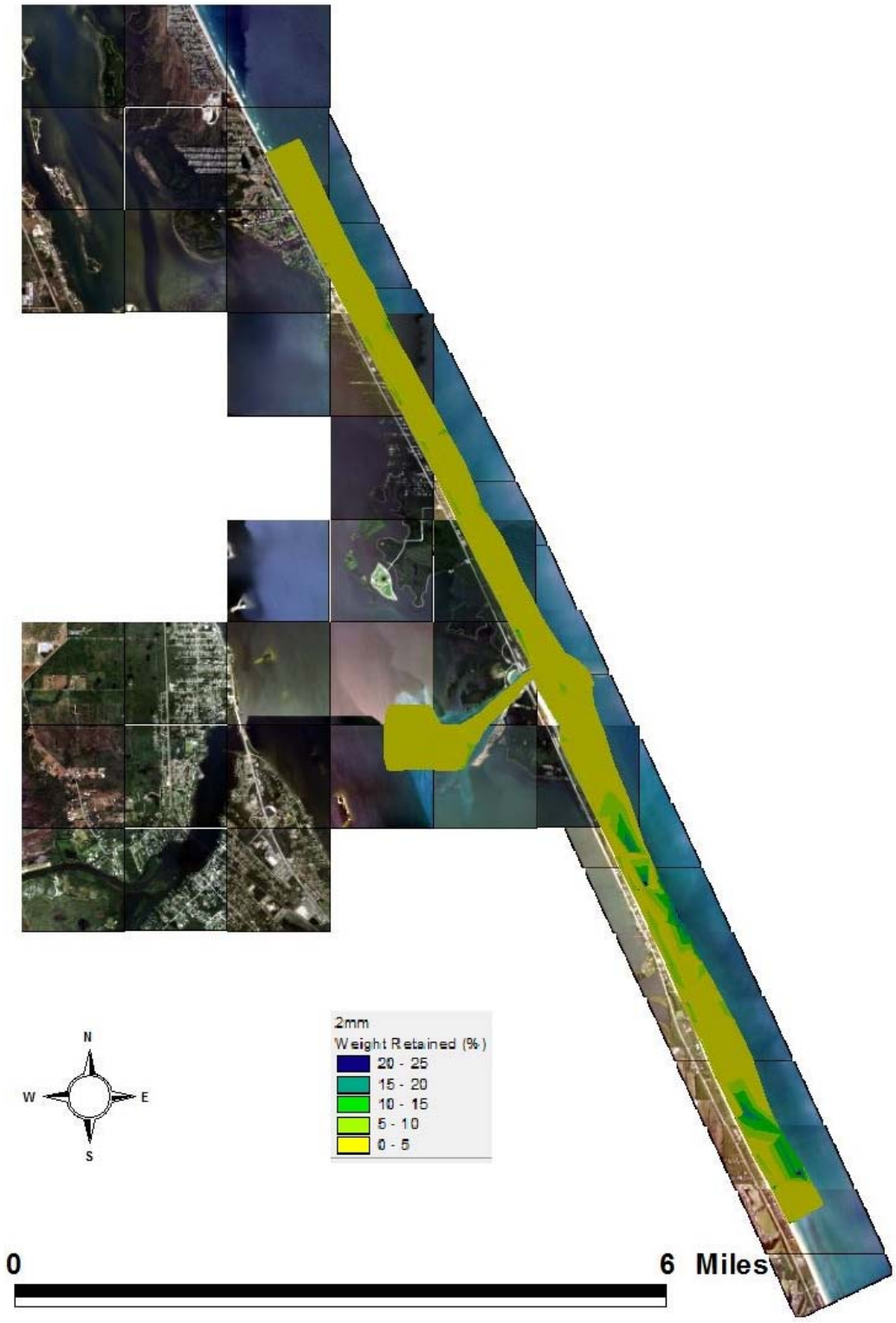

Figure 117. 2.0 mm weight retained (%)

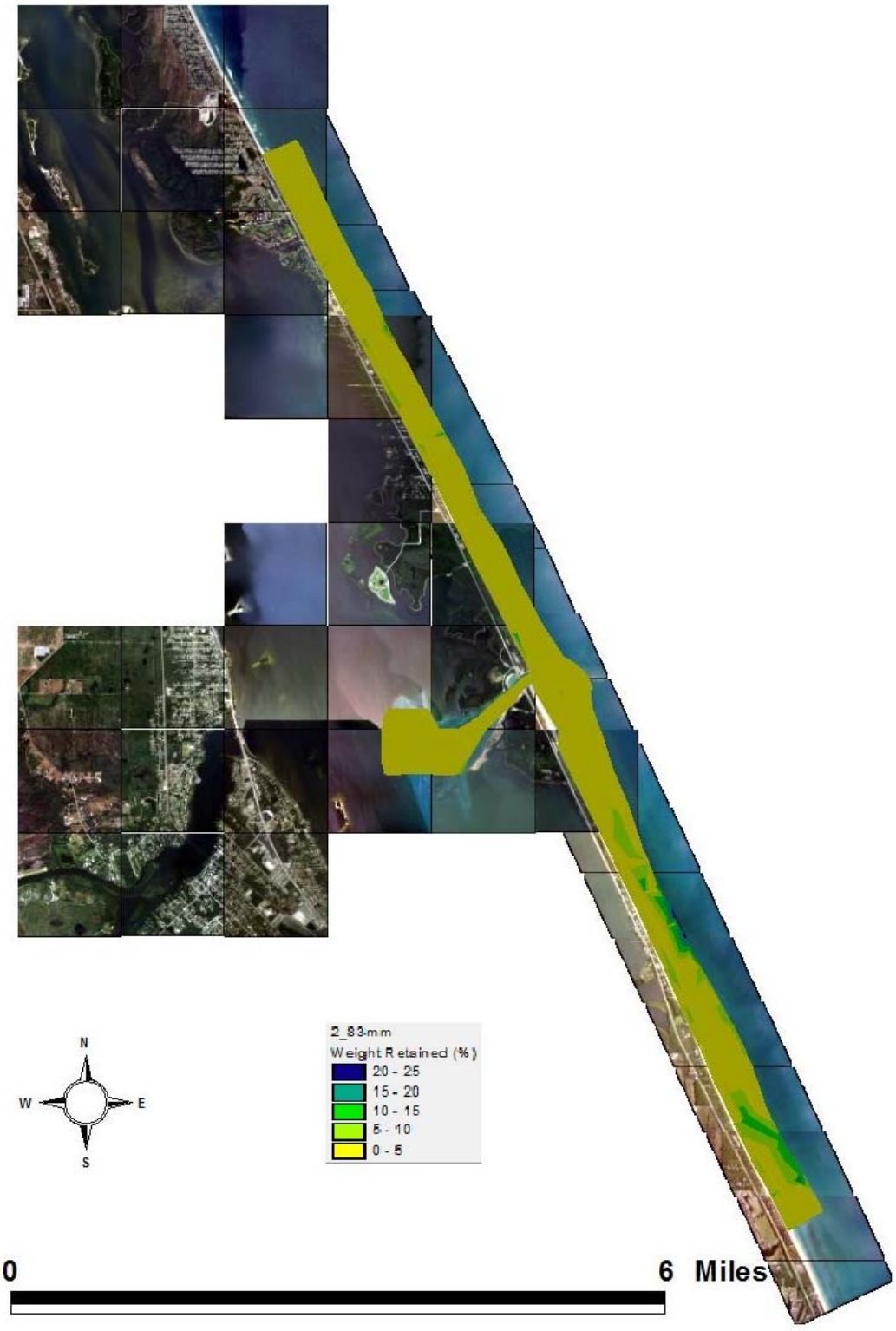

Figure 118.2.83 mm weight retained (%)

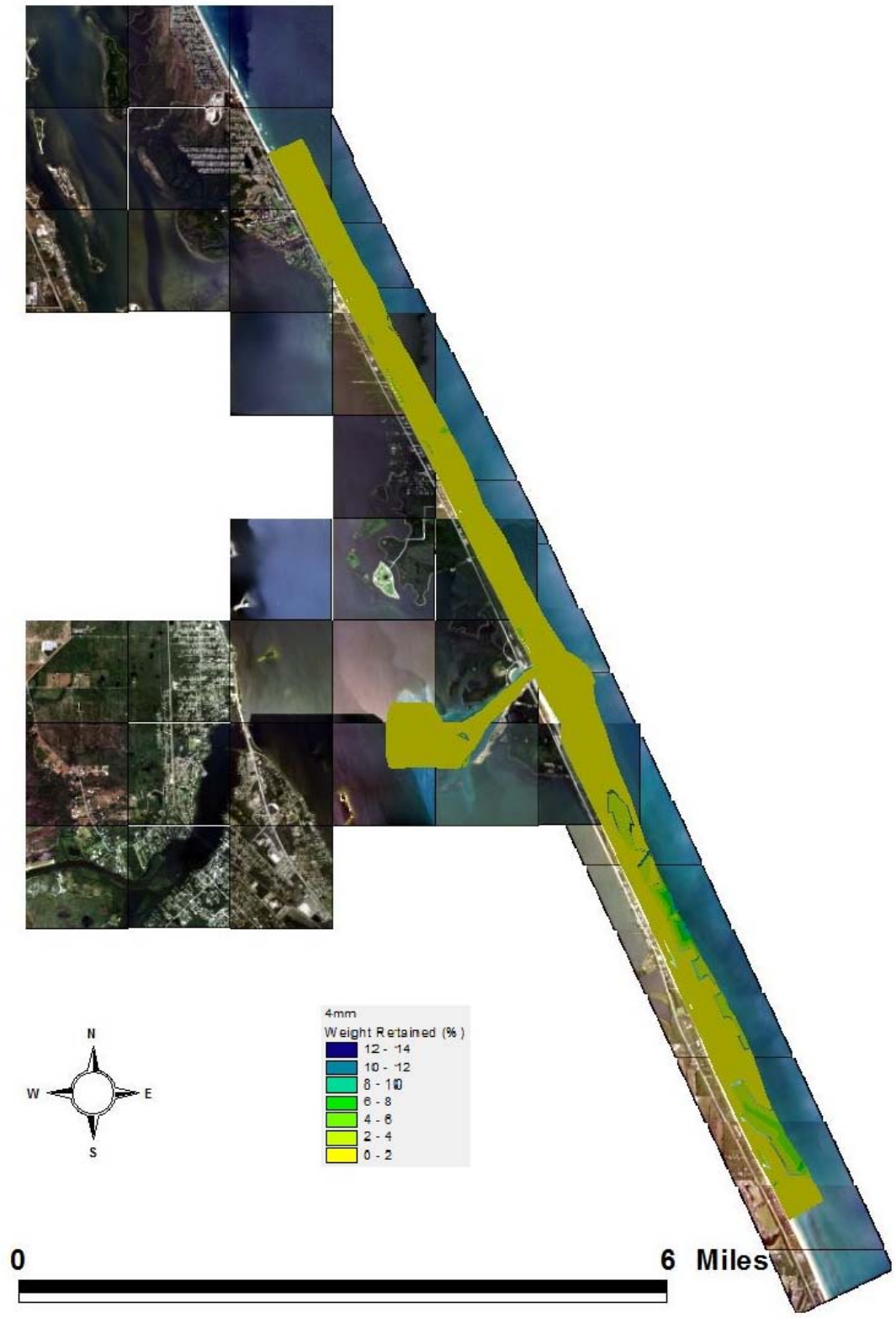

Figure 119.4.0 mm weight retained (%)

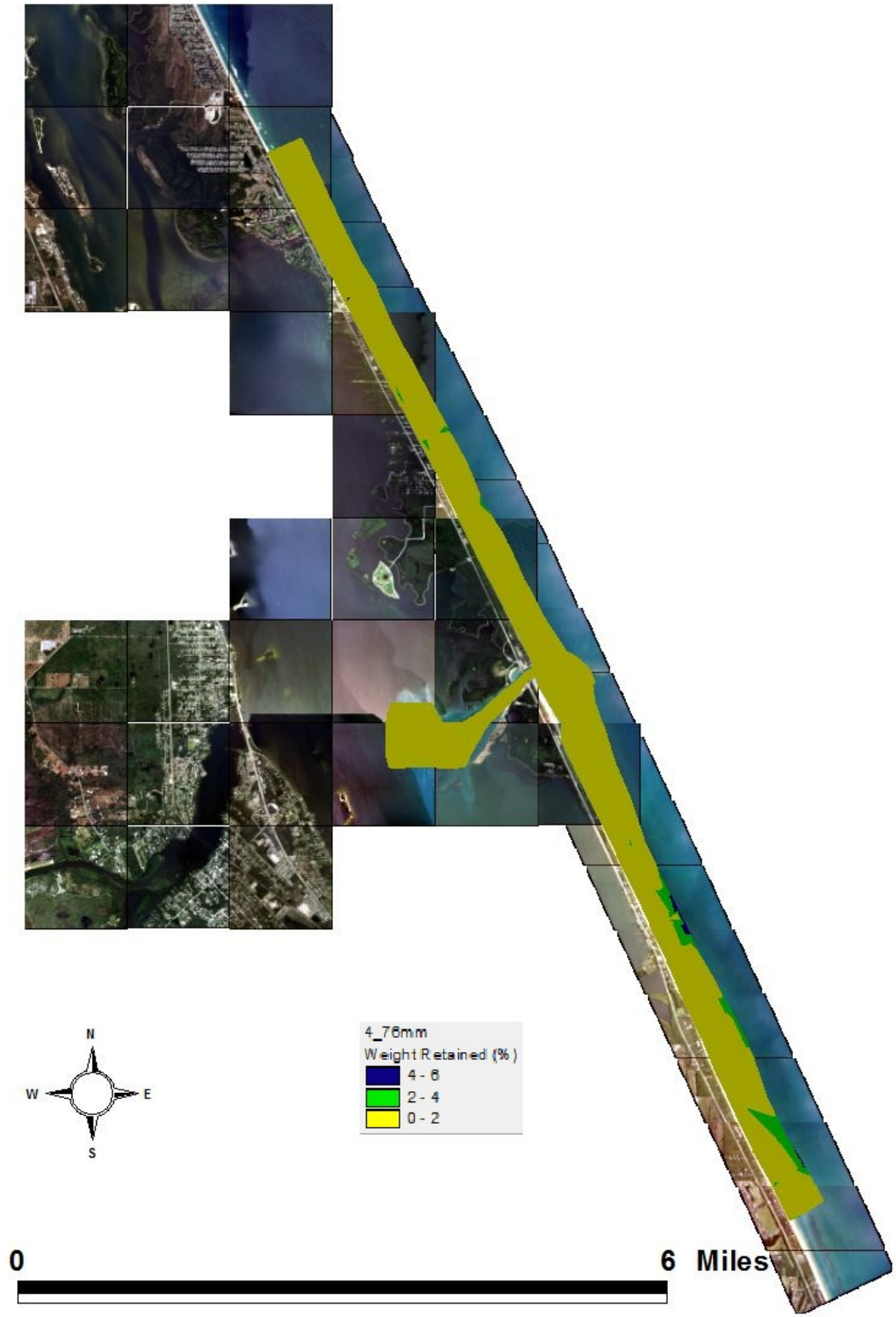

Figure 120.4,76 mm weight retained (%)

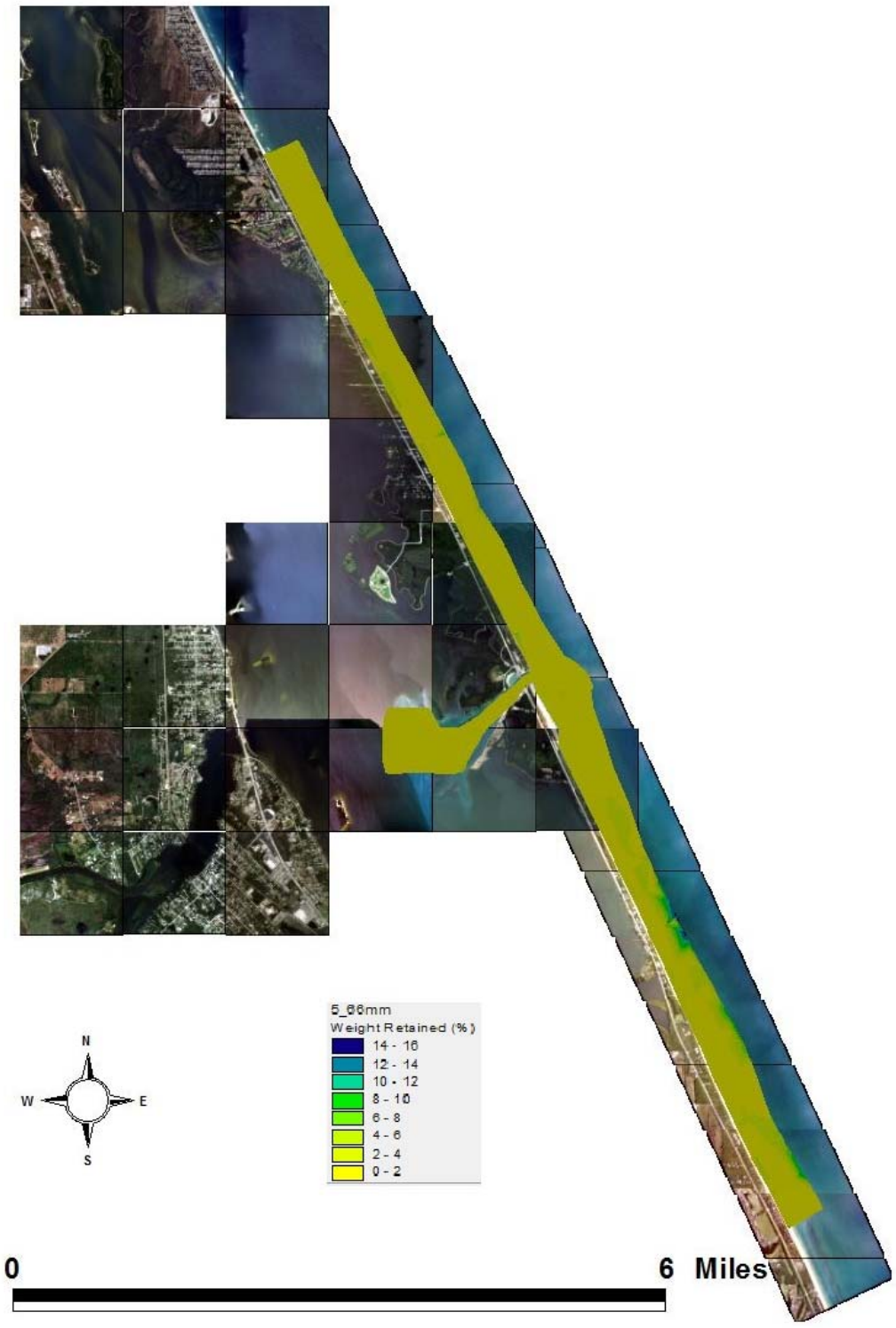

Figure 121.5.66 mm weight retained (%)

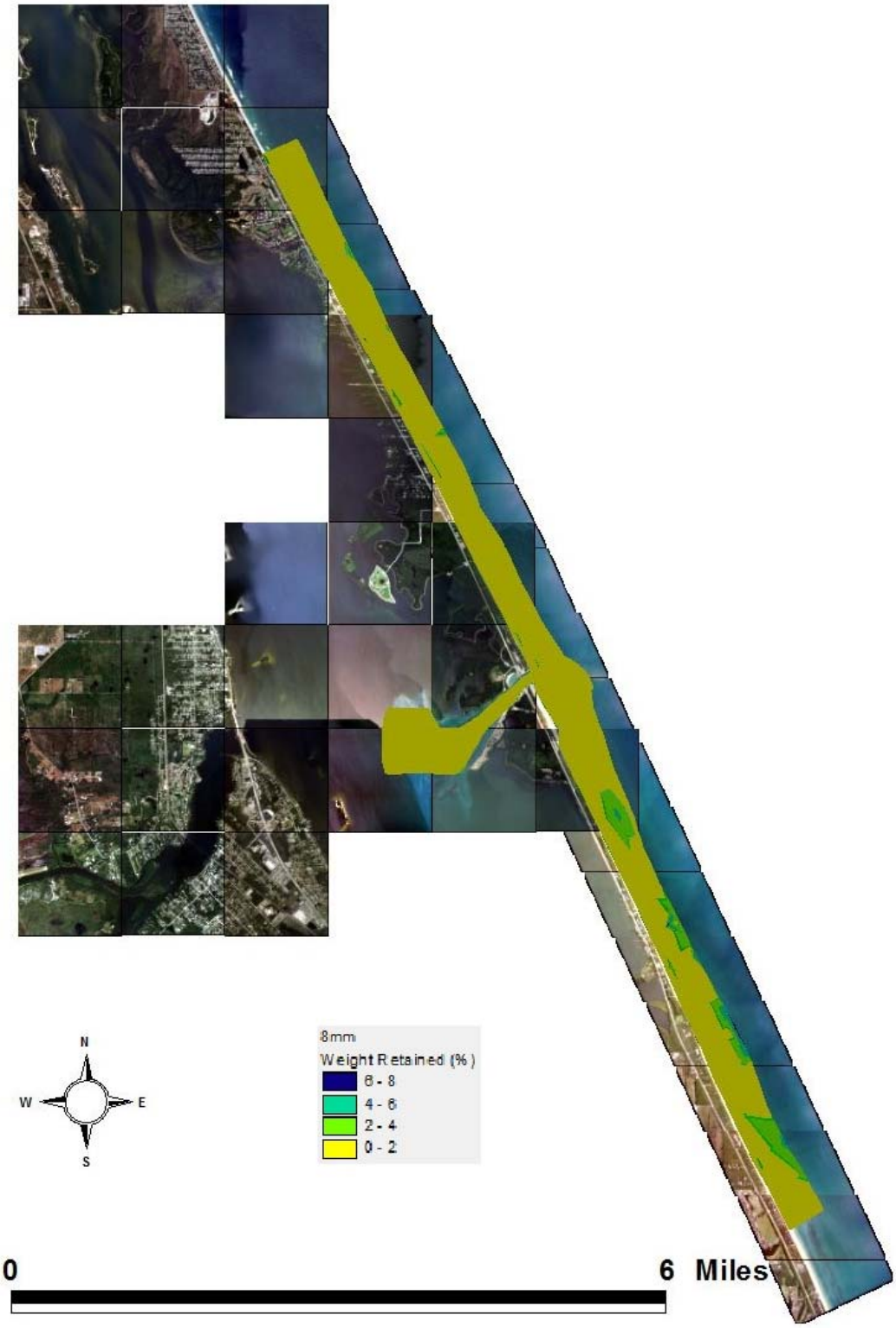

Figure 122.8.0 mm weight retained (%)

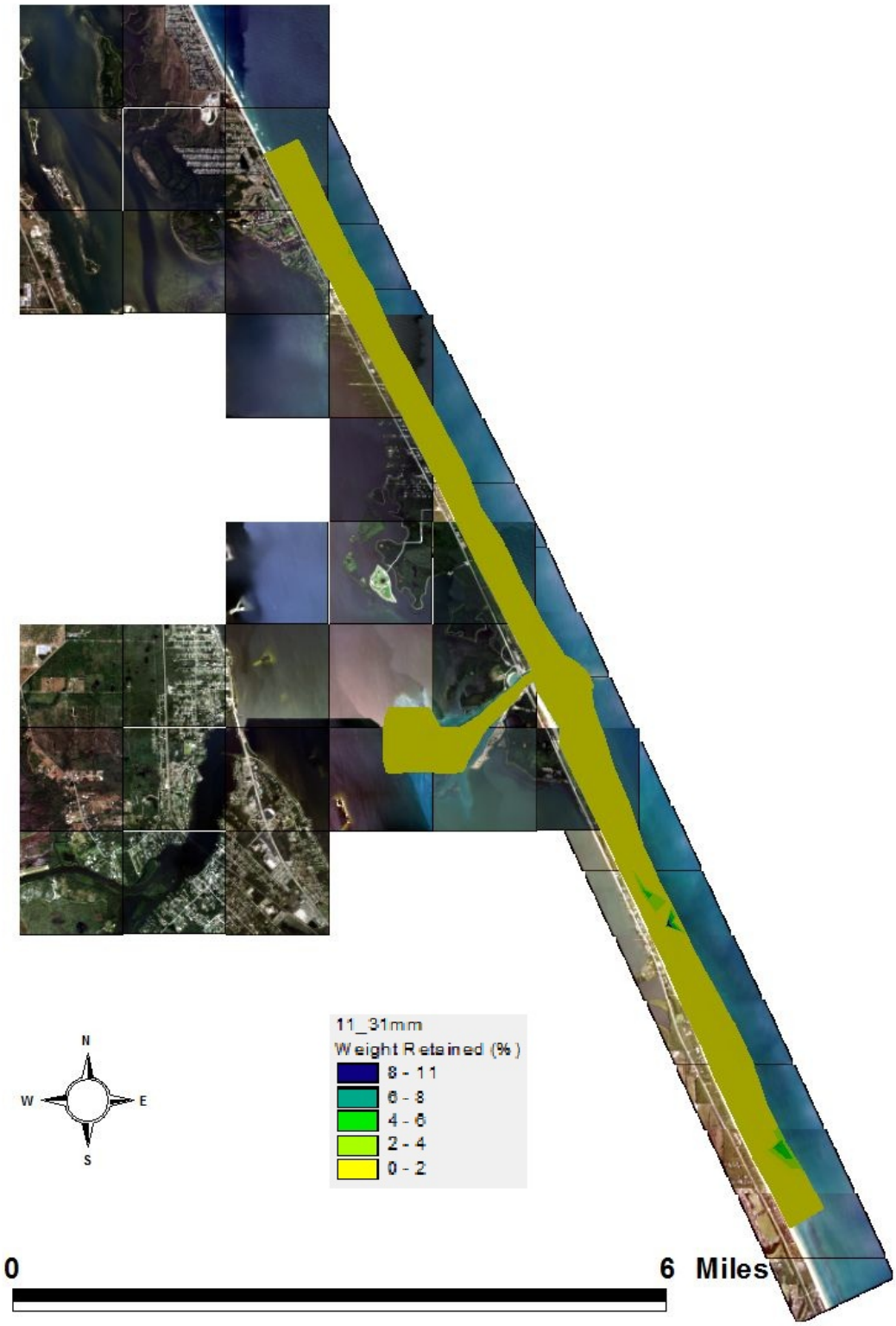

Figure 123.11.31 mm weight retained (%)

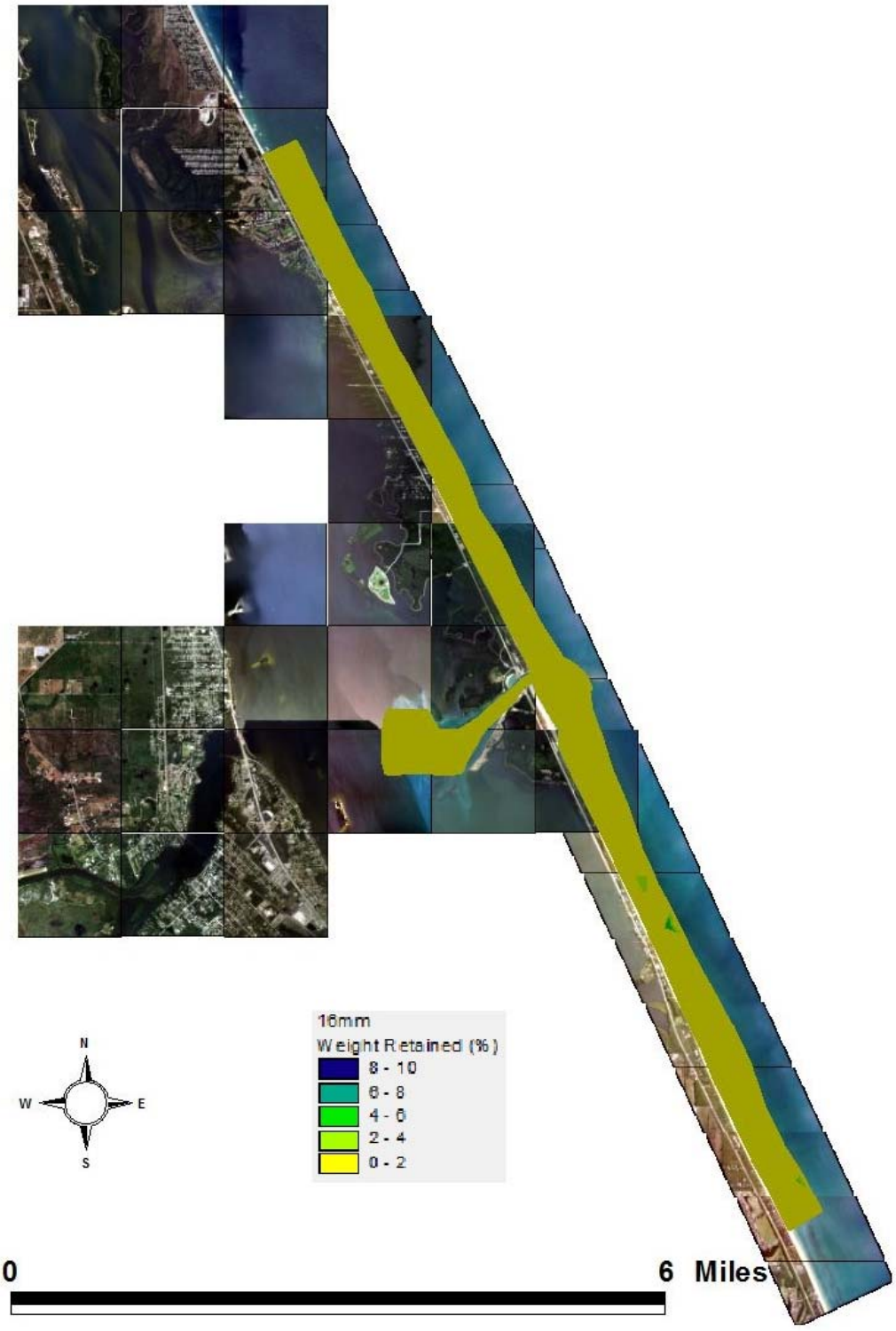

Figure 124.16.0 mm weight retained (%)

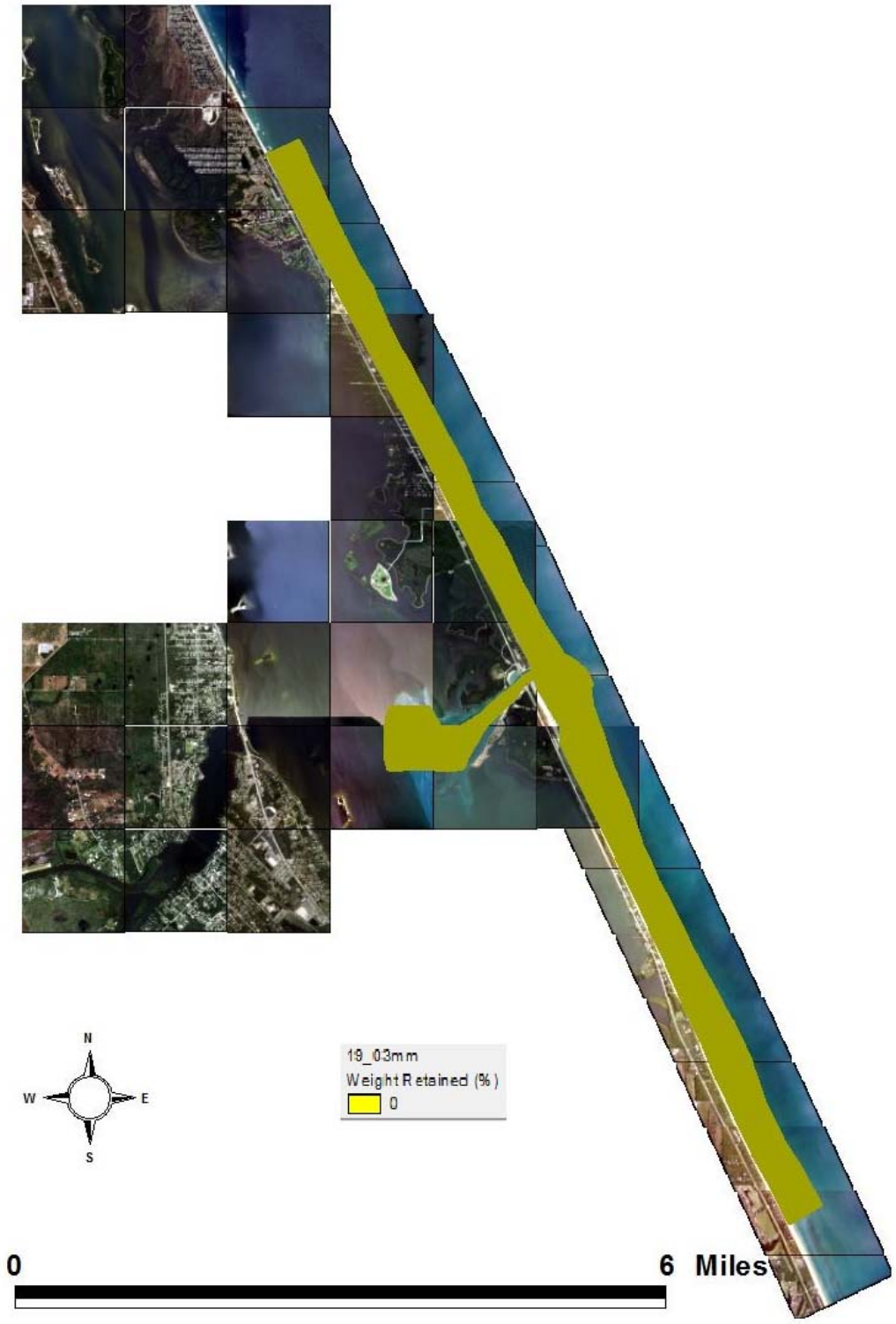

Figure 125.19.03 mm weight retained (%)

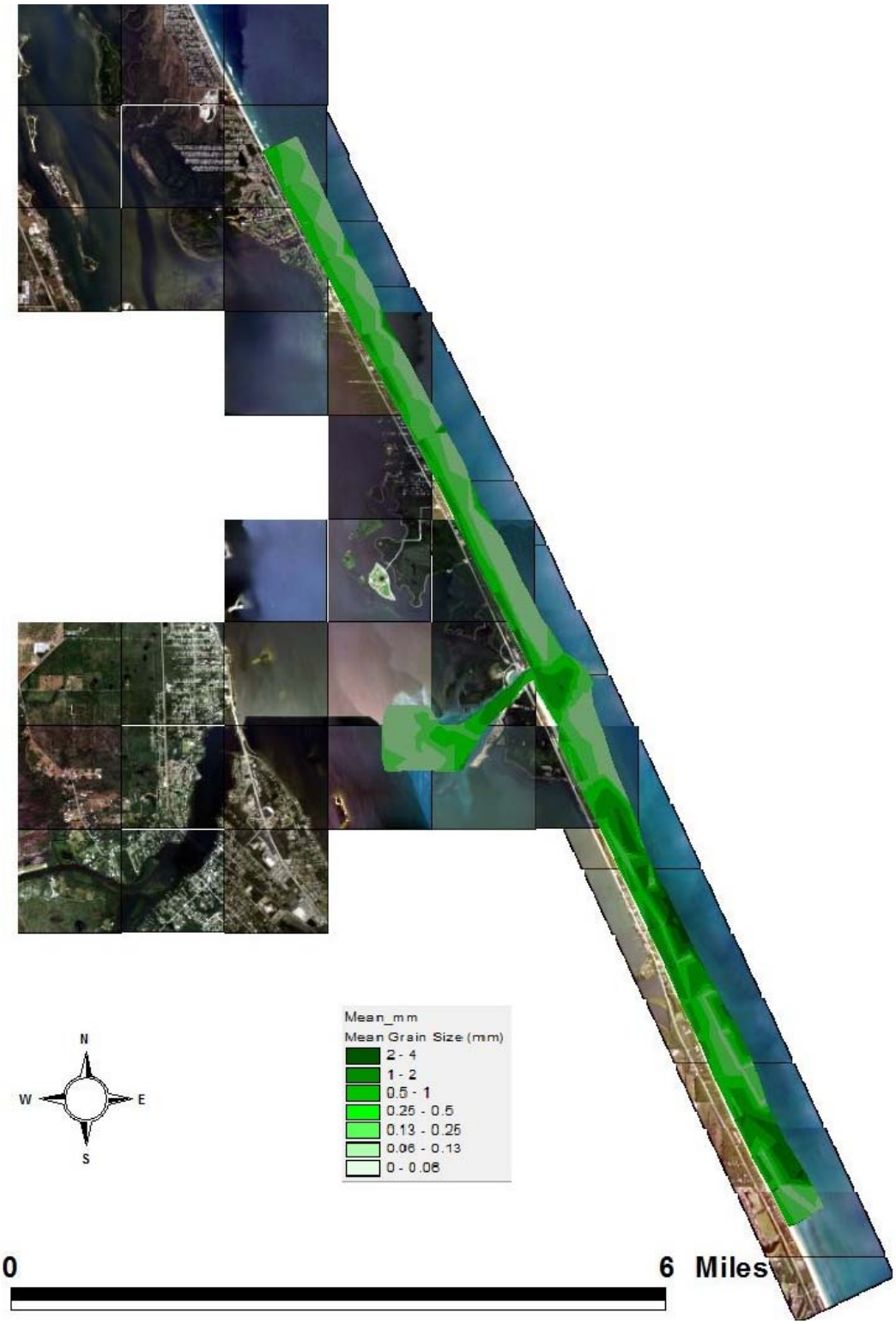

Figure 126. Mean grain size in mm

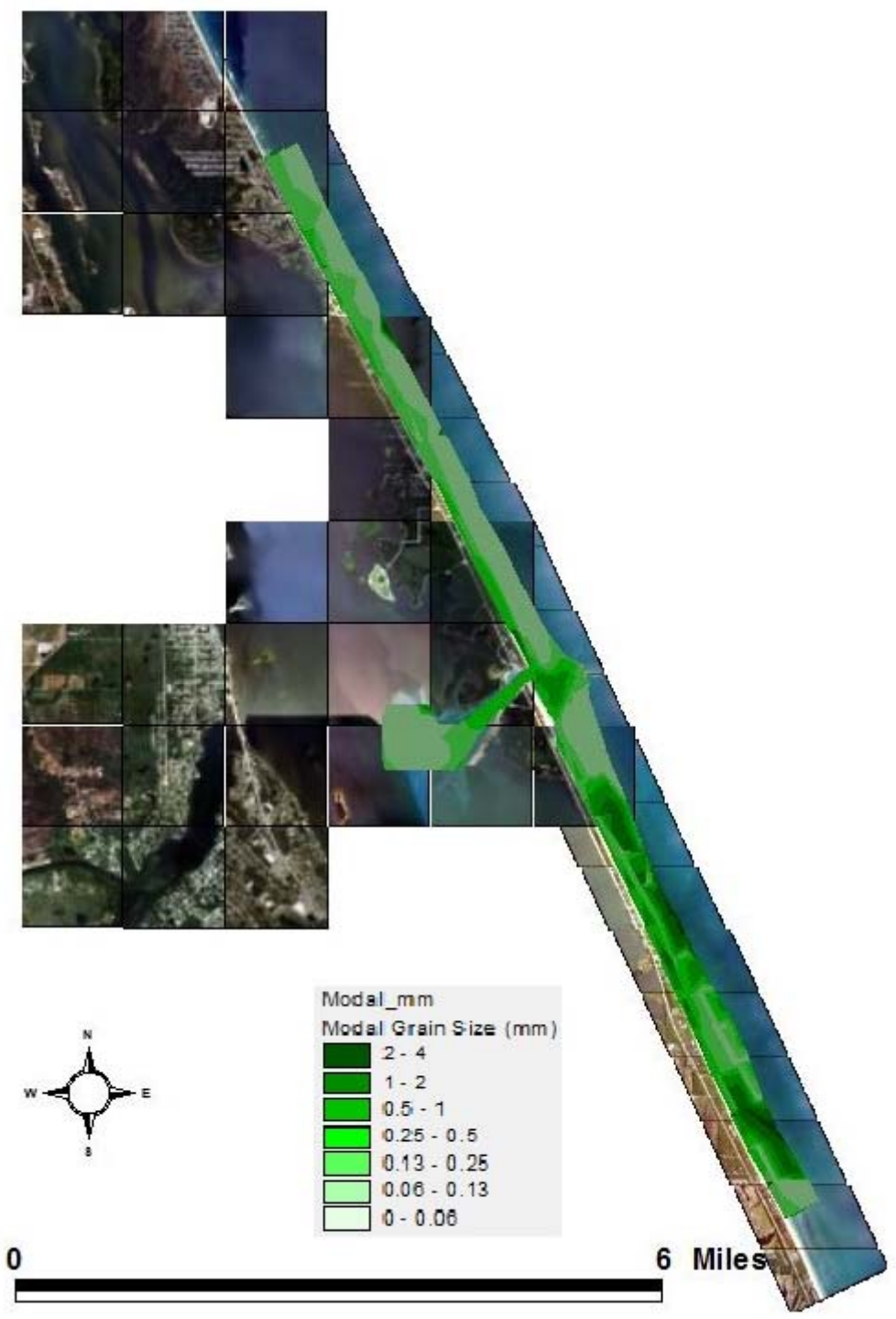

Figure 127. Modal grain size in mm

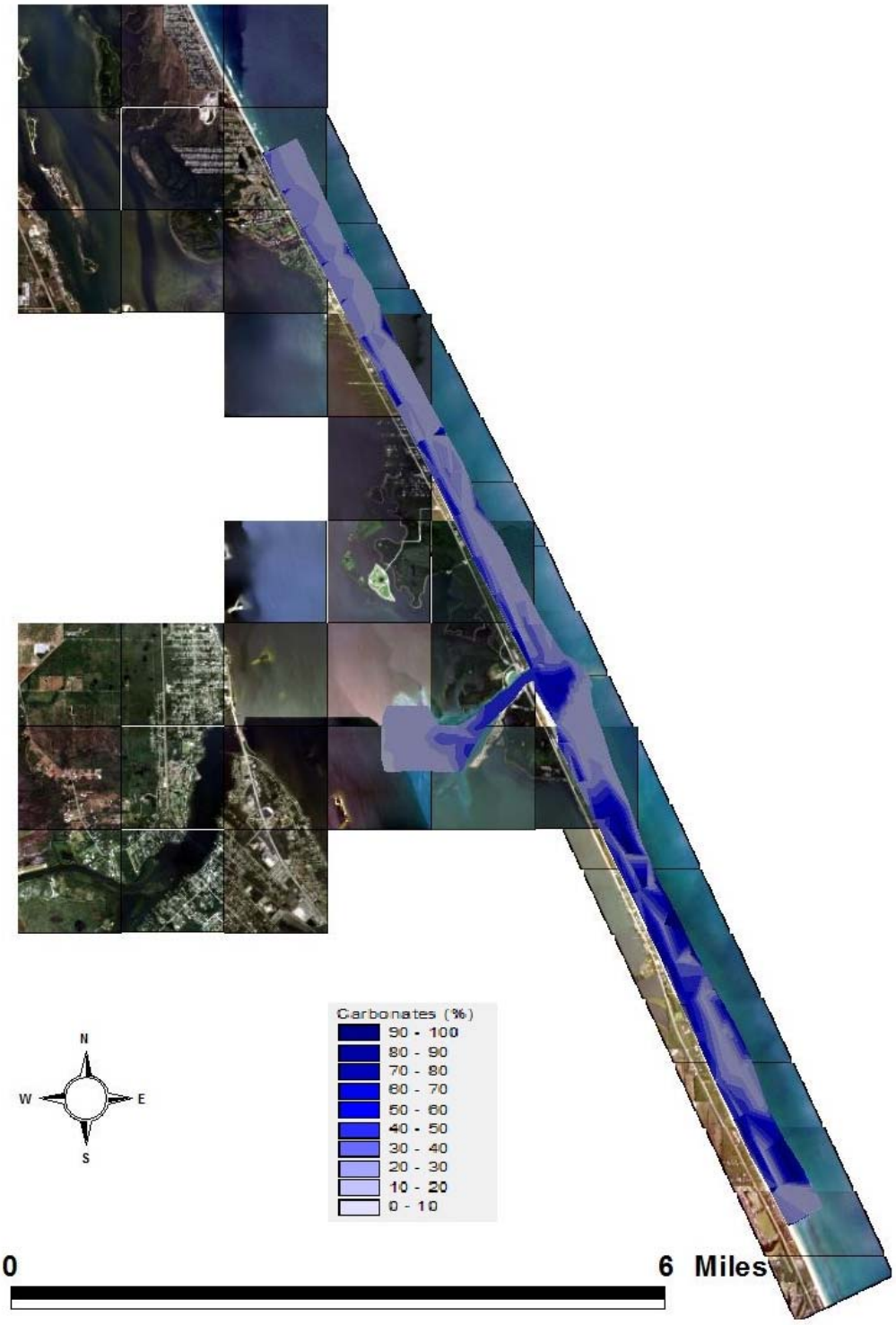

Figure 128. Carbonate fraction percent

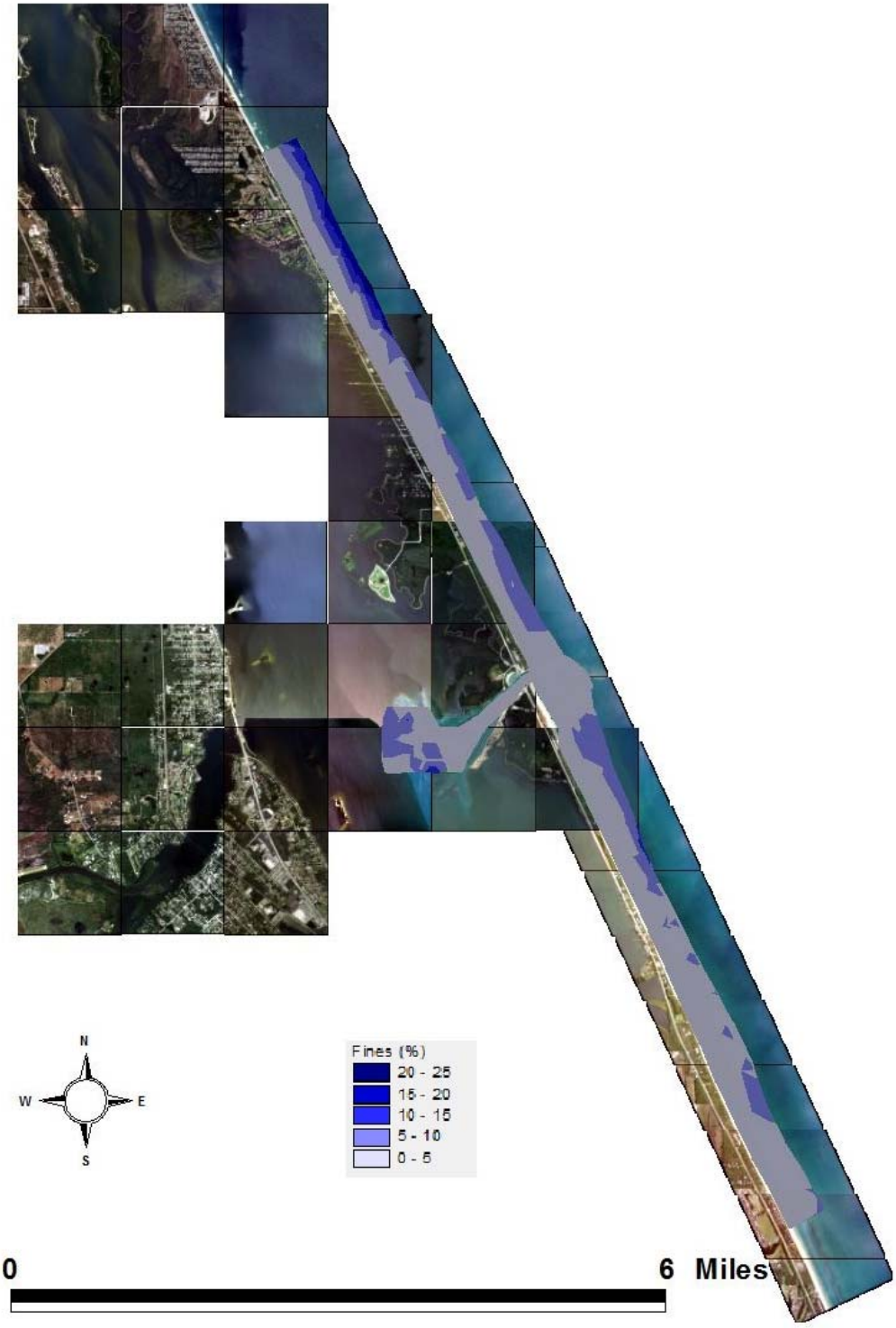

Figure 129. Fine fraction percent.

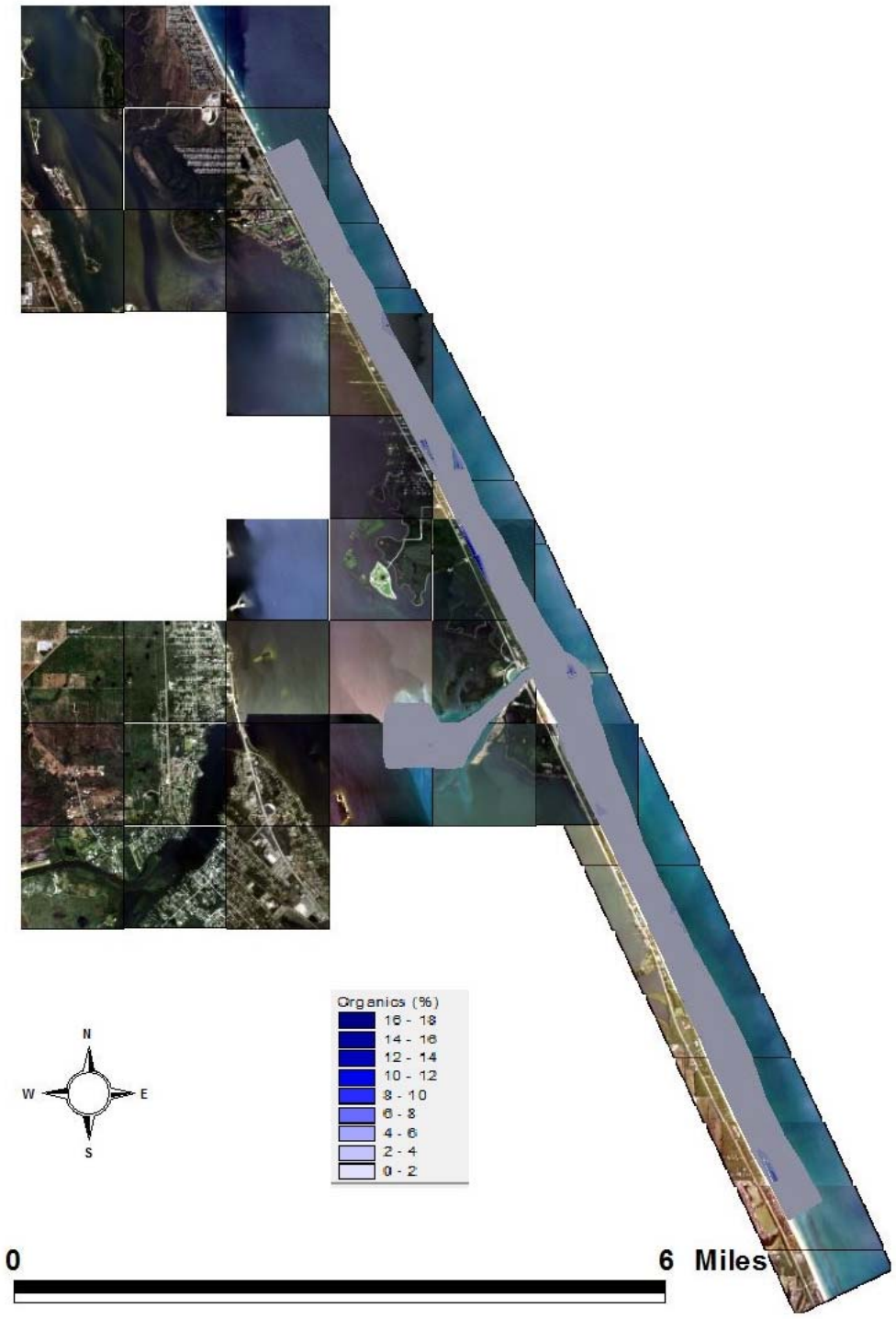

Figure 130. Organic fraction percent from loss on ignition.

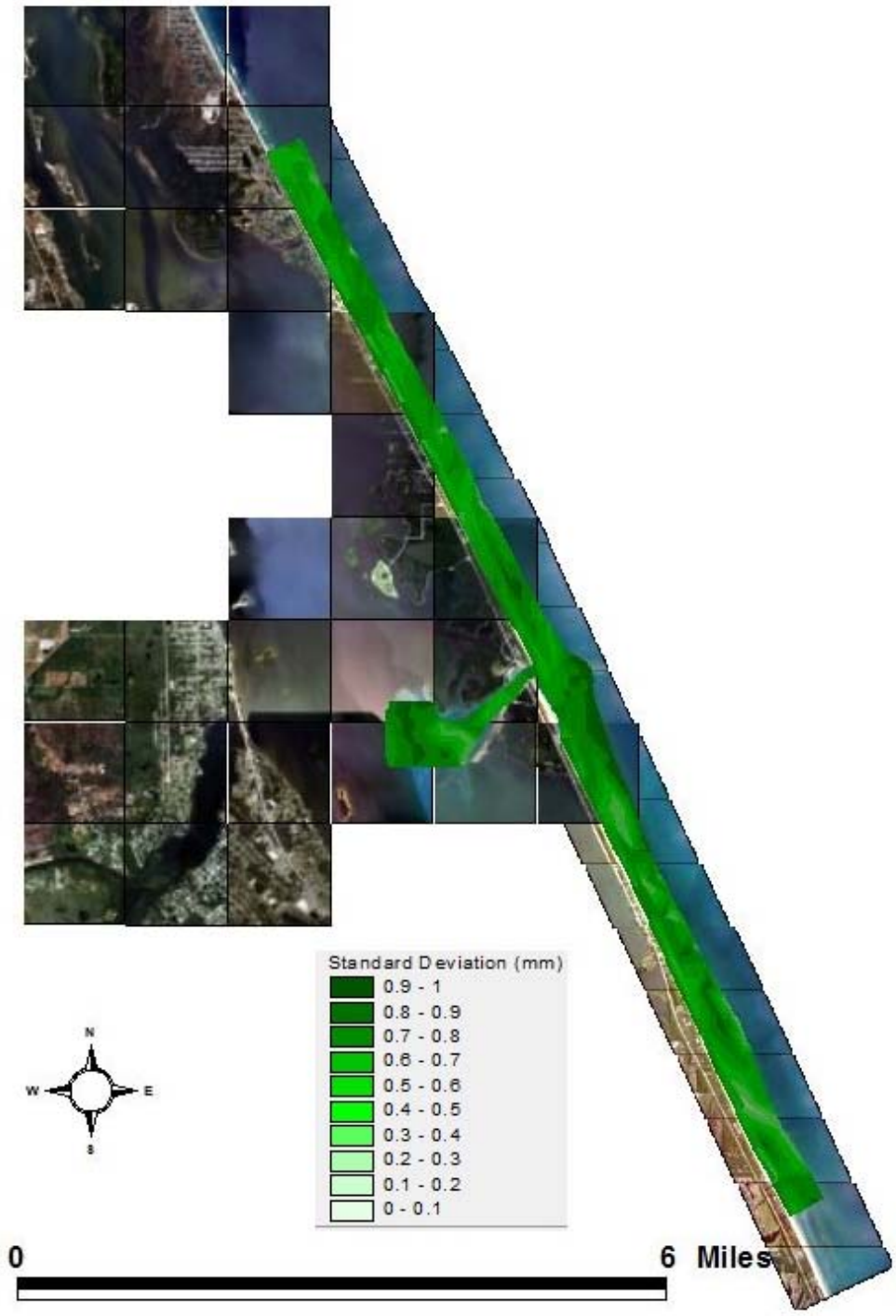

Figure 131. Standard deviation about mean grain size

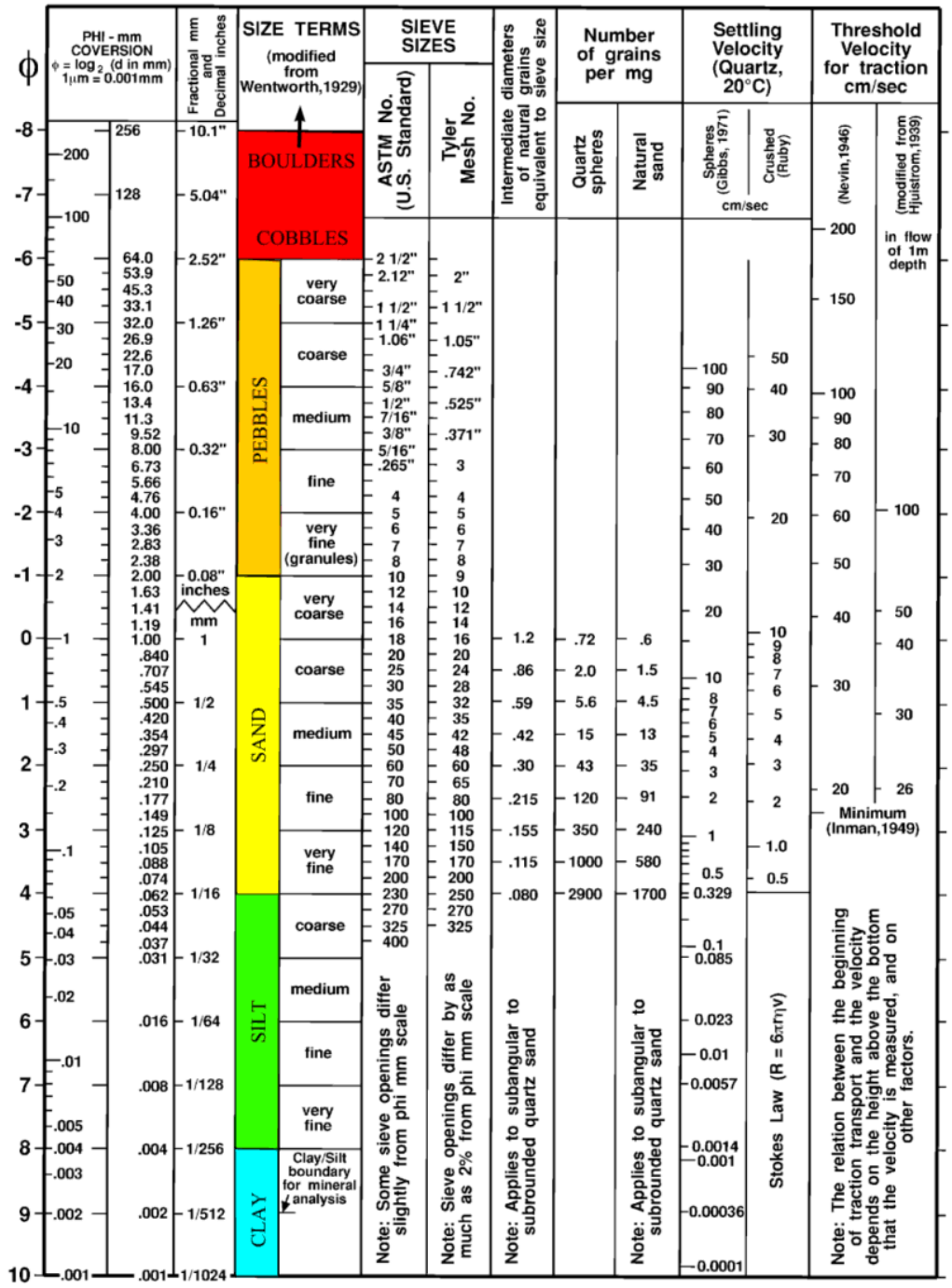

Figure 132. Wentworth grain size classification.